The Role of LKB1-Mediated Signalling in *Dictyostelium Discoideum*

Submitted by
Charlene Farah Kairouz

Bachelor of Medical Science, 2009 La Trobe University
Bachelor of Biochemistry (Honours), 2010 La Trobe University

A thesis submitted in total fulfilment of the requirements

for the degree of

Doctor of Philosophy

School of Life Sciences

College of Science, Health and Engineering

La Trobe University

Victoria, Australia

March **2019**

Table of Contents

List of Figures

List of Tables

List of abbreviations and symbols

ADP	Adenosine diphosphate
AEC	3-amino-9-ethylcarbazole
ATP	Adenosine triphosphate
bp	Base pairs
BSA	Bovine Serum Albumin
cAMP	3',5' cyclic adenosine monophosphate
cDNA	Complementary deoxyribonucleic acid
cfu	Colony forming unit
cm	Centimetres
DEPC	Diethyl pyrocarbonate
dH_2O	Distilled water
DMSO	Dimethylsulfoxide
DNA	Deoxyribonucleic acid
ECF	Enhanced chemifluorescence
EDTA	Ethylenediamine tetraacetic acid
FITC	Fluorescein isothiocyanate
g	Gram
gDNA	Genomic DNA
GFP	Green fluorescent protein
HBS	HEPES-buffered saline
hr	Hour(s)
IPTG	Isopropyl β-D-1-thiogalactopyranoside
kb	Kilobase
kDa	KiloDalton
kV	KiloVolt
l	Litres
LB	Luria Broth
mg	Milligram
min	Minute
ml	Millilitre
mtDNA	Mitochondrial DNA
µF	MicroFaraday
µg	Microgram
µl	Microlitre
mRNA	Messenger RNA
NB	Nutrient Broth
ng	Nanogram
nm	Nanometres
OD	Optical density
OXPHOS	Oxidative phosphorylation
PAGE	Polyacrylamide gel electrophoresis
PBS	Phosphate buffered saline
PCR	Polymerase Chain Reaction
pg	pictograms
PVC	Polyvinyl chloride
PVDF	Polyvinylidene difluoride
rcf	Relative centrifugal force
rpm	Revolutions per minute
RNA	Ribonucleic acid

RNase	Ribonuclease
ROS	Reactive oxygen species
s	Seconds
SBE	Sodium Borate Electrophoresis
SDS	Sodium dodecyl sulfate
SDS-PAGE	SDS-polyacrylamide gel
SM	Standard medium
SOC	Super Optimal broth with Catabolite repression
SS	Sterile Saline
TAE	Tris-acetate-EDTA buffer
TBE	Tris-borate-EDTA-buffer
TBS	Tris-Buffered Saline
TBST	Tris-Buffered Saline Tween-20
TE	Tris-EDTA buffer
TSAP	Thermosensitive Alkaline Phosphatase
U	Units
UV	Ultra-violet light
V	Volts
(v/v)	Volume per volume ratio
(w/v)	Weight per volume ratio

Abstract

Mitochondrial diseases are a poorly understood group of degenerative diseases characterized by a complex array of symptoms affecting major organ systems in unpredictable combinations. *Dictyostelium discoideum* provides a tractable, established model for mitochondrial disease which revealed previously that diverse phenotypes of mitochondrially diseased cells are caused by chronic activation of an energy-sensing alarm protein AMP-activated protein kinase (AMPK). Chronic AMPK hyperactivity impairs *Dictyostelium* growth, cell cycle progression and multicellular morphogenesis as well as promote mitochondrial biogenesis, a feature of mitochondrial disease in humans. In other organisms, AMPK is mainly activated in response to various cellular stresses by the upstream protein kinase LKB1-STRADα-MO25 complex. LKB1 is a serine/threonine kinase, originally identified as a tumour suppressor. Loss of function mutations in the human LKB1 gene can lead to Peutz–Jeghers syndrome, an autosomal dominant disease characterized by benign gastrointestinal tumours (hamartomas).

The thesis aimed firstly to investigate the role of LKB1 expression in *D. discoideum* and whether LKB1's biological functions in the *Dictyostelium* model are mediated by AMPK activation as expected if LKB1 is the main upstream kinase and activator of AMPK. To do this, a genetic approach was utilised to analyse the phenotypic effects of altering LKB1 activity. Transformants with an overexpression LKB1 construct were created to constitutively intensify the effects of LKB1 in *Dictyostelium* and their resultant phenotypes were analysed. To confirm that the phenotypes examined in LKB1-overexpressing cells are due to its kinase activity, transformants that overexpress LKB1 Dead Kinase (mutant LKB1 with its kinase activity ablated) were also created. In this work, I found that overexpression of wild type LKB1 dramatically impaired growth both on a bacterial food source and in axenic medium in *Dictyostelium,* consistent with the growth-suppressing activity of its mammalian homologue in human cells. The overexpression of LKB1 Dead Kinase in *Dictyostelium* resulted in accelerated growth rates; consistent with the upregulation of growth in mammalian cells caused by loss of LKB1. Furthermore, the impaired growth of *Dictyostelium* cells caused by LKB1 overexpression was rescued by antisense-inhibiting AMPK, resulting in growth similar to wild type AX2. The rates of bacterial uptake in phagocytosis and of fluid uptake in

pinocytosis were also reduced in *Dictyostelium* when LKB1 is overexpressed and enhanced in strains expressing LKB1 Dead Kinase. These results show that the regulation of plaque expansion and axenic growth by LKB1 may also depend partly on the ability of the transformants to take up bacteria and fluid through phagocytosis and pinocytosis respectively. AMPK knockdown failed to suppress the impairment of phagocytosis and pinocytosis caused by LKB1 overexpression. These findings imply that LKB1 regulates endocytosis through the activation of kinases other than AMPK. The overexpression of LKB1 in an otherwise wild type *Dictyostelium* background also caused impairment in the morphology of the fruiting bodies. However, overexpression of LKB1 Dead Kinase led to the formation of fewer fruiting bodies which, however, appeared normal morphologically compared to wild type AX2, a phenotype similarly displayed by antisense-inhibiting AMPK. LKB1 in *Dictyostelium* was furthermore shown to lead to increased mitochondrial mass indicative of mitochondrial proliferation, a feature of mitochondrial disease in humans, and in decreased mitochondrial membrane potential. Conversely in *Dictyostelium* cells, overexpressing LKB1 Dead Kinase led to a decrease in the mitochondrial mass and an increase in the mitochondrial membrane potential, as similarly displayed in mice deficient in LKB1 that showed reduced mitochondrial content in muscle and incapability of enhancing mitochondrial biogenesis after exercise. The antisense inhibition of AMPK expression counteracted the effects exerted by the overexpression of LKB1 resulting in mitochondrial mass and membrane potential similar to wild type AX2. From the foregoing results, LKB1 appears to act as an upstream kinase of AMPK in the regulation of cell growth and development as well as mitochondrial biogenesis, but its regulation of phagocytosis and pinocytosis appear to occur independently of AMPK.

The thesis aimed secondly to investigate in *D. discoideum* the effect on the LKB1's function of STRADα, a subunit of the LKB1 heterotrimeric complex. Transformants with concurrent overexpression of STRADα and LKB1 were created and the phenotypic outcomes were analysed. The results revealed that when LKB1 is coexpressed with STRADα, the overexpressed LKB1 has a more potent effect on the phenotypes displayed by the *Dictyostelium* cells than when LKB1 is solely expressed. This result confirms that, as in mammalian cells, STRADα enhances the kinase functions of LKB1.

Statement of authorship

Except where reference is made in the text of the thesis, this thesis contains no material published elsewhere or extracted in whole or in part from a thesis submitted for the award of any other degree or diploma. No other person's work has been used without due acknowledgment in the main text of the thesis. This thesis has not been submitted for the award of any degree or diploma in any other tertiary institution.

Charlene Farah Kairouz

Date: 28th February 2019

Acknowledgements

I would like to express my sincere gratitude to my supervisor, Prof Paul Fisher, for his continuous support of my work, his patience, motivation and immense knowledge. I admire his dedication to his work and am grateful to him for the opportunity of conducting my research as part of his team. His guidance throughout my PhD is immensely appreciated. I also like to acknowledge that this work was supported by an Australian Government Research Training Program Scholarship.

I would also like to thank my co-supervisor, Dr Sarah Annesley, for her insightful comments and nonstop encouragement throughout my candidature. Not only has she been a mentor to me throughout the years on an academic level, but she has also become a good friend whom I respect and admire.

I am also grateful to my fellow labmates for their help and friendship. I will always have fond memories of the fun times we shared, the stimulating discussions we had and the sleepless nights we worked together.

On a personal note, I would like to express my infinite love and respect for my parents, Karim and Juliet. To be deeply loved by them has given me the strength and courage to pursue my dreams and the discipline to make my dreams become a reality. They are my rock and pillar of strength. They have stood by me through all times; especially in moments when I had completely lost hope. Their immense belief in me lifted me back up. I love them immensely and thank them for their emotional support throughout my research.

I am also extremely appreciative to my siblings, Christine, Patrick and Naz, and their beautiful families for their constant love and support. My sister especially, has been my beacon of light on this journey.

I also want to thank each member of my husband's family for their continuous encouragement, positivity and love.

To my husband, Joe, you have constantly made me laugh, wiped my tears and kept me strong. We have become a team that support and encourage each other to become better versions of ourselves. Finishing my PhD would have not been possible if it were not for your support and words of encouragement. I thank you for always nudging me to work harder and achieve more. I love you for the husband you are to me and the father you are to our beautiful children.

To my angelic children, Veronica and William. I love you with every fibre of my heart and soul. You have brought so much joy and love into my life. All the work I have invested into this PhD is for you. I hope my research can play a part, even if miniscule, in creating a better and healthier world for you. You are my world and my everything.

To my Angel Grandma, Angelina, I know you are always looking out for me from Up there. Your unconditional love, acceptance and blessings have always been my refuge on a rainy day.

And last but definitely not least, I would like to thank my Lord, Jesus Christ, for all of his blessings and love.

Publications

Annesley, S. J., Chen, S., Francione, L. M., Sanislav, O., Chavan, A.J., **Farah, C**., De Piazza, S. W., Storey, C.L., Ilievska, J., Fernando, S. G., Smith, P. K., Lay, S. T., Fisher P. R. (2013). *Dictyostelium*, a microbial model for brain disease, *Biochimica et Biophysica Acta*, 1840, 1413-1432.

Conference abstract publications

Farah, C., Annesley, S. J. & Fisher P. R (2014) LKB1-mediated signalling in the *Dictyostelium* mitochondrial disease model. Dicty2014. Annual International *Dictyostelium* Conference. Aug 3rd – Aug 7th, Potsdam, Germany. Abstract p. 69.

Ilievska, J., Annesley, S. J., **Farah, C.**, Bishop, N. E. & Fisher P. R (2012) Roles of ESCRT proteins in Dictyostelium discoideum. Dicty2012. Annual International *Dictyostelium* Conference. July 29th – Aug 2nd, Madrid, Spain. Abstract p. 98.

1. Introduction

Mitochondrial diseases are complex degenerative disorders instigated by mutations in nuclear genes encoding mitochondrial proteins or mitochondrial genes that encode subunits of the oxidative complexes or translational machinery (Wallace, 2010; Alston *et al.,* 2017). In humans, the common pathological outcomes include blindness, deafness, epilepsy, heart disease, stroke-like episodes, ataxia, muscle weakness, exercise intolerance, diabetes and kidney disease (Francione & Fisher, 2010; Zeviani & Carelli, 2007). Mitochondrial dysfunction also plays pathological roles in neurological disorders such as Parkinson's disease and Alzheimer's disease (Zeviani & Carelli, 2007, Bender *et al.,* 2006; Coskun *et al*., 2004; Kraytsberg *et al*., 2006; Hawking, 2016; Haylett *et al.,* 2016; Gao *et al.,* 2017).

1.1. Molecular features of mitochondrial disease

Mitochondrial diseases are an eclectic and poorly understood group of degenerative, genetic diseases caused by mutations that affect mitochondrial proteins encoded either in the nuclear or the mitochondrial genome (Zeviani & Carelli, 2007; Alston *et al.*, 2017). Clinical manifestations normally occur in the affected organs/tissues with a high-energy demand; however, any organ or tissue can be involved. These clinical manifestations include stroke-like episodes, encephalopathy, dementia, ataxia and seizure as well as peripheral neuropathy, ophthalmoplegia and myopathy (Reeve *et al.,* 2008; Vital & Vital; 2012; Pitceathy & McFarland, 2014; Whittaker *et al.,* 2015).

Patients with mitochondrial encephalomyopathies and myopathy were observed to have more than two hundred mutations and/or deletions of mitochondrial DNA (mtDNA) in affected tissues. This demonstrates that genetic defects play a vital role in the pathogenesis of mitochondrial diseases (Tuppen *et al.,* 2010; DiMauro, 2013). Affected tissue cells in patients with mitochondrial diseases often have pathogenic mtDNA mutations resulting in mitochondrial dysfunction. These mutations include point mutations characterized in patients with mitochondrial encephalomyopathy (Rahman & Poulton, 2009; Ienco *et al.,* 2016), MERRF syndrome (Yoneda *et al*., 1990; Agresti *et al.,* 2018), Leigh syndrome (Finsterer, 2008; Ruhoy & Saneto, 2014), Leber's hereditary optic neuropathy (LHON)

(Man & Turnball, 2002; Catarino *et al.,* 2017), stroke-like episodes and ataxia or large-scale deletions demonstrated in patients with Kearns-Sayre syndrome (KSS) (Maceluch & Niedziela, 2006; Yu *et al.,* 2016) and chronic progressive external ophthalmoplegia (CPEO) (Moreas *et al*., 1989; Greaves *et al.,* 2010). Although mitochondrial diseases have well characterized clinical features, the relationship between clinical phenotypes and genotype is fairly complicated and hence the pathophysiology of mitochondrial diseases is poorly understood. To gain further insight into this relationship*, Dictyostelium discoideum* has been used as a model organism to analyse mitochondrial biogenesis and disease (Wilczynska *et al*., 1997; Kotsifas *et al.,* 2002; Bokko *et al*., 2007; Annesley & Fisher, 2009; Francione *et al.,* 2011). The mitochondrial genome of *Dictyostelium* has been fully sequenced (Ogawa *et al*., 2000), and its mitochondrial transcription and RNA processing have been comprehensively studied (Barth *et al*., 1999; Barth *et al*., 2001; Le *et al*., 2009). *Dictyostelium* has been employed to create mitochondrial disease via a variety of methods and the resulting pathological outcomes have been analysed. Many phenotypes can be observed as *Dictyostelium* possess motile unicellular and multicellular stages with multiple cell types. These phenotypes include cell cycle progression and growth, morphogenesis, phototaxis, micropinocytosis and phagocytosis. These various phenotypes represent measurable, reproducible "readouts" of the intracellular signaling pathways that regulate them. Assaying these phenotypes in mitochondrially diseased *Dictyostelium* lines offers a better understanding of genotype- phenotype relationships in mitochondrial disease, without the overlaid complexities coupled with mammalian systems.

To gain a better understanding of the cytopathological pathways associated with mitochondrial diseases, it is essential to pinpoint and study proteins involved in these pathways. One such protein whose signalling was found to be responsible for diverse cytopathologies seen in *Dictyostelium* mitochondrial disease is the AMP-activated protein kinase (AMPK) (Bokko *et al*., 2007 and Francione *et al.,* 2009). AMPK is a ubiquitous, highly conserved protein kinase that maintains cellular energy homeostasis in healthy and diseased cells. In mammalian cells, AMPK activity is regulated by three upstream kinases: Liver Kinase 1 (LKB1), calmodulin-dependent protein kinase kinase (CaMKK) and the transforming growth factor-β-activated kinase (Tak1). Genetic studies of tissue-specific deletion of LKB1 have exhibited that the activation of AMPK is mediated by LKB1 in almost every tissue type tested; hence making it the main upstream kinase of AMPK. *In vitro* studies showed that recombinant LKB1 complex phosphorylates Thr-172 directly on

AMPK resulting in its activation. In LKB1 deficient cells, such as HeLa cells, AMPK is not activated in response to an increase in AMP/ATP ratio (Hawley *et al*., 2003). This finding indicates that the activation of AMPK in response to increased AMP is dependent on the presence of LKB1.

This thesis will highlight the contributions made by the *Dictyostelium* model to our understanding of mitochondrial biology and disease. The role of LKB1 as an upstream kinase of AMPK in *Dictyostelium* is discussed and the associated phenotypes are analysed.

1.2. LKB1- The tumour suppressor protein

1.2.1. The Peutz-Jeghers Syndrome

LKB1 was initially identified as a tumour suppressor, mutations in which were responsible for an inherited susceptibility to cancer (Hemminki *et al*., 1998; Jenne *et al*., 1998). Mutations in the LKB1 gene result in Peutz-Jeugers Syndrome (PJS) that is characterized by benign hamartomas and malignant tumours particularly in the intestine (Sanchez-Cespedes, 2007; Emile *et al.,* 2018).

Peutz-Jeghers syndrome is a hereditary, autosomal dominant disease firstly described by Johannes Peutz in 1921 and further characterized by Harold Jeghers in 1948. This rare disease is mainly characterized by the formation of benign hamartomatous polyps (overgrowth of differentiated tissues), predominantly in the gastrointestinal tract. PJS is also characterized by marked cutaneous pigmentation of the mucous membranes and an increased risk of developing malignant tumours or cancer (Hemminki *et al.*, 1999; Westerman *et al.*, 1999; Giardiello & Trimbath, 2006; Monica & Auerkar, 2018) affecting various organs such as the digestive tract (Banno *et al*., 2013), breast, testis and pancreas (Gan & Li, 2014). The incidences of PJS vary significantly from 1 in 10,000 to 1 in 120,000 births (Alessi *et al.*, 2006; Wang *et al.,* 2016) (Figure 1.1).

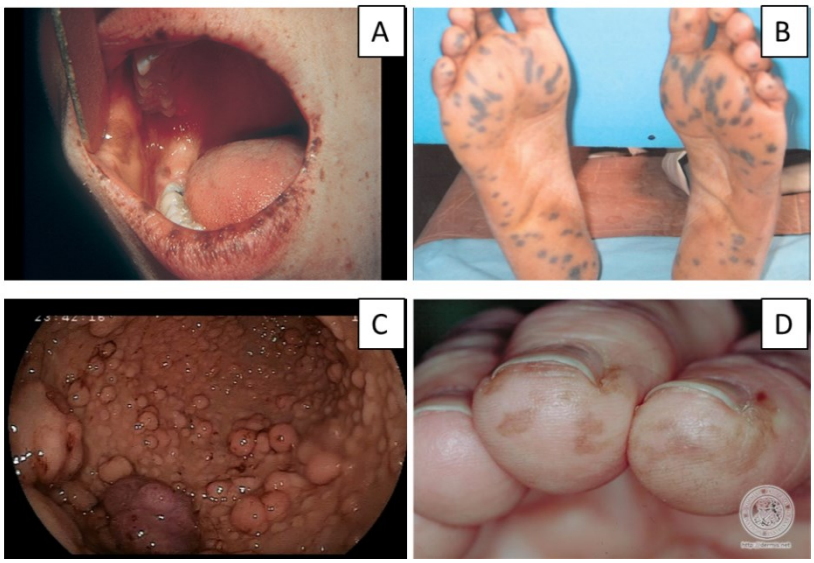

Figure 1.1. Common characteristics of Peutz-Jeghers syndrome in patients.
The PJS is characterized by hyperpigmentation of oral mucosa and the lips (A), of toes (B), of fingers (D) as well as polyposis in the gastrointestinal tract (C).

(A) (http://www.medicinenet.com/image-collection/peutz-jeghers_syndrome_picture/picture.htm), of toes
(B) (http://www.ijdvl.com/articles/2008/74/2/images/ijdvl_2008_74_2_154_39705_2.jpg), of fingers
(C) (http://4.bp.blogspot.com/-ULLXZnuvP5k/UdPi0Zi4TJI/AAAAAAAADPU/B3s7qxY7nzo/s720/18.jpg).
(D) (http://www.dermis.net/dermisroot/en/51592/image.htm)

1.2.2. Germline mutations of LKB1

Hemminki *et al.* (1998) has showed through genetic linkage analysis that Peutz-Jeghers syndrome is caused by a mutation located on chromosome 19p13.3. Positional cloning has identified various mutations in the LKB1 gene in the germline of PJS patients. These mutations include all types of loss of function mutations such as deletions of the LKB1 locus, as well as frameshift and nonsense mutations (Launonen, 2005; Resta *et al.,* 2010; Chen *et al.,* 2017; Xu *et al.,* 2018). The majority of the mutations of LKB1 caused truncations in the kinase domain and ablation of catalytic activity. Missense mutations are mainly positioned in the catalytic domain where they disrupt the LKB1 kinase activity. Some mutations have also been detected in the C-terminal tail of LKB1 resulting in the impairment of the biological activity of LKB1 (Forcet *et al.,* 2005, Zhao & Xu, 2014). However, in the N-terminal non-catalytic region, no point mutations have been detected (Alessi *et al.*, 2006) (Figure 1.2).

The LKB1 gene is the main gene responsible for PJS with mutations detected in more than 80% of the families worldwide (Yajima *et al.,* 2013). However, in a few families without LKB1 mutations, linkage with a locus other than LKB1 has been mapped. Recently, a PJS patient has been found to have a germline mutation of the gene coding MYH11 (myosin heavy chain); however, the importance of this observation is not clear (Alhopuro *et al*., 2008). Hence, notwithstanding circumstantial proof of a genetic heterogeneity, no other genes besides LKB1 have been attributed to PJS.

1.2.3. LKB1 mutations in sporadic cancer

LKB1 mutations have also been characterised in sporadic cancers, more specifically in 30% of human non-small cell lung cancer (NSCLC), 20% of cervical cancers and 4 to 7% of pancreatic cancers (Hardie & Alessi, 2013; Sahin *et al.,* 2003; Banno *et al.,* 2013; Zhao *et al.,* 2014). The loss of LKB1 function has been proven to be critical to pulmonary tumourigenesis with its involvement in different stages from tumour initiation to metastasis (Ji *et al*., 2007; Hermann *et al.,* 2011; Faubert *et al.*, 2014).

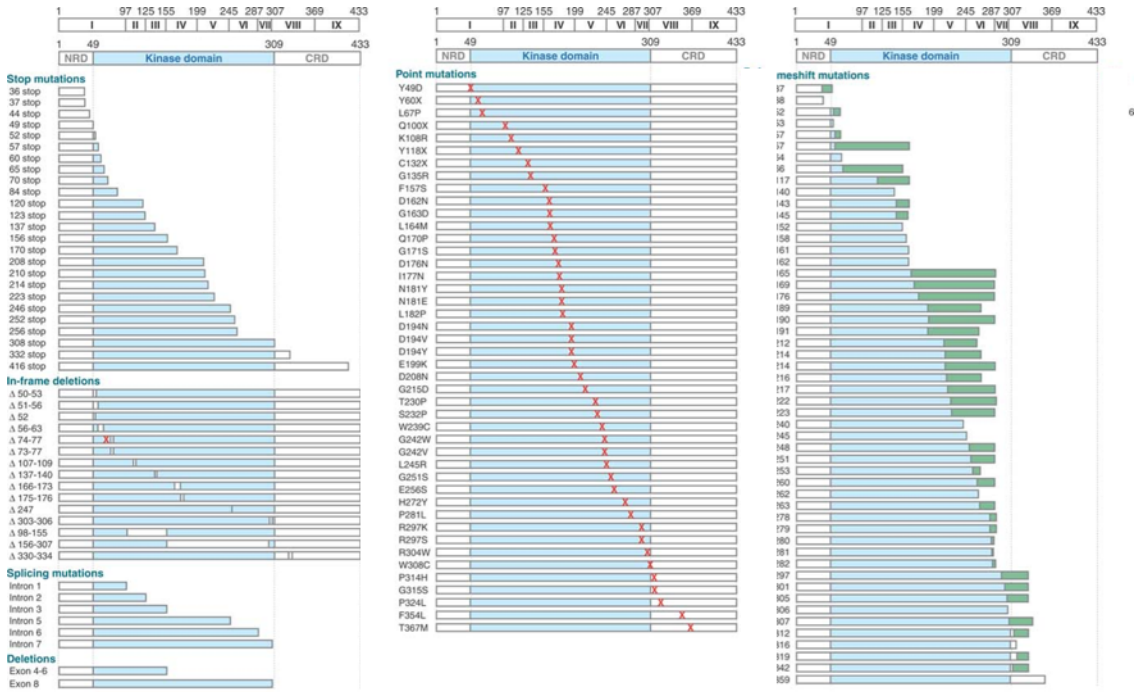

Figure 1.2. Schematic representation of mutations identified in the human LKB1 gene in patients with PJS and sporadic cancer.

The mutations' predicted effects on the primary structure of the LKB1 protein are schematically represented. The genomic organization of the LKB1 gene coding sequence is presented on the top, and the functional domains of the protein are presented below with (a) stop mutations, in-frame deletions (represented by Δ), splicing mutations, and deletions; (b) point mutations (represented by X); (c) frameshift mutations (represented by fs). The abbreviations used are NRD, N-terminal regulatory domain; CRD, C-terminal regulatory domain (white boxes).
The protein kinase domain (blue boxes) and amino acid sequence introduced by the frameshift (green boxes) are also specified. (Adapted from Alessi *et al*., 2006; with permisison).

1.3. LKB1: from gene to protein

LKB1 is a tumour suppressor gene which is evolutionarily conserved. LKB1 in the human genome spans 23 kb and encompasses ten exons, nine of which are coding and one is non-coding (Mehenni *et al.,* 1998). The LKB1 gene is ubiquitously expressed in healthy tissues as well as tumours. In mice, LKB1 (mRNA) is mainly expressed in the lung, gastrointestinal tract and testis during embryonic development (Luukko *et al.,* 1999; Gan & Li, 2014). In humans, LKB1 is chiefly expressed in epithelia and the seminiferous tubules of the testis. The expression levels of LKB1 appear to be higher in foetal than in adult tissues (Rowan *et al.*, 2000; Gan & Li, 2014). Conversely, in *Xenopus*, the ortholog of LKB1, XEEK1, appears to be limited to early embryogenesis (Rowan *et al.*, 2000) whereas in *C. elegans*, the ortholog of LKB1, Par-4, can be expressed in the gonads, oocytes and early embryos (Watts *et al.,* 2000; Alessi *et al.*, 2006; Gan & Li, 2014).

Moreover, LKB1 expression levels are high in some malignant tumours while no expression of LKB1 is detected in some cancer cells. This implies a dual role of LKB1 at different stages of tumourigenesis (Gan & Li, 2014).

1.3.1. LKB1: Splice variants

The human LKB1 gene spans 23kb and is transcribed in the telomere-to-centromere direction. The 3kb transcribed mRNA can be alternatively spliced resulting in two isoforms: $LKB1_L$ (long isoform) and $LKB1_S$ (short isoform). The alternative splicing takes place at exon 9 of the mRNA. In $LKB1_L$, the C-terminal sequence is encoded by exon 9B, whereas in $LKB1_S$ this sequence is encoded by exon 9A resulting in the substitution of the last 63 amino acids of the long isoform by 39 different amino acids in the short isoform (Towler *et al.,* 2008; Denison *et al.,* 2009; Gan & Li, 2014, Kullman & Krahn, 2018) (Figure 1.3). Hence, distinguishing the splice variants of LKB1 is dependent on their molecular weights in which $LKB1_L$ is 50 KDa and $LKB1_S$ is 48 KDa. $LKB1_L$ is expressed ubiquitously throughout tissues, while $LKB1_S$ is prevalent in the testis where it plays a role in spermiogenesis. This is demonstrated in male knockout mice for this isoform which are sterile and display a decrease in the number of mature spermatozoa. The infertility phenotype is mainly due to a defect in the release of mature spermatids from the seminiferous epithelium (spermiation) during spermatozoan development (Denison *et al.,* 2011; Denison *et al.,* 2009; Shaw, 2008).

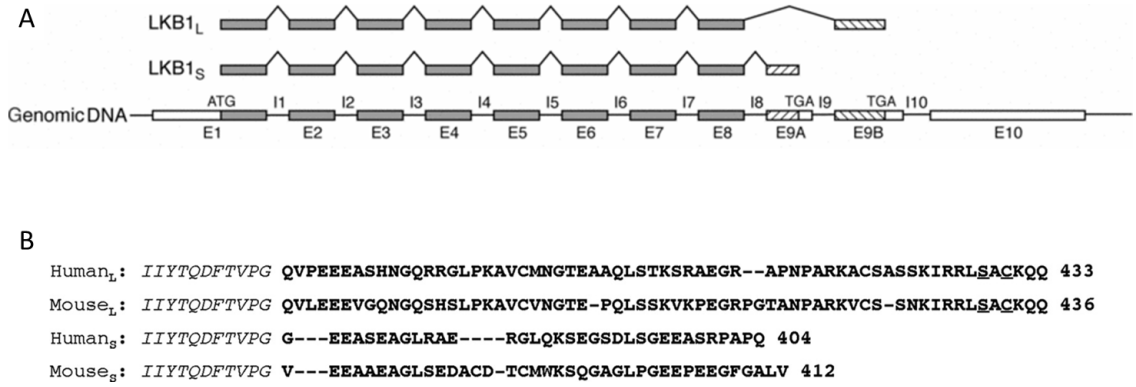

Figure 1.3. The long and short isoforms of LKB1 splice variants.
A. A presentation of the arrangement of exons (E1 through E10) and introns (I1 through I10) of the LKB1 gene. Protein coding regions shared by both isoforms are depicted in grey, whereas the regions encoding the unique C-terminal regions of $LKB1_S$ and $LKB1_L$ found in exons 9A and 9B are depicted with forward or backward cross-hatching respectively. **B.** The deduced amino acid sequences of the C-terminal regions of human and mouse $LKB1_L$ and $LKB1_S$ are presented. A part of the sequence encoded by exon VIII and shared by both forms, is represented in italics. Serine 428/431 (human/mouse) and cysteine 430/433 in $LKB1_L$ that have been found to be post-translationally modified are underlined. The number of amino acids in each of the full-length proteins is specified. (Adapted from Denison *et al*., 2009; with permission).

1.3.2. LKB1: Structure and subcellular localization

LKB1 is a serine/threonine kinase encompassing 433 amino acids in humans. It has a conserved kinase catalytic domain localized between the 49th and 309th amino acid. The C-terminal region of LKB1 holds a prenylation site (Cys433) which plays a role in the localization of LKB1 to the plasma membrane (Houde *et al.,* 2014). The N-terminal region of LKB1 contains in the 38 to 43 amino acid region a nuclear localization signal (NLS); which regulates the shuttling of LKB1 between the nucleus and the cytoplasm. Hence, the localisation of LKB1 can be within the plasma membrane, the nucleus and the cytoplasm in living cells. However, LKB1 can also translocate into the mitochondria during apoptosis (Jansen *et al*., 2009; Alessi *et al.,* 2006; Karuman *et al.,* 2001; Gan & Li, 2014).

1.3.3. Post-translational modifications

LKB1 undergoes post-translational modifications such as phosphorylation, prenylation, ubiquitination as well as acetylation.

1.3.3.1 Phosphorylation of LKB1

LKB1 can either autophosphorylate itself or be phosphorylated by upstream kinases. Phosphorylation has been reported to at least occur at 9 residues of LKB1 (Alessi *et al.*, 2006). Thr185, Thr189, Thr336 and Thr402 are autophosphorylation sites while Ser31, Ser307, Ser325, Thr366 and Ser428 (Ser431 in mice) are phosphorylated by different upstream kinases (Alessi *et al.*, 2006, Xie *et al.,* 2008; Sebbagh *et al.,* 2011, Liu *et al.,* 2012; Kullman & Krahn, 2018) (Figure 1.4). The major autophosphorylation site of LKB1 is on Thr336. Mutation of Ser31, Ser325 and Thr366 did not affect the catalytic activity or subcellular localization of LKB1 and the autophosphorylation on Ser31 and Ser325 remain controversial (Sapkota *et al.,* 2002a).

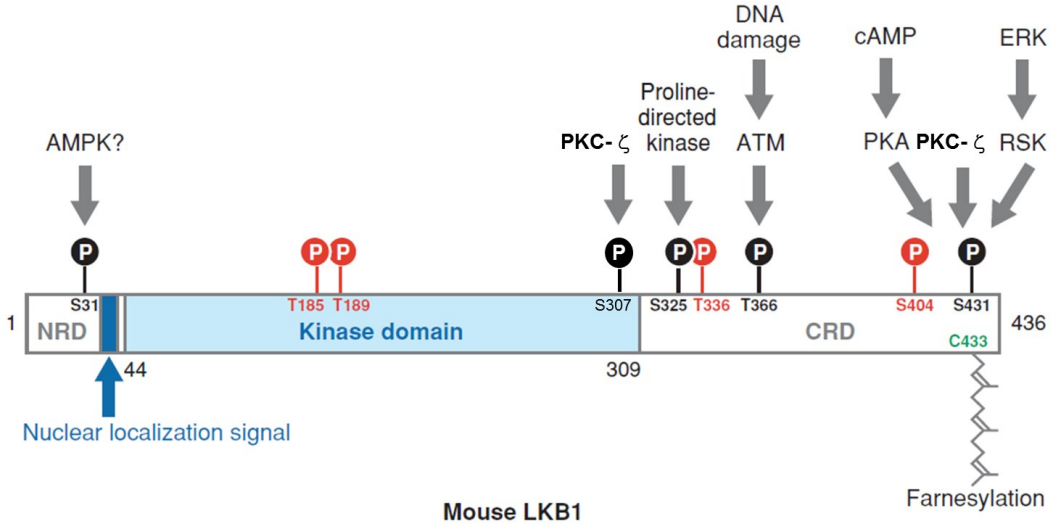

Figure 1.4. Location of the posttranslational modification sites on mouse LKB1.
Sites that are autophosphorylated in mice are portrayed in red, and sites that are phosphorylated by other kinases are depicted in black. The Cys433 farnesylation site is shown in green. The agonists and the upstream protein kinases phosphorylating LKB1 are specified. It must be considered that it is debatable whether Thr189 represents a site of autophosphorylation (Sapkota *et al.*, 2002a). In human and mouse LKB1, the Ser31, Thr185 and Thr189, Ser325 and Ser336 are identical in number; however, in human LKB1, Thr366 is Thr363, Ser404 is Thr402, Ser431 is Ser428 and Cys433 is Cys430. The noncatalytic domains are presented in white, and the kinase domain is depicted in light blue. (Adapted from Alessi *et al.*,2006; with permission).

The mutation of Ser428 to an Ala residue led to LKB1 being retained in the nucleus, signifying that the subcellular localization of LKB1 is regulated by the phosphorylation of this residue (Song *et al.*, 2008; Shen *et al.,* 2014). Indeed, Xie *et al.,* (2008) showed that following metformin treatment, the LKB1 S428A mutant is incapable of translocating into the cytoplasm nor associating with its cytoplasmic substrate AMPK (AMP-activated protein kinase) in HeLa-S3 cells. Nonetheless, this mutation does not affect the catalytic activity of LKB1 (Xie *et al*., 2008; Zhu *et al.,* 2013).

In mice, mutation of the phosphorylation site Ser431 to either Glu or Ala hindered LKB1 from inhibiting the growth of G361 cells in a colony formation assay. G361 is a cancer cell line that does not express endogenous LKB1, and when wild type LKB1 is overexpressed, the growth of these cells is suppressed by inducing a G1 cell cycle arrest (Tiainen *et al*., 1999). This mutation at Ser431 residue signifies that phosphorylation of this residue is crucial for the inhibition of cell growth by LKB1 (Sapkota *et al.*, 2001). Mutation of the major autophosphorylation site on LKB1, Thr336, to Glu, but not Ala, hindered LKB1 from suppressing G361 cell growth, demonstrating that autophosphorylation of this residue may somehow lead to the inhibition of the function of LKB1 in tumour suppression (Sapkota *et al.*,2002a; Bai *et al.,* 2012). On the other hand, mutation of Ser31, Ser325 or Thr366 did not exhibit a profound effect on the ability of LKB1 to abolish G361 cell growth (Sapkota *et al*., 2002a; Gan & Li, 2014).

The Thr336 and Ser431 phosphorylation sites are highly conserved in mammalian, *Xenopus* and *Drosophila* LKB1 but not in *Caenorbabditis elegans* LKB1 (Sapkota *et al.*, 2002). Ser431 is phosphorylated by the p90 ribosomal S6 protein kinase (rsk) and PKA in response to agonists, which prompt their activation (Sapkota *et al.*, 2001; Collins *et al.*, 2000; Houde *et al.,* 2014). Hence these kinases may play a role in regulating cell growth through the LKB1 pathway. LKB1 is phosphorylated at Thr366 only due to the exposure of cells to ionising radiation (Sapkota *et al.*, 2002b). The upstream kinases phosphorylating LKB1 at Ser31 and Ser325 have not yet been characterised.

1.3.3.2 Prenylation

LKB1 is shown to be prenylated in cultured cells and invertebrates (Collins *et al.,* 2000; Martin & St Johnston, 2003; Sapkota *et al*., 2001; Watts *et al*., 2000). Prenylation is a crucial process in mediating protein-protein interactions and protein-membrane interactions. Mouse LKB1 contains a conserved prenylation motif (Cys433–Lys–Gln–Gln436) at the C-terminus directly downstream from a consensus cAMP-dependent protein kinase (PKA) phosphorylation site (Arg428-Arg-Leu-Ser431) (Figure 1.4). In vivo, Cys433 is prenylated and is targeted to the cellular membrane (Collins *et al*., 2000). This prenylation results due to the addition of a farnesyl moiety to Cys433, and mutation of this residue blocks LKB1 prenylation (Sapkota *et al*., 2001). Intriguingly, a study in *Drosophila* showed that a point mutation of the homologous residue to Cys433 forms an allele with dramatically reduced rescue activity. These reports signify the importance of the C-terminus for the function of LKB1 (Jansen *et al.*, 2009).

A study showed that in a $LKB1^{C433S/C433S}$ knockin mouse model, most of the endogenous LKB1 is prenylated (Houde *et al*., 2014). Moreover, a reduced amount of LKB1 was localized at the membrane of the liver cells and fibroblasts in comparison to the wild-type mice; hence corroborating the role of farnesylation in mediating membrane association. Furthermore, LKB1 was unable to activate its substrate AMPK in all of the tested cells and tissues taken from these mice. Consequently, the farnesylation of LKB1 is proven to be imperative to the localization of LKB1 to the cell membrane. These data present the initial confirmation that this farnesylation is necessary for downstream signaling of LKB1 (Houde *et al*., 2014).

1.3.3.3 Ubiquitination

Several studies showed that LKB1 can be ubiquitinated. LKB1 binds to the molecular chaperone heat shock protein 90 (Hsp90) forming a stable complex (Boudeau *et al.,* 2003). Disturbing the LKB1-Hsp90 complex recruits both Hsp/Hsc70 and the U-box dependent E3 ubiquitin ligase CHIP (carboxyl terminus of Hsc70-interacting protein), which in turn prompts the degradation of LKB1 by the proteasome. Hence, LKB1 can be ubiquitinated (Nony *et al*., 2003; Gaude *et al.,* 2012).

1.3.3.4 Acetylation

LKB1 can also be acetylated and deacetylated. In mice, at least ten lysine residues have been identified as potential modification sites (Lysine 44 (K44), K48, K64, K96, K97, K296, K311, K416, K423, and K431) (Calamaras *et al.,* 2012; Lan *et al.,* 2008; Lee *et al.*, 2010; Yang *et al.,* 2014; Zheng *et al*., 2012; Zu *et al.*, 2010, Bai *et al.,* 2016). The enzymes responsible for the acetylation of LKB1 are unknown; however, LKB1 was shown to be deacetylated by Sirtuin 1 (SIRT1) on lysine 48 (K48) which allows the translocation of LKB1 from the nucleus to the cytoplasm (Lan *et al.,* 2008). SIRT1, a conserved NAD^+-dependent deacetylase, enhances the phosphorylation of LKB1 on Ser428 and Thr336 and hence AMPK activation in HEK293T cells (Lan *et al.,* 2008). Overexpression of SIRT1 in HepG2 cells and mouse liver can stimulate basal AMPK signalling through the phosphorylation and activation of LKB1 (Hou *et al*., 2008). The acetylation/deacetylation of LKB1 thus appears to regulate its kinase activity and subcellular localization.

1.3.4. LKB1 complex regulation and activation

The stability, subcellular localization and kinase activity of LKB1 are regulated by its association with several partners.

1.3.4.1. The LKB1-STRAD-MO25 complex

A yeast two-hybrid analysis has shown that LKB1 exists in mammalian cells in a complex with two proteins, called STE20-related adaptor (STRAD) and mouse protein 25 (MO25) (Baas *et al.*, 2003). The formation of the LKB1/STRAD/MO25 complex leads to the activation of LKB1 and its translocation from the nucleus to the cytoplasm (Alessi *et al*., 2006). The components of the LKB1:STRAD:MO25 complex isolated from mammalian and insect cells are found to have similar stoichiometry (1:1:1 ratio) (Baas *et al.*, 2003; Zeqiraj *et al.,* 2009). Two isoforms of STRAD (α and β) and MO25 (α and β) are recognized and found to interact with LKB1.

STRADα and STRADβ have high sequence homology to the STE20 protein kinase family and bind ATP. Ste (from "sterile") genes were discovered by genetic analysis of mating in the budding yeast *Saccharomyces cerevisiae*. Ste20 is the founding member of a kinase superfamily that is divided into two groups, the p21-activated kinases (PAKs) and the germinal center kinases (GCKs) (Hoffman *et al.,* 2004; Strange *et al.,* 2006). Ste20-type kinases play essential roles in signalling pathways that regulate fundamental cellular processes, including cell-cycle control, apoptosis, development, cell growth, and cell stress responses (Dan *et al*., 2001; Pan, 2010; Valeras, 2014; Yu *et al.,* 2015). However, these isoforms are considered pseudokinases due to the lack of several key catalytic residues essential for catalysis, hence rendering them inactive (Baas *et al.*, 2003). The kinase domain of LKB1 and its region spanning the amino acid residues 319 to 343 are crucial for its interaction with STRAD (Baas *et al*., 2003). Homozygous deletion of STRADα (LYK5) is coupled to the polyhydramnios, megalencephaly, symptomatic epilepsy (PMSE) syndrome which is a severe developmental and epileptic disorder in humans. Patients with PMSE suffer from severe mental retardation, gross movement disorders, craniofacial abnormalities and childhood mortality (Puffenberger *et al*., 2007; Veleva-Rotse *et al.,* 2014).

MO25, which was initially recognized as a gene expressed at the early cleavage phase of mouse embryogenesis (Miyamoto *et al.,* 1993, Nozaki *et al.,* 1996) also has two closely related isoforms in mammals, termed MO25α and MO25β (Boudeau *et al.,* 2003a; Filippi *et al.,* 2011). They are found to be extremely evolutionarily conserved (Karos & Fischer, 1999)**.** Structural analysis of MO25α has uncovered an extended α-helical repeat rod-like structure that is faintly related to the armadillo repeat domain. MO25α binds to the C-terminal Trp-Glu-Phe (WEF) motif of STRADα through a hydrophobic pocket in its C-terminal region and hence operates as a scaffold for the assembly of the heterotrimer. MO25 loses the ability to bind to STRAD if mutations occur in any of these three residues (Boudeau *et al.,* 2003a; Milburn *et al.,* 2004). This interaction can significantly enhance the binding of STRAD to LKB1 and increase STRAD-induced kinase activity of LKB1 nucleocytoplasmic transport of LKB1 (Boudeau *et al*., 2003b; Filippi *et al.,* 2011).

Zeqiraj *et al*. (2009) has analysed the structure of the STRADα pseudokinase and its interaction with MO25α. As previously described, STRADα interacts with MO25α through its WEF motif but can also interact extensively with the highly conserved concave surface of MO25α. STRADα, although catalytically inactive, can assume a closed active-

like conformation, with an ordered activation loop akin to active protein kinases. This active-like conformation is stabilized when bound to ATP and/or MO25α. The study showed that STRADα mutants that cannot interact with both ATP and MO25α are unable to activate LKB1, while STRADα mutants that can still bind either ATP or MO25α are able to activate LKB1. Hence, the activation of the tumour suppressor LKB1 by STRADα is rather triggered by the closed active-like conformation of STRADα and not the catalytic phosphoryltransferase activity. Figure 1.5 presents a model of the interaction of STRADα/MO25α with LKB1 based on known mutagenesis and structural data (Zeqiraj *et al.,* 2009).

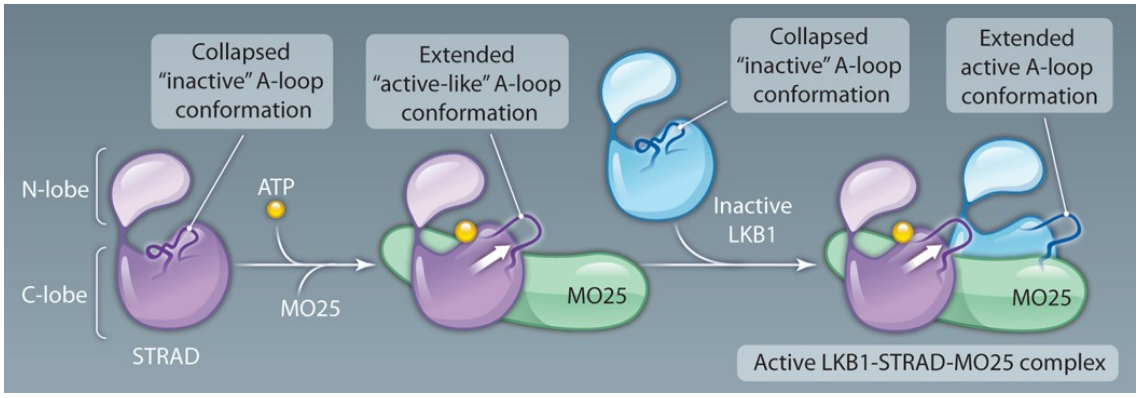

Figure 1.5. The kinase domain of LKB1 is allosterically activated by STRAD.
It is presumed that the kinase domain of STRAD is maintained in an inactive conformation in its inaccessible state. When STRAD binds to ATP and MO25, its kinase domain shifts to an active-like kinase conformation which is characterized by the extended conformation of its A-loop. This active-like conformation permits STRAD to bind LKB1 as a pseudosubstrate. The allostearic binding of STRAD prompts the kinase domain of LKB1 to assume an active kinase conformation, which is further stabilized by the binding of MO25 to the A-loop of LKB1 and positioning the loop in an extended conformation. (Adapted from Rajakulendran & Sicheri, 2010; with permission).

1.3.4.2. Regulation of the subcellular localisation of LKB1

The localization of LKB1 in the cytoplasm has been shown to be essential for its activity. In PJS patients, LKB1 mutants are found to localize solely in the nucleus, to lack catalytic activity and thus to be incapable of suppressing cell growth (Boudeau *et al*., 2003b). However, LKB1 mutants which lack the nuclear localization signal (NLS) situated in the

N-terminal non-catalytic region (residues 38–43) are still able to inhibit cell growth (Tiainen *et al.,* 2002).

LKB1 does not have a nuclear export domain of its own and thus in the absence of metabolic stress (low glucose, low oxygen) remains in the nucleus. The LKB1 protein, once synthesised, is imported to the nucleus by importins α and β (Dorfman & Macara, 2008). LKB1 can then only translocate from the nucleus to the cytoplasm when in a complex with STRADα, which binds to the nuclear export proteins CRM1 and exportin-7. The heterotrimeric complex is stabilised by MO25 (van Veelen *et al.,* 2011) (Figure 1.6). STRADβ on the other hand, lacks the binding sites for exportin-7 and CRM1 and thus cannot translocate LKB1 to the cytoplasm (Dorfman & Macara, 2008). When LKB1 is coexpressed with STRADα, the majority of LKB1 is transported to the cytoplasm, but a substantial amount remains nuclear. However, when LKB1 is coexpressed with STRADα and MO25 in a heterotrimeric complex, LKB1 fully localizes to the cytoplasm (Alessi *et al.,* 2006; Korsse *et al.*, 2013). Thus, the formation of LKB1-STRADα-MO25 complex is essential for LKB1 localization. The phosphorylation of LKB1 on several residues can also regulate its subcellular localization. LKB1 phosphorylation on Ser428 and Ser307 by PKC-ζ23 appears to be essential for the nucleocytoplasmic export of LKB1 and the subsequent AMPK activation. The LKB1 S307A mutant (Ser307 to Ala) displays a diminished interaction with STRADα and fails to associate with CRM1 (Xie *et al*., 2009).

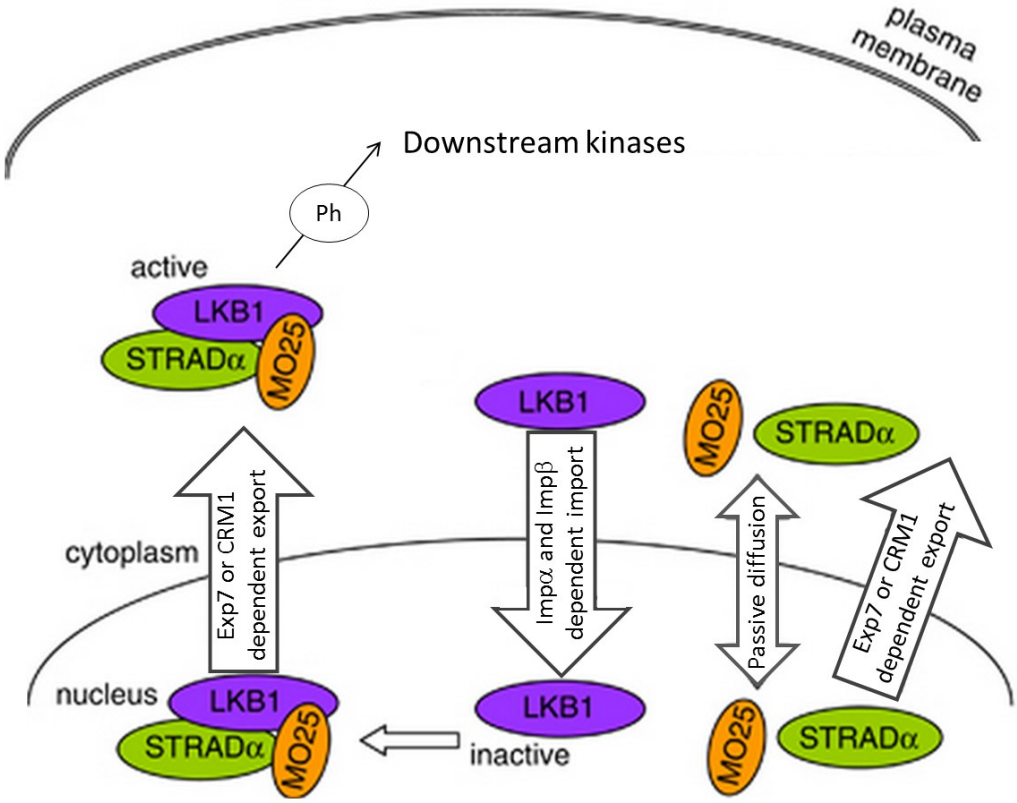

Figure 1.6. The activation and translocation of LKB1.
The activation of LKB1 occurs when it is translocated from the nucleus to the cytoplasm. Usually, LKB1 is found in the nucleus in an inactive state. Upon activation, LKB1 is bound by STE20-related adaptor protein α (STRADα) and mouse protein 25 (MO25), which are actively imported into the nucleus by importins α/β (Impα, Impβ) or enter by passive diffusion. The stable LKB1/STRADα/MO25 complex is actively translocated by exportin-7 and CRM1 out of the nucleus and into the cytoplasm, in which LKB1 exerts its serine/threonine kinase activity by phosphorylating and activating downstream kinases. (Adapted from van Veelen *et al.*, 2011; with permission).

Using the yeast two-hybrid system to screen for LKB1-interacting proteins resulted in the identification of the cytoplasmic scaffolding protein LIP1 (LKB1-interacting protein 1). LIP1 is a leucine-rich repeat containing protein and its overexpression with LKB1 leads to a considerable increase in the levels of LKB1 in the cytoplasm (Smith *et al*., 2001; Gan & Li, 2014). A study has showed that LKB1 interaction with LIP1 negatively regulated TGFβ signaling (Morén *et al* 2011).

Lastly, a study has also revealed that LKB1 can bind to and be sequestered by the orphan nuclear receptor Nur77 in the nucleus. This leads to a decrease in the activation of LKB1 cytoplasmic downstream targets. LKB1 can be released if the chemical compound ethyl

2-[2,3,4-trimethoxy-6-(1- octanoyl)phenyl]acetate (TMPA) interacts with Nur77 with high affinity leading to the release and transportation of LKB1 to the cytoplasm, thus antagonizing the Nur77 function (Zhan *et al*., 2012).

1.3.5. LKB1 regulates downstream kinases

LKB1 is a ubiquitously expressed serine/threonine kinase which is known to phosphorylate 14 protein kinases of the AMPK family (ARKs or AMPK Related Kinases), and hence is termed a "master kinase" (Lizcano *et al.,* 2004; Kullmann & Krahn, 2018) (Figure 1.7). The phosphorylation and subsequent activation of the ARKs occurs at their T-loop threonine residue (Lizcano *et al.,* 2004). The best characterized substrate of LKB1 is the AMP-activated protein kinase (AMPK), an intracellular energy sensor. AMPK is a serine/threonine kinase activated by metabolic stress resulting in the depletion of ATP (adenosine triphosphate) and subsequent increase of AMP (adenosine monophosphate): ATP and ADP (adenosine diphosphate) ratios (Ross *et al.,* 2016; Carling, 2017). In response to an increasing AMP/ATP ratio and to restore normal ATP levels, LKB1, when bound to MO25 and STRAD, has been shown to phosphorylate AMPK at Thr172 and consequently, phosphorylated AMPK stimulates catabolic processes such as fatty acid oxidation and switches off anabolism and other ATP-consuming processes such as lipid and protein synthesis.

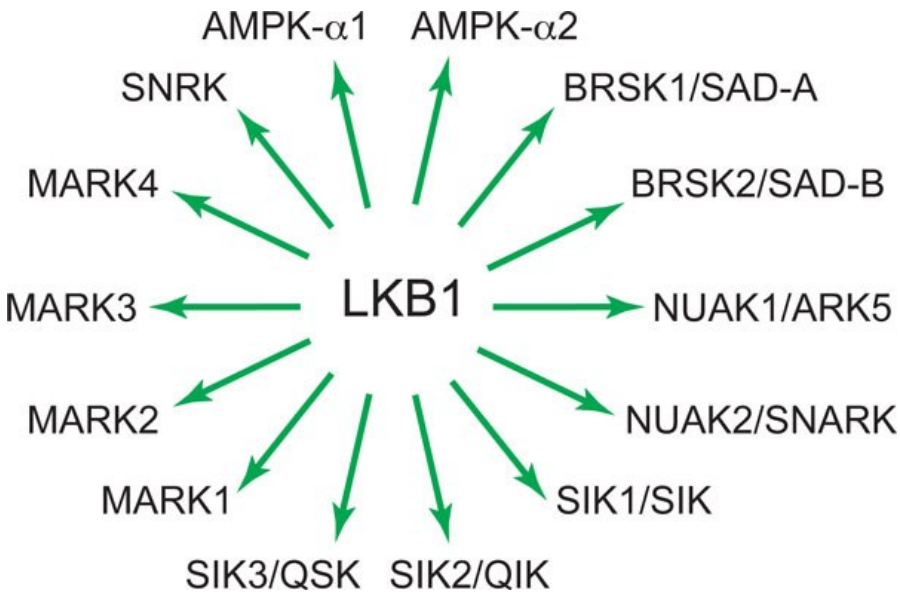

Figure 1.7. Members of the AMPK and AMPK-related kinase (ARK) family.
LKB1 phosphorylates and activates 14 members of the AMPK-related kinase (ARK) family. However, only the mechanisms regulating the phosphorylation of AMPK is known. Alternative names are shown, where applicable. AMP-activated kinase (AMPK), NUAK family SNF1-like kinase 1 (NUAK1), sucrose non-fermenting protein-related kinase (SNRK), brain selective kinase (BRSK), synapses ofamphids-deficient kinase (SAD), Salt-inducible kinase (SIK1), microtubule affinity regulating kinase (MARK). (This figure is adapted from Hardie & Alessi; 2013)[1].

The AMPK-related kinases, other than AMPK, are not regulated by energy stress and AMP:ATP ratios. The role of LKB1 in the regulation of these other ARKs downstream still require further research; however, LKB1 has been found to have an optimal substrate motif for its phosphorylation containing the T-loop phosphorylated threonine residue (Figure 1.8). The implication of this phosphorylation in cell proliferation (NUAKs) and CREB-regulated gene transcription (SIKs) as well as polarity regulation (MARK, BRSK/SAD) has been reported (Gan & Li, 2014; Hardie & Alessi, 2013). Some of these functions are presented in Table 1.1.

	Peptide
NUAK2	LSNLYHQGKFLQ**T**FCGSPLYRRR
SIK	FGNFYKSGEPLS**T**WCGSPPYRRR
AMPK	LSNMMSDGEFLR**T**SCGSPNYRRR
BRSK2	MASLQVGDSLLE**T**SCGSPHYRRR
MARK3	FSNEFTVGGKLD**T**FCGSPPYRRR

Figure 1.8. Optimal substrate motif for LKB1 phosphorylation in ARKs.
Kinetic analysis of the phosphorylation of the indicated T- loop by the LKB1:STRAD:MO25 complex was completed. The T- loop Thr residue in each peptide is depicted in red and is in boldface type. At the C- terminus of each T- loop peptide, three Arg residues were added to enable their capture on phosphocellulose p81 paper (Lizcano *et al*., 2004).

ARKs	Name	LKB1 target residue in human proteins	Role downstream of LKB1	References
AMPK	AMPK-activated protein kinase	Thr172	-Epithelial cell polarity -Lipid homeostasis -Cell growth/survival -Cell migration	See text for details and references
BRSK1/SAD-A	Brain-specific kinase	Thr189	Neuronal polarisation	(Barnes *et al.,* 2007; Kishi *et al.,* 2005)
BRSK2/SAD-B		Thr174		
MARK1/PAR-1c	MAP/microtubule affinity-regulating kinase	Thr215	-Epithelial cell polarity -Microtubule dynamics -Cancer cell migration (inhibition)	(Drewes *et al.,* 1998; Chen *et al.,* 2006; Martin-Belmonte & Perez-Moreno, 2012; Goodwin *et al.,* 2014)
MARK2/PAR-1b		Thr208		
MARK3/PAR-1a		Thr211		
MARK4		?		
NUAK1/ARK5	AMPK-related kinase 5	Thr211	-Axon branching -Cell adhesion -Proliferation -Actin cytoskeleton	(Courchet *et al.,* 2013; Hou *et al.,* 2011; Humbert *et al.,* 2010)
NUAK2/SNARK	SNF/ AMPK-related kinase	Thr208		
SIK1/SIK	Salt-induced kinase	Thr182	-p53-dpendent anoikis (SIK1) -Maintenance of epithelial junctions stability (SIK1) -Cancer cell migration (inhibition) (SIK1) -HTLV1 transcription -Gluconeogenesis	(Cheng *et al.,* 2009; Eneling *et al.,* 2012; Patel *et al.,* 2014; Tang *et al.,* 2013)
SIK1/QIK		Thr175		
SIK1/QSK		Thr163		
SNRK	SNF-related serine/threonine kinase	Thr173	?	

Table 1.1. The role of the ARKs downstream of LKB1.
The phosphorylation sites were based on information attained from UniProt (www.uniprot.org). The following terms Anoikis and HTLV-1 mean respectively a form of programmed cell death that is induced by anchorage-dependent cells detaching from the surrounding extracellular matrix (ECM); and Human T-cell Leukaemia Virus Type 1.

1.4. AMPK: structure and regulation by upstream kinases

The AMP-activated protein kinase (AMPK) is a highly conserved serine/threonine protein kinase, which acts as a sensor of cellular energy status in most eukaryotic organisms. The AMPK complex is activated in mammals due to elevation in AMP: ATP or ADP: ATP ratios resulting from the impairment of the cellular energy status. Activation occurs as a result of metabolic stresses that either speed ATP consumption or interfere with ATP production, in which AMPK functions to maintain energy homeostasis by impeding ATP-requiring processes such as the synthesis of fatty acids, cholesterol and proteins whilst stimulating other catabolic processes generating ATP such as fatty acid oxidation, glycolysis and autophagy (Hardie *et al,* 2012; Ross *et al.,* 2016; Carling, 2017).

AMPK is expressed as a heterotrimeric complex comprised of a catalytic α subunit and regulatory β and Y subunits. Orthologs of genes encoding AMPK-α, -β and -γ subunits are found in almost all eukaryotes where genome sequences have been completed. In mammalian cells, there are two isoforms of the α subunit (α1 and α2), two isoforms of the β subunit (β1 and β2) and three isoforms of the Y subunit (γ1, γ2 and γ3). Theoretically, 12 heterotrimeric AMPKαβγ combinations can occur when these subunits are coexpressed in cells (Hardie *et al*, 2011; Sanli *et al.,* 2014, Ross *et al.,* 2016).

Each of these three subunits performs a particular role in the stability and activity of AMPK. The γ subunit comprises of four Cystathionine beta synthase (CBS) domains which enables AMPK to sense shifts in the AMP:ATP ratio. These four CBS domains form two binding sites for AMP known as Bateman domains (Bateman, 1997; Xiao *et al.,* 2007; Sanli *et al.,* 2014). The binding of an AMP to a Bateman domain results in an increased binding affinity of the second AMP to the other Bateman domain (Adam *et al,* 2004). This subsequently results in a conformational change in the γ subunit which exposes the catalytic domain located on the α subunit. Activation of AMPK occurs in this catalytic domain when phosphorylation takes place at threonine-172 (named due to its position in the rat α2-subunit sequence) by an upstream AMPK kinase (AMPKK) (Hawley *et al*, 1996; Carling, 2017) (Figure 1.9). AMPK activation by the upstream kinases is induced by increased levels of AMP and inhibited by high concentrations of ATP (Hawley *et al.*, 1996).

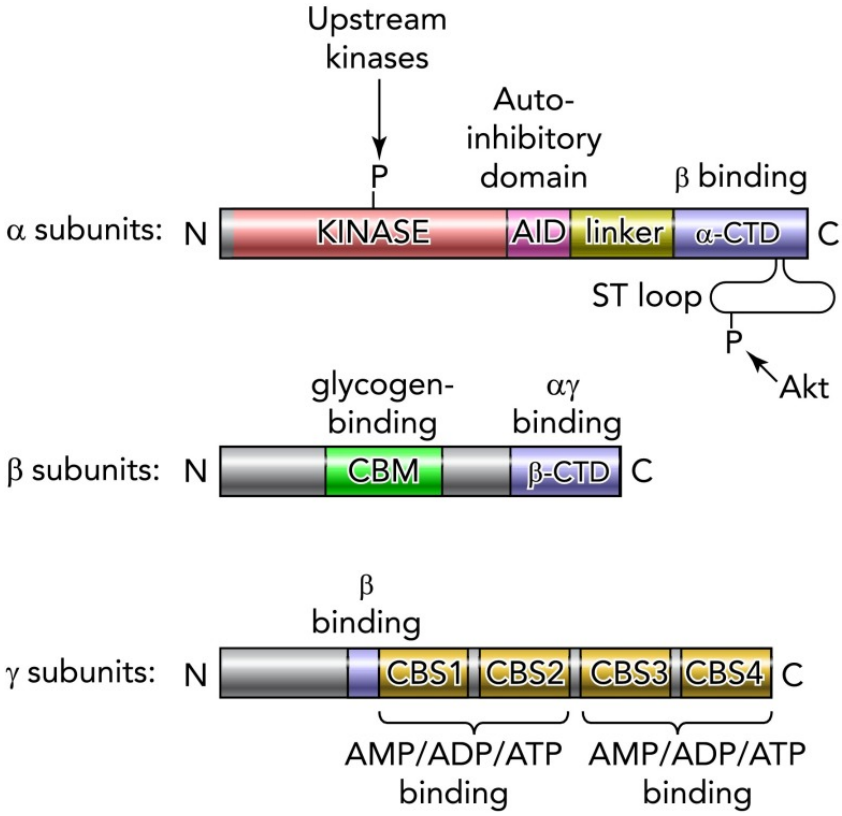

Figure 1.9. Domain structure of eukaryotic AMPK orthologs.
The catalytic α-subunits are comprised of serine/threonine kinase domains containing the threonine residue (Thr172 in rat α2) phosphorylated by upstream kinases. Following the kinase domains are usually auto-inhibitory domains (small domains with a negative effect on kinase activity), which are joined to the COOH-terminal domains (α-CTD) by a less well conserved linker. In vertebrates, there is also a flexible serine-/threonine-rich loop (ST loop) within the α-CTD that is phosphorylated by Akt. The β-subunits hold two conserved regions, a carbohydrate-binding module (CBM) that instigates the binding of mammalian complex to glycogen particles, and a COOH-terminal domain (β-CTD) that provides the connection between the α- and γ-subunits. The γ-subunits are comprised of variable NH2-terminal regions followed by a short sequence involved in binding to the β-subunit, then four tandem repeats of a cystathionine-β-synthase (CBS) motif. The CBS motifs operate in pairs to create the binding sites for adenine nucleotides; in mammalian AMPK, there is one site formed between CBS1 and CBS2 and two between CBS3 and CBS4. (Figure modified from Hardie *et al.,* 2011; with permission).

Hence, AMPKγ binding to nucleotides regulates the enzyme's activity. During energy stress, ADP and AMP levels increase in comparison to ATP levels and function as a cellular read-out of energy exhaustion. This results in an increase of AMPK activity via a conformational change, which exposes and phosphorylates the α subunit Thr-172 as well as prevents the dephosphorylation of Thr-172 by phosphatases via making AMPK complex a less efficient substrate for protein phosphatases (Riek *et al.*, 2008; Xiao *et al*., 2011, Gu *et al.,* 2017).

1.4.1. The heterotrimeric complex of AMPK

1.4.1.1. The catalytic α subunit

The alpha subunit is the catalytic subunit and consists of an N terminal serine/threonine kinase domain (KD), a regulatory domain containing an auto-inhibitory sequence (AIS) that has been revealed to inhibit kinase activity (Pang *et al*., 2007; Chen *et al*., 2009), and an interacting motif on its C-terminus that binds to the β subunit (Hardie & Hawli, 2001). The kinase domain exhibits a canonical fold with 11 subdomains and contains the activation loop (also called T-loop) (Hanks & Hunter, 1995; Oakhill *et al.,* 2010).

Full kinase activity in mammalian cells occurs when a conserved threonine residue 172 is phosphorylated within the activation loop. This threonine residue is conserved in the α subunit sequences of AMPK orthologues within all eukaryotes, and studies revealed that mutations of the corresponding threonine residue result in a complete loss of function *in vivo*, as exemplified in the yeast α subunit (Snf1p) (Estruch *et al.,* 1992). The α-Thr172 phosphorylation leads to a further two- to fivefold allosteric activation caused by AMP, which maintains the active form of the enzyme by inhibiting α-Thr172 dephosphorylation by protein phosphatases PP2c or PP2a (Xiao *et al,* 2011; Gu *et al*., 2017).

Both isoforms of the α subunit, α1 and α2, have a short putative nuclear localization sequence toward the C-terminus of the kinase domain (KKIC in α1 and KKIR in α2) (Suzuki *et al.,* 2007) as well as a well-defined and functional nuclear export sequence at the C-terminus (Kazgan *et al,* 2010). This indicates that α1 and α2 complexes are likely to shuttle in and out of the nucleus.

Following the kinase domain (KD) of AMPK is the regulatory domain containing the autoinhibitory sequence (AIS). This domain is also known as the autoinhibitory domain (AID) and interferes with kinase substrate binding and catalytic function (Crute *et al.*, 1998; Li *et al*., 2015). The AID consists of three α helices that interact with the lobes of the KD and constrain the kinase domain in a less active "open" conformation (Pang *et al.*, 2007). In mammals the AID domain is unstructured yet mutations in the KD:AID interface increased the basal activity of AMPK in the absence of AMP (Chen *et al.,*2009). Mutational studies showed that expression of truncated α subunits comprising of the kinase domain alone had full activity; whereas expression of alpha subunits containing

both the KD and AID had extremely low activity regardless of the phosphorylation state of the conserved threonine residue (Chen *et al.,* 2009).

The C-terminal region of the α subunit (α-CTD) is important for the formation of the heterotrimeric complex. It interacts with the C-terminal domain of the β subunit (Hudson *et al.,* 2003; Xiao *et al,* 2011) and connects to the γ subunit through a linker peptide of extended conformation (Xiao *et al,* 2011; Li *et al.,* 2015). This α-linker wraps around the γ subunit, appearing as two arms stretching out from the KD/AID and the α-CTD that hold the γ subunit in a tight embrace. This "α hook" region interacts with the γ-subunit when AMP is bound, resulting in a configuration change of the complex and promoting activation of the catalytic domain (Xiao *et al,* 2011; Li *et al.,* 2015).

1.4.1.2. The γ subunit

The function of the γ regulatory subunit is to regulate the activity of the α-catalytic subunit (Carling *et al*., 2012). This occurs through binding of adenylates to the cystathionine-β-synthase (CBS) domains (Bateman, 1997). The γ1, γ2 and γ3 isoforms, encoded by *PRKAG1, PRKAG2* and *PRKAG3,* respectively, in humans, are comprised of four tandem repeats known as cystathionine β synthase (CBS) repeats. These repeats occur as two pairs of domains termed Bateman domains (Bateman, 1997), which are assembled in a pseudosymmetrical manner revealing four clefts for AMP, ADP and ATP binding. These clefts are numbered 1-4 (Hardie *et al,* 2013) with three of these sites binding adenine nucleotides, while one site (site 2) is never occupied (Kemp *et al.,* 2007, Calabrese *et al.,* 2014). Moreover, site 4 is associated only with AMP very tightly and does not exchange AMP with ADP or ATP. Binding at this site may have a structural role, while the other two sites (sites 1 and 3) are sensors of cellular energy in which they competitively bind AMP, ADP, and ATP (Hardie, 2014).

1.4.1.3. The β subunit

The β subunit is a scaffolding subunit containing C-terminal domains that form the conserved core of the αβγ complex and links the C-terminal domain of the α subunit to the N-terminal region of the γ subunit to form the functional AMPK heterotrimeric

complex (Amodeo *et al,* 2007; Townley & Shapiro, 2007). The C-terminal domain of the β subunit (β-CTD) binds to the α-CTD exposing a short sequence that interacts with the γ subunit through an intersubunit β sheet (Townley & Shapiro, 2007; Xiao *et al,* 2011). Both isoforms of β subunits are exposed to myristoylation at their N termini; this allows AMP and ADP binding to enhance phosphorylation of Thr-172 (Oakhill *et al.*, 2010; Garcia & Shaw, 2017).

β-subunits also contain carbohydrate-binding modules (CBMs; previously known as glycogen-binding domains (GBD)) that appear to regulate the activity of the kinase (Polekhina *et al,* 2003). CBMs are often linked to the catalytic domains of proteins engaged in the metabolism of starch and glycogen and result in the colocalization of the catalytic domain with their polysaccharide substrates (Machovic & Janecek, 2006). The glycogen-binding domain binds favourably to glycogen with a single glucose α1–6 branch (Koay *et al*., 2007), which prevents AMPK activation by upstream kinases (McBride *et al.,* 2009; Li *et al.,* 2015).

In AMPK, Ser108, within the CBM of the β1 subunit, was found to be critical for activation by mediating the allosteric activation and inhibition of Thr-172 dephosphorylation (Li *et al.,* 2015). These effects were triggered by direct activators such as A769662, a thienopyridone compound which mimics effects of AMP on the AMPK system via an AMP-independent mechanism (Goransson *et al.*, 2007; Sanders *et al.,* 2007). Activation by A769662 entails an interaction between the β subunit CBM and the γ subunit residues that are not involved in AMP binding (Scott *et al.,* 2014). Unexpectedly, A769662 exclusively activates AMPK complexes containing the β1 subunit isoform. Intriguingly, this residue is not conserved in the β2 subunit, which is the predominant isoform expressed within the cells (Steinberg *et al.*, 2010; Scott *et al.,* 2014).

1.4.2. AMPK regulation by upstream kinases

AMPK is phosphorylated by LKB1 on Thr172 within the activation loop of its kinase domain (*Hawley et al.,* 2003; Shaw *et al.*, 2004). AMPK phosphorylation of Thr172 is promoted when ADP and/or AMP binds to its γ subunit initiating an allosteric activation which in turn inhibits AMPK dephosphorylation. This activation is more evident when AMP levels are exceedingly high in response to severe stress (Gan & Li, 2014; Hardie &

Alessi, 2013). Interestingly, LKB1 deficiency in murine embryonic fibroblasts (MEFs) led to an almost complete loss of Thr172 phosphorylation and downstream AMPK signalling in response to different AMPK activators (Ma *et al.,* 2012). In LKB1 deficient cells, such as HeLa cells, AMPK is not activated in response to an increase in AMP/ATP ratio (Hawley *et al*., 2003). This finding indicates that the activation of AMPK in response to increased AMP is dependent on the presence of LKB1. The deletion of LKB1 in certain tissues has been investigated in various animal models. In the heart, deletion of LKB1 has led to a substantial reduction in AMPK α2 activity in response to ischaemia (Sakamato *et al.,* 2006; Salt & Hardie, 2017). Similarly, deletion of LKB1 in skeletal muscle tissues has resulted in a decrease in the activity of AMPK α2 in response to contraction, phenformin (a close relative of the antidiabetic drug, metformin) or 5 amino-4-imidazolecarboxamide riboside (Sakamato *et al.,* 2005). Also, a study has reported that deletion of LKB1 in adult liver caused a considerable decrease in AMPK kinase activity (Shaw *et al*., 2005, Jiang *et al.,* 2015). These findings reinforce the role of LKB1 as the predominant upstream kinase of AMPK in almost every tissue investigated.

While genetic loss of LKB1 in mammalian cells leads to a significant decrease in AMPK phosphorylation on Thr172, a residual phosphorylation remains, implying that other kinases must also phosphorylate this site (Shaw *et al.*, 2004). In fact, AMPK is also activated by CaMKKβ (Ca2+/calmodulin-dependant protein kinase kinase β) and TAK1 (Transforming growth factor beta-activated kinase 1) (Hardie *et al.,* 2012).

AMPK can be activated by an alternative mechanism independent of AMP binding, which involves the phosphorylation of Thr-172 by the upstream kinase CaMKKβ as a result of an increase in the intracellular Ca^{2+} levels (Woods *et al.,* 2005). This normally occurs due to neuronal depolarization (Hawley *et al.,* 2005), stimulation of the antigen receptor in T lymphocytes (Tamas *et al.,* 2006) and Ca^{2+} release due to the activation of phosphatidylinositol-specific phospholipases coupled receptors (Stahmann *et al.,* 2006; Yang *et al.,* 2011). This mechanism can occur independently of AMP, although it can also synergise with the AMP/ADP mechanism (Fogarty *et al.,* 2010). In mouse muscles, after 2 minutes of contraction, AMPK phosphorylation was strongly hindered by CaMKK inhibitors (Corton *et al.*, 1994; Jensen *et al.,* 2007). Intriguingly, none of the ARKs are phosphorylated by CaMKKβ, despite the sequence similarities within the activation loops of AMPK and the ARKs (Fogarty *et al.,* 2010).

TGF-β-activated kinase-1 (TAK1), a member of the mitogen activated protein kinase kinase family, has also been identified as a potential upstream kinase for AMPK (Momcilovic *et al.,* 2006). Several studies support the function of TAK1 as an AMPK upstream kinase, especially under conditions that generate reactive oxygen species and redox imbalance (Xie *et al.,* 2006; Chen *et al.,* 2013; Zippel *et al.,* 2013). The tumour necrosis factor-related apoptosis-inducing ligand (TRAIL) prompts apoptosis in cancer cells while sparing normal cells, and TRAIL receptor agonists are potential anticancer drugs. In this context, a noteworthy study revealed that RNAi -mediated knockdown of TAK1 abolished TRAIL-induced AMPK activation. The TRAIL-induced TAK1–AMPK signalling pathway instigates cytoprotective autophagy to shield normal epithelial cells from TRAIL-induced cell death. However, in MCF10A cells, LKB1 and CaMKKβ depletion had no effect on either TRAIL- induced AMPK activation or autophagy (Herrero-Martín *et al*., 2009). Thus, the physiological role of TAK1 in the activation of AMPK is ambiguous and additional studies are essential to clarify the function of TAK1 in the regulation AMPK *in vivo*.

Finally, phosphorylation of AMPK at Ser485 of the α1 subunit by Akt, protein kinase A (PKA) as well as its autophosphorylation in various cell types and tissues, such as the vascular smooth muscle cells, heart and adipocytes, result in a decrease in AMPK activity (Coughlan *et al.,* 2014).

The different regulators of AMPK are presented in Figure 1.10.

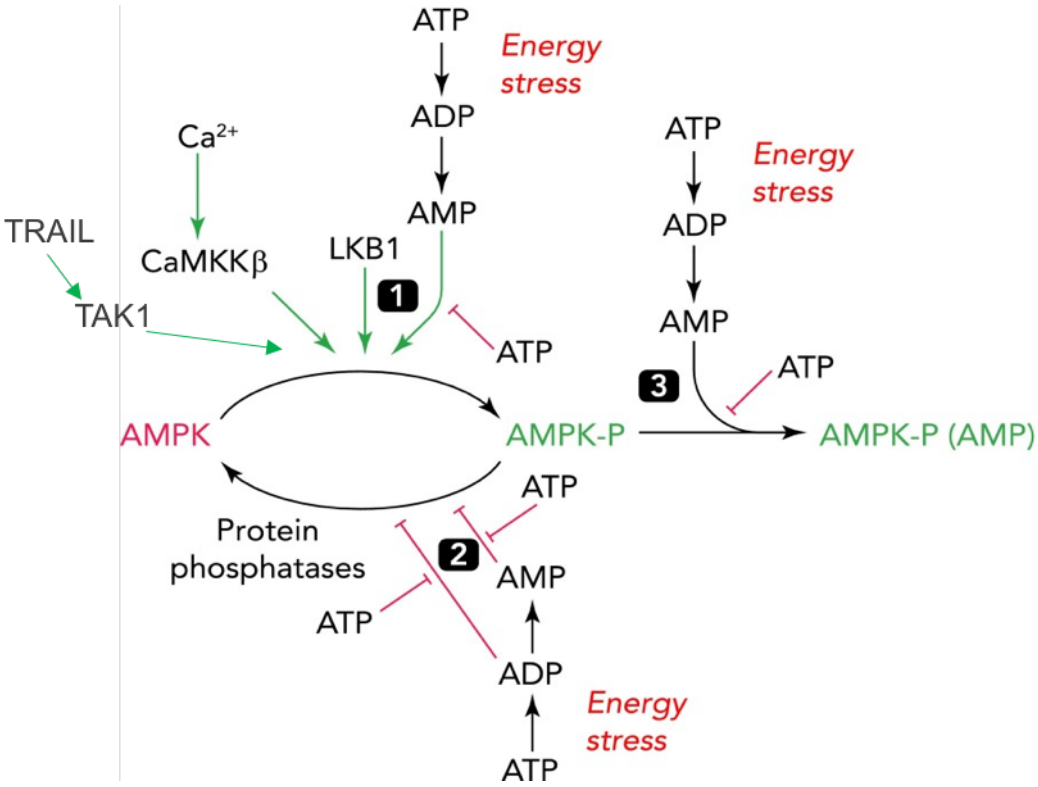

Figure 1.10. Regulation of mammalian AMPK by adenine nucleotides and Ca2+.

Activation of AMPK can occur due to increases in cellular AMP:ATP or ADP:ATP ratio, or Ca^{2+} concentration. AMPK activation is dependent on its conversion from a dephosphorylated form (AMPK) to a form phosphorylated at Thr172 (AMPK-P) catalyzed by at three upstream kinases. The main upstream kinase is LKB1, which seems to be constitutively active; the other two kinases are CaMKKβ, which is activated only when there is an increase in intracellular Ca^{2+}, and TAK1, which is activated by TRAIL. Increases in AMP or ADP activate AMPK by three mechanisms: (1) binding of AMP or ADP to AMPK, causing a conformational change that promotes phosphorylation by upstream kinases (usually this will be LKB1, unless [Ca^{2+}] is elevated); (2) binding of AMP or ADP, resulting in a conformational change that prevents Thr172 dephosphorylation by protein phosphatases; (3) binding of AMP (and not ADP), initiating an allosteric activation of AMPK-P. All three effects are antagonized by ATP, allowing AMPK to act as an energy sensor. (This figure is modified from Hardie & Alessi,2013)[2].

[2] This article (Hardie & Alessi, 2013) is published under license to BioMed Central Ltd. This is an Open Access article distributed under the terms of the Creative Commons Attribution License (http://creativecommons.org/licenses/by/2.0), which permits unrestricted use, distribution, and reproduction in any medium, provided the original work is properly cited.

1.4.3. Activation of AMPK by drugs

In addition to being activated by upstream kinases and low ATP levels, AMPK can also be regulated (activated or inactivated) by a range of pharmacological drugs, hormones (Leptin, adiponectin, interleukin-6) or natural compounds (resveratrol, rooibos, berberine, α-lipoic acid) (Coughlan *et al*., 2014). These drugs can activate AMPK either directly or indirectly. Most activate AMPK indirectly by inhibiting ATP production through the inhibition of oxidative phosphorylation (phenformin) (Owen *et al*., 2000) or glycolysis (2-deoxyglucose) (Hawley *et al.,* 2010), hence increasing cellular AMP:ATP and ADP:ATP ratios. Drugs inhibiting oxidative phosphorylation can be those acting as mitochondrial poisons such as oligomycin and dinitrophenol (Hawley *et al.,* 2010), drugs used in the treatment of type 2 diabetes as phenformin (Owen *et al.,* 2000), rosiglitazone (Fryer *et al*., 2002), phenobarbital (Rencurel *et al*., 2005), and several plant products considered to have health-promoting properties like berberine (Turner *et al.*, 2008), curcumin (Lim *et al.,* 2009) or resveratrol (Baur *et al*., 2006). It has been suggested that metformin, the first-choice drug for treatment of type 2 diabetes, directly interacts with AMPKγ (Zhang *et al.*, 2012). However, the consensus now is that metformin acts on AMPK primarily by inhibiting Complex I, but also has additional AMPK-independent actions (Rena *et al.,* 2017). There are also chemicals that indirectly stimulate the activation of AMPK by interacting with upstream components of the AMPK pathway. These chemicals include Ca^{2+} ionophore A23187 and other Ca^{2+} ionophores, that increase intracellular Ca2+ concentration and in turn activate CaMKKβ and hence AMPK (Hawley *et al.,* 2005; 2010).

AMPK can also be activated through direct interaction. Direct activation occurs when drugs directly bind to AMPK leading to its allosteric activation, promoting phosphorylation of Thr172 and/or inhibiting dephosphorylation of Thr172. Compound A-769662 and salicylate activate AMPK through a mechanism involving an interaction between the β subunit CBM and the γ subunit residues. This interaction leads to an allosteric activation of AMPK and protects it from T172 dephosphorylation (Scott *et al.,* 2008; Hawley *et al.,* 2012). Finally, a commonly used AMPK activator is 5–aminoimidazole-4-carboxamide riboside (AICAR), an analog of adenosine that is phosphorylated by adenosine kinase to ZMP, a riboside that has a similar effect to AMP

on the AMPK complex (Corton *et al.,* 1995). It activates AMPK by binding to the γ-subunit in a similar manner to AMP (Day *et al.*, 2007).

1.4.3.1. AICAR (5- aminoimidazole-4-carboxamide riboside)

The first molecule reported to activate AMPK in intact cells and *in vivo* was AICAR (5-aminoimidazole-4-carboxamide riboside) (Corton *et al*., 1995; Sullivan *et al*., 1994). AICAR entry to the cell is mediated by adenosine transporters and then it is converted by adenosine kinase to the monophosphorylated derivative ZMP. ZMP simulates the effect of AMP by binding to the γ subunit, which in turn prompts the allosteric activation of the kinase while inhibiting its dephosphorylation (Corton *et al*., 1995; Gadalla *et al*., 2004; Hardie *et al.,* 2012). AICAR administration in mouse and rat models with metabolic defects has been shown to increase glucose tolerance, decrease free fatty acid and plasma triglyceride levels, reduce hepatic glucose output and elevate whole-body glucose disposal (Fogarty & Hardie, 2010). AICAR administration in normal mice has also been shown to be beneficial by prompting the induction of genes linked to oxidative metabolism and in boosting running endurance (Narkar *et al*., 2008).

Nonetheless, AICAR can also exhibit AMPK-independent effects by mimicking other actions of AMP in which ZMP interacts with other AMP-regulated enzymes. These effects include AICAR inhibition of the gluconeogenic enzyme fructose-1,6-bisphosphatase (FBPase) and stimulation of the muscle isoform of glycogen phosphorylase. These specificity issues, as well as the poor bioavailability and short half-life, cause AICAR and related adenosine analogues to be unpromising compounds for drug development (Coughlan *et al*., 2014; Fogarty & Hardie, 2010).

1.5. AMPK functions downstream of LKB1

AMPK performs a vital role in the regulation of cellular energy metabolism, but it is also involved in the regulation of transcription, cell growth, autophagy and polarity (Figure 1.11) (Mihaylova & Shaw, 2011; Mirouse & Billaud, 2011; Sanli *et al.,* 2014). The acute functions of AMPK take place through direct phosphorylation of downstream AMPK

targets but can also occur as a long-term effect mediated by phosphorylation of transcription factors and coactivators. In the following section, we will focus on some downstream effectors of AMPK and LKB1/AMPK-regulated processes.

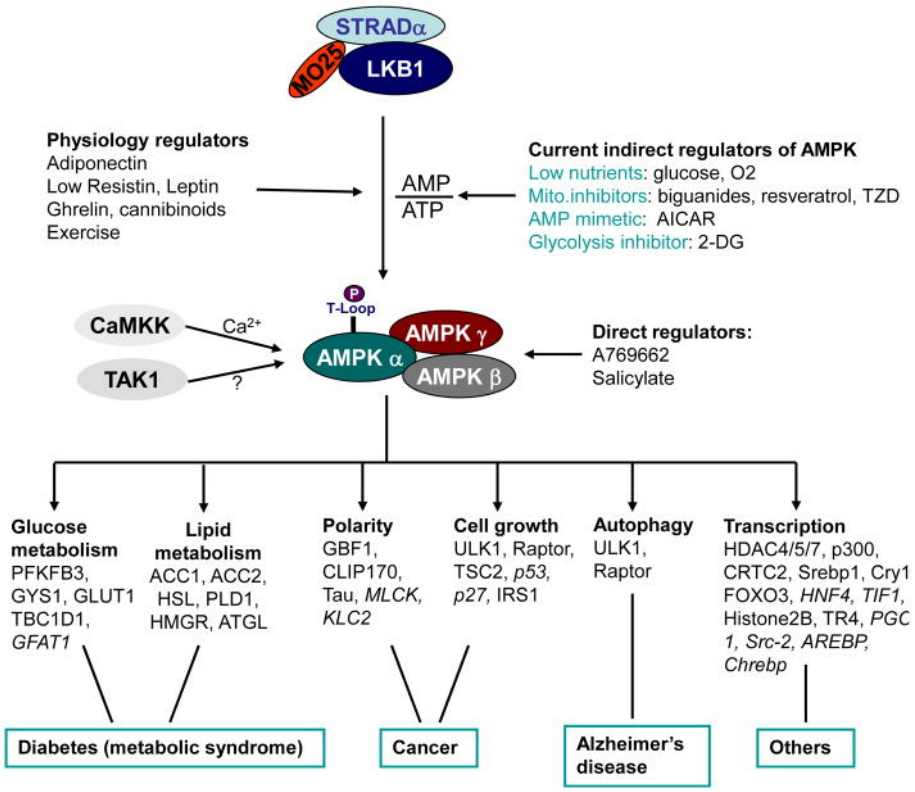

Figure 1.11. Agonists regulate LKB1-AMPK signalling and its functions.
The LKB1-AMPK pathway is involved in the regulation of various cellular processes such as glucose and lipid metabolism, and it also plays a vital role in the regulation of transcription, cell growth, autophagy and polarity. Permission has been granted by the authors to reuse this figure (http://www.ncbi.nlm.nih.gov/pmc/articles/PMC3899349/figure/F1/).

1.5.1. LKB1-AMPK regulates lipid homeostasis

The role of AMPK was originally linked to the regulation of lipid metabolism via the inactivation of HMGR (3-hydroxy-3-methylglutaryl (HMG)-CoA reductase) and ACC (acetyl-CoA carboxylase), which are fundamental regulatory enzymes in the synthesis of cholesterol and fatty acid respectively (Beg *et al*., 1973; Carlson & Kim, 1973). HMGR is attached to the endoplasmic reticulum membrane and controls the mevalonate pathway, a metabolic pathway responsible for the production of cholesterol and other isoprenoid

lipids. Ensuing a reduction in cellular ATP levels, HMGR can be directly phosphorylated and inhibited by AMPK, but can also indirectly be negatively affected by AMPK through the latter's phosphorylation and degradation of FoxO1a (forkhead transcription factor 1a) (Fisslthaler & Fleming, 2009).

Additionally, the activation of AMPK impedes the synthesis of fatty acid in liver and adipose cells and stimulates the oxidation of fatty acid in heart and muscle cells (Figure 1.12). Inhibition of fatty acid synthesis occurs when AMPK phosphorylates and inactivates ACC1 (acetyl-CoA carboxylase 1) or when it inactivates and turns off the expression of lipogenic genes such as fatty acid synthase and ACC1 (Corton *et al*., 1995; Woods *et al.,* 2000; Svensson *et al.*, 2016). Stimulation of fatty acid oxidation occurs when AMPK phosphorylates and inactivates ACC2 (acetyl-CoA carboxylase 2), which reduces malonyl-CoA levels. Subsequently, the uptake of fatty acid into mitochondria is increased (Merrill *et al*., 1997; Fullerton *et al.*, 2013).

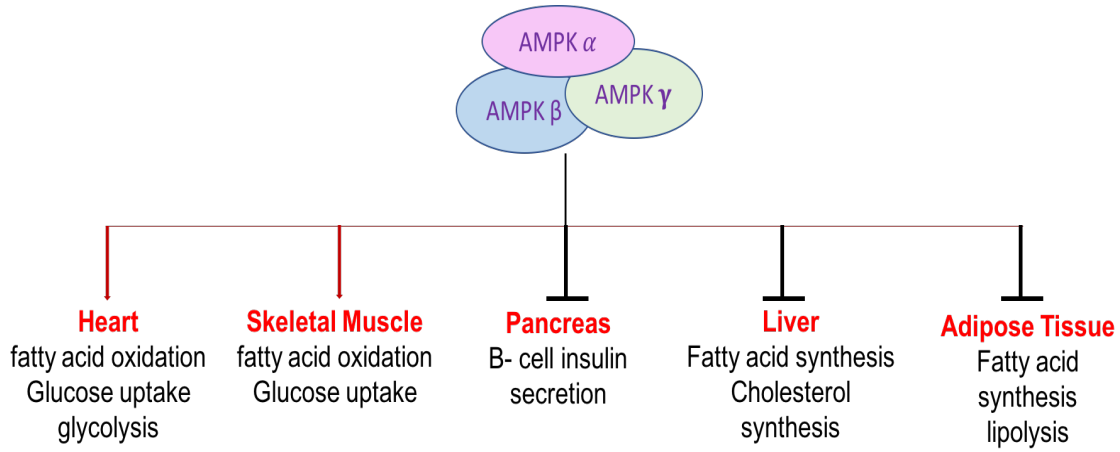

Figure 1.12. The function of AMPK in metabolism regulation in response to incidents such as nutrient- or exercise- induced stress.
The figure displays AMPK-activated mechanisms in various tissues. Activation by AMPK is indicated by red arrows, whereas, the resultant inhibitory effects of AMPK action are indicated by black T-lines. (Adapted from https://themedicalbiochemistrypage.org/ampk.php).

1.5.2. LKB1-AMPK regulates glucose homeostasis

AMPK plays a crucial role in the up-regulation of glucose uptake in heart and skeletal muscle cells. Increase in glucose uptake results due to the enhanced transcription and translocation of GLUT4 (glucose transporter-4) to the plasma membrane (Kurth-Kraczek *et al*., 1999; Zheng *et al.,* 2001; Huang & Czech, 2007) and due to GLUT1 activation at the plasma membrane (Barnes *et al.*, 2002). AMPK indirectly induces the translocation of GLUT-4 through the phosphorylation of the Rab GTPase-activating protein AS160 (Akt substrate 160), which in turn regulates the docking and merging of GLUT4 vesicles with the plasma membrane (Chavez *et al*., 2008).

AMPK is also associated with the regulation of hepatic gluconeogenesis in the liver. CRTC2, a transcriptional coactivator of CREB (cAMP response element–binding protein), is an essential regulator of gluconeogenesis in mice (Hill *et al.*, 2016). It regulates the transcription of PGC1, a transcriptional coactivator involved in energy metabolism, and its gluconeogenic targets glucose 6-phosphatase (G6Pase) and phosphoenolpyruvate carboxykinase (PEPCK). AMPK phosphorylation of CRTC2 results in its translocation to the cytoplasm in primary hepatocytes cultures. In livers lacking LKB1, CRTC2 was dephosphorylated and located in the nucleus, where PGC-1α is transcriptionally activated resulting in gluconeogenesis. Hence, LKB1/AMPK targets CRTC2 in the regulation/inhibition of gluconeogenesis (Shaw *et al*., 2005; Viollet *et al.*, 2009) (Figure 1.13). Intriguingly, the regulation of PGC-1α expression by LKB1/AMPK enhances mitochondrial biogenesis in muscle cells (Sriwijitkamol *et al*., 2006).

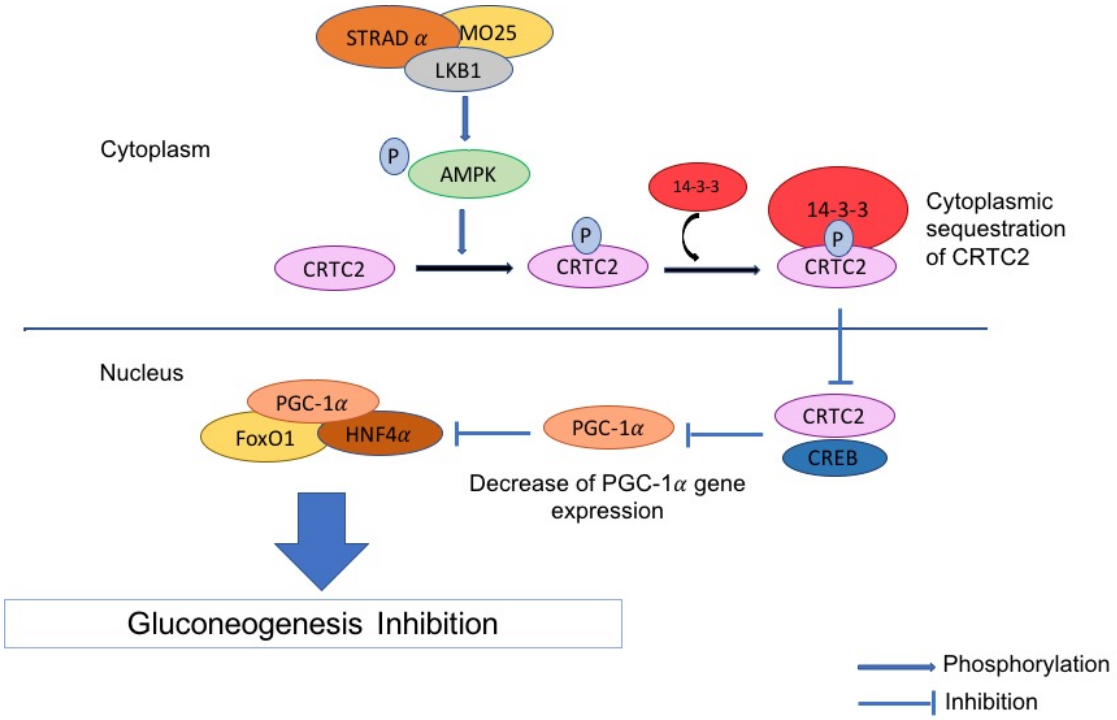

Figure 1.13. Role of LKB1-AMPK pathway in regulating gluconeogenic gene expression. Under metabolic stress, AMPK is phosphorylated and activated by LKB1 resulting in the phosphorylation and subsequent cytoplasmic sequestration of CRTC2 by 14-3-3. Hence, CRTC2 is restricted from translocating into the nucleus and binding to CREB transcription factor. This in turn restrains the expression of the co-activator PGC1α. Hence, the LKB1-AMPK pathway blocks PGC-1α from driving the transcription of crucial gluconeogenic enzymes including G6Pase and PEPCK alongside the transcription factor HNF4α and the forkhead family activator FoxO1.

1.5.3. LKB1-AMPK regulates cell growth, autophagy and metastasis

Protein translation and cellular growth play a substantial role in cellular energy outflow. Under metabolic stress, AMPK conserves energy by inhibiting protein translation and cellular growth. The best understood mechanism by which LKB1/AMPK restricts cell growth is through the inhibition of the mTOR pathway. The mammalian target of rapamycin (mTOR) is a member of the phosphatidylinositol 3-kinase related kinase (PIKK) superfamily that regulates cell growth in all eukaryotes, functioning as a central integrator of nutrient and growth factor inputs (Guertin & Sabatini, 2007; Saxton & Sabatini, 2017). mTOR is the active subunit of two patently distinctive protein complexes called mTORC1 and mTORC2 (van Veelen *et al*., 2011). mTORC1 consists of the

catalytic subunit mTOR, the regulatory associated protein of mTOR (raptor), and mLST8 (mammalian lethal with SEC13 protein 8). mTORC1 is sensitive to inhibition by rapamycin, an immunosuppressive drug, and plays a significant role in initiating protein translation and cell growth through the phosphorylation of two regulatory proteins called p70 ribosomal S6 protein kinase (p70S6K) and eukaryotic initiation factor 4E (eIF4E) binding protein 1 (4E-BP1), which stimulate the translation of cell growth regulators such as c-myc, cyclin D1 and hypoxia inducible factor 1α (HIF-1α) (Holz *et al.,* 2005; Guertin & Sabatini, 2007; van Veelen *et al.,* 2011). mTORC2 is comprised of mTOR, rapamycin-insensitive companion of mTOR (rictor), mSIN1 (mammalian stress-activated protein kinase-interacting protein) and mLST8. mTORC2 phosphorylates Akt and protein kinase C (PKC), which are protein kinases involved in cellular development (Ikenoue *et al.*, 2008). Together, mTORC1 and mTORC2 regulate size and proliferation of cells as well as their cycle progression in mammals (Zoncu *et al.,* 2011).

Upstream components of the mTOR signalling pathway include the tumour suppressor complex formed by TSC1 and TSC2 (the tuberous sclerosis complex). TSC1/TSC2 are a GTPase Activating Protein (GAP) that stimulates GTPase activity of the small G-protein Rheb, a GTPase of the Ras family which activates mTORC1 when in its GTP-bound form (Garrido *et al.,* 2016). AMPK activates TSC2 through the direct phosphorylation of its Ser1345 and Thr1227 residues. This then converts Rheb to a GDP-bound confirmation resulting in its inactivation (Huang & Manning, 2008; van Veelen *et al.,* 2011). When levels of ATP, glucose or oxygen are low, AMPK directly phosphorylates TSC2 at Thr1227 and Ser1345, which leads to an increase in the activity of TSC1/TSC2 complex to inhibit mTOR (Inoki *et al*., 2003). Intriguingly, in lower eukaryotes and in TSC2-/- MEFs, the activation of AMPK still partially suppresses mTORC1, implying an alternative mechanism of mTOR inhibition by AMPK exists. In this context, AMPK was revealed to phosphorylate raptor at Ser722 and Ser792 which prompts the binding to 14-3-3 leading to the inhibition of mTORC1 kinase activity (Figure 1.14) (Gwinn *et al*., 2008; Hahn-Windgassen *et al.,* 2005).

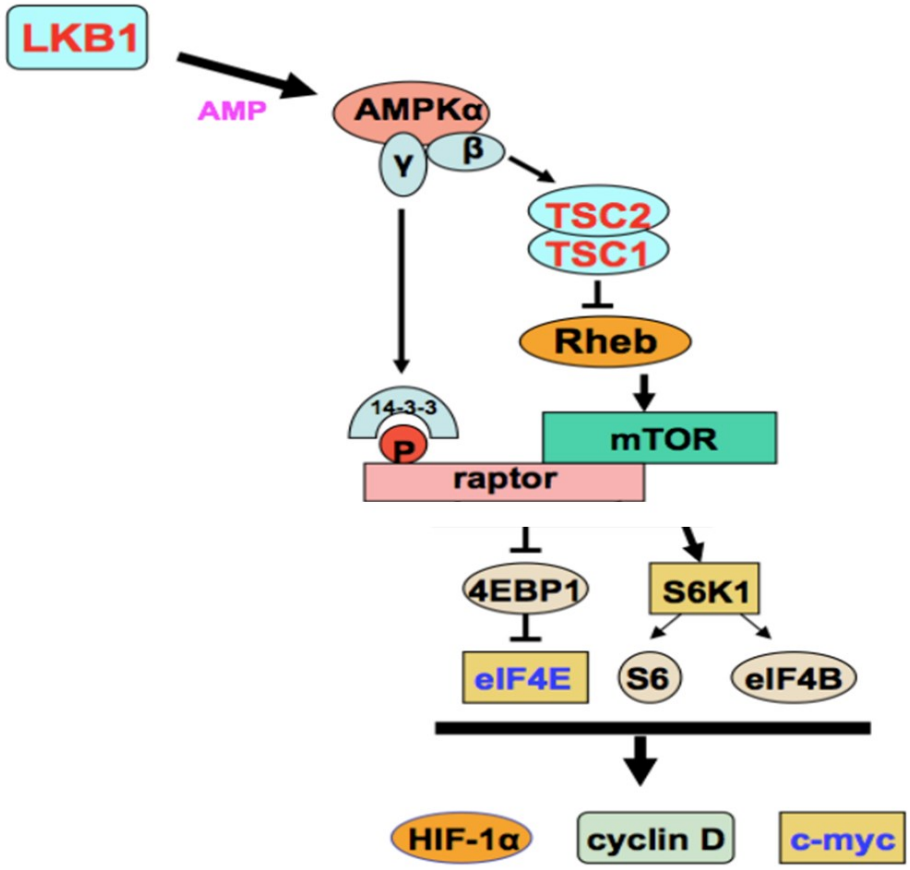

Figure 1.14. The LKB1-AMPK-mTORC1-dependent regulation of protein translation. mTORC1 regulates the translation of numerous cell growth regulators. LKB1 phosphorylation and activation of AMPK results in the direct phosphorylation of both TSC2 and raptor and thus the inhibition of mTORC1 activity by a dual mechanism. mTOR activation leads to the phosphorylation of two regulatory proteins, the eukaryotic initiation factor 4E-binding protein-1 (4E-BP1) and the p70 ribosomal S6 protein kinase (S6K1 or p70S6K). The phosphorylation of 4E-BP1 releases its inhibitory action on eukaryotic initiation factor 4E (eIF-4E), which is able then to bind the mRNA cap and instigate the initiation of protein synthesis. p70S6K phosphorylates several substrates such as the eukaryotic translation initiation factor 4B (eIF4B) and the S6 ribosomal protein (S6). (Adapted from Han et al., 2013, with permission).

Research so far has shown mTORC1 to be the sole signalling pathway downstream of LKB1 that has been deregulated in tumours occurring in humans and mouse models of both NSCLC (non-small cell lung carcinoma) and Peutz-Jeghers syndrome (Han *et al.,* 2013). Current research reveals that LKB1-dependent activation of AMPK as a result of energy stress leads to the inhibition of mTORC1 activity through TSC2 and raptor, although other AMPK substrates may also have a role in the regulation of mTOR (Shaw, 2009; Alexander & Walker, 2011).

In solid tumours, the inner cells are normally less oxygenated and irrigated, creating a hypoxic environment. In such an environment, the expression of the transcription factor HIF-1 (hypoxia inducible factor 1) is induced aiding in cell survival and growth (Powis & Kirkpatrick, 2004; Hashimoto & Shibasaki, 2015). *In vivo,* tumours deficient in LKB1 have upregulated mTORC1 and HIF-1 expression. Indeed, mTORC1 has been well proven to up-regulate HIF-1 and LKB1-AMPK pathway has been established to negatively regulate mTORC1. These results signify that LKB1-AMPK-mTORC1 signalling pathway may be crucial in suppressing the expression of HIF-1 and hence inhibiting cancer cell growth under hypoxic conditions (Gan & Li, 2014). Recent studies have shown that the inhibition of LKB1 or AMPK resulted in a HIF-1-dependent metabolic growth in proliferating cells; whereas the loss of LKB1 or AMPK in tumour cells led to an enhanced glucose and glutamine uptake and utilization. Suppression of HIF-1α reverses these metabolic advantages and hinders the survival and growth of LKB1- or AMPK- deficient tumour cells subjected to low-nutrient conditions (Faubert *et al*., 2013; 2014).

LKB1-AMPK signalling is not only implicated in the regulation of cell growth through the mTORC1 complex, the LKB1-AMPK-mTORC1 pathway is also involved in the regulation of autophagy and metastasis (Han *et al*., 2013; Dunlop & Tee, 2014). Autophagy is induced by ULK1 and ULK2 (unc-51-like kinase), which are orthologues of yeast Atg1 in eukaryotes and have partially redundant roles in starvation-induced autophagy. ULK1/2 creates a complex with 2 other proteins called FIP200 and Atg13. In normal growth environments, mTORC1 interacts with the ULK1/2 via raptor which in turn allows mTOR to phosphorylate ULK1/2 and Atg13, and hence inhibit ULK1/2 kinase activity. On the other hand, mTORC1 is incapable of inhibiting ULK1/2-induced autophagy under starvation conditions or when mTORC1 activity is suppressed by drugs or upstream kinases such as AMPK. Nonetheless, AMPK can directly phosphorylate ULK1 and stimulate its kinase activity (Shang & Wang, 2011) (Figure 1.15). Intriguingly, AMPK and raptor can also be phosphorylated in an ULK1-dependent manner in a negative feedback loop that impairs the initiation of autophagy (Alers *et al*., 2012).

A study performed by Tripathi *et al.* (2013) has indicated that steady-state nitric oxide (NO) led to nitrosative stress resulting in prompt activation of an ATM damage-response pathway and the stimulation of the downstream signalling by the LKB1/AMPK/TSC/mTORC1/ULK1 pathway and hence resulting in an increase in

autophagy. This study is crucial in planning anti-cancer therapies as cancer cells are especially sensitive to nitrosative stress. These therapies can be designed on the aptitude of reactive nitrogen species to stimulate autophagy-mediated cell death (Tripathi *et al.*, 2013).

Overexpression of LKB1 is also implicated in supressing metastasis of cancer cells. In LKB1 deficient MDA–MB-435 breast cancer cells, overexpression of wild-type LKB1 can drastically impede the invasion and metastasis *in vitro* and *in vivo*. This effect accompanies the downregulation of matrix metalloproteinase 2 and 9 (MMP-2 and MMP-9) as well as vascular endothelial growth factor (VEGF). The LKB1-AMPK pathway also plays a crucial role in adiponectin-mediated suppression of breast cancer cells metastasis through the inhibition of p70S6 kinase inhibition (Gan & Li, 2014). In ErbB2-mediated breast cancer, the removal of LKB1 induces tumour initiation and leads to a characteristic change to aerobic glycolysis ('Warburg effect'). mTOR has been found to play a role in the metabolic reprogramming in these tumours, and the loss of LKB1 in these cells exhibited enhanced early tumour growth and improved migratory properties *in vitro* (Dupuy *et al.,* 2013).

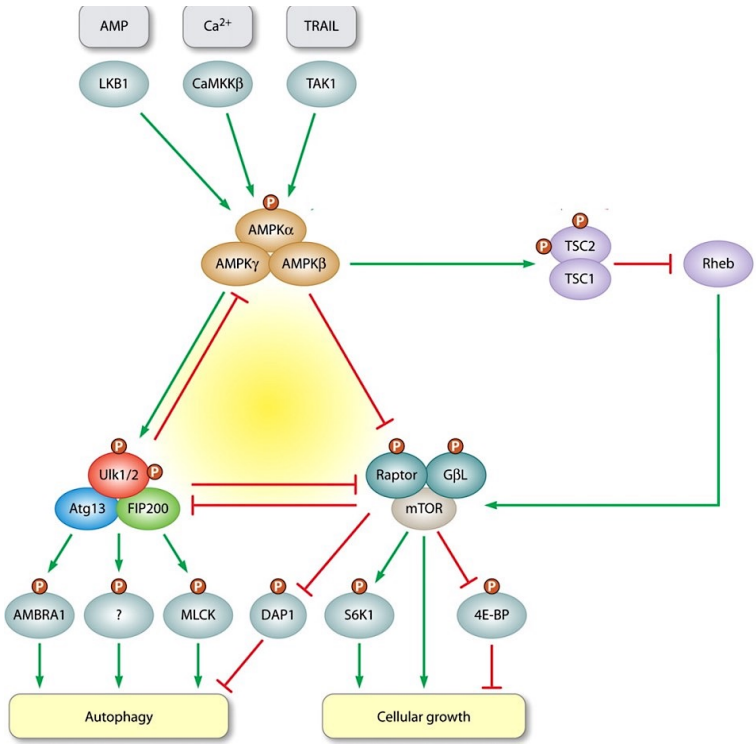

Figure 1.15. Fine adjustment of autophagy by the AMPK-mTORC1-Ulk1/2 kinase network.
AMPK and mTORC1 protein complexes regulate the autophagy inducing complex Ulk1/2-Atg13-FIP200 in opposing manners. Active mTORC1 utilises the sufficient supply of growth factors and nutrients to stimulate growth related processes such as protein translation, for example, by phosphorylation of S6K1 and 4E-BP, while concurrently impeding self-consuming processes such as autophagy. The activation of AMPK by upstream kinases, mainly LKB1 as well as CaMKKβ and TAK1, have shown under low-energy conditions to positively regulate autophagy induction through the inhibition of mTORC1. This relieves the Ulk1/2-Atg13-FIP200 complex from the negative regulation of mTORC, especially that exerted on Ulk1/2 kinase activity. AMPK suppresses mTORC1 activity either through the TSC1/2-Rheb pathway or by direct phosphorylation of raptor. Nonetheless, AMPK can also bind, phosphorylate, and directly activate Ulk1/2. Yet, this interaction is countered by mTORC1. Moreover, mTORC1 does not only suppresses autophagy by inhibiting Ulk1/2 kinase activity, it also simultaneously suppresses the activity of DAP1, a negative regulator of autophagy. Hence, the inhibition of mTORC1 results in both autophagy induction via Ulk1/2-Atg13-FIP200 and its inhibition via DAP1. Two Ulk1-dependent feedback loops also assist in the fine-tuning of the autophagic response. Ulk1 has been found to phosphorylate and inhibit both of its upstream regulators AMPK and mTORC1. The Ulk1 phosphorylation of raptor might maintain mTORC1 inhibition under limited supplies of nutrients, however Ulk1 suppression of AMPK activity antagonizes this action and impedes the autophagic response. This perplexingly complex network of mutual activation and inhibition will eventually establish an applicable response to conflicting demands. (Adapted from Alers *et al.*, 2012; with permission).

1.5.4. LKB1-AMPK regulates cell polarity

LKB1 plays a vital role in the regulation of numerous cellular processes including cell proliferation, cell polarity, migration, transcription and cellular stress and damage responses. In the following sections, I will discuss the regulation of cell polarity by LKB1 and LKB1-AMPK pathway.

1.5.4.1. LKB1 regulates cell polarity

Cell polarity is a biological process in which the asymmetric allocation and organization of cellular components and structures occur. Cell polarity is established and maintained throughout development and in adult tissues in uni- and multicellular organisms. It is controlled via the fine-tuning of signalling pathways, membrane trafficking events and cytoskeletal rearrangements. In fact, the impairment of cell polarity is strongly associated

with developmental maladies as well as cancer. Regulation of cellular polarity is one of the main functions of LKB1.

Prior to the detection of AMPK's role as an LKB1 downstream target involved in metabolism regulation, LKB1 functions were notably associated with the regulation of cell polarization in model organisms: *Drosophila melanogaster* and *Caenorhabditis elegans*. Homologs of LKB1 in *Drosophila melanogaster* and *Caenorhabditis elegans*, *dlkb1* and *Par-4* respectively, have been found to have crucial roles in regulating cellular polarity (Martin *et al.*, 2003; Watts *et al.,* 2000).

Genetic screening for regulators of cytoplasmic partitioning in the early embryo of *C. elegans* resulted in the identification of the par genes (Kemphues *et al.,* 1988). The PAR proteins have been discovered to play a crucial role in the regulation of polarization, not only in *C. elegans*, but also in other diverse models, which emphasises their fundamental role in establishing cell polarization across evolution (Goldstein & Macara, 2007; Jansen *et al.,* 2009; Macara, 2004). The PAR protein members include the serine threonine kinase PAR-4, an ortholog of *Drosophila, Xenopus* and mammalian LKB1. Mutation in *par-4* in *C. elegans* were found to cause defects in the asymmetric cell division of the fertilized worm zygote and thus the loss of intestinal cells. Hence, PAR4 plays a vital role in the establishment of cell polarity through asymmetric cleavage configurations of blastomeres and specification of the intestinal lineage (Watts *et al.,* 2000).

Similarly, in *Drosophila*, mutations in *dlkb1* result in the defective formation of the anterior-posterior oocyte axis. Accordingly, dLKB1 is crucial in regulating the early anterior-posterior (A–P) polarity of the oocyte, as well as the repolarization of the oocyte cytoskeleton that outlines the embryonic A–P axis (Martin & St Johnston, 2003; Nakano & Takashima*,* 2012). dLKB1 has also been discovered to have a crucial role in the regulation of the asymmetric division in neuroblasts. Neuroblasts are neural stem cells from which most neuronal and glial cells of the central nervous system in *Drosophila* originate. As such, mutations of *dlkb1* result in the inhibition of uneven cytokinesis and abolishment of proper localization of Bazooka, PAR-6, Miranda and DaPKC, which are proteins involved in directing asymmetric cell division in neuroblasts in *Drosophila* (Martin & St Johnston, 2003; Bonaccorsi *et al.,* 2007).

LKB1 is not only necessary for the regulation of polarity in invertebrates, it also has an essential role in the regulation of polarity in mammals. It controls Rho GTPases,

phosphoinositide and Wnt/GSK3β signalling involved in epithelial polarization (Gloerich *et al.,* 2012; Martin-Belmonte & Perez-Moreno, 2012). Epithelial tissues are described by the arrangement of cellular sheets exhibiting apicobasal polarity and taut intracellular junctions (Martin-Belmonte & Perez-Moreno, 2012). The function of LKB1 in epithelial polarization was highlighted in a study conducted in the human intestinal epithelial cell line LS174T-W4 in which the expression of STRAD was induced by doxycyclin resulting in the stabilization, activation and translocation of LKB1 into the cytoplasm. Once LKB1 is activated, the cells quickly rebuild the actin cytoskeleton to form an apical brush fringe around which a few junctional proteins, for example, ZO-1 (zonula occludens) redistribute in a dotted circle. Upon LKB1 activation, CD66 (carcinoembryonic antigen/CEA), CD13 (dipeptidyl peptidase IV), and CD26 (amino peptidase-N) are relocalised to the apical membrane, while the basolateral protein CD71 is totally omitted from the brush border domain (Baas *et al.,* 2004). These findings reveal the significance of LKB1 in regulating epithelial cell polarity in mammals. Defects in LKB1 may therefore result in tissue disorganization, polyploidy and misorientation of the plane of division of epithelial cells (Korsse *et al.*, 2013). This commonly occurs in human cancers.

LKB1-deficient cells display altered cell polarity and this phenotype can be rescued by expressing a phosphomimetic version of AMPKα in the same cells. This indicates that LKB1 coordinates epithelial polarity and proliferation through phosphorylation and activation of AMPK.

PJS patients are highly predisposed to developing pancreatic cancer. In this context, *in vivo* conditional deletion of LKB1 in the pancreatic epithelium of the mouse results in defective acinar cell polarity, an abnormal cytoskeletal organization, a loss of tight junctions, and an inactivation of the AMPK/MARK/SAD family kinases. Starting with rapid and progressive postnatal acinar cell degeneration and acinar-to-ductal metaplasia, the mice later develop pancreatic insufficiency culminating with the development of pancreatic serous cystadenomas, a tumour type associated with PJS. LKB1 deficiency also impacts the endocrine pancreas where the Langerhans islets become smaller and scattered and display transient alterations in glucose control. Thus, LKB1 is essential for the establishment of epithelial cell polarity that is vital for pancreatic acinar cell function and viability *in vivo* and for the suppression of neoplasia (Hezel *et al.,* 2008).

1.5.4.2. AMPK mediates LKB1 function in establishing cell polarity

Forcet *et al.* (2005) observed in PJS patients and in sporadic tumours which delineate the C-terminal domain of LKB1 that LKB1 mutations do not disrupt the catalytic or the cell growth suppressing activity of LKB1 but instead adjust its ability to activate AMPK. Subsequently, LKB1 renders incapable of forming and maintaining polarity of both intestinal epithelial cells and migrating astrocytes.

In *Drosophila*, normal development is dependent on AMPK as all AMPK-null mutant flies fail to survive before reaching the mid-pupal stage and entering adulthood, regardless of the presence of adequate nutrients. The embryos display serious defects in cell polarity and mitosis, like those of LKB1-null mutants. Many of the phenotypes displayed by LKB1-null mutants are restored by the constitutive activation of AMPK, signifying that LKB1 controls mitosis and cell polarity by mediating its downstream effects through AMPK (Lee *et al.,* 2007; Sinnett & Brenman, 2016).

LKB1 regulates cell polarity through the activation of the actin motor myosin II. Myosin II activity and stability are regulated in humans via the phosphorylation of the Myosin II Regulatory Light Chain (MRLC); which is a downstream target of AMPK (Watanabe *et al.*, 2007). In AMPK and LKB1-null mutants in *Drosophila* embryos, the polarity defects can be rescued by the expression of a phosphomimetic mutant of MRLC; which can also induce polarization of colon cancer cell line LS174T cells (Lee *et al.,* 2007; Nakano & Takashima, 2012). Hence, MRLC has been suggested to be a direct substrate of AMPK; however, *in vitro*, purified AMPK could not phosphorylate MRLCII efficiently (Bultot *et al*., 2009). Therefore, the postulated phosphorylation of MRLC by AMPK may be mediated by other kinases (Mirouse & Billaud, 2011). An example is the Rock kinase (ROCK), which can be activated by AMPK and which phosphorylates MRLC through MLC kinase (Miranda *et al.,* 2010). NUAK1, a member of the AMPK family, can also indirectly inactivate the MLC phosphatase protein resulting in increased phosphorylation of MRLC (Zagórska *et al.,* 2010). Hence, ROCK and NUAK1 can potentially mediate the phosphorylation of MRLC that is activated by LKB1. Intriguingly, it has been recently shown in cranial neural crest cells (CNCCs) that LKB1 can activate AMPK which then activates ROCK resulting in the phosphorylation of MRLC (Cruezet *et al.,* 2016). This signalling pathway is essential for the directional migration of CNCCs and head

development in chick embryos. Hence, cell polarity is regulated by the LKB1-AMPK pathway which remains conserved amongst species from invertebrates to human.

1.5.5. LKB1-AMPK regulates polarized cell migration

Cellular migration is an essential machinery in embryonic development as well as in adults where it recruits immune cells to wounds and infection sites. Tumour cells also possess the ability to migrate and metastasize. Comprehending the molecular mechanisms enabling tumour cells to separate from the epithelium and migrate via epithelial-to-mesenchymal transition (EMT) is vital in offsetting the spreading of tumours.

Forcet *et al.* (2005) has revealed that mutations in the catalytic or C-terminal domain of LKB1, like those established in PJS patients and sporadic cancers, resulted in defective polarized migration of astrocytes. Moreover, LKB1 has been found to have a crucial role in neuronal migration and centrosome positioning (Shelly *et al*., 2007). Asada *et al.* (2007), has shown that the knock-down of LKB1 in migrating immature neurons leads to the impediment of neuronal migration and alteration of the centrosomal positioning, with the centrosome position being a spatial gauge for the migrational direction of the cell. Furthermore, the impaired capacity of LKB1 to differentiate neurons within the cortical plate prompts the centrosome to malposition at the basal side of the nucleus, instead of the usual apical positioning (Asada *et al*., 2007). Later on, LKB1 has been shown to mediate the phosphorylation of Ser9 of GSK3β (glycogen synthase kinase 3 beta) and inactivate it at the leading tip of migrating neurons in the developing neocortex (Asada & Sanada, 2010, Morgan-Smith *et al.,* 2014). GSK3β inactivation facilitates the localisation of APC (the microtubule plus-end binding protein adenomatous polyposis coli) at the distal ends of microtubules in the tip, and hence stabilizes the microtubules neighbouring the leading edge (Figure 1.16). These are crucial steps for the forward movement of the centrosome and the migration of neurons (Asada & Sanada, 2010).

Whether LKB1 induces neuronal migration through AMPK remains unclear; however, a number of studies point in this direction. The activation of AMPK by AICAR in HepG2 cells, enhances the phosphorylation rate of GSK3 at Ser9 (Horike *et al.*, 2008). AMPK has also been found to phosphorylates CLIP-170 directly at Ser311, bringing it closer to the distal end of microtubules than non-phosphorylated CLIP-170. CLIP-170 is a

microtubule "plus-end-tracking protein" involved in the regulation of microtubule dynamics. siRNA-depletion of AMPK leads to reduced phosphorylation of CLIP-170 and movement of the dissociation pattern of CLIP-170 at the distal end of the microtubules; which in turn causes impairment of cell polarity (Nakano & Takashima, 2012). These data signify that indeed, LKB1-induced migrational polarity might be mediated through its downstream target, AMPK.

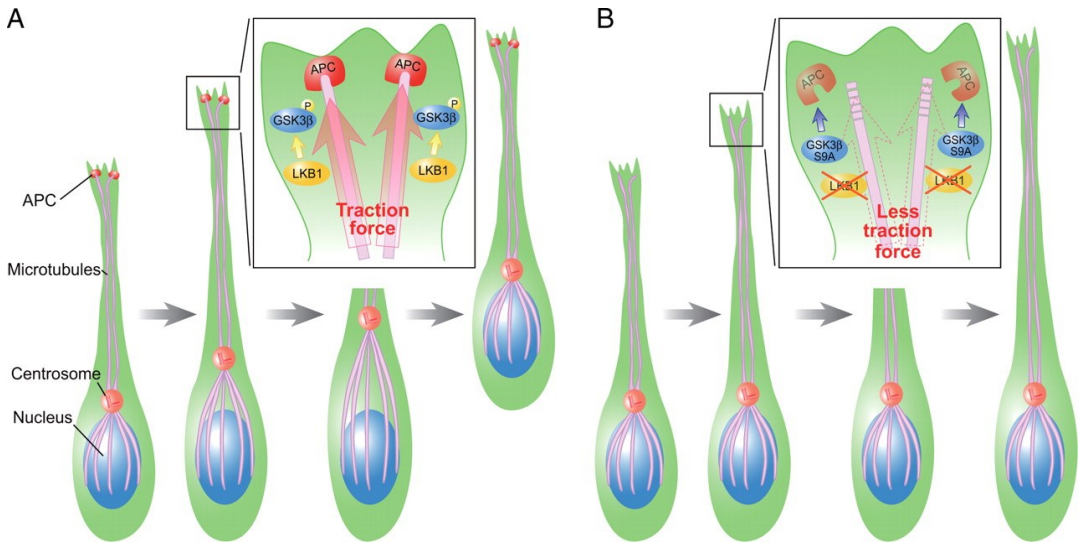

Figure 1.16. A model for a role of LKB1-GSK3β-APC pathway in centrosomal forward movement.

A. In migrating neurons, LKB1 mediates the phosphorylation of Ser9 and inactivation of GSK3β in the leading process tip. This in turn allows APC, a microtubule plus-end protein, to bind to the microtubule ends and anchor and stabilize them to the leading-edge cortex. Certain motor proteins such as dynein/dynactin (not shown) found at the cell cortex exert a traction force on the microtubules causing the centrosome to pull up in the leading process**. B.** The disruption of either Ser9 phosphorylation of GSK3β or APC binding to the microtubule ends leads to the destabilization of microtubules in the leading process tip, most likely as a result of an impairment of microtubule capture at the cell cortex. This may cause less traction force to be exerted on the microtubules and lead to an impairment of centrosomal upward movement and elongation of the leading process. (Adapted from Asada & Sanada,2010; with permission).

1.5.6. Role of LKB1-AMPK in cancer

The role of LKB1 has been demonstrated to regulate metabolism, cell growth and establishing polarity, with the latter providing tissues with resistance to oncogene activities and tumour development. The following section will cover the links between

AMPK-LKB1 signalling, metabolism and cancer as well as the dual role of LKB1 in tumourigenesis.

1.5.6.1. LKB1-AMPK in cancer and metabolism

The switching of tumour cells from oxidative metabolism to increased glucose uptake, glycolysis and lactate output in a poorly oxygenated and irrigated setting is known as the Warburg effect. The Warburg effect enables tumour cells to rapidly enhance macromolecular biosynthesis in order to grow and thrive (Heiden *et al*., 2009; Burns *et al.,* 2017). Under metabolic stress, the LKB1-AMPK pathway decreases cell growth by preventing glycolysis amid other processes, thus operating as a tumour suppressor. By inhibiting mTORC1 activity, LKB1-AMPK reduces the expression levels of the hypoxia-inducible factor-1 (HIF- 1), which is necessary for fast cell growth in low oxygen environments. HIF-1 is a transcription factor that stimulates the expression of enzymes and transporters needed for the Warburg effect. They involve most glycolytic enzymes and also, the transporters GLUT1 and MCT4, needed for glucose uptake and lactate output, respectively (Shackelford *et al.,* 2009; Faubert *et al.,* 2014; Chen & Sang, 2016). Hence, an anti-Warburg effect is exerted by LKB1/AMPK through the inhibition of the mTOR pathway. Indeed, in AMPK-α1/α2 double null or LKB1-null mouse embryo fibroblasts (MEFs), an up-regulated expression of HIF-1α as well as that of the downstream glycolytic genes is detected. In this context, drugs that activate AMPK should be effective in the treatment of cancer. In fact, metformin administered to Type 2 Diabetes (T2D) patients resulted in a lower rate of cancer development; hence, establishing metformin as a potential anti-cancer drug (Evans *et al*., 2005; Faubert *et al.,* 2013). Additional research implies that metformin might stall the initial development of tumours. In a tumour-prone mouse model as a result of heterozygous loss of phosphatase and tensin homolog (PTEN) and reduced expression of LKB1, treating the mice from the time of weaning with metformin or phenformin, or another AMPK activator, A-769662 can delay tumour development (mainly lymphomas) (Huang *et al.*, 2008). Metformin activation of AMPK inhibits cell growth prompting a cytostatic effect on preneoplastic lesions, and

thereby delaying the onset of tumourigenesis.

Alternatively, in LKB1-deficient cells, biguanides (a group of Type 2 Diabetes drugs to which metformin belongs) can suppress tumour growth by inhibiting the mitochondrial respiratory chain (Parker *et al.,* 2016). Indeed, defective LKB1-AMPK signalling reduces the capacity of cells to restore ATP levels in response to metabolic stress. Consequently, a down-regulated LKB1-AMPK pathway in tumour cells makes them less capable of adapting to mitochondrial inhibition by biguanides and more susceptible to cell death (Foretz *et al*., 2010; Hawley *et al.,* 2010; Owen *et al*., 2000; Russell *et al*., 2004; Sakamoto *et al*., 2005). A mouse xenograft study of MC38 colon carcinoma cells has experimentally supported this mechanism of action, in which administering metformin decreased the rate of tumour growth in insulin-resistant mice, as well as in insulin-sensitive mice where LKB1 is knocked-down in the tumour cells by means of RNA interference (Algire *et al*., 2011). Another study performed in another NSCLC mouse model revealed that treatment with phenformin (more powerful inhibitor of the respiratory chain than metformin) resulted in prolonged survival of the mice, in which the tumours were stimulated by the activation of mutant K-Ras combined with the loss of LKB1 (Shackelford *et al*., 2013). Accordingly, LKB1-deficient tumour cells which become more sensitive to the ATP-depleting effects of biguanides can be targeted without disturbing the nearby normal cells in which LKB1-AMPK is functional.

1.5.6.2. A dual role of LKB1 in tumour progression

The role of LKB1 in tumour suppression has been well investigated; however, recent research has also shown that under certain conditions, LKB1 can play a role in promoting cancer.

Recently, a new isoform of LKB1, ΔN-LKB1, has been identified. ΔN-LKB1 isoform lacks the N-terminal domain rendering it catalytically inactive. This isoform is expressed only in the lung cancer cell line NCI-H460, and suppression of its activity results in a decline of the survival of the cells and inhibition of their tumourigenicity when engrafted in nude mice. Hence, the LKB1 isoform, ΔN-LKB1, plays a role in promoting tumourigenesis (Dahmani *et al.,* 2014).

In established tumours in which the role of the LKB1-AMPK pathway is maintained,

AMPK can shield tumour cells from metabolic stress and enable them to subsist. Certainly, in lung adenocarcinoma (A549) cells that lack LKB1, reexpressing LKB1 in cells exposed to glucose starvation results in safeguarding these cells from cell death. Seemingly, this defence mechanism is due to AMPK inhibition of fatty acid synthesis and subsequent sparing of NADPH, which can be employed to offer protection against the oxidative stress triggered by glucose deprivation (Jeon *et al*., 2012). Additionally, AMPK was shown to be activated in hypoxic regions of tumours and to increase survival in metabolically defective cells (Laderoute *et al.,* 2006).

A study conducted by Bouchekioua-Bouzaghou *et al.* (2014) employed a proximity ligation assay (PLA) derived technique, the "Single Detection method" and FFPE analysis to detect the subcellular localization of LKB1 in tumour cells. LKB1 was found to be localised mostly in the cytoplasm of MCF-7 cells; whereas, it was detected mostly in the nucleus in ZR75-1 cells. This dual localization of LKB1 was associated with clinical features, in which the nuclear expression of LKB1 was linked to good prognostic markers; whereas cytoplasmic LKB1 localisation was associated with bad prognostic markers. Interestingly, the activation of 4E-BP1 is shown to correlate with the cytoplasmic expression of LKB1, and that in turn supports the hypothesis that LKB1 is sequestered by the cytosolic complex metERα/Src/PI3K and is functionally inactivated in primary sporadic breast carcinomas. This renders LKB1 incapable of down-regulating the mTOR pathway and suppressing cell growth (Bouchekioua-Bouzaghou *et al.*, 2014).

Therefore, LKB1 signalling can both suppress and promote tumourigenesis, so targeting LKB1 signalling for cancer treatment should be done with caution.

1.5.6.3. The role of LKB1-AMPK in genomic stability and DNA damage response pathways

Tumourigenesis and the acquisition of malignant phenotypes have been found to strongly correlate with genomic instability (Risinger *et al.*, 2004; Harper *et al.,* 2007; Broustas & Lieberman, 2014). Genomic instability generally occurs due to DNA damage, which results in an array of nucleotide modifications and breakage of DNA strands. DNA damage can result from endogenous sources such as errors in DNA replications and recombination as well as cellular metabolism (Risinger *et al.,* 2004; Harper *et al.,* 2007;

Tubbs & Nussenzweig, 2017) or from exogenous sources such as X-rays, oxidative stress, ultraviolet (UV) light and chemical mutagens (Harper *et al.,* 2007). To maintain genomic stability, the cell has developed a DNA damage response (DDR), which is a network of DNA repair processes. The DDR is comprised of sensors that constantly search for damaged DNA in the genome, transducers that transmit the signals, and effectors that collect these signals and coordinate the repair process (Harper *et al*., 2007; Matsuoka *et al.,* 2007; Broustas & Lieberman, 2014).

LKB1 has been found to play a crucial role in DNA repair. The LKB1 protein sequence and structure show that the Thr363 residue in humans (Thr366 in mouse) can be optimally phosphorylated by the phosphoinositide 3-kinase-like kinases. These kinases include ataxia telangiectasia mutated kinase (ATM), DNA-dependent protein kinase (DNA-PK) and ATM- and rad3-related kinase (ATR), which function upstream of DNA damage operating as DNA damage sensors and mediating DNA repair (Sapkota *et al.,* 2002a; Sapkota *et al.*, 2002b; Harper *et al.*, 2007; Matsuoka *et al.,* 2007). An *in vitro* GST pull-down assay revealed that ATM kinase activated by DNA damage mediates the phosphorylation of LKB1 at Thr363 following the exposure of cells to ionizing radiation (IR) (Sapkota *et al.*, 2002b). Research in epithelial cancer cells also revealed AMPK as an effector of ATM in its role as a sensor of DNA damage as well as a regulator of cell cycle progression and cellular sensitivity to genotoxic stress (Sanli *et al.,* 2014). Mutated ATM genes cause ataxia telangiectasia, an autosomal recessive disorder that emerges in children who exhibit symptoms of ataxia associated with loss of motor function (Bensimon *et al.*, 2011; Jeong *et al.,* 2014). Affected patients also display a rise in cellular ROS build-up, increased sensitivity to ionizing radiation and a higher risk of acquiring Type 2 diabetes and cancer (Ditch *et al.*, 2012; Armata *et al.*, 2010). Although ATM is mostly known for its role as a nuclear protein that reacts to DNA damage, ATM is also suggested to be localized in the cytoplasm and regulate cell metabolism, oxidative stress and the activation of AMPK in response to pharmaceutical agents and genotoxic stress (Armata *et al.*, 2010; Alexander *et al.,* 2010; Sun *et al.*, 2007; Alexander & Walker, 2011). Cytoplasmic ATM is found to be sensitive to redox signals (Kozlov *et al.,* 2016). Exposing ATM to hydrogen peroxide (H_2O_2) leads to its activation and phosphorylation of LKB1 at Thr366, which in turn results in an increase in AMPK activation, suppression of mTOR activity and eventually the stimulation and induction of autophagy (Alexander *et al.,* 2010).

Additionally, recent findings have showed that AMPK is involved in ROS- and IR-stimulated DNA damage response (Sanli *et al*., 2014; Alexander *et al.*, 2010a). DNA double-strand breaks (DSB) recruit AMPKα2 in an LKB1-dependent manner, whereas the depletion of AMPKα2 impairs this recruitment. Also, the depletion of LKB1 triggers the development of chromosome breaks and radials (Ui *et al*., 2014). These discoveries suggest that LKB1 may aid in upregulating DNA repair through the AMPK signalling pathway, and hence play a part in the preservation of genomic stability.

1.5.7. The role of LKB1-AMPK in mitochondrial biogenesis

The role of LKB1 has been established to encompass many regulatory processes such as cellular metabolism and growth, polarity and tumourigenesis. The following section will shed some light on the role of LKB1-AMPK in regulating mitochondrial biogenesis.

Mitochondrial biogenesis arises as a result of increased energy expenditure producing a need to generate more ATP. Mitochondrial biogenesis is the growth and division of preexisting mitochondria, in which new material is added to the present mitochondrial network to increase mitochondrial mass. To support the broadening of the surface area of the inner and outer mitochondrial membranes, mitochondrial biogenesis entails the upregulation of mitochondrial proteins as well as an upsurge in lipid production and transfer. The majority of mitochondrial proteins are encoded in the nucleus. Therefore, stimulating mitochondrial biogenesis relies on relaying the signal to the nucleus for the transcription factors to promote expression of genes encoding mitochondrial proteins, a process referred to as retrograde signalling (Quiros *et al*., 2016).

Study has showed that expanded mitochondrial mass can be elicited by an assortment of experimental and physiological conditions, with exercise being well studied and analysed. In the 1950s, muscle activity in birds was found to be associated with muscle fibre mitochondrial content, with more mitochondria being present in active muscles than in less-active muscles (Paul & Sperling, 1952). Current research has proven that exercise and muscle activity stimulate a mitochondrial biogenesis programme designed to enhance the oxidative capacity of muscles (Jornayvaz & Shulman, 2010).

Hence, mitochondrial biogenesis is a critical acclimatisation to chronic energy deprivation such as long-term exercise or chronic metabolic stress (Zong *et al*., 2002). Interestingly,

AMPK has been identified to be a crucial energy sensor in mitochondrial biogenesis in response to chronic energy deprivation. During exercise the level of AMP in relation to ATP increases, which then triggers the activation of AMPK (Jorgensen *et al.,* 2005). This kinase activates cellular processes in order to increase ATP production, one of which is to increase mitochondrial biogenesis (Herzig & Shaw, 2018).

The phosphorylation of AMPK by LKB1 has been shown to enhance mitochondrial biogenesis in skeletal muscle during metabolic stress and nutrient deprivation (Zong *et al*., 2002; Garcia & Shaw, 2017).

Furthermore, chronic AMPK activation has been observed to result in increased mitochondrial biogenesis (Bergeron *et al*., 2001; Garcia & Shaw, 2017) and the AMPK-activating drug AICAR is shown to perform as an exercise mimetic (Narkar *et al.,* 2008). Moreover, increased expression of the constitutively active AMPK γ3 subunit in mice stimulates mitochondrial biogenesis (Garcia-Roves *et al.,* 2008). The role for AMPK-LKB1 in maintaining mitochondrial biogenesis has also been demonstrated in loss-of-function experiments. Under energy stress, mice expressing a dominant-negative mutant of AMPK are unsuccessful in promoting mitochondrial biogenesis (Zong *et al.*, 2002). Mice deficient in the upstream kinase LKB1 (Tanner *et al*., 2013; Jeppesen *et al*., 2013) or AMPK β1/β2 subunits (O'Neill *et al;* 2001) display reduced mitochondrial content in muscle, and mice with muscle-specific LKB1 knockout are incapable of enhancing mitochondrial biogenesis after exercise (Tanner *et al.*, 2013). Muscle-specific knockout of AMPK α-subunits also results in defects in mitochondrial biogenesis and function (Lantier *et al.,* 2014). Furthermore, LKB1-AMPK has also been revealed to regulate mitochondrial content in other tissues, including adipocytes (Mottillo *et al.,* 2016), macrophages (Galic *et al*., 2011) and hepatocytes (Hasenour *et al*., 2014). Together, these studies show the role of LKB1-AMPK signalling as a central regulator of mitochondrial biogenesis.

To stimulate mitochondrial biogenesis, prolonged activation of AMPK triggers and upregulates the expression of nuclear respiratory factor 1/2 (NRF-1 and NRF2), which are transcription factors involved in mitochondrial biogenesis (Bergeron *et al.*, 2001; Kiyama *et al.,* 2018). These factors upregulate the expression of mitochondrial transcription factor A mitochondrial (mTFA), a mitochondria matrix protein, imperative for mitochondrial DNA replication (Canto *et al*., 2009). In this context, NRF-1, a vital transcriptional regulator of genes encoding respiratory chain proteins, regulates cell acclimatization to

energy stress by converting various physiological or metabolic distresses into an increased capacity to produce energy. Of particular importance is the expression of a master regulator of mitochondrial biogenesis; the peroxisome proliferator-activated receptor-γ (PPAR-γ) co-activator 1 α (PGC1) family (Wu *et al.*, 1999; Kiyama *et al.,* 2018). PGC1α is a transcriptional coactivator involved in energy metabolism and regulation of mitochondrial biogenesis and function. It binds transcription factors containing a LXXLL motif, stimulating their activity, and remodels chromatin to upregulate transcription of genes related to mitochondrial biogenesis (Scarpulla, 2011).

In muscles, overexpression of PGC1α is enough to convert type II b (glycolytic) fibres into mitochondria-rich type II and type I fibres, emphasising the role of PGC1α as a master regulator of mitochondrial biogenesis (Lin *et al.*, 2002; Jornayvaz & Shulman, 2010). The coactivation of NRF-1 and PGC1α induces the expression of the mitochondrial transcription factor A mitochondrial (mTFA), which in turn upregulates and increases the expression of mitochondrial genes encoding respiratory chain proteins (Scarpulla, 2011; Handschin & Spiegelman, 2011). Interestingly, the transcriptional upregulation of several genes implicated in oxidative metabolism upon AMPK activation have been reported to require PGC1α (Jäger *et al*., 2007). Further studies showed that overexpression of the constitutively active AMPK γ3 subunit resulted in an increased of PGC1α expression (Garcia-Roves *et al.,* 2008; Herzig & Shaw, 2018). Indeed, in skeletal muscle, increase in the amount of PGC-1α has been shown to occur in an AMPK-dependent manner, as has the proportion that is activated (Jager *et al.,* 2007).

Thus, LKB1-AMPK signalling is crucial in increasing mitochondrial biogenesis, which in turn is essential for maintaining mitochondrial bioenergetics function and energy homeostasis.

1.6. Mitochondrial dysfunction and cytopathology

The following section will examine the mitochondrial function in maintaining cellular health as well as the mitochondrial diseases that arise from disrupting mitochondrial homeostasis. The phenotypic features of mitochondrial disease will be highlighted in the *Dictyostelium discoideum* model and the reason this model has been selected to research the role of LKB1-AMPK in mitochondrial dysfunction.

1.6.1. The mitochondrion: structure and function

Mitochondria are energy-producing organelles located in nearly all eukaryotic cells except mammalian erythrocytes (Taanman, 1999; Attardi *et al.*, 2002). They are most abundant in tissues that require high energy demand such as skeletal muscle, the heart, liver, cochlea and brain. Mitochondria are considered to have developed one to two billion years ago from aerobic α-proteobacteria that colonized primordial eukaryotic cells (DiMauro & Schon, 2003; DiMauro & Davidzon, 2005; Lister *et al*., 2005; Gray, 2012). The symbiotic relationship was fundamental for the production of more efficient energy by oxygen metabolism and hence to the evolution of the eukaryotic cell. As a consequence of this symbiosis, eukaryotic cells possess two genomes: mitochondrial DNA (mtDNA) and nuclear DNA (nDNA). The mtDNA genome has altered considerably from its original autonomy with the course of evolution, as a result of the transfer of genes to the nuclear genome. This in turn has made it reliant on nDNA, which encodes a variety of factors required for the transcription, translation and replication of mtDNA (DiMauro, 2004; Gray, 2012). Additionally, nDNA encodes most of the proteins required for the energy-producing multi-enzyme complexes that form the mitochondrial respiratory chain (MRC).

The largest mitochondrial genome discovered so far belongs to *Reclinomonas americana* of the Jakobid eukaryote order. Their genome spans 69,034 base pairs and codes for 97 gene products, of which 67 are proteins and 30 are structural RNAs (Lang *et al.,* 1997; Burger *et al.,* 2013). In *Dictyostelium,* the mitochondrial genome is 55.5 kb DNA base pair long (Le *et al.,* 2009); whereas the mammalian mitochondrial genome (mtDNA) is much smaller and is a circular 16.6-kb double stranded DNA encoding 37 gene products; 13 of which are components of an electron transport chain (ETC), 2 are 16S and 12S ribosomal RNAs (rRNAs) and 22 are transfer RNAs (tRNAs) that are needed for translation of the protein encoded by the mitochondrial genome (Cooper, 2000; Chinnery & Hudson, 2013). The rest of the mitochondrial proteins (>99%) are encoded by nuclear DNA (nDNA).

1.6.1.1. The mitochondrial structure

Mitochondria are complex specialised organelles organised into a complex interacting mobile reticular network, whose establishment and maintenance is dependent on balanced

mitochondrial fusion and fission events (Frey & Manella, 2000; Paumard *et al.*, 2002; Scott & Youle, 2010). This dynamic behaviour of mitochondria is essential for various cellular functions (Westermann, 2003; Friedman & Nunnari, 2014).

The mitochondria are comprised of two lipid membranes, an outer mitochondrial membrane (OMM) and an inner mitochondrial membrane (IMM), which split the mitochondria into two compartments, the matrix, bounded by the IMM, and an intermembrane space (IMS), between the IMM and OMM. The OMM is smooth and permeable providing a route for molecules less than 5 kDa to enter the IMS, while the IMM is quite impermeable and folded to form cristae, which are tubular invaginations that project into the matrix and greatly increase the surface area of the IMM (Cooper, 2000; Hung *et al.,* 2014). The number of cristae is elevated in cells with a higher demand for ATP (Scheffler, 2001; Kühlbrandt, 2015). The granular mitochondrial matrix contains inclusions such as calcium salts and organic crystals as well as various enzymes for fatty acid oxidation and the citric acid cycle, ribosomal ribonucleic acids (rRNAs), transfer RNAs (tRNAs) and mtDNAs (Calabrese *et al.*, 2001; Hung *et al.,* 2014).

The nuclear-encoded mitochondrial proteins are created in the cytoplasm and imported into the mitochondria via the mitochondrial protein import machinery (Schmidt *et al.*, 2010). This includes the ATP-generating OXPHOS system which is comprised of an electron transport chain (ETC) and ATP synthase. The ETC consists of five multi-protein enzyme complexes (Complex I-V) located in the IMM and two electron carriers, ubiquinone (also known as coenzyme Q) and cytochrome C (CytC), that are situated in the IMM and IMS, respectively (Figure 1.17).

Complex I, better known as NADH ubiquinone oxidoreductase, is comprised of NADH dehydrogenase, the cofactor flavin mononucleotide and six associated iron-sulphur centres (Milane *et al.,* 2015). In humans, Complex I contains 7 subunits encoded by mtDNA (ND1, 2, 3, 4, 4L, 5, 6), and 38 subunits encoded by nDNA (Ryan & Hoogenraad, 2007). Complex II, known as succinate ubiquinone oxidoreductase, is associated with cytochrome b, three iron-sulphur centres and flavin adenine dinucleotide (Milane *et al.,* 2015). All four subunits of Complex II are nDNA encoded (Ryan & Hoogenraad, 2007). Complex III, or ubiquinol-cytochrome c oxidoreductase, contains an iron-sulphur centre, cytochrome b and cytochrome c1. Cytochrome b, is the only subunit of Complex III encoded by mtDNA in humans, whereas, the other 10 subunits are encoded by nDNA (Ryan & Hoogenraad, 2007; Milane *et al*., 2015). Complex IV, known as cytochrome c

oxidase, has CuA, CuB, cytochrome a and cytochrome a3 (Milane *et al.*, 2015). Three subunits of human complex IV (cytochrome oxidase (CO) I, II, III) are encoded by mtDNA, while the other 10 subunits are encoded by nDNA (Ryan & Hoogenraad, 2007). And finally, Complex V, better known as the proton (H^+) translocating ATP synthase is an F1F0-ATPase. Two subunits of human Complex V, ATP6 and ATP8, are mtDNA encoded, while the other 14 subunits are nDNA encoded (Figure 1.17).

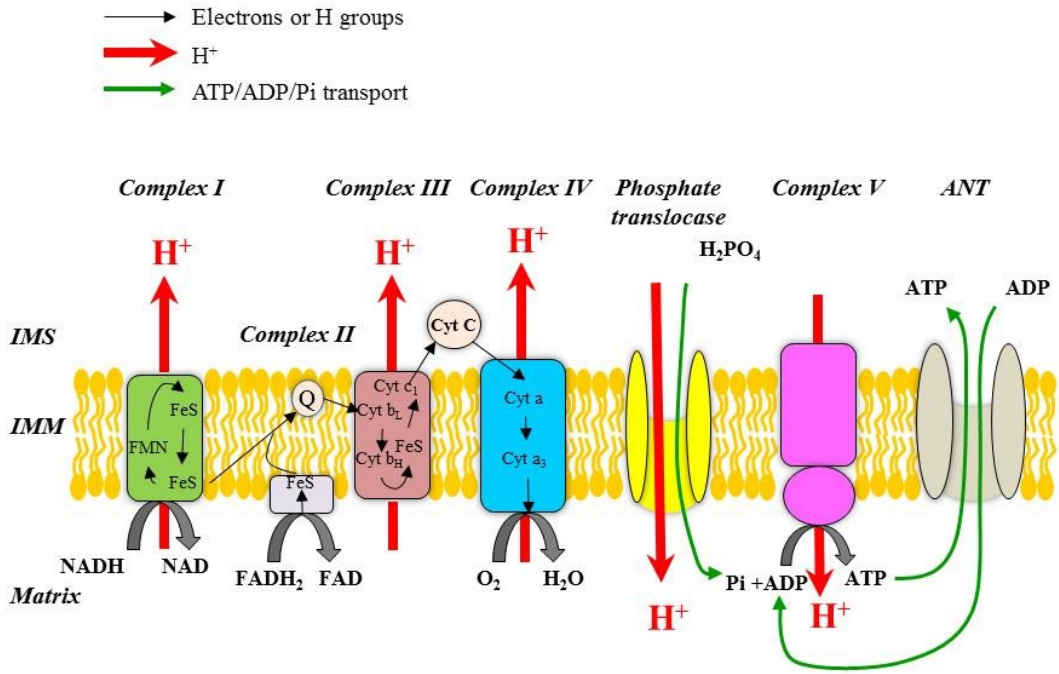

Figure 1.17. The mitochondrial respiratory chain and oxidative phosphorylation.
FeS: Iron-sulfur centre, FMN: Flavin mononucleotide, Q: Ubiquitin, Cyt: Cytochrome, Pi: inorganic phosphorus, ADP: Adenine diphosphate, ATP: Adenosine triphosphate, NAD: Nicotinamide adenine dinucleotide, NADH: reduced form of NAD, FAD: Flavin adenine dinucleotide, FADH2: Hydroquinoneform of FAD, IMS-intermembrane space, IMM: Inner mitochondrial membrane.

The transfer of electrons (red arrows) and proton pumping activity of respiratory complexes (blue arrows) are indicated. (Modified from García-Bermúdez & Cuezva, 2016; with permission)

1.6.1.2. Mitochondrial function

The mitochondria are the cell's powerhouse, generating more than 90 % of the cellular energy, in the form of adenosine 5'-triphosphate (ATP) that is vital for viability and growth (Taanman, 1999). Mitochondrial function in mammalian cells is usually described as the central pathway for energy metabolism, but can also encompass other roles including apoptosis, free radical production, calcium signalling and thermogenesis (Taanman, 1999; Leclerc & Rutter, 2004; Chinnery & Turnball, 2000; Bianchi *et al.,* 2016; Cedikova *et al.,* 2016). In healthy tissues, the mitochondria oxidise a mixture of substrates such as fatty acids, pyruvates, etc. in order to generate NADH and/or FADH2 which are then further oxidised by the respiratory chain. This in turn is used to establish an electrochemical gradient of protons which is utilised by the F1F0 ATP synthase to generate ATP, the main form of energy used by the cells. ATP has an essential function in cellular energetics as an intermediate carrier of chemical energy that associate catabolism with biosynthesis (Lipmann, 1941; Senior *et al.,* 2002; Jonckheere *et al.,* 2011). The pathways of nucleotide metabolism are associated with the function of adenine nucleotides, mainly ATP, in regulating cellular metabolism (Atkinson & Walton, 1967; Chapmann & Atkinson, 1977) and cellular bioenergetics (Haddoch & Hamilton, 1977). Nearly all of the energy-driven processes in the cells are pushed directly or indirectly by the breaking down of one or the other of the acid anhydride bonds in ATP, yielding ADP or AMP. ATP can be directly employed in cellular metabolism, but can also drive specific biosynthetic processes, by being utilised to reversibly transfer the free energy of hydrolysis of its phosphate group to the diphosphates of other intracellular nucleotides as required for biosynthesis. The regulation of cellular metabolism is a result of successful integration of various metabolic control systems at different biochemical levels and time scales extending from genetically regulating the synthesis and activity of enzymes to utilising the kinetic and thermodynamics aspects of the system to achieve fine metabolic tuning (Jones, 1977; Jonckheere *et al.,* 2011; Zala *et al.,* 2017).

1.6.2. Lowered cellular energy state affected by pathophysiological conditions

When excitable cells like skeletal and cardiac muscle, brain and nerve cells or retinal photoreceptor are activated, the turnover of ATP may increase by several degrees of magnitudes; however, the levels of ATP remain remarkably steady. The ratio of ATP/ADP and ATP/AMP are also retained. This situation ensures ideal effectiveness of cellular ATPases that execute countless energy dependent cellular activities such as muscle contraction, ion pumping, cell motility, etc. (Dudley *et al*., 1997, Kuo & Ehrlich, 2015).

However, when the cells are exposed to recurrent stress signals that culminate in lowered high-energy-phosphates or when the enzymes directly engaged in high-energy-phosphates metabolism are removed, the energy status of the cells can become compromised. The depletion in energy then becomes physiologically prominent particularly at high workloads resulting in the stimulation of compensatory reactions and adaptations that lead to an increase in the highest capacity to generate ATP (Wakerhage & Woods, 2002). These adaptations involve the activation of AMPK-sensitive catabolic processes such as the oxidation of fatty acids to generate ATP (Hardie & Hawley, 2001; Long & Zierath, 2006; Hardie, 2011; Garcia & Shaw, 2017), upregulation of the expression of PGC1α coupled with NRFs to promote mitochondrial biogenesis (Barrientos & Moraes, 1999; Lehmann & Kelly, 2002; Zong *et al.,* 2002; Jornayvaz & Shulman, 2010; Suliman & Piantadosi, 2016), stimulation of satellite cell proliferation (Wakerhage & Woods, 2002; Mounier *et al.,* 2015) and the increase of glucose uptake (Zong *et al.,* 2002; Mihaylova & Shaw, 2011).

These events compensate for the deficit in cellular energy with more intense outcomes observed in mitochondrial dysfunction. A deficiency in the mitochondrial oxidative phosphorylation system leads to the generation of energy needed for growth almost entirely via glycolysis (Hofhaus *et al.,* 1996; Pfieffer *et al.,* 2001; Wallace & Fan, 2010). For example, a decline in the production of mitochondrial ATP can be directly counteracted by a comparable increase in glycolysis (Korzeniewski, 2000; Rossingal *et al.,* 2000; Zheng *et al.,* 2016). Where oxidative phosphorylation can generate a high yield of ATP at a low rate, glycolysis generates a lower yield of ATP but at a high rate (Pfeiffer *et al.*, 2001). The major indication of the change in energy production in the cytosol is the (ATP)(ADP)/(Pi) ratio (Hardie & Hawley, 2001).

Given its key roles in energy metabolism, it is not surprising that mitochondrial function is essential in maintaining cellular health and mitochondrial dysfunction results and contributes to various disease states.

1.6.3. Mitochondrial diseases

Mitochondrial diseases are a group of disorders caused by malfunctioning of the mitochondrial oxidative system leading to an array of severe and assorted, degenerative human disorders (Wallace, 1999; Skladal *et al.,* 2003; Martinez-Vincente, 2017). Pathological outcomes include exercise intolerance (Hutchinson *et al*., 2005; Lott *et al.,* 2013) as well as cardiomyopathy, neuromuscular disorders, diabetes mellitus, fatal encephalomyopathies and liver disease (Kirvy *et al.*, 2004; Jain-Ghai *et al.*, 2013). These disorders develop due to defective mitochondrial respiratory chain complexes that arise as a result of mutations in mitochondrial and nuclear genes encoding subunits of the five complexes of the oxidative phosphorylation system (OXPHOS) or other mitochondrial proteins fundamental for maintaining the function of OXPHOS (Rossignol *et al.,* 2003; Alston *et al.,* 2017). The severity of the disorders alters in accordance with the oxidative requirements of the affected tissues (Lehmann & Kelly, 2002; Chinnery & Hudson, 2013).

Respiratory chain deficiency and lactic acidosis are two prominent biochemical features exhibited in most mitochondrial diseases (DiMauro & Schon, 2011, Alston *et al.,* 2017). Mitochondrial disease can virtually affect any organ or tissue in the body, but it severely affects organs, such as the brain, heart and skeletal muscle, which have the highest aerobic demand and lowest regenerative capacity (Rossignol *et al.,* 2003; DiMauro *et al.*, 2013). Tissues can also be affected individually, e.g. mitochondrial encephalomyopathy (Schon *et al*., 1997; Martinez-Vincente, 2017). Regardless of these complexities, insufficient ATP generation persists to be the prevailing parameter in the pathogenesis of mitochondrial diseases (Rossignol *et al*., 2003; McKenzie *et al.,* 2004).

In mitochondrial diseases, the manifestation of various cellular pathologies seems to occur at different thresholds in regard to the severity of the underlying genetic disorder (Helm *et al.,* 1999; Schapira, 1999; Alston *et al.,* 2017). Moreover, different mutations in mtDNA can lead to the same clinical manifestations; and conversely, different clinical phenotypic outcomes can result from the same genetic mutation in mtDNA or biochemical defects

affecting the same respiratory chain complex (Rossignol *et al*., 2003; Thornburn, 2004). This complexity in the genotype-phenotype relationship is due to numerous factors including the nature and variability of the mutations in different individuals and multiple disparate mutations in various tissues. It can also be affected by the increasing impact of mitochondrial damage throughout ageing, the diverse initial loads of maternally inherited mutations and the assorted segregation patterns that mutant mtDNA undergo through in early development (Zeviani *et al.*, 1996; Schon, 2000; Leonard & Shapira, 2000; Shapira, 1999; Tuppen *et al.,* 2010; Mishra & Chan, 2014). This genetic variability can be one reason behind the dissimilar clinical manifestations in various patients resulting from a particular mutation in mtDNA. Further genetic mechanisms can also play a role in associating this defective mitochondrial genome with the manifestation of an array of clinical and biochemical phenotypic outcomes (Morgan-Hughes *et al.*, 1995). The biochemical and genetic intricacy of the respiratory chain also contributes to the extensive variety of clinical phenotypes of mitochondrial disorders (Rossignol *et al.,* 2003; Alston *et al.,* 2017).

These findings indicate that the onset, manifestations and gravity of a mitochondrial dysfunction can differ greatly (Chinnery & Turnball, 1999) and during the progression of the disease, systems which were not affected previously, may become involved (Dahl, 1998; Schapira, 1999; Greaves *et al.,* 2012). Furthermore, clinical reports are not adequate in identifying and explaining the displayed mitochondrial diseases due to the overlapping of syndromes and non-specific phenotypes (Chinnery & Turnball, 1999; Niyazov *et al.,* 2016). Interestingly, environmental and physiological stressors are known to accelerate the clinical manifestations of mitochondrial diseases by expanding the demand for the production of mitochondrial energy such as fasting or exercise, which in turn implies that a mismatch between energy demand and supply triggers organ dysfunction (Kelly & Strauss, 1994, Niyazov *et al.,* 2016). For example, acquired heart diseases are commonly marked by mitochondrial disorder (Kelly & Strauss, 1994; Parikh *et al.*, 2017), and individuals with genetic mitochondrial diseases are frequently diagnosed with cardiovascular defects, demonstrating that mitochondrial energy generation and cardiac energy demand must be balanced (Lehmann & Kelly, 2002; Czubryt *et al.,* 2003). This implication can help explain the down-regulation of fatty acid metabolizing enzymes in heart failure and the shift from fatty acid oxidation toward glucose utilisation (Czubryt *et al.,* 2003).

Research has shown that mitochondrial cytopathy can be initially characterised by renal dysfunction or it may manifest alongside neurological and neuromuscular symptoms (Buemi *et al*., 1997; Kurogouchi *et al*., 1998). mtDNA mutations are commonly associated with various syndromes such as focal segmental glomerulosclerosis (FSGS) (Kurogouchi *et al*., 1998) or tubulointerstitial nephropathy leading to terminal uraemia in infants and adults as well as Fanconi's syndrome (benign renal tubulopathy) in newborns ((Buemi *et al*., 1997; Kurogouchi *et al.,* 1998). Mitochondrial disorders are also accompanied by hyperlactatemia, raised levels of lactate and pyruvate in the cerebrospinal fluid, slight to severe hearing loss (Hameed *et al.,* 2001), severe sensorineural hearing loss (Oshima *et al.*, 1996) and cortical blindness (Rosenthal *et al.,* 1999).

In addition to the clinical manifestations of the mtDNA mutations affecting the oxidative phosphorylation components, a secondary effect of these mutations is displayed by the continual production of reactive oxygen species (ROS). Excessive ROS production results in oxidative impairment of mtDNA, respiratory chain components, cellular proteins, lipids and nucleic acids (Wallace, 1999; Raha & Robinson, 2000). Nonetheless, to compensate for the decrease in the activity of respiratory chain complexes due to ROS production, cells can detect excessive ROS and activate particular transcription factors and to express specific target genes for counteracting the ROS-induced damage (Michiels *et al.,* 2002). Furthermore, studies have revealed that the cytopathology of mitochondrial diseases affecting certain tissues manifests clearly as a result to the damaged induced by ROS and the processing of programmed cell death (Wallace, 1999; Desagher & Martinou, 2000).

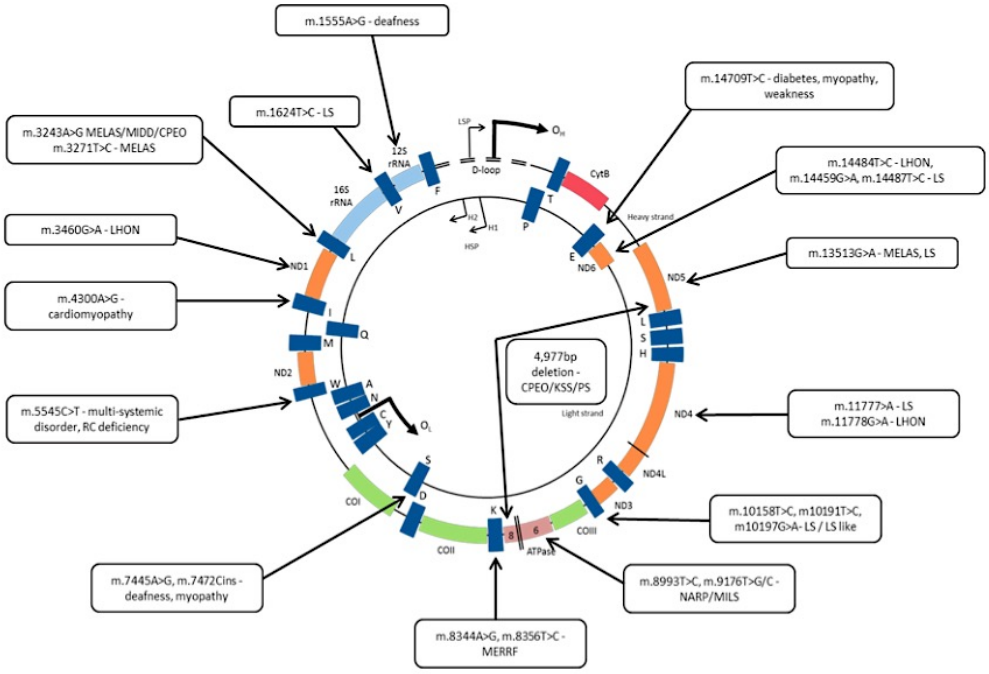

Figure 1.18. Locations of disease-causing mtDNA mutations.
Point mutations are represented by the arrows, the "common deletion" is shown in the centre of the genome. Abbreviations: CPEO – chronic progressive external ophthalmoplegia, LHON – Leber's hereditary optic neuropathy, LS – Leigh syndrome, MELAS – mitochondrial myopathy, encephalopathy, lactic acidosis, stroke-like episodes, MERRF – Myoclonic epilepsy and ragged red fibres, MILS – maternally inherited Leigh syndrome, NARP – neurogenic weakness, ataxia and retinitis pigmentosa, PS – Pearson's syndrome. Adapted from Tuppen et al. 2010, with permission.

1.6.4. Mutations causing mitochondrial diseases

Human mitochondrial disorders can be caused by mutations or deletions/duplication in mitochondrial DNA (mtDNA) encoding any one of the 13 polypeptides as well as in both mtDNA encoding ribosomal RNAs and those encoding 21 of the 22 transfer RNAs. These mutations are located solely in the genomes of the numerous mitochondria found in most cells (Buemi *et al*., 1997; Servidei, 2001; Leonard & Schapira, 2000; Vezier & Lestienne, 2000) (Figure 1.18).

Mitochondrial dysfunction can also be caused by Mendelian mutations that occur due to defects in chromosomal loci that affect the 77 nuclear-encoded OXPHOS proteins, including about 30 proteins necessary for the functioning of the 5 respiratory chain complexes (Letellier *et al.,* 1994; Dahl. 1998; Schapira, 1999). Mitochondrial disease can arise as a result to mutations in any of the 5 complexes involved directly in OXPHOS; however, deficiencies of complex II are very unusual (Rossignol *et al.,* 2003). Moreover,

mitochondrial diseases can also result from flawed interactions between nuclear and mitochondrial genes (Schon, 2000; DiMauro & Schon, 2003; Kirby *et al.,* 2004). The interaction between nuclear and organellar genomes can be accounted for some of the variety in mitochondrial pathologies (Grivennikova *et al.,* 2001). These mutations can affect the introns, exons and even the promoters. Almost any nuclear DNA (nDNA) or mtDNA mutation or deletion that affects an intermediate metabolism pathway that interfaces with the mitochondria can also affect the OXPHOS gene polymorphisms and cause a range of diseases.

1.6.4.1. Mutations of nuclear genes leading to mitochondrial diseases

Mutations in nuclear genes that encode the five enzyme complexes of the respiratory chain or affect their assembly can lead to oxidative phosphorylation deficiency (Thornburn, 2004). For example, mutations in *SURF1* or the SCO2, which are assembly genes required for the proper assembly of COX (Tiranti, 1998; Kirby *et al.,* 2004) result in cardioencephalomyopathy in infants, pure myopathy and Leigh's syndrome (Campos *et al*., 1997; Rossignol *et al*., 2003; Freisinger *et al*., 2001). Nuclear gene defects mainly result in autosomal recessive disorders; as well as a few cases of autosomal dominant and X-linked diseases (Thornburn, 2004). Certain diseases such as Autosomal Dominant Progressive External Opthalmoplegia (adPEO), which is characterised by progressive weakening of external eye muscles, can result from mutations in nuclear genes essential for mtDNA replication (such as *Polg1* and *C10orf2*), which in turn impairs proper interactions between nuclear and mitochondrial genes (Coplenad, 2012; Spelbrink *et al.*, 2001; Rossignol *et al.,* 2003).

As there are around 1100 nuclear encoded mitochondrial proteins already identified, and as more mitochondrial proteins are to be unveiled, it is highly likely that more mitochondrial diseases resulting from nuclear gene mutations will be revealed in the future.

1.6.4.2. Mutations of mitochondrial DNA leading to mitochondrial diseases

1.6.4.2.1. Point mutations of mtDNA leading to mitochondrial diseases

Over 70 detrimental mutations in the mitochondrial DNA have been reported to cause human OXPHOS disorders (Chinnery *et al*., 2000; Thornburn, 2004). Many of these point mutations are reported to be heteroplasmic, a state in which the same mitochondriome contains two or more coexisting mtDNA populations (Chinnery *et al*., 2000; Leonard & Schapira, 2000). The increased prevalence of these heteroplasmic mtDNA is a result of mutations of the human mtDNA at a rate of ten to twenty times quicker than those of nuclear DNA due to poor proofreading by mitochondrial DNA polymerases (Leonard & Schapira, 2000) and restricted repair capacity of mtDNA (DiMauro & Schon, 2001). Although a vast number of pathogenic point mutations have been detected in the mitochondrial genome, there are five mutations reported to be the most recurrent (DiMauro & Schon, 2001).

The A3243G transition in transfer RNA$^{Leu(UUR)}$ gene is the most common point mutation for MELAS (mitochondrial encephalomyopathy with lactic acidosis and stroke-like episodes) disease and accounts for ~80% of the cases (Goto *et al.,* 1990, Kurogouchi *et al.,* 1998; Fan *et al.*, 2006). It is also linked to other mitochondrial diseases including maternally inherited diabetes and deafness (MIDD). This mutation inhibits 5-taurinomethyluridine modification of the uridine wobble-position in tRNA$^{Leu(UUR)}$, resulting in a decrease in the translation. (Kirino *et al*. 2004). In Cybrid cells (Cytoplasmic hybrid cells used to integrate human subject mitochondria and maintain its mitochondrial DNA (mtDNA)-encoded components in order to examine the impact of mtDNA on cell function), the level of aminoacylated tRNA$^{Leu(UUR)}$ and total tRNA$^{Leu(UUR)}$ are both reduced with research revealing that the mitochondrial 3243A>G mutation can dimerize the tRNA by encoding a self-complementary region in the D-loop of the tRNA. This in turn leads to a decrease in the aminoacylation of the mutated species resulting in reduced levels of tRNA$^{Leu(UUR)}$ present for translation (Wittenhagen & Kelley, 2002). A reduction in the rate of protein synthesis results in a reduced availability of the OXPHOS

complexes required for oxidative phosphorylation, and hence in an overall lower OXPHOS activity (Ciafaloni *et al*., 1992).

The A8344G in the $tRNA^{Lys}$ gene is another common mutation, most frequently associated with Myoclonic Epilepsy with Ragged Red Fibres MERRF) (Shoffner *et al*., 1990; Yoneda *et al.,* 1990; Fan *et a*l., 2006). This point mutation is located in the TψC loop of mitochondrial $tRNA^{Lys}$ and results in the taurine modification of the uridine wobble-position similar to that exhibited by m.3424A>G (Yasukawa *et al*. 2000) leading to decreased translation rates. Faulty modification can lead to a reduction in the correct codon-anticodon binding due to the diminished stability of the codon-anticodon interaction which enhances the misincorporation of lysine into nascent peptides (Yasukawa *et al.,* 2001).

The T8993G mutation occurs in the ATPase subunit 6 and is mainly associated with Neuropathy, ataxia, retinitis pigmentosa (NARP) disease (Thyagarajan *et al*., 1995; Carrozzo *et al.,* 2001). This mutation affects the ATP synthase subunit 6 by changing Leu156 to Arg which results in phenotypic manifestations of NARP as the heteroplasmy levels reach 90-95% mutant (Tatuch *et al.* 1992).

The T8993G or T8993C point mutation also leads to maternally inherited Leigh's syndrome (MILS) in humans (Tatuch *et al*., 1992; Carrozzo *et al*., 2001). MILS is associated with respiratory abnormalities, dystonia and optic atrophy. The disease is often terminal and post mortem examination displays necrotic lesions of the brain stem, basal ganglia and thalamus. Symptoms related with MILS normally manifest when the mutant heteroplasmy level is greater than 95% (Tatuch *et al.,* 1992).

These associated mitochondrial disorders are generally agreed to occur as a consequence of the impairment in the synthesis of ATP. This mutation occurs close to Glu58 in subunit c of ATP synthase, which is a crucial amino acid residue for the transport of protons. Further research has also revealed that the ability of the c ring subunits to rotate is altered by the mutation which then prevents F_1 subunit from manoeuvring the rotational torque to generate ATP from ADP and P_i (Sgarbi *et al.,* 2006).

Finally, the point mutation G11778A is commonly found in Leber's hereditary optic neuropathy (LHON) (Fischel-Ghodsian, 1988), one of the most common mitochondrial diseases (Chinnery *et al*., 2000). This mutation occurs in Complex I subunits and leads to

the loss of retinal ganglion cells in the optic nerve. The resultant symptoms encompass acute or subacute visual loss that affects both eyes usually within 2 months, predominantly in males aged 15-35 (Chinnery *et al*., 2000).

The mutation rate in mtDNA is exceptionally high allowing the mtDNA to amass an extensive variety of population-specific base substitutions (Rossignol *et al.,* 2003). Although the majority of these variants are neutral, some are mildly deleterious. These latter mutations might not have a drastic effect on reducing fitness; nonetheless, they may interconnect with nuclear and environmental elements and increase the risk of developing neurodegenerative diseases in predisposed individuals later in life (Schon *et al.*, 1997; DiMauro & Schon, 2001; Servidei, 2001; Rossignol *et al.,* 2003). Furthermore, interdependent mild deleterious polymorphisms may affect mitochondrial function and hence the severity of a mitochondrial disorder (Schon, 2000; DiMauro & Schon, 2001). Certain point mutations are linked to a particular phenotype whilst other point mutations lead to an extensive array of clinical symptoms.

1.6.4.2.2. Deletions of mtDNA leading to mitochondrial diseases

Mitochondrial diseases can also occur as a result of single large-scale deletions or multiple deletions of mtDNA (Yamamoto *et al*., 1991; Schon *et al.,* 1997).

The large-scale deletions commonly occur between 13-base pair direct repeat from nucleotide (nt) 8470 to nt 8482 and from nt 13447 to nt 13459 in the ATPase8 and the ND5 gene respectively (Moraes *et al.,* 1989). The resulting 4997 bp deletion (the common deletion) represents arounds 50% of ocular myopathy patients (Moraes *et al*., 1989; Porteous *et al.,* 1998).

Single large-scale deletions are usually acquired through the germ-line and are associated with certain paediatric-onset mitochondrial diseases such as Kearns-Sayres syndrome (KSS) (Lestienne & Ponsot, 1988; Zeviani *et al.,* 1988). KSS is a multisystem disorder resulting in cerebellar ataxia and cognitive impairment and is associated with the progression of retinitis pigmentosa and progressive external ophthalmoplegia (PEO) in patients before the age of 20 (Tuppen *et al.* 2010).

Multiple deletions are associated with mutations in the Twinkle mitochondrial helicase

(*PEO1*) and the mitochondrial catalytic subunit of DNA polymerase γ (*POLG*) and are linked to chronic progressive external ophthalmoplegia (CPEO) disease which is characterised by advanced paresis of the eye, bilateral ptosis, proximal weakness and in some causes problems with cardiac conduction (Agostino *et al.* 2003). This was initially discovered in 1989 when an autosomal dominant inherited mutation was reported to cause multiple mitochondrial deletions (Zeviani *et al*. 1989).

The proportion of deletion-bearing mitochondrial genomes has the most effect on developing defective tissues rather than the location or size of the deletion in mtDNA (Rossignol *et al*., 2003). The size of deleted mtDNA has been revealed to be inversely correlated to age of onset (Yamamoto *et al.,* 1991). mtDNA deletions as well as other mitochondrial function defects have also been found to occur with ageing as well as in an assortment of attained pathophysiologic disorders including ischaemic heart disease and hypertrophied and failing heart (Zhu, 1998; Lehman *et al.*, 2000).

1.6.4.2.3. Duplication of mtDNA leading to mitochondrial diseases

Deletions in mtDNA are additionally accompanied by mtDNA duplications compensating for the corresponding deleted region in the mtDNA; although duplications occur at a much scarcer rate (DiMauro & Schon, 2001). Partial duplications detected in mtDNA have been revealed to also be associated with ocular myopathy and Pearson's syndrome. mtDNA duplications can be maternally inherited or acquired sporadically (Rossignol *et al.,* 2003). Duplications as well as deletions in mtDNA are heteroplasmic, and can exist concurrently on occasional basis (Schroder *et al*., 2000; Hiyashi *et al*., 2002). Since essentially all deletions eradicate at least one tRNA, it is possible they cause a generalised defect in translation (Zhou *et a*l., 1997; Helm *et al*., 1999). The severity of the inherited phenotypic manifestations and the acquired mitochondrial diseases emphasise the significance of generating high capacity mitochondrial energy to maintain normal body function (Lehmann *et al.*, 2000).

1.6.4.3. Threshold effect

mtDNA mutations in cells can reach high levels (>60%); however, a critical level of mutated mtDNA needs to be reached before a cell displays a deficient phenotype or clinical signs of mitochondrial disease. This phenomenon is called the threshold effect. If the threshold is not reached, the mutated molecules can be compensated for by wild type mtDNA resulting in no biochemical deficit in cells. If the threshold is reached and exceeded, it is improbable for the cells to generate enough ATP to function properly (Sciacco *et al.*, 1994). The threshold differs amongst individuals as a result of diverse nuclear backgrounds and also differs between tissues where it is found to be lower in high energy demand tissues such as the skeletal muscle, heart, brain, retina, renal tubules and endocrine glands (DiMauro & Schon 2003, Korpelainen 2004). The threshold for tRNA mutations is generally required to exceed 80% to overcome the compensation of wild type mtDNA for their deficiencies (Taylor & Turnbull, 2005; Chinnery & Hudson, 2013).

The severity of mitochondrial diseases has been found to be positively correlated with heteroplasmic mtDNA point mutations in which increased levels of heteroplasmy lead to more severe phenotypic outcomes, particularly in post-mitotic tissues such as skeletal muscle (DiMauro & Schon, 2003; Korpelainen, 2004; McKenzie *et al.,* 2004; Alston *et al.,* 2017). Low heteroplasmy pathogenic mutations have also been documented including the mt-tRNA^{Glu} m.14723 T>C mutation and the tRNA^{Trp} m.5545C>T mutation which display mitochondrial disease phenotypes at 7% mutation heteroplasmy (Alston *et al.,* 2010) and <25% mutation heteroplasmy respectively (Sacconi *et al.,* 2008).

1.6.4.4. Mitochondrial diseases in *D. discoideum*

mtDNA mutations associated with human mitochondrial diseases have been widely researched and characterised; however, the relationship between genotype and phenotype is complex and not well understood. The variation in the proportion of mutated mtDNA in different individuals and in different tissues or in the same individuals and in the same tissues at different ages, combined with variations in energy requirements in tissues and expressions of nuclear-encoded mitochondrial proteins, all can lead to the manifestation of either similar or very different phenotypic outcomes depending on the proportion and distribution of the mutant mitochondria (Schapira, 2006; Zeviani &

Carelli, 2007). An example is the same underlying molecular pathology of mitochondrial disease can lead to blindness if it is produced in photoreceptor cells in the retina, however it can cause parkinsonism if it occurs in the *substantia nigra* (Schapira, 2006; Zeviani & Carelli, 2007).

These complications in understanding the genotype-phenotype relationship of mitochondrial diseases can be avoided in *Dictyostelium discoideum*. *D. discoideum* is an amoeba that have a distinctive life cycle in which its unicellular stage represents a single, clonally grown, haploid, totipotent stem cell type, while its multicellular development is commenced by aggregation and undergoes a terminal differentiation forming a fruiting body consisting of a basal disc, a stalk and a spore droplet. The stalk and spores are formed from prestalk cells and prespore cells respectively (Williams, 2006). Eventually, the stalk cells undergo autophagic cell death and the spores are released into their surroundings and germinate under favourable conditions continuing the life cycle (Chisholm & Firtel, 2004) (Figure 1.19). This life cycle does not have a sexual stage, involves relatively few cell types and takes place without the overlaid complications of cell growth and division (Francione *et al.,* 2011). Moreover, the mitochondrial genome of *Dictyostelium* has been fully sequenced (Ogawa *et al*., 2000), and its mitochondrial transcription and RNA processing have been well studied (Barth *et al.,* 1999; Barth *et al.,* 2001; Fisher *et al*., 2009). Research has revealed that in *D. discoideum,* mitochondrial mutations affecting oxidative phosphorylation lead to common impaired phenotypic outcomes despite of the causal mutation (Francione *et al.,* 2011).

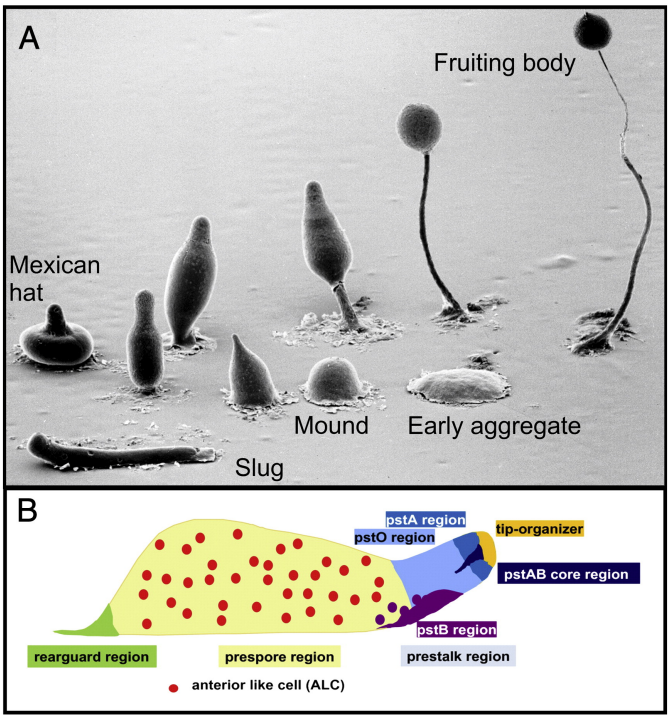

Figure 1.19. Life cycle of *Dictyostelium discoideum*.

A. The initiation of a multicellular developmental programme in *Dictyostelium di*scoideum is triggered by starvation. Pulses of cAMP are emitted by individual amoebae which are attracted to it resulting in the aggregation of about 100,000 cells. The cells then differentiate into prestalk and prespore cells resulting in the formation of a finger, which in turn falls over to form a motile slug for a variable period of time. The slug stops migration and further differentiates into a fruiting body comprising of two main cell types forming the long slender stalk and spore cells enclosed in a sorus atop the stalk. Each spore can then germinate to release a vegetative amoeba and renew the life cycle.

B. Cell types in the motile *Dictyostelium* slug. Most of the cells are prespore cells, which later become spores in the sorus and reside in the rear two-third of the slug. The figure displays the distribution of the prestalk cell subtypes at the front as well as the tip, rearguard and anterior like cells.

(Adapted from Annesley *et al.*, 2014; with permission).

Previously, it was believed that mitochondrial disease and its resultant phenotypic manifestations were caused by a depletion of ATP; however, diverse cytopathological outcomes in *Dictyostelium* have been revealed to result from the chronic activation of the cellular energy sensor AMPK (Bokko *et al.*, 2007; Francione *et al.*, 2011). Chronic activation of AMPK and the ensuing dysregulation of its signalling pathways lead to the phenotypic outcomes associated with mitochondrial disease. Separate to this discovery in *Dictyostelium*, AMPK has been revealed to be chronically activated in several mammalian neurodegenerative disorders that involve mitochondrial dysfunction (Chou *et al.*, 2005; Lopez *et al.*, 2007; Lim *et al.*, 2012) in which AMPK plays a cytopathological role.

Chronic AMPK activation in mitochondrially diseased *Dictyostelium* results in common phenotypic outcomes including the formation of short, thickened and misshapen stalks in the final stages of morphogenesis. The prestalk/stalk differentiation pathway is also a form of autophagic cell death, uncomplicated by the presence of apoptosis. Other common phenotypes displayed include AMPK-dependent defects in growth, as well as aberrant slug phototaxis and thermotaxis (Bokko *et al.,* 2007). These AMPK-dependent phenotypic outcomes result from generalised OXHPOS defects in which multiple respiratory complexes are coordinately affected.

1.6.4.4.1. Generalised mitochondrial OXPHOS defects result in common defective phenotypes in *Dictyostelium*

To gain a better understanding of mitochondrial diseases in *D. discoideum,* several approaches have been used to create mitochondrial respiratory dysfunction. The first is to antisense inhibit the expression of chaperonin 60 (Cpn60), an essential nuclear-encoded mitochondrial protein (Kotsifas *et al*., 2002). The knockdown of chaperonin 60 produces a general defect in the folding of mitochondrial proteins. The other two approaches involve the depletion of mitochondrial DNA with ethidium bromide treatment (Chida *et al.,* 2004) and heteroplasmic gene disruption i.e. disruption of mitochondrial genes in a subset of the mitochondrial genomes in the cell (Wilczynska *et al.,* 1997; Inazu *et al*., 1999; Francione & Fisher, 2011). The latter two approaches cause a decrease in the expression of the entire mitochondrial genome (Chida *et al.,* 2004, Francione & Fisher, 2011). All these methods result in a generalised respiratory dysfunction which coordinately affects at least Complex I, III, IV and V of OXPHOS, all of which consist of subunits encoded in the mitochondrial genome.

To establish whether the phenotypic outcomes of mitochondrial disease are consistent irrespective of the mitochondrial gene that is targeted, a study was conducted of the heteroplasmic disruptions of 9 different genes spread around the mitochondrial genome (Francione & Fisher, 2011) (Figure 1.20). It was expected that the sequences at different distances downstream of the targeted gene might be affected differentially due to the unidirectional transcription of the entire *Dictyostelium* mitochondrial genome from a single promoter. However, there was no detectable polar effect on mitochondrial gene expression so that no correlation was found between the relative levels of expression and

the position of the targeted gene in the mitochondrial disruptants (Francione & Fisher, 2011). In fact, genetic examination utilising quantitative northern hybridisation analysis showed that the expression of genes throughout the entire mitochondrial genome were reduced relative to cellular mRNA levels in the mutants compared to the wild type strain. This decrease implies that the plasmid insertions either lead to an increased instability of the RNA transcripts or reduced rates of transcription.

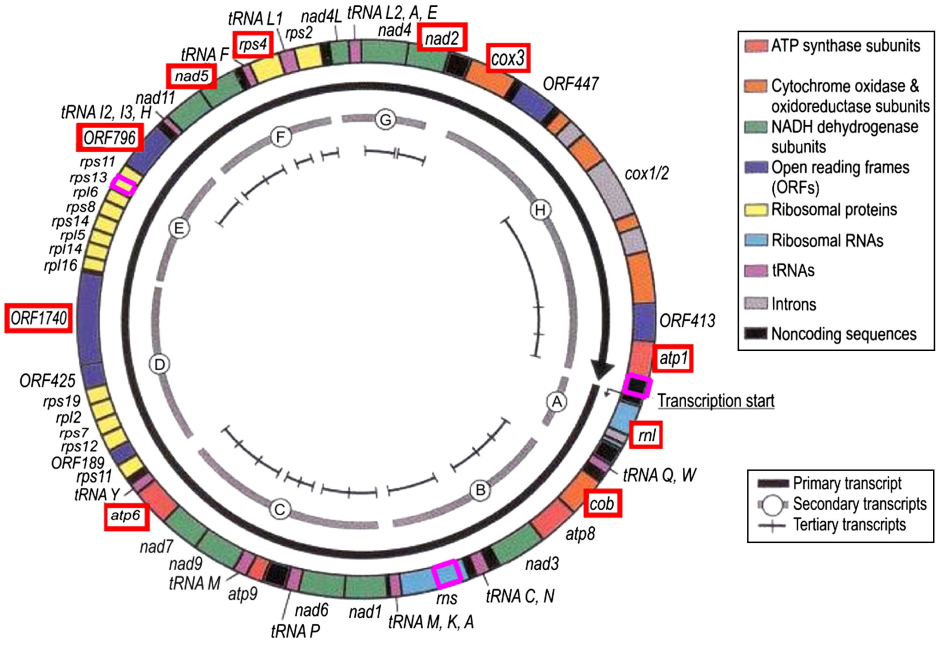

Figure 1.20. The *Dictyostelium discoideum* mitochondrial genome map portraying genes targeted for heteroplasmic disruption.

A single transcription start site is used to initiate transcription of a large primary transcript, which spans the entire genome. This primary transcript is cotranscriptionally processed into secondary and tertiary transcripts. The figure highlights the genes targeted for disruption in the mitochondrial genome map by outlining them in red boxes. Six genes encode subunits of respiratory chain enzymes — *atp1*, *atp6*, *cob*, *cox3*, *nad2* and *nad5*; one encodes the large subunit ribosomal RNA — *rnl*; one encodes a small ribosomal subunit protein — *rps4*; two encode the open reading frames *ORF1740* and *ORF796*–ORF1740 encodes a ribosomal S3 C-terminal domain-containing protein, whereas the function of the ORF796 product is unknown. (Figure is adapted from Francione & Fisher, 2011; with permission).

The heteroplasmic disruption of mitochondrial genes in *Dictyostelium* resulted in aberrant phenotypes including abnormal multicellular development, slow growth, both on plates and in liquid medium (Francione & Fisher, 2011), and impaired slug phototaxis and thermotaxis. This display of phenotypic manifestations was consistent, regardless of the

position of the gene in respect to the single transcription initiation site and irrespective of whether the targeted gene product was known to be necessary for energy production. These phenotypic patterns are mirrored in *Dictyostelium* in which Cpn60 expression is antisense inhibited (Kotsifas *et al.,* 2002; Francione & Fisher, 2011) and mtDNA replication is inhibited by ethidium bromide (Chida *et al.,* 2004).

The *Dictyostelium* model has hence shed new light on mitochondrial disease by showing regularities in the fundamental cell biology of mitochondrial disease which have been otherwise unnoticed in humans due to the complexities of mammalian development. Unlike the complicated genotype-phenotype relationships in human mitochondrial disease resulting in unpredictable clinical outcomes even when the underlying genetic defect is known, the *Dictyostelium* model has provided a consistent pattern of mitochondrial disease phenotypes. The latter implies that all generalised defects in mitochondrial respiratory function are caused by a common cytopathological mechanism and not by a gene-specific process. This cytopathological mechanism appears to be a consequence of chronic activation of an energy-sensing protein kinase, AMPK.

1.7. Scope and objective of this study

Bokko *et al.* (2007) reported that it is the chronic activation of AMPK that leads to the cytopathological effects of mitochondrial dysfunction in *Dictyostelium,* and this can be suppressed by AMPK inhibition. Therefore, pharmacological inhibition of AMPK may be utilised as a treatment possibility for mitochondrial disease. Moreover, research has revealed that AMPK inhibition in otherwise healthy cells can stimulate cellular proliferation and even be tumourigenic. Decrease in the functional activity of AMPK such as observed in Peutz-Jeghers Syndrome due to mutations in LKB1 predisposes humans to increased risk of cancers (Boudeau *et al.,* 2003b; Zhao & Xu, 2014; Faubert *et al.,* 2014). Additionally, AMPK acts synergistically with LKB1, a known tumour suppressor, to cause death or offset growth of cancer cells (Shaw *et al.,* 2004; Wei *et al*., 2012; Zhao & Xu, 2014).

Given the role of LKB1 as the main upstream kinase and activator of AMPK and as well as a key regulator in various cellular process mediated by AMPK activation, this study aims to investigate the role of LKB1 as an upstream kinase of AMPK and whether its

function is involved in the pathophysiology of mitochondrial diseases. The working hypothesis is that chronic activation of LKB1 will result in phenotypic outcomes that are similar to those displayed by chronic activation of AMPK in *Dictyostelium discoideum* and hence associated with mitochondrial disease.

The *Dictyostelium* genome contains genes encoding homologues to LKB1 as well as its two binding partners, STRADα and MO25, allowing it to be an exploitable model for this study. Moreover, previous research conducted in *Dictyostelium* has shown that LKB1 phosphorylates and activates AMPK under osmotic and oxidative stresses. Knocking down LKB1 has not only abrogated the phosphorylation of AMPK in response to these stresses, it also severely impaired starvation-induced aggregation and subsequent multicellular development. This phenotype is not dissimilar to that caused by AMPK knockdown in strains with very high copy numbers of an AMPK antisense construct (Veeranki *et al*., 2011). These results are consistent with a possible role for LKB1 in *Dictyostelium* as the main upstream kinase responsible for AMPK activation in mitochondrially diseased cells, which will be addressed in this thesis.

1.8. The aims of this study

The aims of this thesis are the following:

1. Investigate the functions of LKB1 in LKB1-overexpressing *Dictyostelium* cells
2. Create a kinase-dead version of LKB1 to associate the phenotypic outcomes with the kinase activity of LKB1
3. Determine whether the function of LKB1 is mediated by AMPK activity, by antisense-inhibiting AMPK in LKB1-overexpressing cells
4. Determine the effects of STRADα overexpression in augmenting the function of LKB1 in LKB1-overexpressing cells

2. Materials and Methods

2.1. General Procedures

2.1.1. Sterilization

All glassware, tips and media were sterilized by autoclaving at 100 kPa for 20 minutes at 121 ^{o}C.

2.1.2. Chemicals and reagents

The chemicals, reagents, and their suppliers are listed in Appendix 1.

2.1.3. Media, Antibiotics and Buffers

The composition of the media, buffers and solutions used are listed in Appendix 2 and Appendix 3 respectively. The solvent used for all media and buffers was sterile dH_2O, unless otherwise stated.

The composition of the antibiotics used are listed in Table 2.1.

Table 2.1. The composition and concentrations of the antibiotics utilised.

Antibiotic stock solutions (All filter sterilized)		
Ampicillin	100 mg ml^{-1}	Ampicillin (sodium salt)
Streptomycin	100 mg ml^{-1}	Streptomycin (sulfate)
Kanamycin	25 mg ml^{-1}	Kanamycin (monosulfate)
Tetracycline	10 mg ml^{-1}	Tetracycline (hydrochloride)
Geneticin	30 mg ml^{-1}	Geneticin or G418 (sulfate)

2.1.4. Centrifugation

Bacterial and *D. discoideum* strains grown in < 50 mL of media were harvested by centrifugation at 12,000 x *g* for 1 minute and 250 x *g* for 2 minutes respectively, unless stated otherwise. An Eppendorf™ microcentrifuge 5424 or 5702 was used for all centrifugation. All strains grown in > 50 ml of media were harvested by centrifugation at 12,000 × *g* for 10 minutes at 4 ^{o}C using a GSA rotor in the Sorvall® RT6000B centrifuge.

2.1.5. Enzymes and Kits

The enzymes utilized and the kits employed (with their reagent compositions) are detailed in Appendix 4 and Appendix 5 respectively. The protocols were followed according to manufacturer instructions, unless otherwise specified.

2.1.6. Plasmid vectors

The plasmid vectors utilized and their schematic maps are briefly described in Figures 2.1-2.3. The plasmid constructs derived from these vectors and used in this work are listed in Table 2.2.

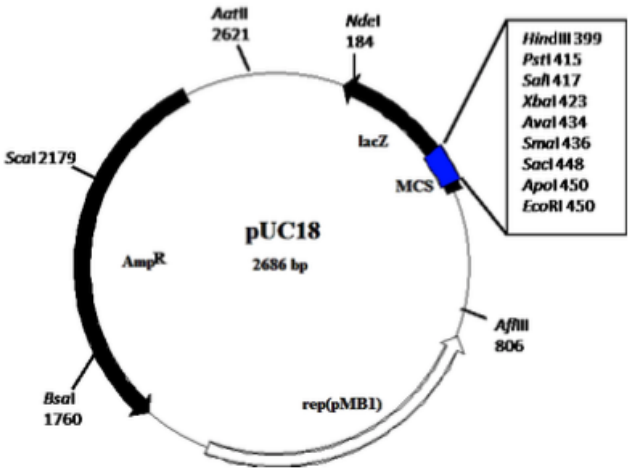

Figure 2.1. Circular map of *E. coli* cloning vector pUC18.

pUC18 holds an ampicillin resistance cassette (Amp^R), a pMB1 replication origin (rep) required for the replication of plasmid and a multiple cloning site (MCS) positioned in the lac Z operon, which can facilitate visual blue/white screening with the use of IPTG and X-gal (Vieria & Messing, 1982). Several restriction enzyme sites are displayed on the map followed by a number indicating their position. The units of map numbers are base pairs (bp).

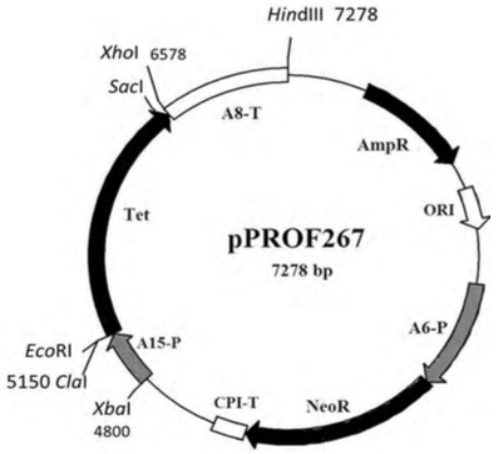

Figure 2.2. Circular map of *D. discoideum* expression vector pPROF267.

pPROF267 was created by the substitution of the GFP cassette in pA15GFP with the Tet cassette from pPROF74. Additional restriction enzymes sites were also included both sides of the Tet cassette for cloning purposes (Annesley *et al*., unpublished).

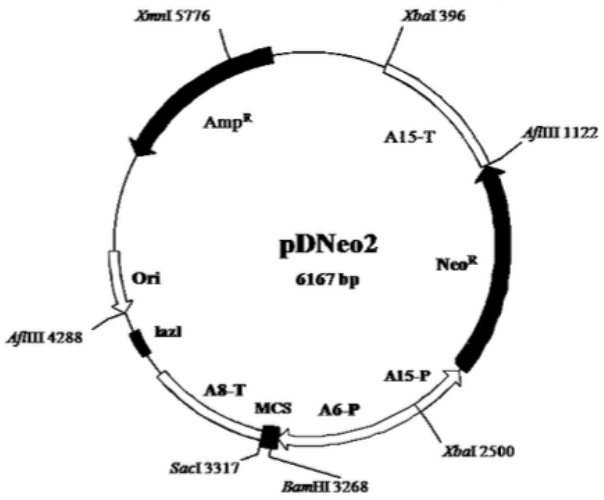

Figure 2.3. Circular map of *D. discoideum* expression vector pDNeo2.
pDNeo2 is comprised of the pUC19 backbone, with the polylinker substituted by two cassettes; one exhibiting G418 resistance (Neo^R) and an expression cloning cassette. The G418 resistance cassette is controlled by the actin-15 promoter and terminator (A15-P and A15-T). The expression cloning cassette is regulated by the actin-6 promoter (A6-P) and the actin-8 terminator (A8-T). The presence of the Ampicillin cassette (Amp^R) from pUC19 allows selection in *E. coli*, whereas the presence of the G418 cassette enables selection of *D. discoideum* transformants (Witke *et al*., 1987). The units of map numbers are base pairs (bp).

Table 2.2. Created bacterial and *D. discoideum* constructs.

Construct	Plasmid vector	Gene Fragment	Reference
pPROF780	pUC18	pUC18 containing full length of the LKB1 gene cloned into the *Eco*RI restriction enzyme site.	This thesis
pPROF781	pPROF267	pPROF267 containing full length of the LKB1 gene cloned into the *NotI* and *Xho*I restriction enzyme site in the sense orientation.	This thesis
pPROF782	pPROF781	pPROF781 containing the full LKB1 gene with two point mutations (K69M and D186A) created through mutagenesis. This would enable expression of LKB1 Dead Kinase.	This thesis
pPROF783	pUC18	pUC18 containing full length of the STRADα gene cloned into the *Sal*1 restriction enzyme site.	This thesis
pPROF784	pUC18	pUC18 containing full length of the MO25 gene cloned into the *Eco*RI restriction enzyme site.	This thesis
pPROF785	pPROF267	pPROF267 containing full length of the STRADα gene cloned into the *NotI* and *Xho*I restriction enzyme site in the sense orientation.	This thesis
pPROF362	pDNeo2	pDNeo2 containing a 1120 bp gDNA fragment of the AMPK gene cloned into the *EcoR*I restriction enzyme site in the antisense orientation.	Bokko *et al*. (2007)

2.1.7. Bacterial and D. discoideum strains

The genotypes and phenotypes of all bacterial and *Dictyostelium discoideum* wildtype

strains are listed in Table 2.3. The strains expressing the genes encoding LKB1; LKB1 Dead Kinase; LKB1 overexpression+AMPK antisense RNA; and LKB1+STRADα are listed in Tables 2.4.

Note: Copy number for all strains listed was determined by quantitative PCR (qPCR) (Section 2.3.4).

Table 2.3. Genotypes/phenotypes of *E. coli* strains.

Strain	Genotype/Phenotype	Reference
TOP10	F^-, *mcrA*, Δ(*mrr-hsdRMS-mcrBC*), ϕ80*lacZ*ΔM15, Δ*lacX*74, *recA*1, *araD*139 Δ(*ara-leu*)7697, *galU*, *galK* *rpsL*(Str^R), *endA*1, *nupG*	Invitrogen® www.invitrogen.com
DH5α	F^-, *endA1*, *hsdR17(*rk^-*,*mk^+*), φ80dlacZΔM15*, *Δ(lacZYA-argF)U169*, *deoR*, *recA1*, *phoA*, *supE44*, *thi-1*, *gyrA* (Nal^r), *relA1*	Hanahan (1983)
M15 (pREP4)	nal^S, str^S, rif^S, thi^-, lac^-, ara^-, gal^-, mtl^-, F^-, $recA^+$, uvr^+, lon^+	Qiagen® www.qiagen.com
JC11451	F^-, *thr-1*, *leuB6*, *proA2*, *his-4*, *thi-1*, *argE3*, *lacY1*, *galK2*, *rpsL31*, *supE44*, *ara-14*, *xyl-15*, *mtl-1*, *tsx-33*, *kdgK51*, *sbcB*, sup^+	Kushner *et al*., 1971.

In this table, the genotype symbols are italicized whereas the phenotype symbols are not.

Key to genotype/phenotype symbols:

Genotype	Phenotype
ara	Defective in arabinose sugar utilization
argE	Requires arginine for growth
endA	Mutation suppressing endonuclease A-dependent degradation of plasmid DNA
galK	Defective in galactose sugar utilization
gyrA(Nal^r)	DNA gyrase mutation (nalidixic acid resistance)
his-4	Requires histidine for growth
hsd	Restriction negative and modification positive
leuB6	Requires leucine for growth
mtl-1	Defective in mannitol sugar utilization
proA2	Requires proline for growth
recA	Recombination defective
relA1	Relaxed regulation of RNA synthesis
sbcB	Recombination defective
supE44	Carries a tRNA suppressor gene
thi-1	Requires thiamine for growth

Table 2.4. Genotypes of the *D. discoideum* strains.

Strain	Parent	Genotype or integrated construct and gene/fragment expressed*	Construct Copy No.*	Reference
Ax2	NC4	*axe*A1, *axe*B1, *axe*C1		Watts & Ashworth (1970); Darmon *et al*. (1975)
HPF1338	AX2	pPROF781 expressing LKB1	8	This thesis
HPF1339	AX2	pPROF781 expressing LKB1]	14	This thesis
HPF1340	AX2	pPROF781 expressing LKB1	16	This thesis
HPF1341	AX2	pPROF781 expressing LKB1	26	This thesis
HPF1342	AX2	pPROF781 expressing LKB1	35	This thesis
HPF1343	AX2	pPROF781 expressing LKB1	42	This thesis
HPF1344	AX2	pPROF781 expressing LKB1	66	This thesis
HPF1345	AX2	pPROF781 expressing LKB1	76	This thesis
HPF1346	AX2	pPROF781 expressing LKB1	84	This thesis
HPF1347	AX2	pPROF781 expressing LKB1	91	This thesis
HPF1348	AX2	pPROF781 expressing LKB1	113	This thesis
HPF1349	AX2	pPROF781 expressing LKB1	121	This thesis
HPF1350	AX2	pPROF781 expressing LKB1	166	This thesis

HPF1351	AX2	pPROF781 expressing LKB1	170	This thesis
HPF1352	AX2	pPROF781 expressing LKB1	183	This thesis
HPF1353	AX2	pPROF781 expressing LKB1	339	This thesis
HPF1354	AX2	pPROF781 expressing LKB1	423	This thesis
HPF1355	AX2	pPROF781 expressing LKB1	486	This thesis
HPF1356	AX2	pPROF781 expressing LKB1	532	This thesis
HPF1357	AX2	pPROF781 expressing LKB1	549	This thesis
HPF1358	AX2	pPROF781 expressing LKB1	942	This thesis
HPF1359	AX2	pPROF782 expressing LKB1 Dead Kinase	45	This thesis
HPF1360	AX2	pPROF782 expressing LKB1 Dead Kinase	57	This thesis
HPF1361	AX2	pPROF782 expressing LKB1 Dead Kinase	78	This thesis
HPF1362	AX2	pPROF782 expressing LKB1 Dead Kinase	92	This thesis
HPF1363	AX2	pPROF782 expressing LKB1 Dead Kinase	102	This thesis
HPF1364	AX2	pPROF782 expressing LKB1 Dead Kinase	114	This thesis
HPF1365	AX2	pPROF782 expressing LKB1 Dead Kinase	167	This thesis
HPF1366	AX2	pPROF782 expressing LKB1 Dead Kinase	231	This thesis
HPF1367	AX2	pPROF782 expressing LKB1 Dead Kinase	376	This thesis
HPF1368	AX2	pPROF782 expressing LKB1 Dead Kinase	415	This thesis
HPF1369	AX2	pPROF782 expressing LKB1 Dead Kinase	520	This thesis

HPF1370	AX2	pPROF782 expressing LKB1 Dead Kinase	554	This thesis
HPF1371	AX2	pPROF781 and pPROF362, expressing LKB1 and antisense AMPK	43,55	This thesis
HPF1372	AX2	pPROF781 and pPROF362, expressing LKB1 and antisense AMPK	53,74	This thesis
HPF1373	AX2	pPROF781 and pPROF362, expressing LKB1 and antisense AMPK	61,215	This thesis
HPF1374	AX2	pPROF781 and pPROF362, expressing LKB1 and antisense AMPK	122,148	This thesis
HPF1375	AX2	pPROF781 and pPROF362, expressing LKB1 and antisense AMPK	134,154	This thesis
HPF1376	AX2	pPROF781 and pPROF362, expressing LKB1 and antisense AMPK	143,130	This thesis
HPF1377	AX2	pPROF781 and pPROF362, expressing LKB1 and antisense AMPK	143,148	This thesis
HPF1378	AX2	pPROF781 and pPROF362, expressing LKB1 and antisense AMPK	154,121	This thesis
HPF1379	AX2	pPROF781 and pPROF362, expressing LKB1 and antisense AMPK	176,149	This thesis
HPF1380	AX2	pPROF781 and pPROF362, expressing LKB1 and antisense AMPK	195,16	This thesis
HPF1381	AX2	pPROF781 and pPROF362, expressing LKB1 and antisense AMPK	245,86	This thesis
HPF1382	AX2	pPROF781 and pPROF785, expressing LKB1 and STRADα	14,92	This thesis

HPF1383	AX2	pPROF781 and pPROF785, expressing LKB1 and STRADα	15,31	This thesis
HPF1384	AX2	pPROF781 and pPROF785, expressing LKB1 and STRADα	20,60	This thesis
HPF1385	AX2	pPROF781 and pPROF785, expressing LKB1 and STRADα	21,7	This thesis
HPF1386	AX2	pPROF781 and pPROF785, expressing LKB1 and STRADα	21,25	This thesis
HPF1387	AX2	pPROF781 and pPROF785, expressing LKB1 and STRADα	26,14	This thesis
HPF1388	AX2	pPROF781 and pPROF785, expressing LKB1 and STRADα	28,4	This thesis
HPF1389	AX2	pPROF781 and pPROF785, expressing LKB1 and STRADα	32,66	This thesis
HPF1390	AX2	pPROF781 and pPROF785, expressing LKB1 and STRADα	33,8	This thesis
HPF1391	AX2	pPROF781 and pPROF785, expressing LKB1 and STRADα	35,27	This thesis
HPF1392	AX2	pPROF781 and pPROF785, expressing LKB1 and STRADα	36,6	This thesis
HPF1393	AX2	pPROF781 and pPROF785, expressing LKB1 and STRADα	57,100	This thesis
HPF1394	AX2	pPROF781 and pPROF785, expressing LKB1 and STRADα	59,113	This thesis
HPF1395	AX2	pPROF781 and pPROF785, expressing LKB1 and STRADα	63,13	This thesis

HPF1396	AX2	pPROF781 and pPROF785, expressing LKB1 and STRADα	89,22	This thesis

*Where two constructs are present in cotransformants, the copy numbers refer to the constructs in the order in which they are named in the "Genotypes…" column.
Key to genotype symbols:

GENOTYPE	PHENOTYPE
axe	Able to grow in axenic medium if all 3 loci *axeA,B,C* are mutant.

2.1.8. 2.1.8. Storage of bacterial and D. discoideum strains

All *E. coli* strains were grown in Luria broth (LB) medium at 37 ^{o}C to an optical density of 600nm (OD_{600nm}) of 0.5-0.7. 1.5 ml aliquots of cell culture were harvested in an Eppendorf tube, the supernatant was discarded and the pellet was resuspended in 100 µl of 10% (v/v) glycerol solution and stored at -80 ^{o}C immediately.

D. discoideum cells were grown at 21 ^{o}C on Standard Medium (SM) agar with *Klebsiella aerogenes* as a food source for several days until they contained a mixture of plaques and mature fruiting bodies. The mixture of amoebae and spores were scraped from the surface of the plate using sterile tips and added to Eppendorf tube containing 200 µl of storage buffer and frozen at -80 ^{o}C immediately. Cells were recovered by thawing and aliquots were streaked on geneticin plates inoculated with *K. aerogenes* lawns.

2.1.9. 2.1.9. Growth and maintenance of bacterial and D. discoideum strains.

Ampicillin-resistant *E. coli B2* strains were grown on Luria Broth (LB) agar plates containing 100 µg ampicillin ml^{-1}. The strains were purified by streak plating every 5-8 days and incubated at 37 ^{o}C for 24 hours.

E. coli B2 was also grown on LB agar plates with no antibiotics and incubated at 37 ^{o}C for 24 hours. *Micrococcus luteus* and *K. aerogenes* were inoculated onto SM plates and incubated at 27 ^{o}C for 3 days or 37 ^{o}C for 24 hours respectively.

Dictyostelium strains were subcultured as follows for periods no longer than 1-2 months before being freshly resuscitated from frozen stocks.

Klebsiella aerogenes was provided as a food source for *D. discoideum*, by spreading 0.2 ml aliquots of bacterial suspension in Sterile Saline (SS) on standard medium (SM) plates supplemented with 30 μg ml^{-1} of G418 (geneticin). *D. discoideum* test stains were streak plated onto the dried *K. aerogenes* lawns and the plates were incubated at 24 ^{o}C for 3 days. Strains were subcultures this way by streak dilution once or twice a week. Note: *D. discoideum* wildtype strains were always streaked on SM plates without geneticin and incubated under the same conditions as the test strains.

D. discoideum cell cultures were grown in liquid media by inoculating a single fruiting body from an SM agar plate (with or without geneticin) into a single well of a 24 well Costar plate (Nunc^{TM}) containing 1 ml of HL-5 supplemented with 20-35 μg ml^{-1} geneticin, 100 μg ml^{-1} ampicillin, 100 μg ml^{-1} tetracycline, 100 μg ml^{-1} streptomycin and 25 μg ml^{-1} kanamycin to inhibit the growth of bacteria. Note: Axenic wildtype strains were grown in HL-5 without geneticin. Strains in Costar wells were subcultured every 1-2 weeks.

The vegetative cells in growth phase were transferred to a conical flask containing 10 ml or 50 ml HL-5 and incubated at 21 ^{o}C shaking at 130 rpm to a desired density of 1-3 × 10^{6} ml^{-1}. Cells in conical flasks were subcultured every second day.

2.2. Molecular biological techniques

2.2.1. Small scale extractions of plasmid DNA (Alkaline Lysis Mini-preps)

The alkaline lysis miniprep method was adapted from Birnboim & Doly (1979) and Birnboim (1983) and used for the extraction of small amounts of DNA. This technique allows for screening large numbers of bacterial transformants.

A single bacterial colony was inoculated into 3 ml of LB containing 100 µg ampicillin ml^{-1} and incubated overnight at 37 ^{o}C on a rapidly reciprocating shaker. 1.5 ml of the bacterial culture was harvested by centrifugation at 12,200 *x g* for 30 seconds at room temperature and the supernatant was discarded. The cell pellet was resuspended in 100 µl of resuspension buffer containing 20 µg ml^{-1} RNase A and incubated at room temperature for 5 minutes. The cells were then lysed by the addition of 200 µl of NaOH/SDS solution and gently inverted several times. 150 µl of 5M potassium solution was then added to the lysate to neutralize the DNA and the mixture was vortexed at maximum speed for 2 seconds. The mixture was incubated on ice for 5 minutes and centrifuged at 12,200 *x g* for 5 minutes to precipitate the cell debris, proteins and chromosomal DNA. The supernatant containing the plasmid DNA was transferred to a fresh microcentrifuge tube and the DNA was precipitated by adding 900 µl of 100% ethanol (v/v) and 45 µl of 3M sodium acetate and then incubated for 5 minutes at room temperature. The plasmid DNA was harvested by centrifugation for 5 minutes at 12,200 *x g*. The pelleted DNA was washed with 1 mL of 70% (v/v) ethanol and air dried for 20-30 minutes or dried in a speed vacuum for 5 minutes. The dried pellet was resuspended with 20-25 µl of Milli-Q water and stored at 4 ^{o}C for short-term use and -20 ^{o}C for long-term use.

2.2.2. Large scale extraction of plasmid DNA (Maxi-prep)

The large-scale extraction of highly pure plasmid DNA was performed using the PureLink™ HiPure Plasmid Filter Purification Kit and the PureLink™ HiPure Precipitator Module (Invitrogen) according to the manufacturer's instructions.

A single *E. coli* colony containing the plasmid DNA of interest was inoculated into 200 ml of LB with Ampicillin and shaken at 37 ^{o}C overnight. The cells were harvested by centrifugation at 4,000 *x g* for 10 minutes at 4 ^{o}C in a GSA rotor of a Sorvall centrifuge. The supernatant was discarded and the cell pellet was resuspended in resuspension buffer containing 20 µg ml^{-1} RNase A and lysed with Lysis Buffer by incubation at room

temperature for 5 minutes. The lysate was then precipitated by the addition of Precipitation Buffer. The resultant lysate was poured into a Hipure Filter Maxicolumn in which it ran through by gravity flow. The DNA bound to the Maxicolumn was washed with 50 ml of Wash Buffer. The plasmid DNA was then eluted from the column by adding 15 ml of Elution Buffer and precipitated by adding 10.5 ml isopropanol. The DNA solution was loaded into a 30 ml syringe (Terumo) with a Hipure Precipitator module attached (Invitrogen). The pure DNA was pushed through the precipitator module, washed twice with 5 ml of 70 % (v/v) ethanol and then eluted from the precipitator using 400 µl of TE buffer. The DNA was stored immediately at -20 ^{o}C.

2.2.3. Isolation of genomic DNA

Small scale genomic isolation was carried out using DNazol® Genomic DNA Isolation Reagent (Molecular Research Center Inc) and large scale genomic DNA was isolated using a method adapted from Murray & Thompson (1980).

2.2.3.1. Small scale isolation of genomic isolation (DNAzol method)

The DNAzol method was used as a quick and efficient DNA extraction method to screen *D. discoideum* transformants. Approximately 2 x 10^7 *D. discoideum* cells were harvested from mass plates and centrifuged at 10,000 x g for 10 seconds. The cell pellets were washed in sterile SS multiple times and then resuspended in 1 ml of DNAzol to lyse the cells and incubated at 4 ^{o}C for 30 minutes. The lysate was centrifuged at 12,200 *x g* for 10 minutes and the supernatant was transferred to a fresh Eppendorf tube and precipitated with 0.5 ml absolute ethanol then centrifuged at 8,600 *x g* for 5 minutes. The DNA was washed with 1ml of 70 % (v/v) ethanol, dried in a Speed-Vac low speed vacuum centrifuge for 5-10 minutes and resuspended in 30-50 µl 8 mM NaOH or milliQ water. DNA was stored at 4 ^{o}C for short-term use or -20 ^{o}C for long-term use.

2.2.3.2. Large scale isolation of genomic Dictyostelium DNA (CsCl method)

This procedure was used to extract large and highly concentrated amounts of genomic DNA. *D. discoideum* AX2 was grown axenically in 1 L of HL-5 media at 21 ^{o}C, shaking at 150 rpm on an orbital shaker to a density of 2-3 x 10^{6} cells ml^{-1}. The cells were harvested by centrifugation at 2,000 × g for 5 minutes at 4 ^{o}C. The supernatant was discarded and the pelleted cells were washed twice with 250 ml of cold milliQ water. The cell pellet was resuspended in 200 ml of cold nuclear lysis buffer and incubated for 5 minutes on ice. The nuclei were then pelleted by centrifugation at 6000 × g for 10 minutes and the nuclear pellet was resuspended in 4 ml of nuclear lysis buffer and transferred to a 50 ml Falcon tube (Sarstedt©). 20 ml of hot (65 ^{o}C) EDTA/Sarkosyl buffer was added to lyse the nuclei and allowed to stand in a 65 ^{o}C water bath for 10 minutes. The lysate was transferred to a Falcon tube, 0.92 g of CsCl per gram of lysate was added, the mixture was inverted gently and placed at 65 ^{o}C until the CsCl dissolved. 400 µl of ethidium bromide (10 mg ml^{-1}) was added as an indicator to the mixture and transferred to an ultracentrifuge tube. The tube was heat sealed and centrifuged in a Beckman™ 50 Ti angle rotor at 45,000 × g for 48 hours at 20 ^{o}C in a Beckman™ L80 ultracentrifuge. The genomic DNA appeared as a single fluorescing band under UV light. This DNA was removed using a 22-gauge needle (Terumo®) with a 5 ml syringe and transferred to a Falcon tube. An equal volume of TE and 2 volumes of absolute ethanol were added to the DNA at RT to precipitate the DNA. The DNA was extricated using a fine glass hook and washed twice with 1 ml of 70 % (v/v) ethanol. The genomic DNA was then air dried for a few minutes and stored in 500 µl TE buffer in an Eppendorf tube at -20 ^{o}C.

2.3. Molecular manipulation of DNA

2.3.1. Standard polymerase chain reaction (PCR)

The polymerase chain reaction (PCR) was used for *in vitro* amplification of the *D. discoideum* LKB1, STRADα and MO25 genes, using *D. discoideum* genomic DNA and gene specific oligonucleotide primers. Additional bases (GC) were added at the 5' ends to ensure efficient cutting of PCR products by restriction enzymes during cloning. Full

sequences of the genes are in Appendix 6. The forward and reverse primers to amplify full length LKB1, STRADα and MO25 were synthesised by Geneworks and their sequences are shown in Figure 2.4. The restriction enzyme cut sites used in the primer design for cloning purposes are listed in Table 2.5. The PCR was carried out using an automated MiniCycler^{TM} apparatus (M.J. Research PTC-150) with a heated lid. The reagents used for gene amplification are listed in Table 2.6 and the PCR conditions used for optimal amplification of all genes are listed in Table 2.7.

Primer sequences for amplification of LKB1

Forward primer: GC **GAATTC GCGGCCGC**
ATGGAAGTTGAACAACAACCATCATATACATCG
Reverse primer: GC **GAATTC CTCGAG**
TTAATTAATGATACATTTTGACTTATTATGTGGAG

Primer sequences for amplification of STRADα

Forward primer: GC **GTCGAC GCGGCCGC**
ATGTCCGATGATAAATATCATCATGATAAACATC
Reverse primer : GC **GTCGAC CTCGAG**
TTATTGAGTTTGTGGTCTACTATTATTACTACTATTACTC

Primer sequences for amplification of MO25

Forward primer: GC **GAATTC GCGGCCGC**
ATGAAATTAGAGAAAGGGATTTTC
Reverse primer: GC **GAATTC CTGCAG**
CTAAAAATAAATAAATATATATATGAAATATACCTGATCG

Figure 2.4. Primer sequences for amplification of LKB1, STRADα and MO25 genes.
Primers are listed in the 5' to 3' direction with GC provided at the 5' end for more efficient restriction digestion. Restriction cut sites are indicated in bold.

Table 2.5. Restriction enzyme sites used in the primer design for LKB1, STRADα and MO25 genes.

Enzymes	LKB1	STRADα	MO25
*Eco*RI: G▼AATTC	√	-	√

*Not*I : GC▼GGCCGC	√	√	√
*Xho*I : C▼TCGAG	√	√	√
*Sal*I : G▼TCGAC	-	√	-
*Pst*1 : C▼TGCAG	-	-	√

Table 2.6. PCR reaction mixture for amplification of LKB1, STRADα and MO25.

Components	**Volume (µl)**	**Final concentration**
dH_20	78	
10 x PCR $MgCl_2$ buffer	10	1 x
50mM $MgCl_2$	5	2.5 mM
10mM dNTPs mixture	2	0.2 mM each
AX2 genomic DNA (2-5 µg $µl^{-1}$)	2	40-100 ng l^{-1}
Forward primer (10 µM ^{1})	1	0.1 µM
Reverse primer (10 µM)	1	0.1 µM
pfu Taq polymerase enzyme (5 U $µl^{-1}$)	1	5 U
Total:	100	

Table 2.7. Minicycler program for PCR reaction to amplify LKB1, STRADα and MO25.

Step	**Reaction**	**Temperature /duration For LKB1 and MO25**	**Temperature /duration for STRADα**

1	Initial template denaturation		95 ^{0}C/ 2 minutes	95 ^{0}C/ 2 minutes
2	35 Cycles of amplification	Denaturation	95 ^{0}C/ 1 minutes	95 ^{0}C/ 1 minutes
		Annealing	52 ^{0}C/ 1 minutes	52 ^{0}C/ 1 minutes
		Elongation	72 ^{0}C/ 2 minutes	72 ^{0}C/ 4 minutes
3	Final elongation		72 ^{0}C/ 5 minutes	72 ^{0}C/ 5 minutes
4	Storage		4^{o}C/ 24-48 hours	4 ^{o}C/ 24-48 hours

2.3.2. Cloning into plasmid DNA

2.3.2.1. Restriction endonuclease digestion of DNA and vector

The restriction endonuclease digestions of the PCR-amplified DNA fragments and plasmid DNA were performed in the corresponding appropriate buffer as recommended by the supplier (Promega^{TM}) and presented in Table 2.8. The reaction mixture was incubated in a sterile Eppendorf tube at 37 ^{o}C for 1.5 h before the reaction was terminated by either heat inactivation at 65 ^{o}C for 15 minutes or 80 ^{o}C for 20 minutes or by adding one third volume of blue juice/SBE loading buffer. The digested DNA were loaded onto an agarose gel and electrophoresis was carried out as described in Section 2.3.2.2.

Table 2.8. Restriction endonuclease digestion reactions.

Component	**Volume**
Buffer (10 x)	1 µl
DNA sample (0.2-1 µg µl^{-1})	1-2 µl
Enzyme (each) (10 U)	1 µl
milliQdH_2O	△ µl
Final	10 µl

△: The volume of milliQdH_2O varied depending upon the amount of DNA used.

2.3.2.2. Agarose gel electrophoresis

Agarose gels of 1-2% (w/v) were made with 1 x Tris-Borate-EDTA (TBE) buffer and supplemented with 0.005 % (v/v) ethidium bromide (0.5 µg ml^{-1}) as an indicator to visualize the DNA under ultraviolet (UV) light. The gel was immersed in 1.5 L of 1 x TBE in a gel electrophoresis tank (Bio-Rad®). The DNA samples were mixed with SBE (3 x) or Blue Juice™ Gel loading buffer (2 x) (Life Technologies™) and loaded into the wells of the agarose gel. A 1 kb Gene Ruler™ DNA ladder (Fermentas™) was used as a size standard. Electrophoresis was carried out at 110 V for 1.5 h at room temperature and the DNA bands were visualized with a UV transilluminator and photographed with an Olympus Camedia C-5060 camera.

2.3.2.3. DNA extraction and purification from gel

The DNA was extracted from the agarose gel using the PureLink™ Quick Gel Extraction Kit (Invitrogen®). The fragment DNA of interest was excised by means of a surgical blade and the gel piece holding the DNA was weighed to a maximum of 300 mg. The gel was placed into a 1.5 ml Eppendorf tube and dissolved in 3 volumes of solubilization buffer. It was then incubated at 50 °C for 10-15 minutes, after which one gel volume of isopropanol was added to precipitate the DNA. A maximum volume of 650 µl of the solution was loaded into a Quick Gel Extraction Column inside a Wash Tube and centrifuged at 12,200 *x g* for 1 minute. This step was repeated until all the DNA solution was passed through the column. The Extraction Column was washed with 500 µl wash buffer containing ethanol and centrifuged at 12,200 *x g* for 1 minute. A further 2-minute spin was performed to ensure any residual wash buffer or ethanol was removed. The column was then placed into a new Eppendorf tube and the DNA was eluted by adding 30-50 µl of milliQdH_2O followed by centrifugation at 12,200 *x g* for 1 minute. The purified DNA was stored at -20 °C or used immediately in a ligation reaction (Section 2.3.2.5).

2.3.2.4. Dephosphorylation of linearised vector DNA

To prevent religation of linearized vector DNA during cloning experiments, thermosensitive Alkaline Phosphatase (TSAP, Promega) was added to remove the 5' phosphate groups from the vector DNA.

The enzyme used to linearize the vector was irreversibly heat inactivated at 65 ^{o}C for 15 minutes. 15 units TSAP and 1 µl of 10 x buffer (Promega) were added to 1 µg of vector DNA and incubated at 37 ^{o}C for 30 minutes. TSAP was then heat inactivated at 75 ^{o}C for 15 minutes, and the DNA was microdialysed in order to reduce electrolyte concentration (Section 2.3.2.6).

2.3.2.5. Ligation of vector and insert DNA

The vector and the insert DNA were both digested with the appropriate enzymes and added to the ligation mix in a 1:7 ratio of vector to insert DNA. Ligations were generally carried out in a 30 µl total volume of dH_20, 10 x ligation buffer and 2 µl of T4 DNA ligase (Promega). The components for ligation are listed in Table 2.9. The reaction mix was incubated overnight at 16 ^{o}C. The ligation reaction was microdialysed prior to transformation (Section 2.3.2.6).

Table 2. 9. Reaction mix for ligation.

Component	**Volume (µl)**
T4 ligase buffer (10 x)	3
Insert DNA	22
Vector	3
T4 ligase 30	2
Total	30

2.3.2.6. Microdialysis

Microdialysis was carried out to decrease the concentration of electrolytes added from restriction and ligation buffers and therefore allow electroporation without the buffer short-circuiting the electrical flow (Section 2.4.1.2). The DNA solution was pipetted onto Millipore™ filter paper (type VS, pore size 0.025 µm) and floated on dH_20 in a sterile Petri dish for approximately 1-1.5 hours at room temperature. An Eppendorf pipette was then carefully used to recover the microdialysed sample from the filter paper.

2.3.2.7. DNA sequencing

Gene sequencing was carried out by the Australian Genome Research Facility (AGRF), Melbourne, Australia. The primers designed for sequencing are presented in Appendix 7 and the components and their respective concentrations used for sequencing are presented in Table 2.10.1 and Table 2.10.2 respectively. The sequencing alignments are presented in Appendix 8.

Table 2.10.1. Sequencing mix.

Component	**Volume or quantity**
milliQdH_2O	$\triangle^1$ µl
DNA sample	$\triangle^2$ ng
Primer	10 pmol
Total	12 µl

$\triangle^1$: Varies according to volume of DNA added. $\triangle^2$: Depends on fragment size as shown below.

Table 2.10.2. The DNA size and required quantity for sequencing.

Fragment size (bp)	Recommended quantity (ng)
PCR Product 100-200	3-8
PCR Product 200-400	6-12
PCR Product 400-600	12-18
PCR Product 600-800	18-30
PCR Product >800	30-75
Plasmid, single-stranded	150-300
Plasmid, double-stranded	600-1500

https://www.agrf.org.au/docs/sanger-sequencing-sample-preparation-guide.pdf

2.3.3. Site-directed mutagenesis of LKB1 to create LKB1 Dead Kinase

Site-directed mutagenesis of DNA constructs was performed using Stratagene QuikChange® II site-directed mutagenesis kit according to manufacturer's instructions. It is a rapid three-step procedure that allows site-specific mutation in virtually any double-stranded plasmid. Site-directed mutagenesis was used to mutate single amino acids in the LKB1 gene to create a dead kinase version of it. The mutagenesis reactions were set up in sterile 0.2 ml PCR tubes and were made of 10X reaction buffer, 5–50 ng of template plasmid dsDNA, 0.5µM of forward and reverse mutagenic oligonucleotide primer respectively, 1 mM dNTPs, 2.5 U/µl *Pfu Ultra* HF DNA polymerase made up to a final volume of 50 µl with MilliQ-H_2O.

The PCR reactions were carried out in an automated MiniCycler™ apparatus (M.J. Research PTC-150) with a heated lid using the conditions described in Table 2.11.

Table 2.11. PCR conditions for site-directed mutagenesis reaction.

Step	Reaction		Temperature	Time
1	Initial template denaturation		95 ^{0}C	30 seconds
2	35 Cycles of amplification	Denaturation	95 ^{0}C	30 seconds
		Annealing	55 ^{0}C	1 minutes
		Elongation	68 ^{0}C	1 minute/kb of plasmid length
3	Final Extension		68 ^{0}C	10 minutes

After cycling, 10 U/µl of *Dpn*I restriction endonuclease was added and the reaction incubated at 37°C for 1 hour. *Dpn*I digests the methylated parental (i.e., the non-mutated) supercoiled dsDNA. The RE digestion product was transformed into DH5α bacterial competent cells as described in the Section 2.4.1.2. DNA constructs were verified by DNA sequencing to confirm the mutagenesis.

Site-directed mutagenesis of LKB1 was first used to create the mutant LKB1[K69M], which was then used as a template to create the final LKB1 mutant, pPROF782, containing the mutations [K69M/D186A] (Appendix 9). LKB1 containing both mutations was referred to as LKB1 Dead Kinase and used in all experiments performed in this thesis that required expression of the kinase-dead form of the enzyme.

The primers used in this site-directed mutagenesis are outlined in Tables 2.12.1 and the mutated oligonucleotides are highlighted. Mutants created as part of this thesis are outlined in Table 2.12.2.

Table 2.12.1. Primers used to create mutations in LKB1.

Mutation	Forward Primer	Reverse Primer
LKB1[K69M]	GAGTAGCAGTTATGATATTAAAAAGAGC	GCTCTTTTTAATATCATAACTGCTACTC
LKB1[D186A]	GCAAATGTATTGAAATTGAGTGCTTTTGGAGTTGCAGAGGATAGTAGCC	GGCTACTATCCTCTGCAACTCCAAAAGCACTCAATTTCAATACATTTGC

Table 2.12.2. Mutants created by site directed mutagenesis in LKB1.

Mutant plasmid	Mutation	Plasmid template DNA	Primers
	LKB1 [K69M]	LKB1	LKB1 [K69M]
pPROF782	LKB1 [K69M/D186A]	LKB1 [K69M]	LKB1 [D186A]

2.3.4. Copy number analysis using qPCR

qPCR analysis was used to calculate the number of vector DNA present in a cell derived from a single *D. discoideum* transformant. In other words, it was used to determine the construct copy numbers in *D. discoideum* transformants.

Around 1 x 10^7 cells were harvested from each test strain and their genomic DNA was extracted using the DNazol method (Section 2.2.3.1) and then diluted 1:5 with milliQdH_2O supplemented with 100 µg/µl of RNAse I. The genomic DNA of the wildtype strains used for the qPCR standard curve (Section 2.4.2.2) was extracted using the CsCl method (Section 2.2.3.2). Standard curves to estimate the quantity of gDNA were prepared using the genomic DNA of wildtype strains (Section 2.2.3.2) and the purified DNA maxipreps of the constructs expressing the genes of interest (pPROF781 (LKB1), pPROF782 (LKB1 Dead Kinase), pPROF785 (STRADα) and pPROF362 (AMPK antisense-inhibited)) (Section 2.2.2). The Maxiprep DNA concentrations were measured at 260 nm absorbance using spectrometer and diluted five times to form a 10-fold dilution

series with fragment quantities ranging from 0.01-1,000 pg for estimation of the construct copy numbers.

The filamin gene was used as a reference housekeeping gene and primers were designed by amplifying a 100 bp fragment from the endogenous filamin gene using Primerquest software (the primers designed to amplify a fragment from the DNA of interest and filamin are shown in Figure 2.5).

FILAMIN qPCR (amplified fragment size 100 bp)
Forward primer: CCCTCAATGATGAAGCC
Reverse primer: CCATCTAAACCTGGACC

LKB1 qPCR (amplified fragment size 105 bp)
Forward primer: GCGCACCGTGCTGATAGAGTTGGCTCA
Reverse primer: GCGCAAGGTGGTTGAGGTGAAGAACGGT

LKB1 Dead Kinase qPCR (amplified fragment size 105 bp)
Forward primer: GCGCACCGTGCTGATAGAGTTGGCTCA
Reverse primer: GCGCAAGGTGGTTGAGGTGAAGAACGGT

STRADα qPCR (amplified fragment size 101 bp)
Forward primer: GCGCACATAGTAATGTTCATGG
Reverse primer : GGTTTGAGGTTGTTGAGTGTTATT

AMPK antisense qPCR (amplified fragment size 90 bp)
Forward primer: CAAGTTGTGGTTCACCCAATTAC
Reverse primer: CACCACAAGACCAAACATCAAC

Figure 2.5. Primer sequences used in qPCR analysis for fragment amplification of the FILAMIN, LKB1, STRADα and AMPK antisense inhibition. Primers are in a direction of 5' to 3'.

The components used for the qPCR reaction are presented in Table 2.13.1. 1 µl of gDNA was mixed with 19 µl of reaction mix and duplicates were prepared for each sample. The reaction was performed using an iCycler IQ Multicolor Real-Time PCR Detection System (Bio-Rad) and the cycling parameters of the program used is presented in Table 2.13.2. A negative control containing no DNA template was also included in each experiment.

Table 2.13.1. Reaction mixture for qPCR amplification.

Components	Volume (µl)
DNA template (100ng-1pg)	1
Gene specific forward primer (10 nM)	1
Gene specific reverse primer (10 nM)	1
iQ™SYBR® Green Super-Mix (1x) (Bio-Rad®)	10
milliQdH_2O	7
Total:	20

Table 2.13.2. Program for qPCR reaction.

Step	**Reaction**		**Temperature /duration**
1	Initial template denaturation		95 ^{0}C/ 3 minutes
2	40 Cycles of amplification	Denaturation	95 ^{0}C/ 30 seconds
		Annealing	58 ^{0}C/ 30 seconds
		Elongation	72 ^{0}C/ 30 seconds
3	Final elongation		72 ^{0}C/ 3 minutes

In order to verify the correct amplification, 2 µl of the qPCR products were mixed with 8 µl dH_2O and 5 µl SBE (3 x) and run on a 1.5 % (w/v) agarose gel for approximately 1 h at 110 V (Section 2.3.2.2).

Copy numbers for each gene were calculated based on comparison of their average Ct values of the threshold cycle with those for filamin (control for gDNA concentration) in the unknowns and parental AX2 (control for gene's quantity in chromosomal DNA). The amount of DNA for the test sample was estimated using the SQ (starting quantity). The average was calculated for each test sample with duplicates (SQ mean). The Starting Quantity of the DNA amount and its Ct value have a linear relationship which allows the following formula for calculation of gene copy numbers in mutants:

$$\text{Copy number} = \frac{SQ1}{SQ2} \times \frac{6 \times 10^7}{S}$$

where SQ1 and SQ 2 is the average starting quantity (SQ) for insert DNA of interest and filamin respectively, S is the size of insert DNA (in base pairs) and 6 x 10^7 is the approximate size of the *D. discoideum* genomic DNA genome (in base pairs, including multicopy and repeated sequences). This yields a raw copy number which was then normalized against the raw copy number obtained from AX2, whose genome is known to contain a single copy of each of the target genes of interest. This has been found to improve the accuracy of the final copy number determination (Fisher, pers. comm.)

2.4. Transformation of *E. coli* and *D. discoideum* cells with plasmid DNA

2.4.1. E. coli cell strains

2.4.1.1. Preparation of electrocompetent cells

Preparation of competent *E. coli* cells was performed according to the protocol of Dower *et al*. (1988). 1 L of LB medium was supplemented with ampicillin 100 µg ml^{-1} and inoculated with 5 ml (1/50 volume) of fresh overnight *E. coli* culture. The culture was incubated at 37 °C vigorously shaking until it reached an OD_{600} of approximately 0.5-0.6. Cells were harvested at 4,000 *x g* for 10 minutes at 4 °C using a GSA rotor in a Sorvall centrifuge and the pellet was washed twice with ice cold sterile water. The cell pellet was resuspended in 20 ml of 10 % (v/v) glycerol to prevent the formation of ice crystals which can cause cell damage and re-centrifuged. The cells were resuspended in a final volume of 2-3 ml of 10 % (v/v) cold glycerol and 100 µl aliquots of the electro-competent cells suspension were stored at -80 °C.

2.4.1.2. Electroporation of competent cells

E. coli strains DH5α, Top10 and M15 (pREP4) were used as competent cells for electroporation. An aliquot of 100 µl competent cells was thawed on ice and 0.5 pg to 1 µg plasmid DNA was added to it. The mixture was added into a precooled sterile Gene Pulser / *E. coli* Pulser cuvettes (Bio-Rad®) with a 0.2 cm gap. After the cuvette was wiped dry, it was placed into the cuvette chamber of a Gene Pulser (Bio-Rad) and pulsed at a voltage of 2.5 kV, capacitance of 25 µF and resistance of 200 Ω. Following electroporation, 1 ml of ice cold SOC solution was immediately added to the cuvette and the cell suspension was transferred into a 10 ml polypropylene tube and incubated at 37 ^{o}C for 1 hour.

2.4.1.3. Selection of transformants on LB agar plates

A dilution series of the cell suspension (Section 2.4.1.2) was prepared and plated onto LB agar plates containing ampicillin (100 µg ml^{-1}) for DH5α cells, kanamycin (25 µg ml^{-1}) for Top10 cells and both ampicillin (100 µg ml^{-1}) and kanamycin (25 µg ml^{-1}) for M15 (pREP4) cells. This antibiotic selection was accompanied by blue/white screening to detect insertion of genes into the pUC18 vector. Blue/white screening was performed via the addition of 0.1 M IPTG and 40 µl of filter sterilized X-gal to each plate. The plates were incubated overnight at 37 ^{o}C. In the blue/white screening, white colonies were selected as they indicate that an insert had disrupted the *lacZ* gene. For other constructs, screening was performed for random colonies via minipreps and restriction enzyme analysis.

2.4.2. D. discoideum cell strains

2.4.2.1. Calcium phosphate transformation of *D. discoideum* cells

The transformation of the *D. discoideum* cells was achieved via the calcium phosphate method developed by Nellen *et al.* (1984) with minimal alterations. The *D. discoideum* AX2 cells were grown in HL-5 medium to a density of 1-2 x 10^6 cells ml^{-1} and around 1-1.5 x 10^7 cells were dispensed into a 9 cm tissue culture Petri plate. The cells were allowed

to settle and adhere onto the surface of the Petri dish for approximately 30 minutes to 1 hour. The HL-5 medium was removed and replaced with 10 mL of MES-HL-5 (pH 7.1) and the cells were incubated for 2 hours at room temperature. Concurrently, 20 µg of plasmid DNA was added to a mixture of 600 µl of Sterile Saline and 600 µl of 2 x HBS in a 10 ml Falcon tube and then precipitated slowly by drop wise addition of 76 µl of 2 M $CaCl_2$. This was performed with gentle vortexing of the mixture for 10 seconds and then the mixture was incubated at room temperature for 25 minutes.

MES-HL-5 medium was aspirated from the Petri dish and the precipitated DNA was added gently and softly spread to cover the cells. The Petri dish with the mixture was then incubated for 1 hour at room temperature after which 10 ml of fresh MES-HL-5 medium was added. The Petri dish was incubated furthermore for another 4-5 hours.

The medium was then removed and 2 ml of 15 % (v/v) glycerol in 1 x HBS was added and gently spread over the attached cells for less than 2 minutes to osmotically shock the cells. The glycerol solution was carefully removed and 10 ml of fresh HL-5 medium was added. The cells were left to recover for 15-18 hours at 21 ^{o}C. The cells were selected on *M. luteus* as in Section 2.4.2.2.

2.4.2.2. Selection of *D. discoideum* transformants on *M. luteus*

The procedure for selection of *D. discoideum* on *M. luteus* lawns was portrayed by Wilczynska & Fisher (1994). After incubation, the transformed *D. discoideum* cells were gently resuspended in 10 mL of HL-5 medium and 1 ml of cell suspension was inoculated onto SM gar plates each covered with a 2-3 day old *M. luteus* lawn and containing 25-30 µg ml^{-1} geneticin (G418). The *D. discoideum* cell suspension and the *M. luteus* cells were mixed well and spread evenly on the surface of the plate using a glass spreader.

The inoculum was left to dry for 30 minutes to an hour in a laminar hood and the plates were incubated for approximately 10-20 days at 21 ^{o}C until transformants were visible as plaques on the plates. When plaques appeared, approximately 40-50 transformants were chosen and subcultured onto SM plates containing 30 µg G418 ml^{-1} and a lawn of *K. aerogenes* using sterile toothpicks or pipette tips. The transformants were further purified

by streak dilution 2-3 times on *K. aerogenes* lawns on geneticin plates. These transformants were either stored in storage buffer at -80 ^{o}C or used for plaque expansion (Section 2.5.1) and morphology analysis (Section 2.5.3).

2.5. Phenotypic analysis of *D. discoideum* transformants

2.5.1. Plaque expansion on bacterial lawns

Amoebae from the edges of *D. discoideum* plaques (AX2 and transformants) growing on *K. aerogenes* lawns were scraped with a flat edged sterile toothpick and gently inoculated onto the centre of an NA plate covered with a lawn of *E. coli* B2. Each strain had 3 replicates. The plates were incubated at 21^{o}C and the diameter of the growing plaque was measured in mm twice a day at approximately 7-9 hour intervals for a period of 100 hours.

The results were analysed and the plaque expansion rate (mm h^{-1}) for each strain was calculated by linear regression analysis using the statistics software package "R".

2.5.2. Growth in axenic medium

Exponentially growing axenic strains of *D. discoideum* at a density of 1-2 x 10^{6} cells ml^{-1} were inoculated into 50 ml of Hl-5 medium to a final density of 1 x 10^{4} cells ml^{-1} in 250 ml sterile conical flasks. The cultures were incubated at 21^{o}C on an orbital shaker (Ratek^{TM}) shaking at a speed of 150 rpm. Cell counts were taken twice daily at an interval of 7-8 hours using a Haemocytometer (Bright Line, 0.1 mm deep) for 5 days in total. To obtain statistically viable results, a minimum of 30-300 cells per strain were counted at each time point. The programmeable software package "R" was used for statistical analysis of the log linear regression during the exponential growth of the cells and calculation of the generation times.

2.5.3. Morphogenesis

The *D. discoideum* strains were streak diluted onto *K. aerogenes* lawns on SM plates and

incubated at 21 ^{o}C until fruiting bodies were formed. The fruiting body morphology was observed using the Olympus SZ61^{TM} dissecting microscope (top view at 2.5 magnification & side view at 4.5 magnification) and photographs were captured using an attached Moticam 2300^{TM} camera. The morphology of mutant strains was compared to that of wild type AX2 (all strains were observed under the same magnification).

2.5.4. Phagocytosis

Bacterial uptake by *D. discoideum* strains was measured by using an *E. coli* strain that expresses the fluorescent protein DsRed (DsRed-Ec) (Maselli *et al.,* 2002).

E. coli DsRed cells were inoculated onto multiple LB agar plates supplemented with 100 µg ampicillin ml^{-1} and incubated at 37 ^{o}C for approximately 3 days or until all the colonies became pink. The DsRed-Ec cells were harvested and inoculated into 100 ml of LB medium containing 75 µg ampicillin ml^{-1} and 1mM IPTG. The cell suspension was then incubated overnight with shaking at 150 rpm at 37 ^{o}C, during which time the cells became maximally fluorescent.

Simultaneously, wildtype AX2 and test strains of *D. discoideum* were grown axenically at 21^{o}C in 50 ml flasks containing HL-5 shaking at 150 rpm until the cells reached a density of 1-2 x 10^{6} cells ml^{-1} . 5 x 10^{6} cells were then harvested by centrifugation at 2,500 x g for 5 minutes at room temperature and resuspended in 1 ml of 20 mM phosphate buffer.

The cells were counted to ensure that their density was between 4-6 x 10^{6} cells ml^{-1}. The 1 ml cell suspensions were added to scintillation vials and kept shaking at 150 rpm for 30 minutes at 21^{o}C.

In the meantime, the *E. coli* DsRed cells were harvested by centrifugation at 2,500 *x g* for 10 minutes at room temperature, washed with 50 ml SS and pelleted again. The pellet was resuspended in 10-15 ml of 20 mM sodium phosphate buffer at a density of 2-4 × 10^{10} bacteria/ml and left on ice.

The DsRed-Ec suspension was vortexed vigorously to break up aggregates and 1 ml of the *E. coli* DsRed cell suspension was added to all scintillation vials holding the *D. discoideum* cells. A 400 µl aliquot was transferred into duplicate 10 ml Falcon tubes

(labelled T_0) containing 3 ml of ice cold 20mM sodium phosphate buffer with 5 mM sodium azide (NaN_3) and left on ice. The azide treatment is performed to release the surface bound but not the internalized bacteria from the amoebae (Maselli *et al.,* 2002). The cell mixtures in the T_0 tubes were harvested by centrifugation at 2,500 *x g* for 2 minutes and washed with 3 ml of sodium phosphate buffer with 5 mM NaN_3. The washing was performed twice followed by centrifugation before resuspending the pelleted cells in 2 ml of 20 mM phosphate buffer.

The remaining *E. coli* and *D. discoideum* mixtures in the scintillation vials were left shaking at 21 ^{o}C for 30 minutes. After 30 minutes incubation, 400 µl aliquots of the cell suspensions were transferred to duplicate Falcon tubes (labelled T_{30}) containing 3 ml of ice cold 20mM sodium phosphate buffer with 5 mM NaN_3 and left on ice. The cells were centrifuged and washed as for the T_0 tubes and resuspended in 2 ml of 20 mM phosphate buffer. These suspensions for T_0 and T_{30} tubes were used to count cells for accuracy and data analysis.

The T_0 and T_{30} tubes were centrifuged again as previously stated and resuspended in 2 ml of 0.25 % (v/v) Triton X-100 in 100mM Na_2HPo4 (pH 9.2) buffer to lyse the cells, vortexed for 5-8 s and left on ice.

The OD_{640} of the *E. coli* DsRed cells was measured via a spectrophotometer to calculate the number of bacterial cells and the fluorescence signal per million bacteria (Maselli *et al*., 2002). The fluorescence signal per million bacteria was determined from the density and fluorescence of the bacterial culture used in a given experiment. The relationship between OD_{600} and the density of the bacterial suspension was determined in a separate calibration curve.

The fluorescence of the transformants was measured in a Modulus® fluorometer (Turner Biosystems™) by using a custom manufactured module designed for DsRed (530 nm excitation and 580 nm emission) for each duplicate sample. The fluorometer was preprogrammed to return the fluorescence as numbers of bacteria. The calculation of the phagocytosis rate to determine the hourly rate of consumption of bacteria by a single amoeba was performed according to the following formula:

$$\text{Phagocytosis rate (}\textit{E. coli}\text{ DsRed cells h}^{-1}\text{ amebae}^{-1}\text{)} = \frac{\Delta F \times 10^6}{\text{cell counts} \times \text{time}}$$

ΔF: fluorescence difference between T_0 and T_{30}

Cell counts: cell counts from T_0

Time: 0.5 h (time period during which the *D. discoideum* cells take up *E. coli* DsRed cells)

2.5.5. Pinocytosis

Pinocytosis was measured by using the protocol adapted from Klein & Satre, (1986) that relies on the fluorescent dye Fluorescein Isothiocyanate (FITC)-dextran.

D. discoideum strains were grown axenically in 50 ml HL-5 medium at 21°C, shaking at a speed of 150 rpm to a density of 1-2 x 10^6 cells ml^{-1}. 1 x 10^7 cells were harvested by centrifugation at 2,500 x *g* for 2 minutes and resuspended in 1 ml of HL-5 medium, which was then transferred into scintillation vials and incubated at 21°C for 30 minutes, shaken at 150 rpm.

Following the incubation, 100 µl FITC-dextran of 20 mg ml^{-1} stock was added to a working concentration of 2 mg ml^{-1} to each vial. 200 µl was transferred from each strain into duplicate 10 ml Falcon tubes (T_0) on ice containing 3 ml Sorensen buffer. The vials with the remaining samples were further incubated at 21°C for 70 minutes. In parallel, T_0 tubes were centrifuged at 2,500 x *g* for 2 minutes to harvest the cells. The cells were then washed with 3 ml Sorensen buffer and resuspended in 2 ml Sorensen buffer, in which they were counted using a haemocytometer.

Once the 70 minutes incubation time elapsed, 200 µl was transferred from each sample into duplicate 10 ml Falcon tubes (T_{70}) on ice containing 3 ml Sorensen buffer. In similar fashion to the T_0 samples, the cells in the T_{70} tubes were harvested and washed in Sorensen buffer. T_0 and T_{70} tubes were then centrifuged to harvest the cells, and 2 mL of 0.25% (v/v) Triton X-100 in 100 mM Na_2HPo4 (pH 9.2) was added to lyse the cells.

The fluorescence of the lysate was measured in a Modulus® fluorometer (Turner Biosystems ™) using the "Green Module". The fluorometer was preprogrammed to return the fluorescence in units of nanolitres of FITC-containing medium. The pinocytosis rate was calculated based on cell counts and the increase of fluorescence over 70 minutes (1.17 h) according to the following formula.

$$\text{Pinocytosis rate (nl h}^{-1}\text{ amoeba}^{-1}) = \frac{\Delta F \times 10^7}{2 \times \text{cell counts} \times \text{time}}$$

where ΔF is the fluorescence difference between T_0 and T_{70}

Cell counts: cell counts from T_0

Time: 1.17 h (time period during which the *D. discoideum* cells take up liquid medium)

2.5.6. Mitochondrial mass and mitochondrial membrane potential measurements

D. discoideum strains were grown axenically in 10 ml HL-5 medium at 21°C, shaking at a speed of 150 rpm to a density of 0.8 - 3 x 10^6 cells ml^{-1}. 3 x 10^6 cells were harvested and washed once with Lo-Flo medium by centrifugation at 2,500 *x g* for 2 minutes. The pellet was resuspended in 4 ml of Lo-Flo medium and cell count was performed and then cell concentration was adjusted to 0.5 x 10^6 cells ml^{-1}. (A blank control of any cells was also set up, in which the cells will not be stained with a dye). 2 ml of cell suspension was aliquoted into two 10 ml Falcon tube, one labelled MitoRed and the other MitoGreen. The Falcon tubes are then incubated at 21°C for 2 hours whilst shaking at 150 rpm to equilibrate the cells. After incubation time, 10 µl of 2 µM MitoTracker Red and 4 µM Mitotracker were added into the appropriate labelled tubes respectively. The blank tubes

were left unstained. The tubes were then covered with foil and incubated further for 1 hour whilst shaking. Afterwards, the cells were centrifuged at 2,500 x *g* for 2 minutes and the supernatant was removed.

The fluorescence of the cells was measured in a Modulus® fluorometer (Turner Biosystems ™) using the "Green Module" for the MitoTracker Red signal and the "Blue Module" for the MitoTracker Green signal.

The mitochondrial mass value is provided by the MitoTracker Green signal and is calculated after subtraction of the background fluorescence in the unstained cells.

The mitochondrial membrane potential (MMP) was determined as a ratio of the Red signal over the green signal as per the following formula: MMP = MitoTracker Red/MitoTracker Green.

2.6. Analysis of proteins

2.6.1. Estimation of protein concentration (Bradford assay)

The protocol for estimating protein concentration was adapted from the Bradford colorimetric method (Bradford, 1976) and the Bio-Rad protein assay. A standard was created by diluting 0, 2, 4, 6, 8 or 10 µl BSA protein (1 mg ml^{-1}) with milliQdH_2O to make a total volume of 800 µl in 1.5 ml Eppendorf tubes. To each 800 µl of BSA dilutions, 200 µl of Bio-Rad reagent (1 x) that were previously filtered with Whatman paper to remove particulates was added. The diluted BSA protein samples were then incubated for 10 minutes at room temperature and their optical density OD_{595} was measured using a spectrophotometer and stored to construct a standard curve. 10 µl of each protein samples was added to a mixture of 790 µl of milliQdH_2O and 200 µl of Bio-Rad reagent (1 x) and incubated as previously. The OD_{595} for unknown protein samples were measured and the protein concentration was calculated using the BSA standard curve.

2.6.2. SDS-PAGE analysis

Proteins were separated by SDS polyacrylamide gel electrophoresis according to their molecular mass using the Mini PROTEAN™II (Bio-Rad®) cell instructions manual. For the preparation of total *D. discoideum* cell lysates, 2×10^6 cells were harvested, centrifuged at 5000 × *g* for 2 minutes at 4 °C and washed twice with cold Sorensen buffer. The cell pellets were resuspended in Laemmli buffer and denatured by boiling for 10 minutes then cooled down at -20 ^oC for 1 minute. 1 µl of proteinase inhibitor (25 x, cocktail tablet, Roche) was added to prevent protein degradation.

The SDS-PAGE gel was put into a 2-Gel Tetra Module (Bio-Rad®) and submerged in 1 x Electrophoresis running buffer. 10 µl of protein samples were loaded onto pre-cast Mini-PROTEAN TGX 4-20 % gels (Bio-Rad®) with a BenchMark-Prestained protein ladder (Invitrogen®) as a size standard. The gel was electrophoresed at 200 V for 40-50 minutes using a PowerPac HC (Bio-Rad®). Once electrophoresis was complete, the gel was removed from the plastic plate and used in a Western blot to transfer the separated proteins to a membrane as described in Section 2.6.3.

2.6.3. Western blotting

Protein gels were transferred onto a PVDF membrane (Hybond-P) (GE Healthcare Life Sciences©) and electro-blotted using the Mini Trans-Blot® Electrophoretic Transfer Cell Apparatus (Bio-Rad®) as recommended by the manufacturer's manual. The PVDF membrane was cut to the same size of the gel and soaked in methanol for 1 minute for activation then washed with dH_20 to remove any excess methanol. The gel holder cassette transfer pack consisted of a black panel (cathode) and a clear panel (anode) sandwiching the gel, activated membrane, fiber pads and Watmann™ 3MM filter papers (GE Healthcare Life Sciences©) that were presoaked in transfer buffer. A fiber pad followed by 4 pieces of pre-soaked filter paper were placed on the cathode of the gel holder. The SDS-PAGE gel was then placed on top of the filter papers followed by the membrane, another 4 pieces of filter paper and a fiber pad. The gel holder cassette was closed after ensuring there are no air bubbles present and put into the electrophoresis transfer tank with a magnet at the bottom. A Bio–Ice cooling unit used to maintain appropriate buffer temperature was also placed in the tank filled with cold transfer buffer. The transfer apparatus was positioned on top of a magnetic stirrer for even distribution of the heat generated during transfer and electrophoresis was conducted at 4 ^{o}C at 100 V for 1 hour. After transfer, the membrane was removed from the cassette and proteins were detected using specific antibodies as described in Section 2.6.4.

2.6.4. Immunological detection of proteins with the ECF detection kit

After protein transfer, the PVDF membrane was blocked to prevent unspecific antibody binding by shaking for 1 hour at room temperature in blocking buffer consisting of 5 % (w/v) skim milk in TBS. The membrane was then washed twice with TBS-Tween/Triton (TBST) buffer for 10 minutes and once with TBS buffer. A primary antibody (diluted 1:500 with 5 % (w/v) skim milk in TBS) was added to the membrane and left on an orbital shaker at 4 ^{o}C overnight. Unbound antibody was removed by washing the membrane three times in TBST for 10 minutes intervals and the membrane was consequently incubated with anti-rabbit fluorescein-linked secondary antibody (diluted 1:5000 in TBST) for 1

hour rocking gently in the dark at room temperature. The membrane was washed again as previously stated and incubated with the third antibody, anti-fluorescein alkaline phosphatase conjugate (diluted 1:2500 in TBST) for 1 hour at room temperature. Afterwards, the membrane was washed as previously and incubated with 25ul of ECF substrate per cm^2 membrane for 5-10 minutes in the dark at room temperature. The membrane was dried with Whatmann 3MM filter paper and scanned and visualized using the blue fluorescence mode of a Storm 860™ Fluoroimager (Amersham Biosciences™).

2.7. Fluorescence microscopy

D. discoideum strains used for immunoflourescence were grown at 21°C in HL-5 medium to a density of 1-2 x 10^6 cells ml^{-1}. 2 ml of cell suspension was transferred into each well of a six-well Costar plate (NunC™) containing a sterile coverslip and left to settle for 1 hour in order to allow cells to adhere to the coverslips. HL-5 medium was then removed and replaced with 1 ml of Lo-Flo-HL-5 medium and the cells were incubated for 2 hours to reduce autofluorescence from ingested HL-5 medium.

The Lo-Flo-HL-5 medium was removed from the Costal wells and the coverslips were washed twice with phosphate buffer solution (PBS) (pH 6.5) and fixed by carefully adding 1 ml of 3.7 % (v/v) formaldehyde in PBS to each well and incubated for 30 minutes. The formaldehyde was removed and replaced with 100 % methanol and incubated at -20 °C for 10 minutes to make the cells permeable.

The coverslips were washed twice with PBS and incubated shaking for 1 hour at room temperature with LKB1 rabbit polyclonal antibody raised against *Dictyostelium* LKB1 protein (GenScript®) diluted 1:10 in 1% bovine serum albumin (BSA)/PBS plus 1% cold water fish skin gelatin (FSG) to a final concentration of 3 μg ml^{-1}.

The cells were then washed twice for 5 minutes with 0.1% BSA in PBS and incubated in the dark for 45 minutes at room temperature with secondary antibody Alexa-Fluor® 488 goat anti-rabbit (Invitrogen®) diluted 1:500 in 1% BSA/PBS to a final concentration of 8 μg ml^{-1}.

The coverslips were washed twice with PBS then incubated with 0.1 µg DAPI in PBS for 5 minutes in the dark at room temperature to stain nucleic acids. The cells were washed twice with PBS for 5 minutes to remove excess stain followed by a wash with milliQdH_2O. The coverslips covered with the fixed, stained cells were air dried and consequently mounted onto a microscope slide with 10 µl 90 % (v/v) glycerol in PBS.

The cell preparation was observed immediately with an Olympus Provis AX70 microscope at x 1000 magnification with oil immersion. Digital images were captured using an Olympus U-CMAD3 camera.

3. RESULTS

3.1. The kinase activity of LKB1 is essential for its function in LKB1-overexpressing cells.

3.1.1. Identification and bioinformatics analysis of LKB1 in D. discoideum

66,251.3 Da

To gain a better understanding of the biological roles of LKB1 in *Dictyostelium*, a BLAST (Basic Local Alignment Search Tool) search at dictyBase (the international dictyostelid genomics resource at http://dictybase.org) was carried out to identify homologues in the *D. discoideum* proteome using the protein sequence of human LKB1. The *Dictyostelium* homologue was identified to be DdLKB1: DDB0229349 and exhibits 46% identity and 63% similarity in the sequence aligned to the human protein (local sequence alignment shown in Figure 3.1A). *DdLkb1* cDNA is of 1761 bp length and the protein size is . The C-terminal part of the LKB1 has homo-polymeric tracts which are responsible for reduced sequence similarity of *Dictyostelium* in this region (not shown). The amino terminus is not conserved and not shown in the sequence alignment. In *Caenorhabditis elegans* and *Drosophila*, the amino and carboxyl terminal of the DdLKB1 are also not conserved when compared with human LKB1 (Alessi *et al.,* 2006). The *Dictyostelium* LKB1 kinase domain (261 aa) showed 48% identity to that of the human LKB1 (250 aa) (Figure 3.1B). Unlike human LKB1, DdLKB1 apparently lacks a nuclear localization signal at its N-terminus, while the farnesylation motif at its C-terminus is CIIN instead of the typical CLIQ signal. Out of the four known autophosphorylation sites for human LKB1 (Alessi *et al.,* 2006), DdLKB1 has only one conserved autophosphorylation site (T177) (Highlighted in yellow).

The *Dictyostelium* LKB1 will be referred to in this thesis as simply LKB1.

A.

Query sequence: Human LKB1, Length: 587

Subject Sequence: *Dictyostelium* LKB1

Score:	Expect:	Identities:	Positives:	Gaps:	Method:
266 bits (681)	1e-87	138/303(46%)	193/303(63%)	4/303(1%)	Compositional matrix adjust

```
Query  24   TFIHRIDSTE---VIYQPRRKRAKLIGKYLMGDLLGEGSYGKVKEVLDSETLCRRAVKIL  80
            FI  ++  E   + Y+ R+   KL+  Y++G++LGEG+YGKVK+ +DS T  R AVKIL
Sbjct  12   NFIIHLNENEDNGISYRSRKSTPKLVKHYILGEVLGEGAYGKVKDGMDSFTQKRVAVKIL  71

Query  81   KKKKLRRIPNGEANVKKEIQLLRRLRHKNVIQLVDVLYNEEKQKMYMVMEYCVCGM-QEM  139
            K+ +L++IP GEA+V KEI + ++L +K++I+L+D    EEK K+Y+V EY   G  Q +
Sbjct  72   KRARLKKIPGGEASVLKEINITKKLHNKHIIKLIDHFIIEEKGKLYIVYEYVGGGTSQNI  131

Query  140  LDSVPEKRFPVCQAHGYFCQLIDGLEYLHSQGIVHKDIKPGNLLLTTGGTLKISDLGVAE  199
            L++ P  R P  Q+   F QLI+  EY+HSQ I+H+DIKP N+L T    LK+SD GVAE
Sbjct  132  LENAPNGRLPPHQSQFIFRQLIEACEYIHSQKILHRDIKPDNILFTHANVLKLSDFGVAE  191

Query  200  ALHPFAADDTCRTSQGSPAFQPPEIANGLDTFSGFKVDIWSAGVTLYNITTGLYPFEGDN  259
                    +    S GSPAFQPPE+     TFS FK+DIW+ GVTLY +T G +PF G N
Sbjct  192  DSSQLEDFECLSRSYGSPAFQPPELTQFQTTFSPFKIDIWAMGVTLYLMTIGKFPFSGAN  251

Query  260  IYKLFENIGKGSYAIPGDCGPPLSDLLKGMLEYEPAKRFSIRQIRQHSWFRKKHPPAEAP  319
            ++ LFENI K     P D    L +L+KG+L+ +  +RFS+ QI+ H W  K  P  E
Sbjct  252  MFVLFENISKCKIEFPNDLDKDLVNLIKGILQVDHIQRFSLGQIKNHPWCIKYIPEVEPF  311

Query  320  VPI  322
            VP+
Sbjct  312  VPL  314
```

B.

Query sequence: *Dictyostelium* LKB1

Subject Sequence: Human LKB1, Length: 261

Score:	Expect:	Identities:	Positives:	Gaps:	Method:
234 bits (596)	8e-82	126/261(48%)	174/261(66%)	1/261(0%)	Compositional matrix adjust

```
Query  1    YILGEVLGEGAYGKVKDGMDSFTQKRVAVKILKRARLKKIPGGEASVLKEINITKKLHNK  60
            Y++G++LGEG+YGKVK+ +DS T  R AVKILK+ +L++IP GEA+V KEI + ++L +K
Sbjct  1    YLMGDLLGEGSYGKVKEVLDSETLCRRAVKILKKKKLRRIPNGEANVKKEIQLLRRLRHK  60

Query  61   HIIKLIDHFIIEEKGKLYIVYEYVGGGTSQNILENAPNGRLPPHQSQFIFRQLIEACEYI  120
            ++I+L+D    EEK K+Y+V EY   G  Q +L++ P  R P  Q+   F QLI+  EY+
Sbjct  61   NVIQLVDVLYNEEKQKMYMVMEYCVCGM-QEMLDSVPEKRFPVCQAHGYFCQLIDGLEYL  119

Query  121  HSQKILHRDIKPDNILFTHANVLKLSDFGVAEDSSQLEDFECLSRSYGSPAFQPPELTQF  180
            HSQ I+H+DIKP N+L T    LK+SD GVAE        +    S GSPAFQPPE+
Sbjct  120  HSQGIVHKDIKPGNLLLTTGGTLKISDLGVAEALHPFAADDTCRTSQGSPAFQPPEIANG  179

Query  181  QTTFSPFKIDIWAMGVTLYLMTIGKFPFSGANMFVLFENISKCKIEFPNDLDKDLVNLIK  240
              TFS FK+DIW+ GVTLY +T G +PF G N++ LFENI K     P D    L +L+K
Sbjct  180  LDTFSGFKVDIWSAGVTLYNITTGLYPFEGDNIYKLFENIGKGSYAIPGDCGPPLSDLLK  239

Query  241  GILQVDHIQRFSLGQIKNHPW  261
            G+L+ +  +RFS+ QI+ H W
Sbjct  240  GMLEYEPAKRFSIRQIRQHSW  260
```

Figure 3.1. Sequence relationships between human and *Dictyostelium* LKB1.

A. BLAST sequence alignments using the canonical *H. sapiens* LKB1 amino acid sequence as the query to search the predicted *D. discoideum* proteome. The LKB1 protein in *H. sapiens* is 433 amino acids long, whereas in *D. discoideum*, it contains 586 amino acids. T185 (highlighted in yellow) in *H. sapiens* LKB1 is the only site out of the four known autophosphorylation sites to be conserved in *Dictyostelium* LKB1. This residue appears at site 177 in *D. discoideum*.

B. BLAST sequence alignment using the *D. discoideum* LKB1 kinase domain amino acid sequence as the query to search the *H. sapiens* proteome for similarity. Kinase domain blast of human LKB1 (49-309) to *Dictyostelium* LKB1 yielded at 48% similarity. Out of the four known autophosphorylation sites for human LKB1, DdLKB1 has only one conserved autophosphorylation site (T177) (Highlighted in yellow).

3.1.2. Cloning lkb1 in E. coli vectors

To investigate the function of LKB1 in *D. discoideum*, transformants with overexpression levels of LKB1 were created. A two-phase cloning strategy was employed due to the difficulties of cloning PCR products and cloning AT-rich genes into AT-rich *D. discoideum* vectors. The full-length sequence of *lkb1* was first amplified and cloned into the *E. coli* cloning vector pUC18 (Figure 3.2). The DNA fragment was then excised from this vector, and subcloned into the *D. discoideum* expression vector pPROF267 as shown in Figure 3.3.

The gene fragments were amplified via PCR using gene-specific primers and *D. discoideum* AX2 genomic DNA (gDNA) as the template (Section 2.3.1). The LKB1 amplicon was cloned into the *Eco*RI site of pUC18 as shown in Figure 3.2.

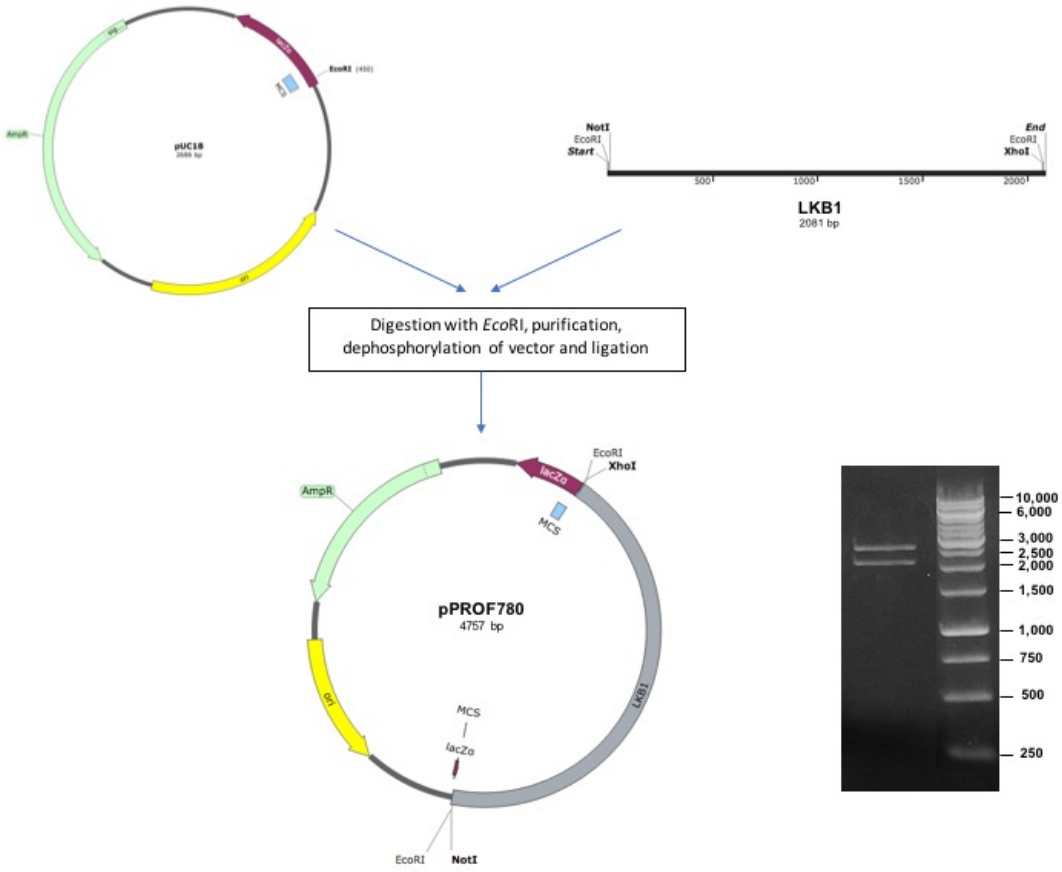

LANE	DNA	RESTRICTION ENZYME	FRAGMENT SIZE (bp)
1	1 kb DNA ladder		
2	pPROF780	*Eco*RI	2686 bp 2081 bp

Figure 3.2. Generation and restriction endonuclease digestion of pPROF780.
LKB1 of length 2081 bp, was amplified using primers LKB1F and LKB1R, digested with *Eco*RI and cloned into pUC18 to produce the construct pPROF780. The constructs were verified by restriction enzyme analysis (the enzymes and fragment size are listed in the above table) and sequenced by AGRF.

3.1.3. LKB1 gene sequencing

The cloned gene was sequenced by AGRF using the primers listed in Section 2.3.1. The sequences were then aligned with the native gene sequence using the software BioEdit and were used for BLAST searches at the NCBI website to confirm that they represented the *D. discoideum* homologue of human LKB1. The results of the sequencing are shown in Appendix 8.

3.1.4. Creation of LKB1 expression constructs in D. discoideum vectors

To create an overexpression construct, the full length LKB1 gene was excised from pPROF780 and subcloned into the *Not*I and *Xho*1 sites of the *D. discoideum* expression vector pPROF267 (Figure 3.3).

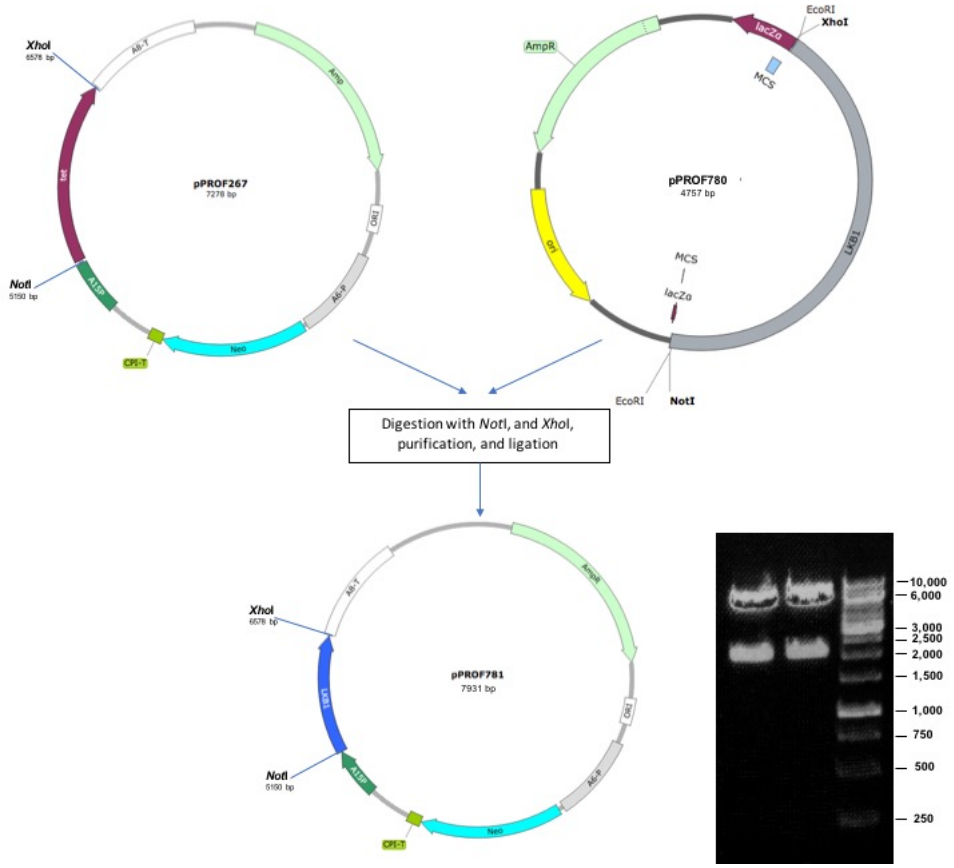

LANE	DNA	RESTRICTION ENZYME	FRAGMENT SIZE (bp)
1	1 kb DNA ladder		
2	pPROF781	*Not*I and *Xho*1	5850 bp, 2081 bp
3	pPROF781	*Not*I and *Xho*1	5850 bp, 2081 bp

Figure 3.3. Generation and restriction endonuclease digestion of pPROF781.
LKB1 was excised from pPROF780 and inserted into the *Not*I and *Xho*I sites of the *D. discoideum* expression vector pPROF267 effectively removing the Tet cassette to produce the construct pPROF781. The construct was verified by restriction enzyme analysis as listed in the table.

3.1.5. Subcellular Localisation of LKB1 in AX2 wild type cells

The subcellular localization of LKB1 in mammals is in both the cytoplasm and the nucleus (Boudeau *et al.*, 2003a; Dorfman & Macara, 2008). LKB1 is mainly localized in the nucleus due to the nuclear localization signal (NLS) found in its N-terminal noncatalytic region (residues 38-43); however, a mutation in this motif leads to the localization of LKB1 throughout the cell (Alessi *et al.,* 2006). These mutants still maintain the ability to inhibit cell growth like wildtype LKB1, implying that the cytoplasmic LKB1 mediates its tumour suppressor properties. Indeed, the importance of the cytoplasmic localization of LKB1 for its function has been demonstrated in PJS patients, in whom mutant forms of LKB1 localize exclusively in the nucleus and are unable to suppress cell growth (Boudeau *et al.,* 2003). Coexpression of LKB1 and STRADα targets the majority of wild type LKB1 to the cytoplasm, although a significant amount remains nuclear. However, when LKB1 is coexpressed with both STRADα and MO25, it becomes fully localised in the cytoplasm (Alessi *et al.,* 2006). The subcellular localization of LKB1 in *D. discoideum* is predicted to be cytoplasmic as the LKB1 protein in *Dictyostelium* lacks the nuclear targeting signal. To determine its localization, immunofluorescence was performed as described in Section 2.7. Figure 3.4 shows that LKB1 in *Dictyostelium discoideum* is cytoplasmic.

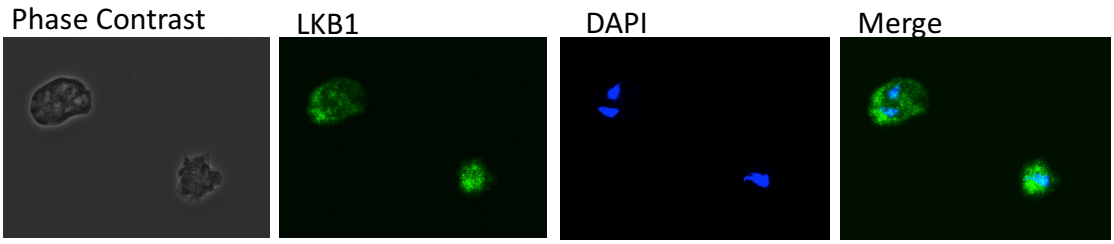

Figure 3.4. LKB1 is localised in the cytoplasm of wild type AX2.
Immunofluorescence using anti-LKB1 antibody shows that unlike in mammalian cells, the *Dictyostelium* LKB1 protein is only localised to the cytoplasm and not to the nucleus. This is predicted as the LKB1 protein in *Dictyostelium* lacks the nuclear targeting signal.

3.1.6. Creation of kinase-dead LKB1 expression constructs in D. discoideum vectors through mutagenesis

To determine whether the kinase activity of LKB1 is responsible for the phenotypes that will be examined in LKB1-overexpressing cells, a kinase-dead version of LKB1 was created using site-directed mutagenesis (refer to Section 2.3.3). Two mutations were introduced into LKB1: K69M which disrupts the binding of ATP to LKB1 and abolishes the LKB1 kinase activity and D186A in subdomain VII of the kinase domain rendering LKB1 catalytically inactive. In mammalian cells, kinase-dead LKB1 is retained within the nucleus, however since LKB1 in *Dictyostelium* does not have a nuclear targeting signal, it is expected to be expressed in the cytoplasm similar to wild type LKB1.

A.

Mammalian Protein	*Dictyostelium* Protein	*Dictyostelium* CDNA	*Dictyostelium* gDNA
K87M	K69M	AAA(207-209)ATG	AAA(305-307) ATG
D194A	D186A	GAT(558-560)GCT	GAT(740-742)GCT

B.

ATGGAAGTTGAACAACAACCATCATATACATCGAATTTTATAATTCATTTAAATGAAAATGAAGATA
ATGGCATTTCATATAGATCAAGAAAATCTACACCAAAATTAGTTAAACATTATATATTAGGTGAAGT
TTTAGGTGAAGGTATTTTTCAATCGATTATATATATATATATATATATATATATCATTATATATA
TAGTATGAAATATATTAATTTATTATTTATTAATTATTTTTAGGTGCTTATGGTAAAGTTAAAGATG
GCATGGATTCATTTACACAAAAAAGAGTAGCAGTTAATGTATTAAAAAGAGCAAGATTAAAAAAGAT
TCCTGGCGGGGAAGCATCAGTTTTAAAAGAGATTAATATTACAAAAAAGTTACACAATAAACATATA
ATCAAATTAATTGATCATTTCATTATAGAGGAAAAAGGTAAACTGTACATTGTCTATGAATATGTTG
GTGGTGGAACTTCACAAAATATTTTAGAAAATGCACCAAATGGTAGATTACCACCACACCAATCACA
ATTGTATGTATTATTTATTTTTTAAAATTTTTATATTTTATTTTTATTATTAAATAAAATATTTTAT
TAATAATAATAATAATTACAGTATATTTAGACAATTAATTGAAGCATGTGAATATATTCATTCACAA
AAGATATTACATCGTGATATTAAACCTGATAATATACTATTTACACATGCAAATGTATTGAAATTGA
GTGCTTTTGGAGTTGCAGAGGATAGTAGCCAATTGGAAGATTTTGAATGTTTATCAAGAAGTTATGG
TTCACCAGCATTTCAACCACCAGAGTTAACACAATTTCAAACTACATTTTCACCATTTAAAATCGAT
ATTTGGGCAATGGGTGTAACATTATACCTTATGACCATTGGTAAATTCCCTTTTTCCGGTGCAAATA
TGTTTGTACTTTTTGAAAATATCTCTAAATGTAAAATAGAATTTCCAAATGATCTCGATAAAGATTT
GGTTAATTTAATTAAAGGTATTTTACAAGTTGATCATATTCAAAGATTTTCATTAGGTCAAATTAAA
AATCATCCGTAAAGTATTAAATAAATAAATAATAATAATAATAATAATAAAACTATTTAAATAGATA
AGAGAGAGATAAATATTAATACCTTTTTTTTTATTTTCATAAATTTAGGTGGTGTATTAAATATATA
CCAGAGGTAGAACCATTTGTGCCATTATTAGAAGAAAGTAAATTTTTACCATTAGAGATGGCATATG
GTGATGATGAAGGTGATGATGGTGGAGGTGGTAGAGGAGGAGGAGGAGATGATGAACTTATTTTTGG
TTATGAAAATGATGGAAATACAATAGATTTACAAGATCCAGAATATATACCCTCTATATCAGTGGGT
GATCAACCACCATCAACTCCAATATTACATAGTAGTGATCATCATCATCATCATCATCATAATAACC
AACATCAACATCAACAACAACAACAGCAACTACAACAATCACAACAATTTCATGGTAATGGAGATAA
TAATTTATTATTTGATTCAAATAATAATTTAATATTTGATTCAAATAATAATTTATTATTTAATACA
AATAATAATGAACATTTAATTAATGGTTTACCAGTGCACCCAATTGAACTCGACCCTGTAAATATTA
AAAAGAGTTCAATTGGTACAAATATTTCTGATGTGGCTTTAATTCGTGAGAATTATATATGCTCTGA
TAATGATGCTAGTAGTGGTCAAGATGATGAAGACTATTCAGATGATAATGAAATTAGTGGTGAAGAT
TTAAATCCAACAAATCACCACCACCACCGTGCTGATAGAGTTGGCTCACGTGATAAGAGTTCAAGAT
CAAGTAAAAGAAAGAATAGTAGTAGTAATAATAATAATAATTCCACTTCTCCAAAAGTTGAATT
TAATCCAAACCGTTCTTCACCTCAACCACCTTTAAGAAATTCAAGTAATAGAAGGCCAAAAATTACT
TTTGAATCTCCACATAATAAGTCAAAATGTATCATTAATTAA

Figure 3.5. Creating a kinase-dead version of LKB1 using site directed mutagenesis.
A. The table shows the two sites at which the mutations were introduced and their respective conserved sites in mammalian cells as well as their location within the cDNA and gDNA of *Dictyostelium*. The mutations in the gDNA sequence are highlighted in red in **B**. K69M prevents the binding of ATP to the kinase domain of LKB1 and D186A renders the catalytic activity of LKB1 inactive.

3.1.7. Kinase-dead LKB1 gene sequencing

The mutated gene was sequenced by AGRF using the primers listed in Section 2.3.3; Table 2.11.1 to verify successful introduction of the desired mutations. The sequences were then aligned with the native gene sequence using the software BioEdit and were used for BLAST searches at the NCBI website to confirm that they represented the *D. discoideum* LKB1. The results are shown in Appendix 8.

3.1.8. Confirmation of D. discoideum kinase-dead LKB1 expression constructs

The kinase-dead LKB1 sequence was created by site-directed mutagenesis of the pPROF781 plasmid and hence a restriction analysis was necessary to verify the presence of the mutated construct in the plasmid. The kinase-dead LKB1 protein will be referred to in this thesis as LKB1 Dead Kinase. The *Dictyostelium* plasmid expressing LKB1 Dead Kinase was named pPROF782.

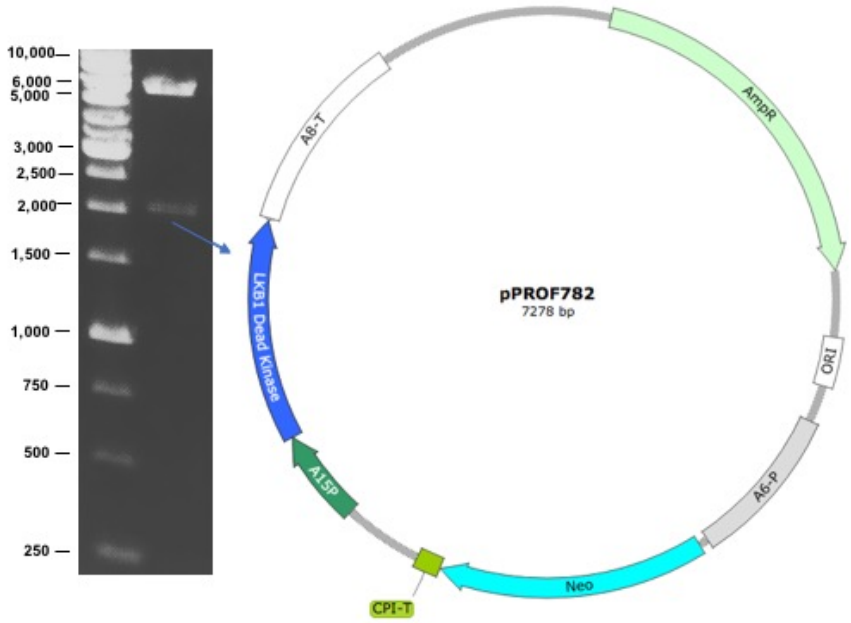

LANE	DNA	RESTRICTION ENZYME	FRAGMENT SIZE (bp)
1	1 kb DNA ladder		
2	pPROF782	*Not*I and *Xho*1	5850 bp, 2081 bp

Figure 3.6. Restriction endonuclease digestion of pPROF782.
The kinase-dead LKB1 construct in the *D. discoideum* expression vector (pPROF782) was verified by restriction enzyme analysis as listed in the table at the *NotI* and *Xho*I sites of the *D. discoideum* expression vector.

3.1.9. Creation of transformants with altered LKB1 expression

To create transformants with altered levels of LKB1 expression, the overexpression

construct of LKB1 (pPROF781) and of LKB1 Dead Kinase were transformed into parental *D. discoideum* strain AX2. During this process, multiple copies of the constructs are generated through the rolling circle replication of the plasmid constructs, which are integrated in a random manner into the *D. discoideum* genome via recombination (Barth *et al.,* 1998). The resultant transformants contain different numbers of copies of the construct and hence, express different levels of the gene. The number of copies of the inserted constructs in each transformant was determined by qPCR (Section 2.3.4) and the relative expression levels were revealed by Western blots using LKB1-antibody (Figure 3.7). The relationship between the LKB1 and LKB1 Dead Kinase levels and the copy numbers of the overexpression constructs were as predicted. Accordingly, this thesis deploys the formerly established convention of utilising the copy numbers as an expression index and assigning positive numbers to the overexpression construct copy numbers (Bokko *et al*., 2007).

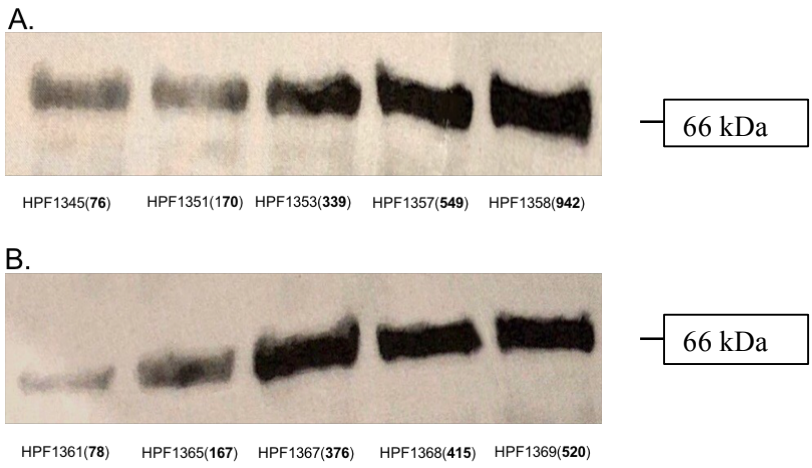

Figure 3.7. Western blot analysis of LKB1 and LKB1 Dead Kinase overexpression in *Dictyostelium*.

Total protein was isolated from *Dictyostelium* overexpressing LKB1 and LKB1 Dead Kinase of increasing copy numbers respectively. Equal amounts of protein from each suspension (50 µgktotal protein as measured by BCA) were loaded onto a 15-well 1 mm thick gel and *Dictyostelium* LKB1 protein was visualized by incubation with a rabbit polyclonal antibody raised against *Dictyostelium* LKB1 protein, followed by incubation with goat-anti-rabbit ECL Prime Detection antibody. The western blot shows that with increasing copy number of both LKB1 (A.) and LKB1 Dead kinase (B.), there is an increase in protein expression. The copy numbers of LKB1 overexpression and LKB1 Dead Kinase overexpression constructs are as shown in brackets underneath the protein bands.

3.1.10. Phenotypic analysis of LKB1 and LKB1 Dead Kinase transformants

To establish the effects of altering the levels of LKB1 and LKB1 Dead Kinase *in vivo* and the role of the LKB1 kinase in projecting these effects, the *D. discoideum* transformants overexpressing wild type LKB1 and LKB1 Dead Kinase were analysed phenotypically. It has been reported that chronic hyperactivation of AMPK results from mitochondrial dysfunction and phenocopies mitochondrial disease (Bokko *et al.,* 2007). As the primary upstream kinase of AMPK, overexpression of LKB1 in *D. discoideum* is expected to phenocopy that of AMPK overexpression and hence exhibit phenotypes of mitochondrial disease. In *D. discoideum,* mitochondrial dysfunction is characterized by a distinctive pattern of defective phenotypes including slow growth and defective fruiting body morphology (Annesley *et al.,* 2014).

Overexpressing LKB1 in *D. discoideum*, examining the relevant phenotypes and then comparing them with the phenotypes detected in mitochondrially diseased *D. discoideum* may thus reveal whether the cytopathology accompanying LKB1 overexpression could be mediated by AMPK hyperactivity which phenocopies mitochondrial dysfunction. The phenotypes resulting from overexpression of LKB1 Dead Kinase, on the other hand, would reveal if the effects of LKB1 are due to its kinase activity.

3.1.10.1. Selection of LKB1 and LKB1 Dead Kinase overexpression transformants

124 LKB1 overexpression transformants and 105 LKB1 Dead Kinase overexpression transformants were obtained in the AX2 parental background. Each transformant had a different number of copies of the expression construct and initially 50 of these transformants were assessed on their ability to grow on bacterial lawns. Out of these 50 strains, for each construct 10-13 were chosen which displayed a range of growth rates, most likely due to them containing a range of different copy numbers. These selected transformants were then used for the ensuing phenotypic analysis.

3.1.10.2. LKB1 overexpression negatively affects plaque expansion in *D. discoideum.*

A phenotype which was identified in AMPK overexpression and in mitochondrially

diseased strains was decreased growth on bacterial lawns (Bokko *et al.*, 2007). Figure 3.8A shows that LKB overexpression also caused a copy number-dependent decrease in plaque expansion rates in comparison to wild type AX2. On the other hand, overexpression of the LKB1 Dead Kinase construct resulted in increased plaque expansion rates in comparison to wild type AX2 (Figure 3.8B), a phenotype similar to that resulting from AMPK knockdown (Bokko *et al*., 2007). These results indicate that, like AMPK, chronic LKB1 hyperactivity causes slow growth and that the kinase-dead form of LKB1 is able to inhibit the endogeneous protein, for example by competing for substrates such as AMPK.

A.

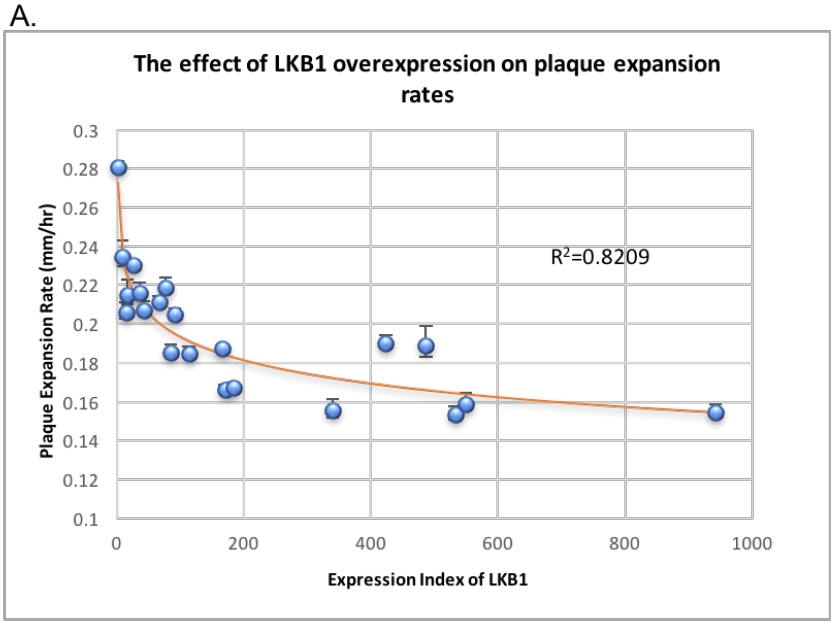

B.

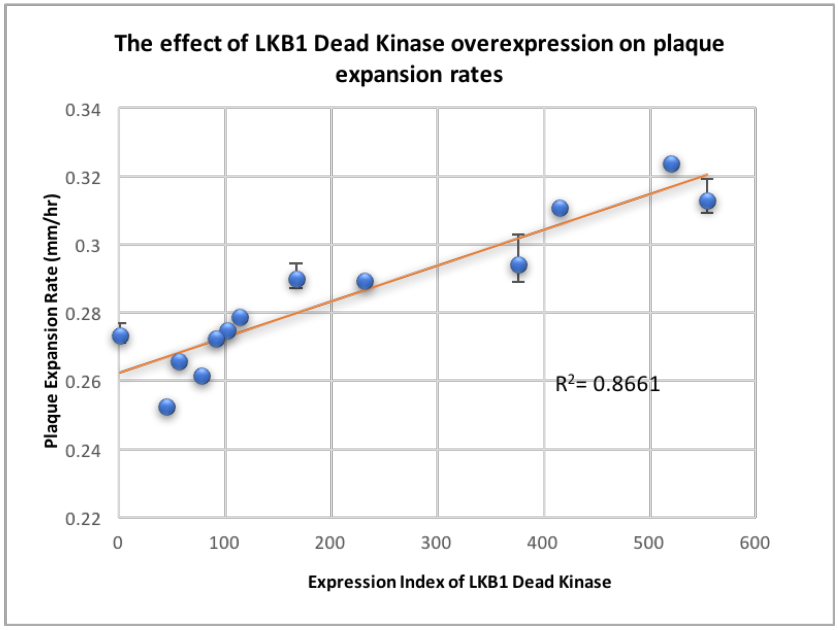

Figure 3.8. Plaque expansion rates of transformants with increased LKB1 and LKB1 Dead Kinase expression levels.

The plaque expansion rates for the transformants were normalized against the rates for AX2 and plotted against the expression index (construct copy number) for each of the wild type and kinase-dead forms of the protein. **A**. An increase in the LKB1 overexpression construct copy number and hence in the levels of expression, resulted in a decrease of the plaque expansion rates. **B**. An increase in the LKB1 Dead Kinase overexpression construct copy number and hence in the levels of expression, resulted in an increase of the plaque expansion rates. The figures show the coefficient of variation, R^2, representing the fraction of the variance in plaque expansion rates that was attributable to the regression relationship. The regressions were highly significant in **A**. at p = 0.00025217 (F test, n=21) and in **B.** at p = 1.96462E-06 (F test, n=13). Error bars are standard errors of the mean from 3 replicate measurements. In some cases, the error bars are too small to be visible.

3.1.10.3. LKB1 overexpression negatively regulates phagocytosis in *D. discoideum*.

Plaque expansion rates of *D. discoideum* on bacterial lawns are determined by the phagocytosis rate, growth rate and motility of the amoebae. Since LKB1 and LKB1 Dead Kinase expression levels affected the rate of plaque expansion, it was essential to establish whether this could be attributed to the ability of the transformants to take up bacteria through phagocytosis. The phagocytosis rates of AX2 and the LKB1 and LKB1 Dead Kinase overexpression transformants were measured as described in Section 2.5.4. The phagocytosis rate correlated with LKB1 and LKB1 Dead Kinase overexpression expression levels and the plaque expansion rates of the transformants. Increased expression levels in LKB1 transformants resulted in decreased phagocytosis rates, suggesting that the decrease in plaque expansion may be due to a decrease of the phagocytosis rate. Conversely, the phagocytosis rates were increased by elevated expression of LKB1 Dead Kinase, showing that the effect of LKB1 on phagocytosis depended on its kinase activity, as did the plaque expansion rate (Figure 3.9). This phenotypic outcome suggests that the increase in plaque expansion was due to an increase of the phagocytosis rate.

However, these findings do not phenocopy AMPK overexpression or mitochondrial disease in *Dictyostelium*, in both of which growth on bacterial lawns is impaired but phagocytosis is unaffected (Bokko *et al.,* 2007; Francione *et al*., 2011). The slower growth elicited by AMPK activity in mitochondrial disease was not a result of the impaired ingestion of nutrients but a consequence of the pathways that control cell growth and proliferation (Bokko *et al.,* 2007; Francione *et al*., 2011). My findings imply that LKB1 may play a role in the activation of nutritional stress responses through the activation of kinases other than AMPK.

A.

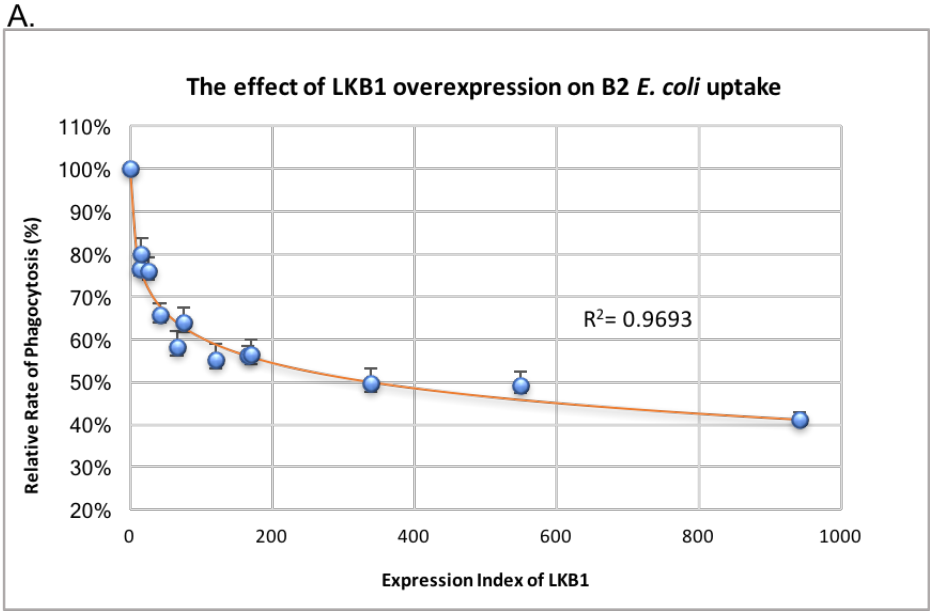

B.

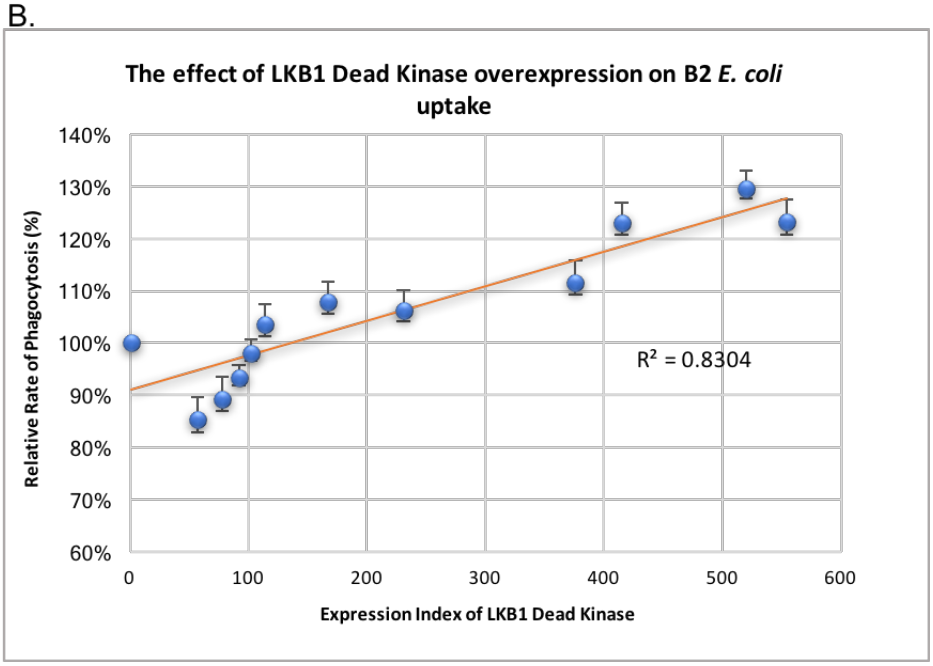

Figure 3.9. Phagocytosis rates of LKB1 and LKB1 Dead Kinase overexpression transformants.

Bacterial uptake by LKB1 overexpression transformants were determined using an *E. coli* strain expressing DsRed. The hourly rate of consumption of bacteria by a single amoeba was calculate from the increase in fluorescence over 30 minutes, the fluorescence signal per million bacteria and the amoebal density. The phagocytosis rates of the wild type AX2 and the transformants with altered LKB1 expression were measured and normalized against AX2. **A**. Overexpression of LKB1 leads to a decrease in phagocytosis which correlates with lower plaque expansion rates. **B**. Overexpression of Dead Kinase LKB1 results in an increase of bacterial uptake which is reflected by the increase in the plaque expansion rates on B2 *E. coli* lawns. The figures show the coefficient of variation, R^2, representing the fraction of the variance in phagocytosis rates that was attributable to the regression relationship. The regression was highly significant for **A**. at $p = 0.0033$ (F test, n=13) and for **B.** at $p = 1.86 \times 10^{-5}$ (F test, n=12). Error bars are standard errors of the mean from 3 replicate measurements.

3.1.10.4. Increased LKB1 expression negatively regulates axenic growth in HL5 media

Increased expression of LKB1 was found to negatively affect the growth of transformants on bacteria while the overexpression of the dead kinase version of LKB1 had the reverse effects. Since *D. discoideum* strains are able to grow axenically in HL-5 medium, I cultured transformants overexpressing LKB1 and LKB1 Dead Kinase in HL-5 to determine whether they had similar effects on axenic growth. The generation times of wild type AX2, LKB1 and LKB1 Dead Kinase overexpression transformants were measured as described in Section 2.5.2. Figure 3.10 shows that increasing LKB1 expression results in a significantly increased generation time. By contrast, expression of the LKB1 Dead Kinase had little effect on growth in liquid except at very high copy numbers of the expression construct (>400) when it did cause a modest reduction in growth rates. This result suggests that the kinase activity of LKB1 is required for its ability to impair growth in liquid medium at expression copy numbers up to 400. This is consistent with the impairment of growth in axenic medium observed in *Dictyostelium* strains overexpressing a constitutively active form of AMPK as well as mitochondrially diseased *Dictyostelium* strains (Francione *et al*., 2011).

At the highest expression levels, the LKB1 Dead Kinase appears to either exert a separate, kinase-independent inhibition of growth or to competitively inhibit a separate kinase-dependent enhancement of growth by the endogenous wild type LKB1. Such an enhancement could have been obscured by the large inhibition of growth by active, overexpressed LKB1. In either case the simplest explanation would involve at least one additional downstream LKB1 target relevant to growth in liquid medium, apart from AMPK.

A.

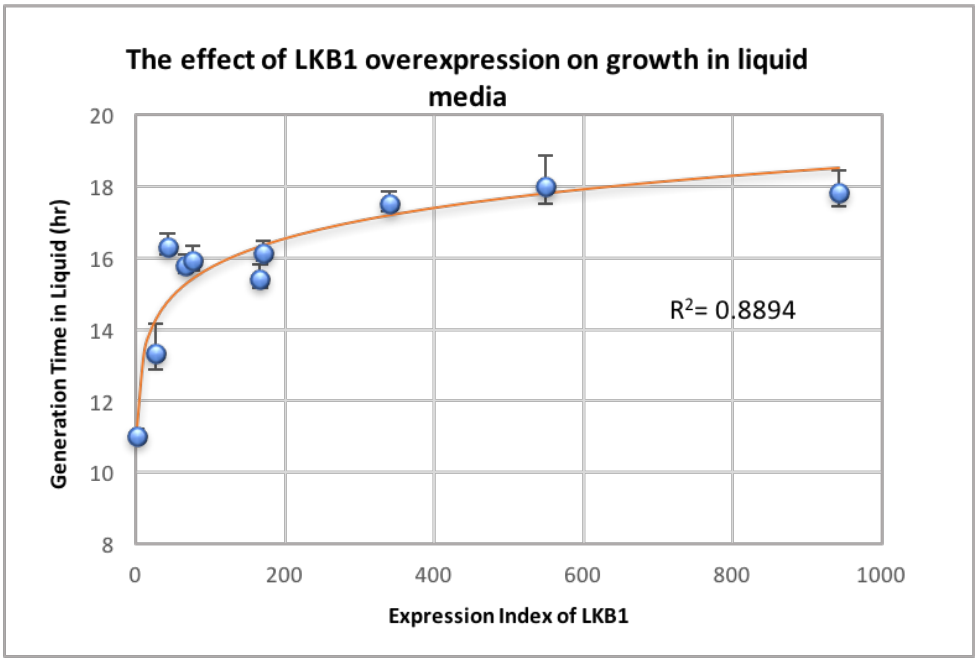

B.

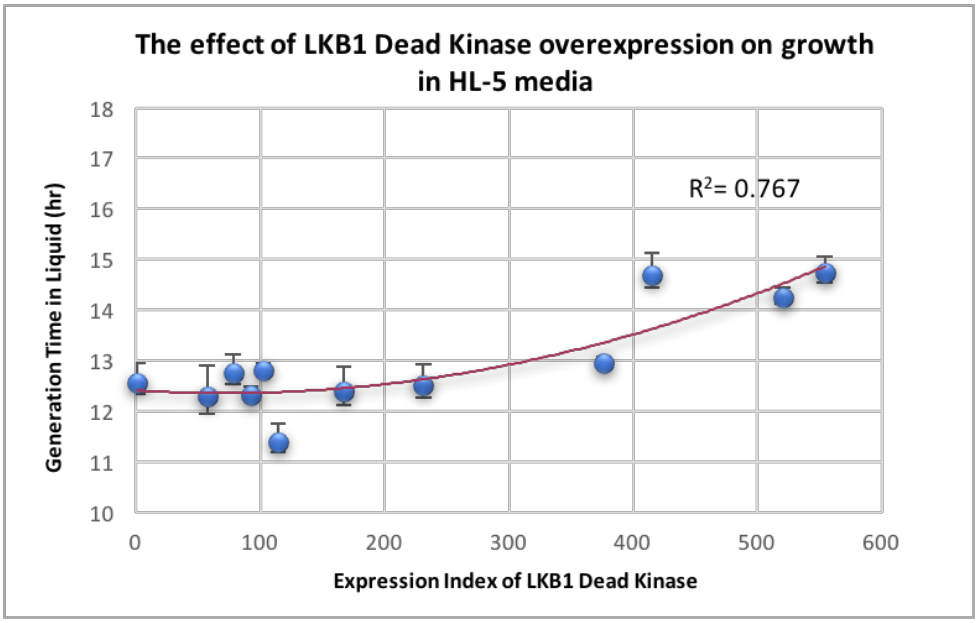

Figure 3.10. The effect of the overexpression of LKB1 and LKB1 Dead Kinase on the axenic growth of the transformants.

The generation times (the doubling time during exponential growth) of LKB1 and LKB1 Dead Kinase overexpression transformants were measured and compared with the parent strain, AX2. **A**. Increased LKB1 expression resulted in an increase in the generation time. **B**. LKB1 Dead Kinase expression had no significant effect at copy numbers below 400, but at higher copy numbers it caused a modest impairment of growth. The figure shows the coefficient of variation, R^2, representing the fraction of the variance in generation time that was attributable to the regression relationship. The regression was significant at $p = 0.000337556$ (F test, n= 10) and $p = 0.018470475$ (F test, n=12) for LKB1 and LKB1 Dead Kinase respectively. Error bars are standard errors of the mean from 3 independent experiments. Lines were fitted by least squares to a power curve in **A.** and a 2nd order polynomial in **B**.

3.1.10.5. LKB1 overexpression negatively regulates pinocytosis in *D. discoideum*.

An increase in the expression levels of LKB1 impaired the growth of the transformants in liquid medium, whereas a kinase-dead version of LKB1 had little effect except at the highest copy numbers where it also impaired growth, albeit modestly so. In order to determine the relationship between the growth of LKB1 overexpression transformants in liquid and their ability to ingest nutrients from the liquid medium, the rates of pinocytosis were assessed (Section 2.5.5). Figure 3.11A shows that overexpression of LKB1 did result in copy number-dependent decreases in the rate of pinocytosis. LKB1 Dead Kinase transformants had little effect on pinocytosis except at construct copy numbers greater than 400 when it caused a modest increase in pinocytosis rates.

These results indicate that, as was the case for phagocytosis, LKB1 inhibits pinocytosis by a mechanism that depends on its kinase activity. At the highest expression levels LKB1 Dead Kinase even enhances pinocytosis, suggesting that it begins to competitively restrain the pinocytosis-inhibiting activity of endogeneous wild type LKB1 in the cells. Phagocytosis and pinocytosis rates depend upon signalling pathways coupled to the cell's nutritional status and containing both shared and distinct elements (Maniak, 2003). My results show that LKB1 kinase activity is one of these shared elements.

Previous studies showed that, with the exception of some Complex I-specific defects, neither mitochondrial disease in *Dictyostelium* nor chronic hyperactivity of AMPK affects phagocytosis or pinocytosis (Bokko *et al*., 2007; Francione *et al*., 2011). Thus, LKB1 must regulate endocytosis through the phosphorylation of downstream targets other than AMPK.

A.

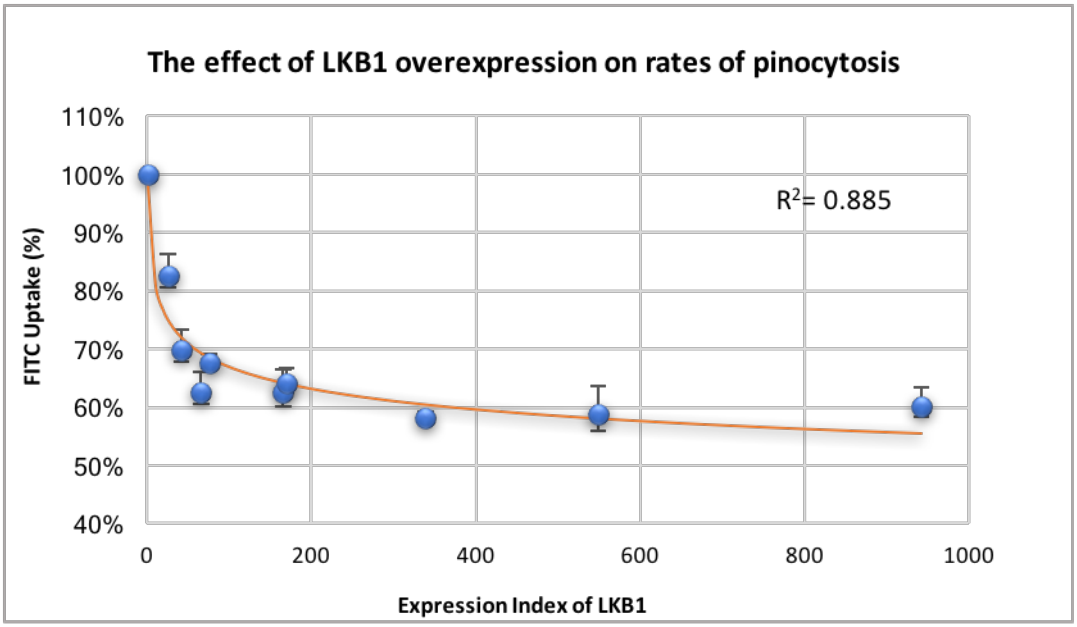

B.

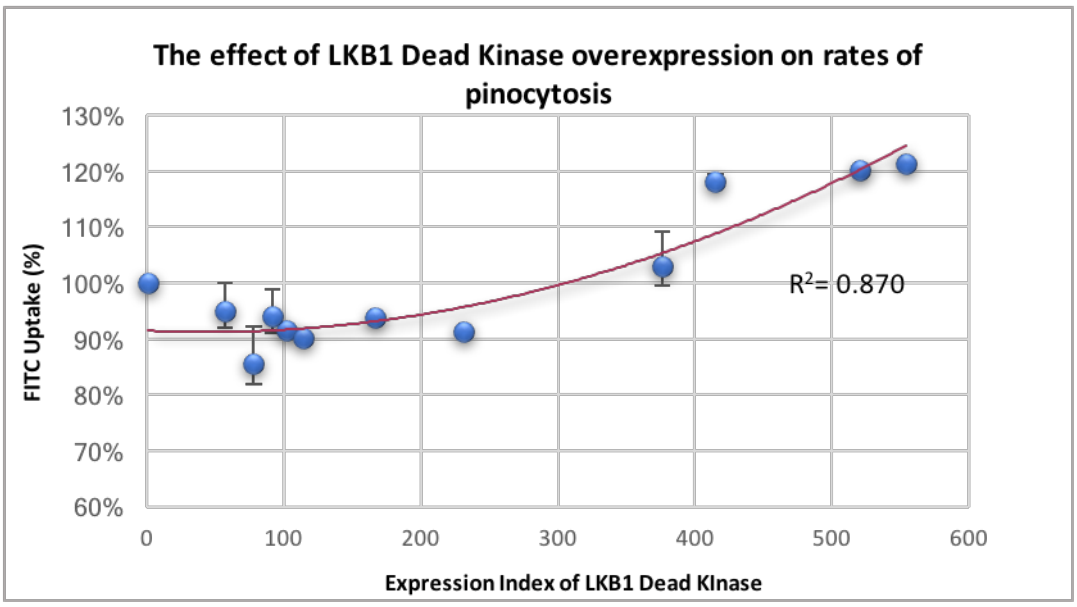

Figure 3.11. The pinocytosis rates of LKB1 and LKB1 Dead Kinase overexpression transformants.

AX2 and LKB1 and LKB1 Dead Kinase overexpression transformants were grown in low fluorescence HL-5 medium containing FITC-dextran. **A**. As the expression levels of LKB1 increased, the pinocytosis rates of the transformants decreased. **B**. The increased expression of LKB1 Dead Kinase showed to have similar and enhanced pinocytosis rates compared to wild type AX2. The figure shows the coefficient of variation, R^2, representing the fraction of the variance in pinocytosis rates that was attributable to the regression relationship. The regression was significant at p= 0.000121824 (F test, n= 10) for transformants with LKB1 overexpression and p= 0.058227824 (F test, n= 12) for transformants with LKB1 Dead Kinase overexpression. Error bars are standard errors of the mean from 3 independent experiments. Lines were fitted by least squares to a power curve in **A.** and a 2nd order polynomial in **B.**

3.1.10.6. LKB1 expression affects the fruiting body morphology

Development in *Dictyostelium* involves starvation-induced differentiation, as a result of which the amoebae undergo chemotactic aggregation followed by multicellular differentiation and formation of a fruiting body - a sorus (spores) held aloft by a stalk and basal disk comprising of vacuolated cells (Strmecki *et al*., 2005; Williams, 2006). Chemotactic aggregation of food starved cells is arbitrated by a cAMP sensory system (Chisholm & Firtel, 2004). Whilst aggregating, the cells identify cAMP gradients and reorganise their cytoskeleton to respond accordingly (Liu *et al*, 2016). A family of surface cAMP receptors (cARs), exhibiting a typical heptahelical structure of G-protein-coupled receptors, detect the extracellular cAMP and bind to it. This leads to the activation of energy-consuming signal transduction cascades which in turn mediate the chemotactic response (Swaney *et al*., 2010). These processes involve the activation of heterotrimeric G-proteins, small GTP-binding proteins and ion fluxes, guanylyl cyclase activity and protein kinase signalling cascades (Wu *et al.*, 1995; Meena & Kimmel, 2016), all of which entail high energy turnover. These pathways are possibly subject to AMPK and hence LKB1 signalling and thereby sensitive to the depletion of energy resulting from mitochondrial disease.

Mitochondrial disease in *Dictyostelium* and the chronic hyperactivity of AMPK have been shown to result in impaired morphogenesis, characterised by fewer fruiting bodies and short thick stalks (Kostifas *et al*., 2002; Bokko *et al*., 2007) resulting from misregulation in the stalk differentiation pathway (Chida *et al.,* 2004). Due to the role of LKB1 as the main upstream kinase of AMPK, I decided to explore whether LKB1 was also involved in the regulation of normal fruiting body morphogenesis and whether its effects are attributable to its kinase activity. LKB1 and LKB1 Dead Kinase transformants as well as the wild type AX2 were subcultured on plates containing a lawn of *K. aerogenes* and incubated at 21 °C for several days until fruiting bodies emerged. The fruiting bodies of the transformants were then inspected and compared to that of the wild type AX2 as described in Section 2.5.3. Increases in LKB1 expression resulted in aberrant fruiting bodies with short thick stalks, a similar phenotype to that presented in cells with AMPK overexpression and mitochondrial dysfunction; whereas the overexpression of LKB1 Dead Kinase in healthy cells led to the formation of fewer, slightly smaller fruiting bodies that were relatively normal morphologically. This is similar to the morphology of AMPK antisense transformants (Bokko *et al*., 2007; Fisher, personal communication). The results

show that chronic LKB1 kinase hyperactivity produces a similar morphological phenotype as that caused by chronically elevated AMPK activity and by mitochondrial disease.

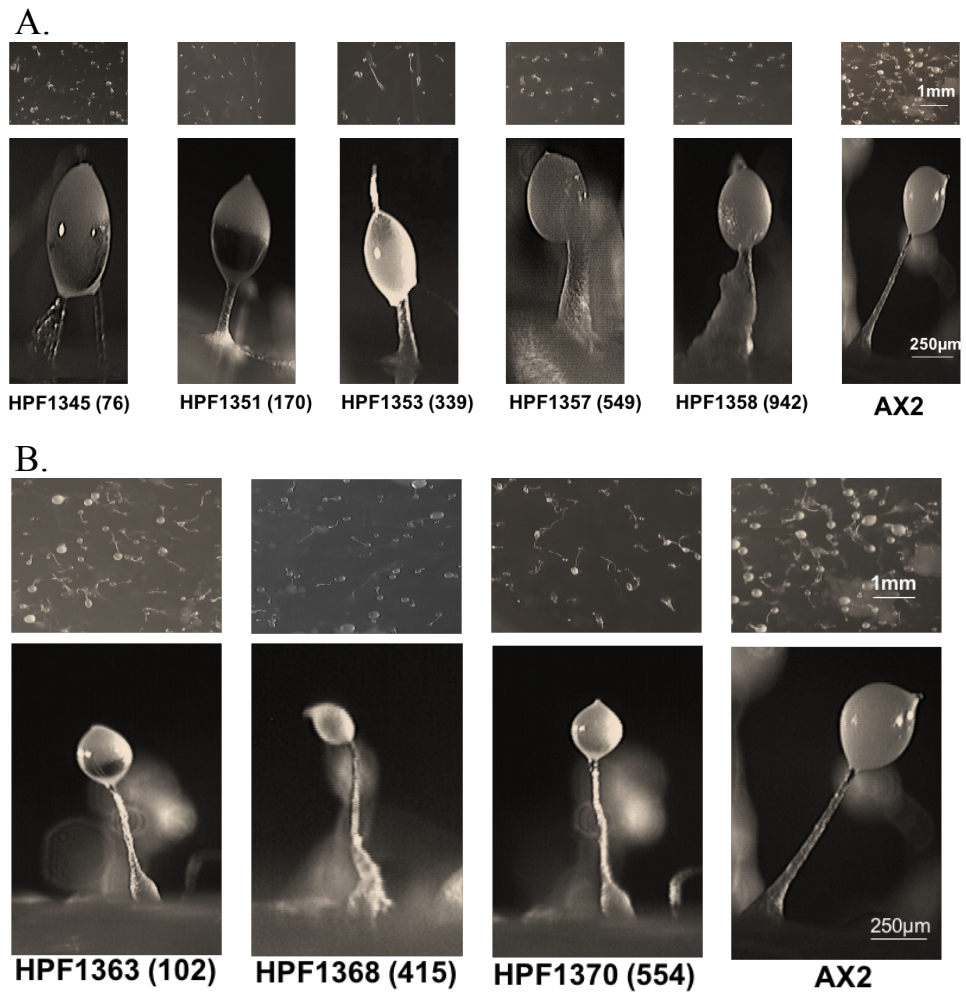

Figure 3.12. Fruiting body morphogenesis of transformants with altered LKB1 expresssion.

A. The fruiting bodies of LKB1 overexpression transformants. Each picture is represented by the strain name followed by the copy number of pPROF781 (LKB1 overexpression construct). **B:** The fruiting bodies of LKB1 Dead Kinase overexpression transformants. Each picture is represented by the strain name followed by the copy numbers of pPROF782 (LKB1 Dead Kinase overexpression construct). Wild type AX2 fruiting bodies contain long slender stalks whereas transformants with increased expression of LKB1 have short, aberrant and thicker stalks in comparison to wild type AX2. The severity of the defect correlates with the increase in LKB1 expression. Transformants with increased expression of LKB1 Dead Kinase have fewer, slightly smaller fruiting bodies of otherwise similar morphology to wild type AX2.

3.1.11. The role of LKB1 kinase activity in mitochondrial biogenesis

3.1.11.1. LKB1 kinase activity regulates mitochondrial mass and mitochondrial membrane potential

In mammalian cells, AMPK plays a crucial role in energy homeostasis of healthy cells. In muscle tissues particularly, the activity of AMPK results in mitochondrial proliferation as a response to strenuous physical training (Bergeron *et al.*, 2001; Zong *et al.*, 2002). Nevertheless, mitochondrial proliferation can also be a feature of mitochondrial diseases (Campos *et al.*, 1997; Agostino *et al.*, 2003). Bokko *et al.* (2007) reported an increase in mitochondrial mass of *Dictyostelium* cells overexpressing active AMPK. By contrast there was no change in mitochondrial mass in cells in which expression of chaperonin 60, an essential mitochondrial protein, had been antisense inhibited; most probably because in these cells a reduction in mitochondrial biogenesis caused by chaperonin 60 knockdown was countermanded by chronic hyperactivation of AMPK (Bokko *et al*., 2007).

In view of the role of AMPK in stimulating mitochondrial biogenesis, I examined whether LKB1 as its major upstream activating kinase might cause this same cytopathology. Mitochondrial "mass" was measured by fluorescence with MitoTracker Green, a mitochondrion-specific dye whose binding is not dependent upon the membrane potential. The mitochondrial membrane potential was assessed by another fluorescent stain, MitoTracker Red, normalized against the Mitotracker Green staining. Figure 3.13A shows that overexpression of LKB1 resulted in an increase in mitochondrial mass indicated by a stronger MitoTracker Green fluorescence signal per cell. Conversely, LKB1 Dead Kinase overexpression reduced the fluorescence signal (Figure 3.13B), consistent with competitive inhibition of the endogenous LKB1 activity and similar to the effect of AMPK antisense inhibition (Bokko *et al.*, 2007). These results show that, like AMPK, the kinase activity of LKB1 stimulates mitochondrial biogenesis in *Dictyostelium*.

The effects of AMPK overexpression on the mitochondrial membrane potential in *Dictyostelium* have not been reported. However, my mitochondrial membrane potential measurements showed that LKB1 overexpression caused a reduction in the mitochondrial membrane potential (Figure 3.13C), whereas LKB1 Dead Kinase resulted in an increase in mitochondrial membrane potential (Figure 3.13D). The mitochondrial membrane

potential is a result of the balance between proton pumping by the respiratory electron transport chain and consumption of the resulting proton motive force by ATP synthesis and other mitochondrial membrane transport processes. Its reduction by LKB1 overexpression suggests the possibility that LKB1 not only stimulates mitochondrial biogenesis but also the "consumption" of the mitochondrial membrane potential by ATP synthesis and membrane transport. Consistent with this, Bokko *et al*. (2007) reported that hyperactivity of AMPK, a downstream target of LKB1, caused elevation of cellular steady state ATP levels.

My results confirm that mitochondrial biogenesis in *Dictyostelium* is stimulated by LKB1 kinase activity and strongly insinuate that LKB1 acts as an upstream kinase of AMPK in the regulation of mitochondrial biogenesis.

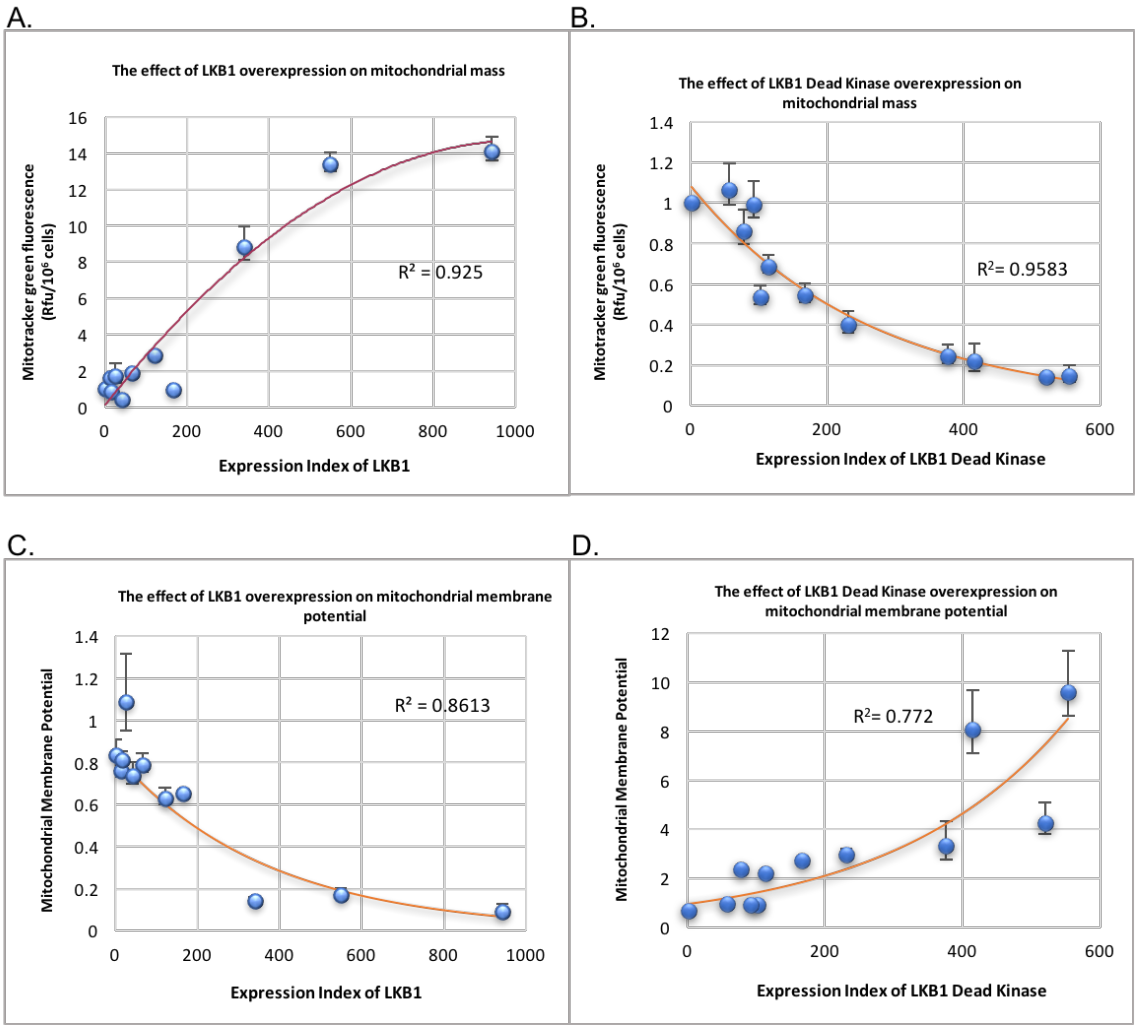

Figure 3.13. Effect of LKB1 expression levels on mitochondrial mass and ATP levels in *Dictyostelium*.

The expression index indicates the copy numbers of the overexpression constructs of LKB1 and LKB1 Dead Kinase constructs. Copy numbers of zero refer to the wild-type parental strain AX2. **(A, B)** Mitochondrial mass is measured by fluorescence with the mitochondrion-specific dye MitoTracker Green after subtraction of autofluorescence from unstained cells from the same suspension. LKB1 overexpression transformants exhibit an increase in mitochondrial mass whereas LKB1 Dead Kinase transformants exhibit a decrease. **(C, D)** In LKB1 overexpression cells, the membrane mitochondrial biogenesis decreases dependent on copy number; however, the LKB1 Dead Kinase strains show an increase in mitochondrial membrane potential. The figure shows the coefficient of variation, R^2, representing the fraction of the variance in mitochondrial mass and mitochondrial membrane potential that were attributable to the regression relationship. For mitochondrial mass measurement, the regression was significant at $p = 9.02 \times 10^{-6}$ (F test, n= 11) for transformants with LKB1 overexpression and $p = 1.72 \times 10^{-5}$ (F test, n = 12) for transformants with LKB1 Dead Kinase overexpression. For mitochondrial membrane potential measurements, the regression was significant at $p = 0.00027$ (F test, n= 11) for transformants with LKB1 overexpression and $p= 0.00018$ (F test, n= 12) for transformants with LKB1 Dead Kinase overexpression. Error bars are standard errors of the mean from 3 independent experiments.

3.2. AMPK activity is responsible for some but not all of the functions of LKB1

AMPK performs a vital role in the regulation of energy metabolism at a cellular level and helps defend the body from metabolic diseases, such as obesity and type 2 diabetes. Conversely, mutations of AMPK can lead to cardiac arrhythmia and hypertrophy. LKB1 is an essential upstream kinase of AMPK in mammalian cells (Hong *et al.,* 2003; Shaw *et al.,* 2004) where it can phosphorylate Thr172 on the activation loop of the AMPK catalytic subunit and consequently activate AMPK (Shaw *et al.,* 2004; Woods *et al.,* 2003). The inhibition of LKB1 activity in cells significantly decreases the activation of AMPK by different stimuli (Woods *et al.,* 2003). I wanted to assess whether the function of LKB1 in *Dictyostelium discoideum* is mediated by the activity of AMPK, so I created cotransformants overexpressing LKB1 and antisense-inhibiting AMPK and then analysed the phenotypic outcomes. If the abnormal phenotypes resulting from LKB1 overexpression are mediated by its activation of AMPK, knockdown of AMPK expression in the same cells should suppress these phenotypes.

3.2.1. Creation of cotransformants with increased expression of LKB1 and antisense-inhibited expression of AMPK.

To create cotransformants containing both LKB1 overexpression and AMPK antisense inhibition constructs, parental *D. discoideum* strain AX2 cells were transformed with the LKB1 overexpression construct (pPROF781) and the AMPK antisense-inhibition construct (pPROF360). Because of independent integration and coinsertional rolling circle replication of the two constructs (Barth *et al.,* 1998), the resultant transformants contain different numbers of copies of both and so express different levels of both genes. The numbers of copies of the constructs were determined by qPCR (Section 2.3.4; Table 2.3) and relative expression levels were verified by western blots using antiLKB1 antibodies (Section 3.2.2.2). The relationship between the cotransformants and the copy numbers of the overexpression and antisense-inhibited constructs were as predicted. As in the earlier sections of the thesis, the copy numbers were therefore used as an expression index.

3.2.2. Phenotypic analysis of LKB1 overexpression and AMPK antisense-inhibited cotransformants

In Section 3.1, I showed that LKB1 overexpression produces similar phenotypes as those reported for both mitochondrial disease and overexpression of active AMPK with respect to growth and morphogenesis, but not endocytosis. To establish the effects of decreasing AMPK expression levels in LKB1 overexpression transformants and whether the role of LKB1 in *Dictyostelium* is mediated through its activation of AMPK, LKB1 overexpression/AMPK antisense inhibition cotransformants were analysed phenotypically.

3.2.2.1. Selection of LKB1 overexpression/AMPK antisense-inhibited cotransformants

94 LKB1 overexpression/AMPK antisense-inhibited cotransformants were obtained in the AX2 parental background. Each transformant had a different number of copies of both expression constructs and initially 45 of them were assessed on their ability to grow on bacterial lawns. Out of these 45 strains, 10-12 were chosen which exhibited a range of growth rates, most likely due to them holding a range of diverse copy numbers. These selected transformants were then used for the following phenotypic analysis.

3.2.2.2. Western blot to verify increased expression of LKB1 in LKB1 overexpression/AMPK antisense inhibition cotransformants

To establish that LKB1 was expressed in the cotransformants, a western blot was performed on strains with relatively high copy numbers of LKB1. Figure 3.14 shows that LKB1 is overexpressed in the expected manner in cotransformants with various copy numbers of the LKB1 overexpression construct. AMPK knockdown could not be similarly verified at the protein level for lack of a suitable antibody.

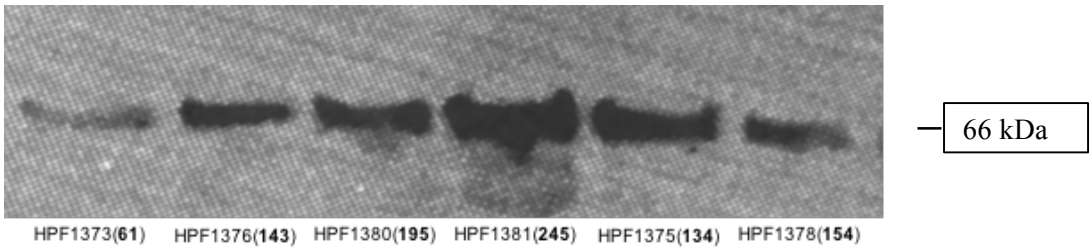

Figure 3.14. Western blot analysis of LKB1 expression in *Dictyostelium* cotransformants with LKB1 overexpression and antisense-inhibited AMPK expression.
Total protein was isolated from cotransformants and equal amounts of protein from each suspension (~50 µg total protein as measured by BCA) were loaded onto a 15-well 1 mm thick gel, subjected to SDS PAGE and western blotted. *Dictyostelium* LKB1 protein was visualized by incubation with a rabbit polyclonal antibody raised against *Dictyostelium* LKB1 protein, followed by incubation with goat-anti-rabbit ECL Prime Detection antibody. The western blot shows LKB1 expression at the following various copy numbers of 61, 143, 195, 245, 134 and 154 respectively (left to right).

3.2.2.3. Antisense inhibition of AMPK rescues impaired growth caused by the overexpression of LKB1 in *D. discoideum*.

A phenotype which was identified in AMPK overexpression and in mitochondrially diseased strains was decreased growth on bacterial lawns, while AMPKα antisense inhibition actually enhanced growth in healthy cells and restore impaired growth in mitochondrially diseased cells to normal (Bokko *et al.,* 2007). To explore whether the slow growth rate of LKB1 overexpression transformants can be rescued by inhibiting the expression of AMPK, the cotransformants were observed for their ability to grow on normal agar plates covered with a lawn of *E. coli* B2. The rate of plaque expansion was calculated as described in Section 2.5.1. The cotransformants showed similar plaque expansion rates to wild type AX2 indicating a rescue in the phenotype observed previously to result from LKB1 overexpression. This result shows that the effect of LKB1 on plaque expansion is regulated by AMPK.

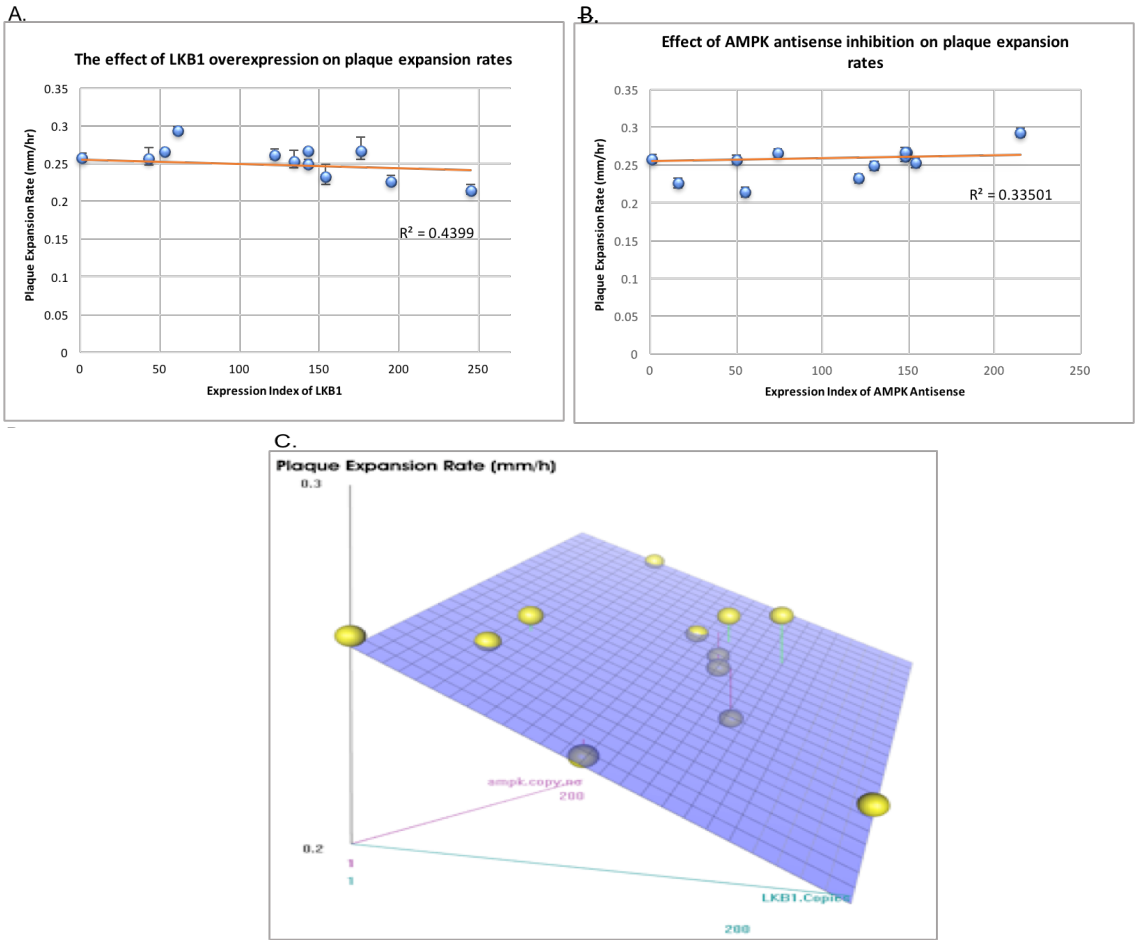

Figure 3.15. Plaque expansion rates of cotransformants with LKB1 overexpression and AMPK antisense inhibition constructs.

The plaque expansion rates for the transformants were measured and plotted against the expression indices (construct copy numbers for the LKB1 overexpression and AMPK antisense constructs). All cotransformants exhibited plaque expansion rates in the range between 0.2 and 0.3, similar to the wild type parental strain AX2. In simple regressions, the plaque expansion rates were unaffected by the LKB1 overexpression construct copy number (**A**) or the AMPK antisense inhibition construct copy number (**B**). However, 3D plots showed that this was because a copy number-dependent inhibitory effect of LKB1 overexpression was suppressed in a copy number-dependent manner by AMPK antisense inhibition (**C**). In multiple regression analysis, this decrease due to LKB1 overexpression was significant at $p = 3.2 \times 10^{-5}$ (*t* test) and its suppression by AMPK antisense inhibition was significant at $p = 4.2 \times 10^{-5}$ (*t* test). Error bars are standard errors of the mean from 3 independent experiments.

3.2.2.4. Nutrient ingestion rates in phagocytosis are inhibited by LKB1 overexpression and are not rescued by AMPK antisense inhibition

Cell division and growth relies on the continued ability of the cells to take up nutrients. In *Dictyostelium,* this is achieved by phagocytosis during growth on bacterial lawns.

Assays for the rate of bacterial uptake by phagocytosis (Figure 3.16) showed that phagocytosis was dramatically affected by increase LKB1 levels; however, it was not significantly affected by antisense inhibition of AMPK. This implies that although antisense inhibition of AMPK rescues the slow rate of plaque expansion caused by increased LKB1 expression, it has not affected the role of LKB1 in negatively regulating phagocytosis. Thus, the activity of AMPK does not mediate the slow rate of nutrient ingestion through phagocytosis caused by LKB1 hyperactivity. This shows that the dramatically slow growth elicited by LKB1 activity in *Dictyostelium* cells is mediated by AMPK; however not as a result of AMPK's effects on the rate of ingestion through phagocytosis.

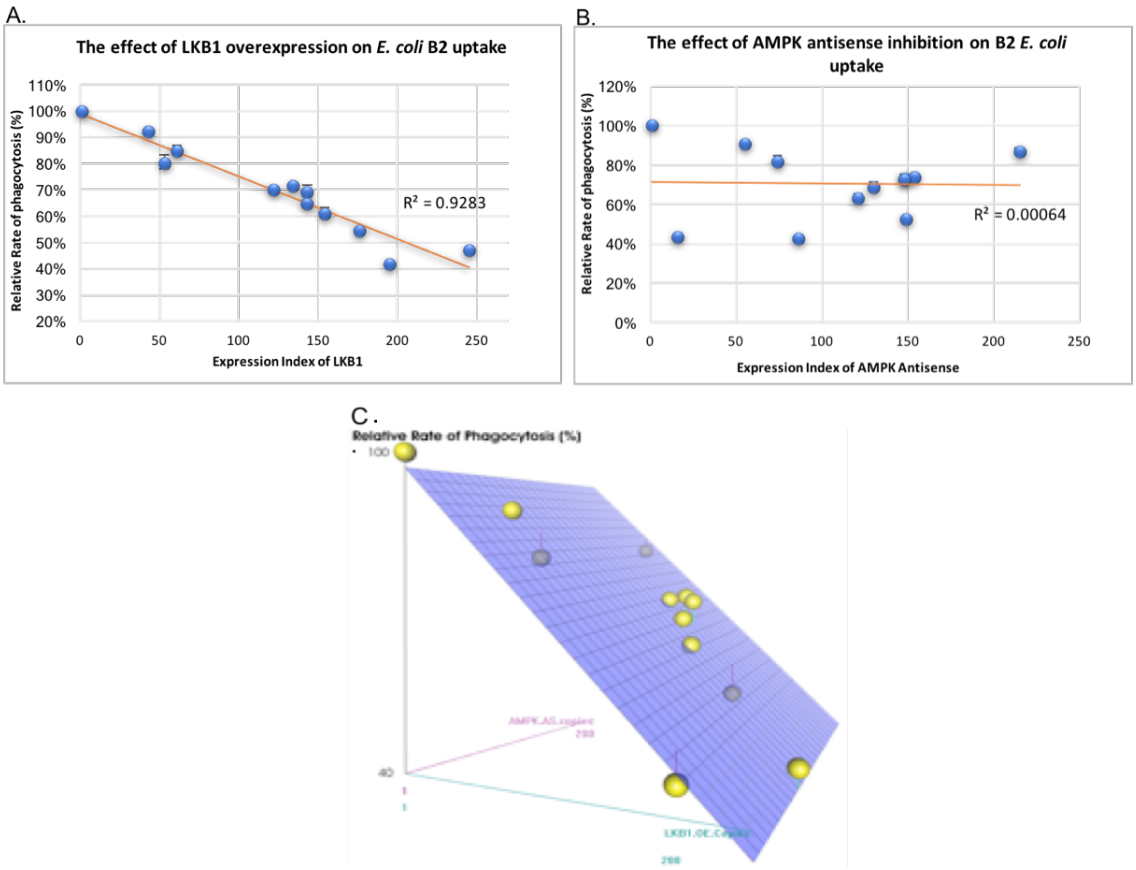

Figure 3.16. Phagocytosis rates of LKB1 overexpression and AMPK antisense-inhibited co-transformants.

The phagocytosis rates of the wild type AX2 and the cotransformants with LKB1 overexpression and AMPK antisense inhibition were measured and normalized against AX2. Bacterial uptake was determined using as prey an *E. coli* strain expressing DsRed. The hourly rate of consumption of bacteria by a single amoeba was calculate from the increase in fluorescence over 30 minutes, the fluorescence signal per million bacteria and the amoebal density. In simple regressions, the overexpression of LKB1 produced a copy number-dependent decrease in phagocytosis rates (**A**), whereas there was no copy number-dependent effect of AMPK antisense inhibition on phagocytosis (**B**), the lower rates of phagocytosis by the cotransformants being due to the overexpression of LKB1 in the same strains. This was confirmed by 3D plots (**C**) and multiple regression analysis, which showed that LKB1 overexpression caused copy number-dependent reductions in the rate of phagocytosis ($p=5.0x10^{-7}$, *t* test), that were unaffected by AMPK antisense inhibition ($p=0.11$, *t* test).

3.2.2.5. AMPK antisense inhibition rescues the slow growth in HL-5 broth caused by LKB1 overexpression

Antisense inhibition of AMPK showed to rescue the slow growth of transformants with LKB1 overexpression on bacterial lawns to resemble the normal growth of wild type AX2. These co-transformants were also subcultured in HL-5 media to determine whether they had similar effects on axenic growth; that is if AMPK antisense-inhibited levels can reverse the effects caused by LKB1 overexpression.

The generation times of wild type AX2 and the co-transformants were measured as described in Section 2.5.2. Figure 3.17 shows that the generation time is relatively similar in comparison to wild type AX2 indicating a rescue in the phenotypes depicted previously by LKB1 overexpression. This result shows that the effect of LKB1 on axenic growth is regulated by AMPK.

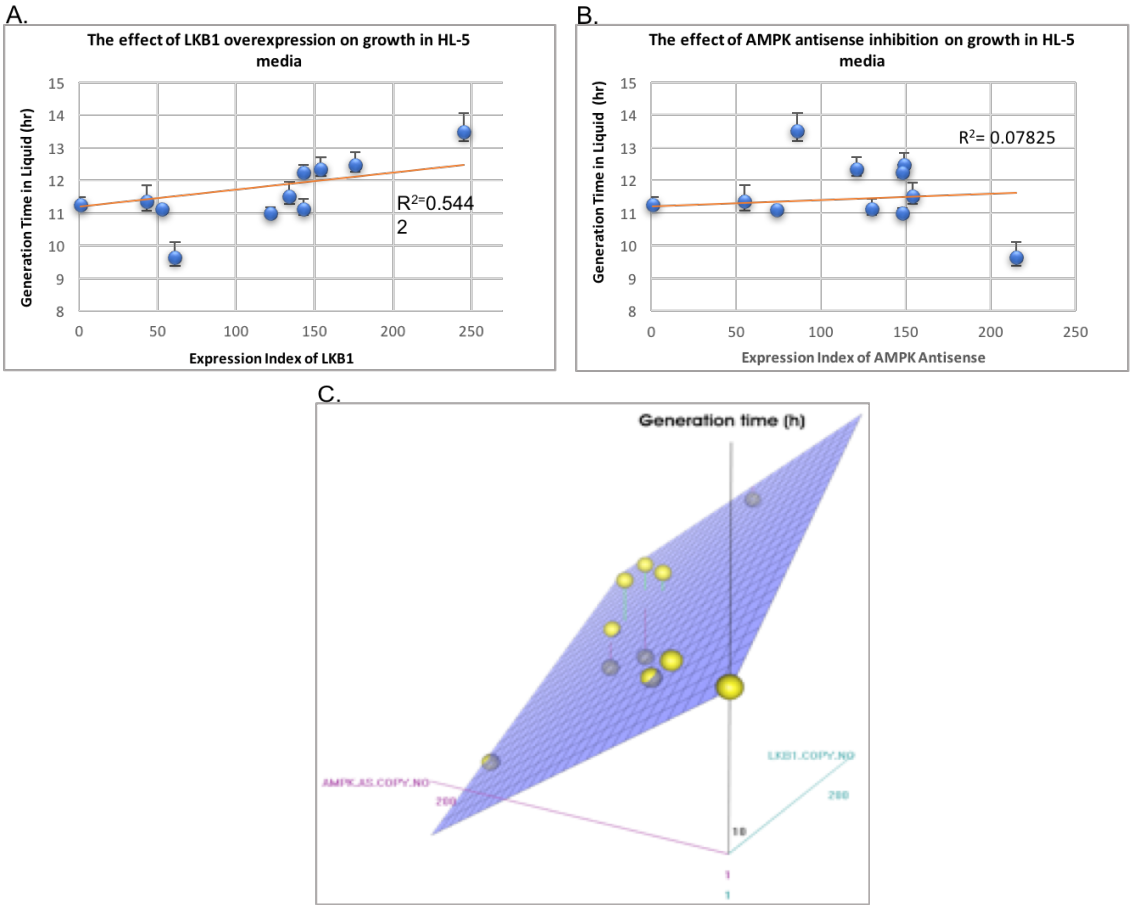

Figure 3.17. The effect on axenic growth of antisense inhibition of AMPK expression in cotransformants overexpressing LKB1.
The generation times (doubling times during exponential phase) were measured and compared with the parent strain, AX2. In a simple regression, increased LKB1 expression in the cotransformants resulted in an increase in the generation time (p=0.01, *t* test), but the effect was only modest (**A**) compared to what had been previously observed to result from LKB1 overexpression (Fig. 3.10). The generation times of the cotransformants were normal compared to AX2 and not significantly affected by the copy number of the AMPK antisense inhibition construct (p=0.45, *t* test) in a simple regression (**B**). 3D plots showed that these results were caused by a copy number-dependent inhibition of growth by LKB1 overexpression that was reversed in a copy number-dependent manner by AMPK antisense inhibition (**C**). In multiple regression analysis, the increased generation time due to LKB1 overexpression was significant at $p = 9.9 \times 10^{-5}$ (*t* test) and its suppression by AMPK antisense inhibition was significant at $p=1.9 \times 10^{-3}$ (*t* test). Error bars are standard errors of the mean from 3 independent experiments.

3.2.2.6. Nutrient ingestion rates by pinocytosis are not affected by AMPK antisense inhibition in *Dictyoselium* cells overexpressing LKB1.

An increase in the expression levels of LKB1 inhibited the growth of the transformants in

liquid medium, whereas a cotransformation of LKB1 with AMPK antisense-inhibition construct rescued this phenotype. To determine if this phenotypic suppression was a result of restoration of normal rates of pinocytosis, the ability of the cotransformants to take up liquid medium was measured. The unaltered rate of pinocytosis with respect to the increased expression levels of AMPK antisense-inhibited construct (Figure 3.18) shows that the growth of LKB1 in axenic media is mediated by AMPK; however not as a result of AMPK's effects on the rate of nutrient ingestion through pinocytosis.

This lack of effect of AMPK on pinocytosis and phagocytosis correlates with previous findings that the regulation of growth by AMPK activity in mitochondrial disease is not influenced by the rate of ingestion even though pinocytosis and phagocytosis are energy expending activities (Bokko *et al.,* 2007). Hence, certain cellular activities affected by mitochondrial dysfunction are not dependent on the consumption of energy but rather on being a downstream target of AMPK signalling.

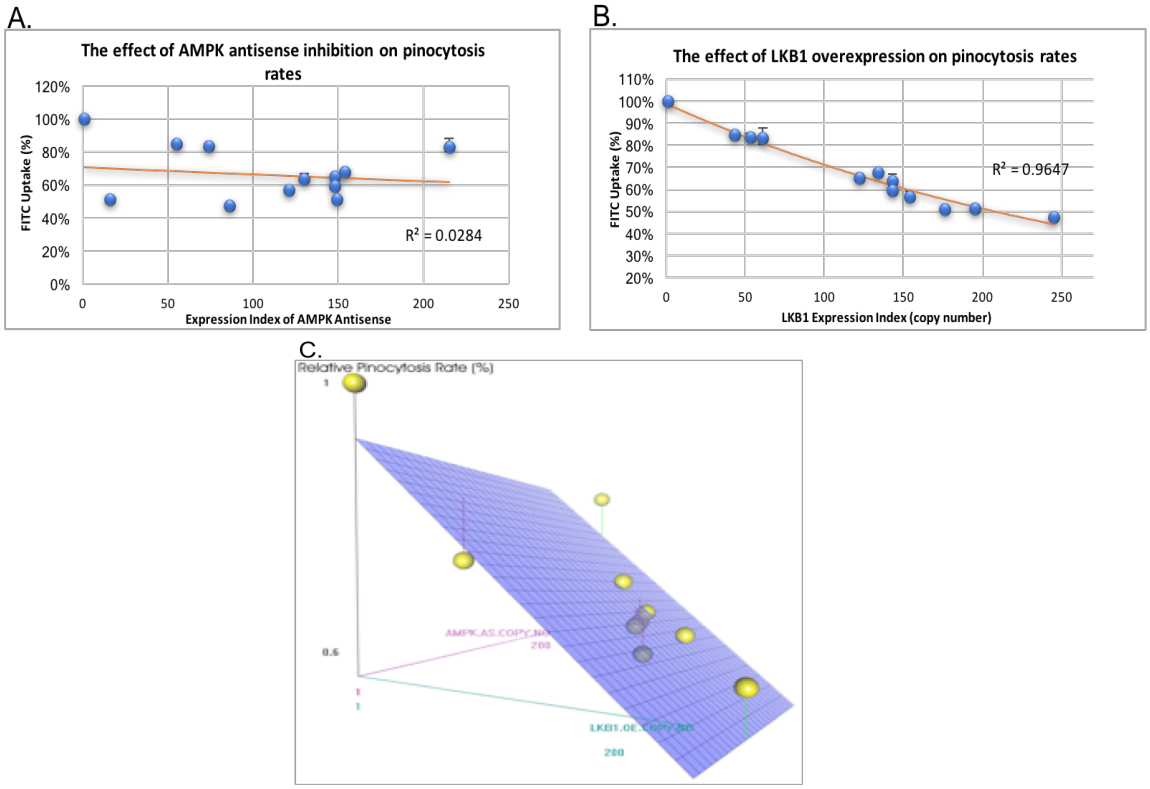

Figure 3.18. The pinocytosis rates of LKB1 overexpression and AMPK antisense-inhibited transformants in *Dictyostelium*.

AX2 and the cotransformants were grown in low fluorescence HL-5 medium containing Fluorescein isothiocyanate (FITC)-dextran. The hourly rate of uptake of medium was calculated from the cell density, the increase of fluorescence over 70 minutes and a separate calibration curve relating the fluorescence signal to the volume of fluorescent medium. **A.** Increased expression the AMPK antisense RNA has no effect on the rate of pinocytosis whereas **B.** the overexpression of LKB1 leads to a decrease in pinocytosis rates. Multiple regression and 3D plotting (**C**) confirmed that LKB1 overexpression impaired pinocytosis in a copy number-dependent manner ($p=2.0x10^{-3}$, *t* test), while AMPK antisense inhibition had no effect ($p=0.67$, *t* test). Error bars are standard errors of the mean from 3 independent experiments.

3.2.2.7. Effects of cotransformation with LKB1 and AMPK antisense construct on multicellular development.

The development of the fruiting bodies in *Dictyostelium discoideum* has been shown to be affected by mitochondrial dysfunction in *Dictyostelium discoideum* (Kotsifas *et al.,* 2002; Bokko *et al*., 2007). Like other mitochondrial disease phenotypes, this was shown to be mediated by chronic hyperactivation of AMPK, so that AMPK overexpression phenocopies mitochondrial disease resulting in impaired morphogenesis characterised by fewer fruiting bodies and short thick stalks (Kostifas *et al*., 2002; Bokko *et al*., 2007). This aberrant morphogenesis was also found in *Dictyostelium* strains with LKB1

overexpression (Section 3.1.10.6).

To determine whether the role of LKB1 in regulating fruiting body morphogenesis is mediated by AMPK signalling, cotransformants containing the LKB1 overexpression and AMPK antisense-inhibited constructs were subcultured on plates containing a lawn of *K. aerogenes* and incubated at 21 °C for several days until fruiting bodies emerged. The fruiting bodies of the transformants were then inspected and compared to that of the wild type AX2 as described in Section 2.5.3.

Cotransformation of *Dictyostelium discoideum* cells with AMPK antisense-inhibition and LKB1 overexpression constructs suppressed the impaired fruiting body morphology that would otherwise have been caused by LKB1 overexpression. When the LKB1 overexpression construct was in large excess compared to the AMPK antisense inhibition construct, the fruiting bodies began to exhibit the abnormalities observed previously in LKB1 overexpression strains. However, the fruiting bodies formed appear relatively normal morphologically compared to wild type AX2 when the ratio of copy numbers was closer to 1. This result indicates that morphogenesis in *Dictyostelium* is regulated via the LKB1-AMPK signalling pathway.

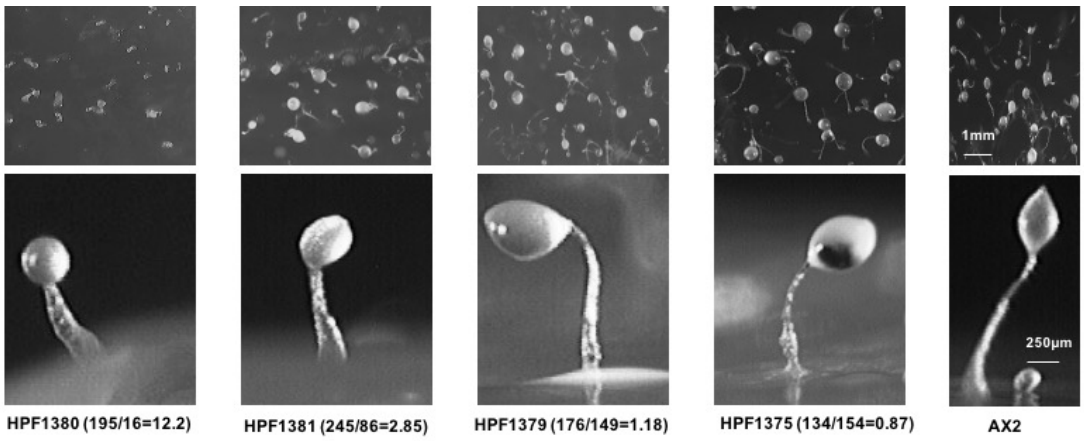

Figure 3.19. Fruiting body morphology of cotransformants with LKB1 overexpression and AMPK antisense inhibition constructs.

The numbers below each set of images represent the ratios of the copy numbers of the LKB1 overexpression and AMPK antisense inhibition constructs in each transformant. Transformants with copy number ratios closer to 1 appear to have more normal fruiting body development indicated by the similar morphology to wild type AX2.

3.2.3. The role of LKB1-AMPK Kinase activity in mitochondrial biogenesis

AMPK has been shown to be a proximal signal in mitochondrial proliferation and biogenesis (Zong *et al.,* 2002). Bokko *et al*. (2007) evaluated the role of AMPK activation in mitochondrial biogenesis in *Dictyostelium* revealing that increased AMPK expression resulted in elevated mitochondrial mass whereas a decrease in AMPK attenuated expression resulted in decreased mitochondrial mass. An elevation in mitochondrial mass was indicative of increased mitochondrial proliferation. An increase or decrease in LKB1 expression appeared to phenocopy the regulation of mitochondrial mass and biogenesis caused by AMPK overexpression or antisense inhibition respectively.

To determine whether the role of LKB1 in mitochondrial biogenesis is mediated through the AMPK signalling pathway, mitochondrial mass was assessed in cotransformants of LKB1 overexpression and AMPK antisense-inhibited constructs. Mitochondrial "mass" was measured by fluorescence with MitoTracker Green, a mitochondrion-specific dye whose binding is independent of the mitochondrial membrane potential. The mitochondrial membrane potential was assessed by another fluorescence stain, MitoTracker Red, normalized against the MitoTracker Green signal. The results show that the mitochondrial mass (Fig. 3.20A, B) and membrane potential (Fig. 3.20D, E) were at normal levels in the cotransformants. 3D plots and multiple regression analysis confirmed that the copy number-dependent elevation in mitochondrial mass (Fig. 3.20C) and reduction of mitochondrial membrane potential (Fig. 3.20F) caused by LKB1 (Section 3.1.11.1) was suppressed in a copy number-dependent manner by AMPK antisense inhibition. Hence, LKB1 appears to act as an upstream kinase of AMPK in the regulation of mitochondrial biogenesis.

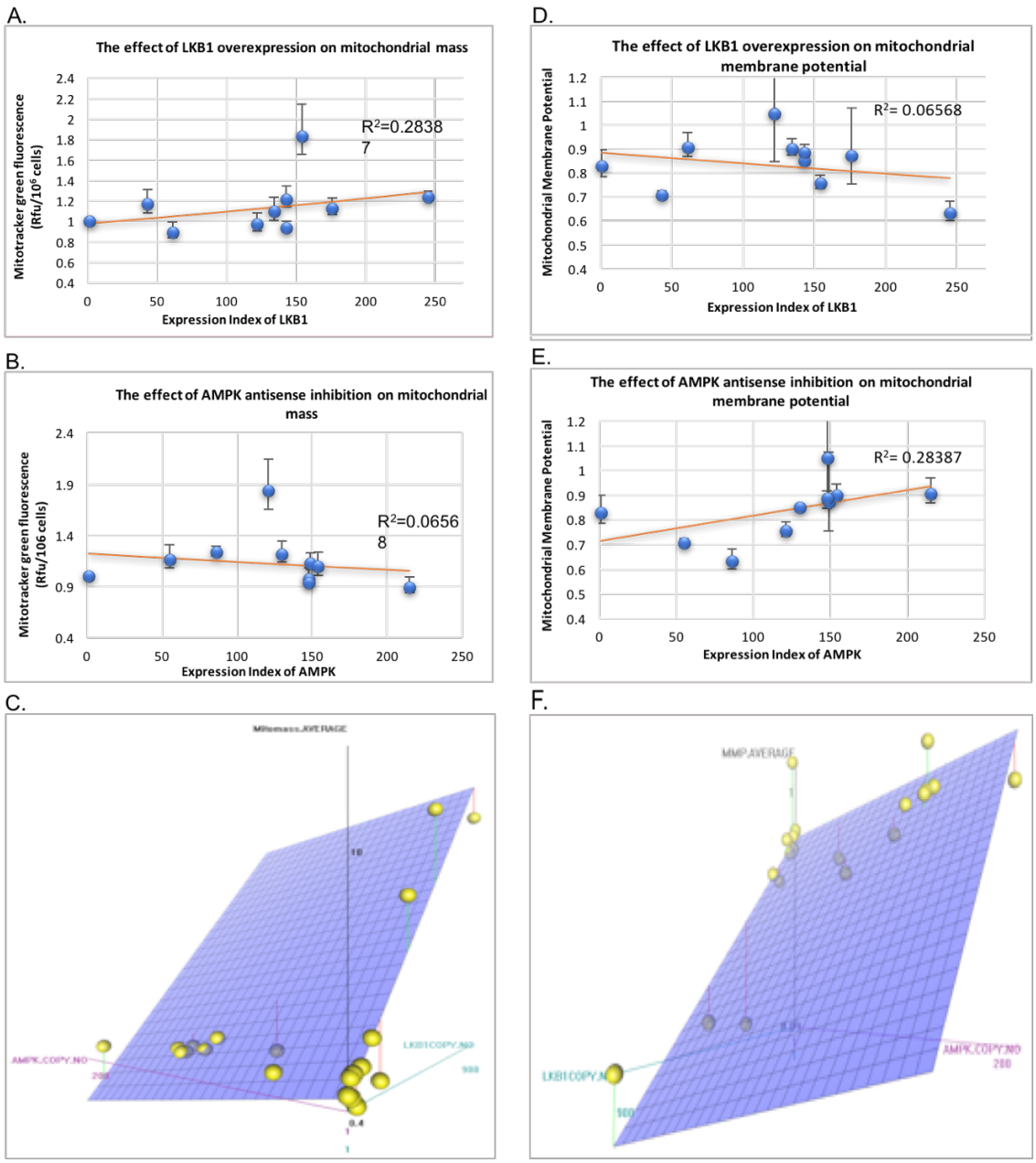

Figure 3.20. Effect of LKB1 overexpression and AMPK antisense-inhibition expression on mitochondrial mass and mitochondrial membrane potential in *Dictyostelium*.

The expression index indicates the copy numbers of the overexpression constructs of LKB1 and antisense-inhibited construct of AMPK. Copy numbers of zero refer to the wild-type parental strain AX2. **A-C.** Mitochondrial mass was measured by fluorescence with the mitochondrion-specific dye MitoTracker Green after subtraction of autofluorescence from unstained cells from the same suspension. The results were normalized against the values for the wild type strain AX2 which served as an internal control within each experiment. The LKB1 overexpression/AMPK antisense-inhibited transformants exhibited a range of mitochondrial masses similar to wild type AX2 as shown by simple regressions against the expression indices for LKB1 (**A,** p=0.32, *t* test) and AMPK antisense RNA (**B**, p=0.67, *t* test). A 3D plot (**C**) and multiple regression analysis showed that the normal mitochondrial masses of the cotransformants were due to the reduced mitochondrial mass caused by LKB1 overexpression ($p=6.7x10^{-9}$, *t* test) being suppressed by AMPK antisense inhibition in a copy number-dependent manner ($p=1.5x10^{-2}$, *t* test). **D-F.** The mitochondrial membrane potential of the cotransformants is not altered and resembles that of wild type AX2 as shown by simple regressions against the expression indices for LKB1 (**D,** p=0.53, *t*

test) and AMPK antisense RNA (**E**, p=0.11, *t* test). A 3D plot (**F**) and multiple regression analysis showed that the normal mitochondrial masses of the cotransformants were due to the reduction in mitochondrial membrane potential caused by LKB1 overexpression ($p=2.5x10^{-6}$, *t* test) being reversed by AMPK antisense inhibition in a copy number-dependent manner ($p=6.3x10^{-3}$, *t* test).

Error bars are standard errors of the mean from 3 independent experiments. The multiple regression analyses and 3D plots included data from LKB1 overexpression transformants (AMPK antisense construct copy number of zero) as well as the cotransformants. Similar outcomes were found using the cotransformants only, but the regression coefficients were not statistically significant ($p>0.05$) because of the small sample sizes and limited construct copy number ranges.

3.3. Concurrent STRADα overexpression augments the function of LKB1 in LKB1-overexpressing cells.

LKB1 is normally found in its active form as a complex with two other subunits, STE20 related adapter (STRAD, a pseudokinase) and Mouse Protein 25 (MO25), in a 1:1:1 ratio to form the LKB1-STRAD-MO25 complex. In mammalian cells, STRAD has two closely related isoforms, α and β, which possess high sequence similarity to protein kinases but lack several essential residues required for catalytic function, hence rendering them inactive. They have therefore been termed pseudokinases (Bass *et al*., 2003). As a pseudokinase, STRAD does not possess any catalytic activity but still binds ATP and assumes a closed conformation that is akin to that of active kinases (Zeqiraj *et al*., 2009). This conformation of STRAD is crucial for the activation of LKB1, as mutation of residues in the ATP-binding pocket of STRAD blocks association with MO25 and activation of LKB1 (Zeqiraj *et al.,* 2009). MO25, which was initially recognized as a gene expressed at the early cleavage phase of mouse embryogenesis (Miyamoto *et al.,* 1993, Nozaki *et al.,* 1996), also has two closely related isoforms in mammals, termed MO25α and MO25β. They were found to be extremely evolutionarily conserved (Karos & Fischer, 1999). MO25α binds to the C-terminal Trp-Glu-Phe (WEF) motif of STRADα through a hydrophobic pocket on its C-terminus and serves as a scaffold for the stabilization of the heterotrimer. This interaction can significantly enhance the binding of STRAD to LKB1 and increase STRAD-induced kinase activity of LKB1.

LKB1 phosphorylates STRAD at multiple Thr residues while STRAD, for its part, escalates the kinase activity of LKB1 and prompts its translocation to the cytoplasm (Baas *et al*., 2003; Alessi *et al*., 2006). The binding of MO25 to the LKB1-STRAD complex further enhances the stability and activity of LKB1 (Boudeau *et al*., 2003). MO25 alone was found not to have any effect on the localization of LKB1, but nevertheless cooperates with STRAD to facilitate cytosolic relocalization of LKB1 from the nucleus (Boudeau *et al*., 2003a; Filippi *et al.,* 2011).

To gain a better understanding of the role of LKB1 in *Dictyostelium discoideum*, it is essential to characterize its phenotypic outcomes when overexpressed with its partners STRAD and MO25 in *Dictyostelium*. Although *Dictyostelium* has putative homologues of STRAD and MO25, not much information is available with regard to their function. The *Dictyostelium* gene DDB0229911 shares 34% sequence identity with STRADα, while

DDB0218587 shares 55% identity with MO25.

I ventured to clone the homologues of STRADα and MO25, which will be referred to by the same names, and then cotransform them concurrently with LKB1 in *Dictyostelium.* The aim was to explore whether the activity of LKB1 in *Dictyostelium* would be amplified once the other two subunits are also overexpressed in the same cells.

3.3.1. Identification and bioinformatics analysis of STRADα in D. discoideum

To gain a better understanding of the biological roles of STRADα AND MO25 in *Dictyostelium*, a BLAST (Basic Local Alignment Search Tool) search at dictyBase (the international dictyostelid genomics resource at http://dictybase.org) was carried to identify homologues in the *D. discoideum* proteome using the protein sequence of human STRADα and MO25. A number of homologous proteins encoded in the *D. discoideum* genome were identified; however local sequence alignment shown in Figure 3.21 revealed that the kinase Fray2 is the closest relative to STRADα with a 34% homology. Interestingly, Fray2 also contains WIF (Trp-Ile-Phe) sequence motif, which is involved in aiding the binding of the pseudokinase STRAD to MO25 at a similar distance to the catalytic domain as in STRADα (Boudeau *et al.,* 2003a; Appendix 6; 8). This reveals it as putative interacting partner of M025. Local sequence alignment shown in Figure 3.22 shows that DDB0304446 is the closest relative to human MO25 with a 55% identity.

Query sequence: Human STRADα			Subject Sequence: *Dictyostelium* STRADα (Fray2)		
Score: 168 bits (426)	**Expect:** 2e-49	**Identities:** 108/317(34%)	**Positives:** 150/317(47%)	**Gaps:** 53/317(16%)	**Method:** Compositional matrix adjust

```
Query  69   YELLTVIGKGFEDLMTVNLARYKPTGEYVTVRRINLEACSNEMVTFLQGELHVSKLFNHP  128
            YEL   IGKG   L  V  A   P  E V ++ I+LE C N  +  ++ E+    L +HP
Sbjct  71   YELKETIGKGGSGL--VQRAICLPFQENVAIKIIDLEHCKNVSLEEIRKEIQAMSLCHHP  128

Query  129  NIVPYRATFIADNELWVVTSFMAYGSAKDLICTHFMDGMNELAIAYILQGVLKALDYIHH  188
            N+V Y  +F+ +  LWV+  F++ GS  D++   F  G  E  IA IL+  LKA+ Y H
Sbjct  129  NVVAYHTSFVYNESLWVIMDFLSAGSCSDIMRFSFPQGFEEHVIATILKEALKAICYFHK  188

Query  189  MGYVHRSVKASHILISVDGKVYLSGLRSNLSMISHGQRQRVVHDFPKYSVKVLPWLSPEV  248
             G +HR +K+ +ILI  +G + LS    + ++I  G+  R          V    W++PE+
Sbjct  189  TGRIHRDIKSGNILIDSNGNIQLSDFGVSATLIDTGETSRNTF------VGTPCWMAPEI  242

Query  249  LQQNLQGYDAKSDIYSVGITACELANGHVPFKDMPATQMLLEKLNGTVPCLLDTSTIPAE  308
            ++Q    YD   DI+S GITA ELA G  PF + P  ++LL
Sbjct  243  MEQ--VNYDYAVDIWSFGITALELARGKAPFAEYPPMKVLL------------------  281

Query  309  ELTMSPSRSVANSGLSDSLTTSTPRPS-NGDSPSHPYHRTFSPHFHHFVEQCLQRNPDAR  367
                              LT   P PS  GD  S   H      F   VE+CLQ++P  R
Sbjct  282  ------------------LTLQNPPPSLEGDGESKWSHS-----FKDLVEKCLQKDPSKR  318

Query  368  PSASTLLNHSFFKQIKR  384
            P  S LL H FFKQ K+
Sbjct  319  PLPSKLLEHRFFKQAKK  335
```

Figure 3.21. BLAST sequence alignment using the *H. sapiens* STRADα amino acid sequence as the query to search the predicted *D. discoideum* proteome.

The STRADα protein in *H. sapiens* is 431 amino acids long encoded by 39,138 bp with 13 exons (Bass *et al.*, 2003), whereas in *D. discoideum*, it contains 1028 amino acids encoded by a gene of only 3184 bp with only one intron.

Query sequence: **Human MO25α**			**Subject Sequence:** ***Dictyostelium*** **MO25- like family protein**		
Score: 392 bits (1008)	**Expect:** 6e-137	**Identities:** 200/363(55%)	**Positives:** 260/363(71%)	**Gaps:** 30/363(8%)	**Method:** Compositional matrix adjust

```
Query  1    MPFPFGKSHKSPADIVKNLKESMAVLEKQDISDKKAEKATEEVSKNLVAMKEILYGTNEK  60
            M   F K  K+P+++VK++KES+A ++K   + K  EKA+EE+SK L  +K+IL+G +E
Sbjct  1    MNIFFNKKQKTPSELVKSIKESLASMDKSGPNSKSTEKASEEISKCLQEIKKILHGDSEH  60

Query  61   EPQTEAVAQLAQELYNSGLLSTLVADLQLIDFEGKKDVAQIFNNILRRQIGTRTPTVEYI  120
            EP  E VA L+ E+  S L+  L+ DL  ++FE KKDVAQIFN +LR + G R+P VEYI
Sbjct  61   EPNQEVVAVLSNEICTSDLVQILIKDLNKLEFEAKKDVAQIFNILLRHKNGARSPIVEYI  120

Query  121  CTQQNILFMLLKGYESPEIALNCGIMLRECIRHEPLAKIILWSEQFYDFFRYVEMSTFDI  180
                 IL  L+KGYE  +IALNCG MLRECI+HE LAKI+++S  F++FF +VE+S FD+
Sbjct  121  AKNPEILDSLVKGYEQQDIALNCGTMLRECIKHESLAKILIYSPNFWEFFEFVEVSNFDV  180

Query  181  ASDAFATFKDLLTRHKLLSAEFLEQHYDRFFSEYEKLLHSENYVTKRQSLK---------  231
            ASD FATFK++LT+HK LSAEFLE++YD+ F +Y  LL+S+NYVT+RQS+K
Sbjct  181  ASDTFATFKEILTKHKTLSAEFLEKNYDQVFEKYTTLLNSQNYVTRRQSIKVNNNSNNNN  240

Query  232  --------------------LLGELLLDRHNFTIMTKYISKPENLKLMMNLLRDKSRNIQ  271
                                LLGELLLDR NF IM  YIS   NLK MMNLLRDKS++IQ
Sbjct  241  NNNNNNNNNNNNNNNNAAILLGELLLDRSNFNIMPLYISSAANLKFMMNLLRDKSKSIQ  300

Query  272  FEAFHVFKVFVANPNKTQPILDILLKNQAKLIEFLSKFQNDRTEDEQFNDEKTYLVKQIR  331
            +EAFHVFKVFVANPNKT+PIL+IL KN+ KLI FLS+F ND+ ED QF+DEK +LVKQI+
Sbjct  301  YEAFHVFKVFVANPNKTKPILEILTKNKEKLIAFLSQFHNDKEED-QFSDEKNFLVKQIQ  359

Query  332  DLK  334
              ++
Sbjct  360  AIQ  362
```

Figure 3.22. BLAST sequence alignment using the *H. sapiens* MO25 amino acid sequence as the query to search the predicted *D. discoideum* proteome.

The MO25 protein in *H. sapiens* is 341 amino acids long encoded by 108,233 bp with 8 exons (Bass *et al*., 2003) resulting in 1024 bp of cDNA, whereas in *D. discoideum*, it contains 363 amino acids encoded by a gene of only 1897 bp with 7 exons.

3.3.2. Predicted Subcellular Localisation of STRADα in Dictyostelium discoideum.

In mammalian cells, STRADα and MO25α expressed on their own are localized throughout the cytoplasm and nucleus. However, when MO25α and STRADα were coexpressed, both proteins were relocalized to the cytoplasm and were excluded from the nucleus (Boudeau *et al*., 2003a). Mammalian LKB1, when expressed with STRADα and MO25, becomes relocalised to the cytoplasm (Bass *et al*., 2003). The subcellular localization of both STRADα and MO25 in *D. discoideum* is predicted to be cytoplasmic (Euk-mPLoc 2.0; Chou & Chen, 2010; Chou & Chen, 2008)

3.3.3. Creation of STRADα and MO25 constructs in E. coli vectors

To investigate the effect of STRADα and MO25 on the function of LKB1 in *D. discoideum*, I aimed to create transformants that overexpressed STRADα and MO25. A two-phase cloning strategy was employed due to the difficulties of cloning PCR products and cloning AT-rich genes into AT rich *D. discoideum* vectors. The full-length STRADα and MO25 genes were first cloned into the *E. coli* cloning vector pUC18. The STRADα gene was then excised and subcloned into the *D. discoideum* vector pPROF267. Despite many attempts, I was only able to subclone STRADα, but not MO25, into the *D. discoideum* vector pPROF267.

The gene fragments were amplified via PCR using gene-specific primers (Figure 2.5) and *D. discoideum* AX2 genomic DNA (gDNA) as the template (Section 2.3.1). The PCR amplicon STRADα was cloned into the *Sal*I site of pUC18 as shown in Figure 3.23 and the resultant pUC18-STRADα plasmid was named pPROF783. MO25 was cloned into the *Eco*RI site of pUC18 as shown in Figure 3.24 and the resultant pUC18-MO25 plasmid was named pPROF784.

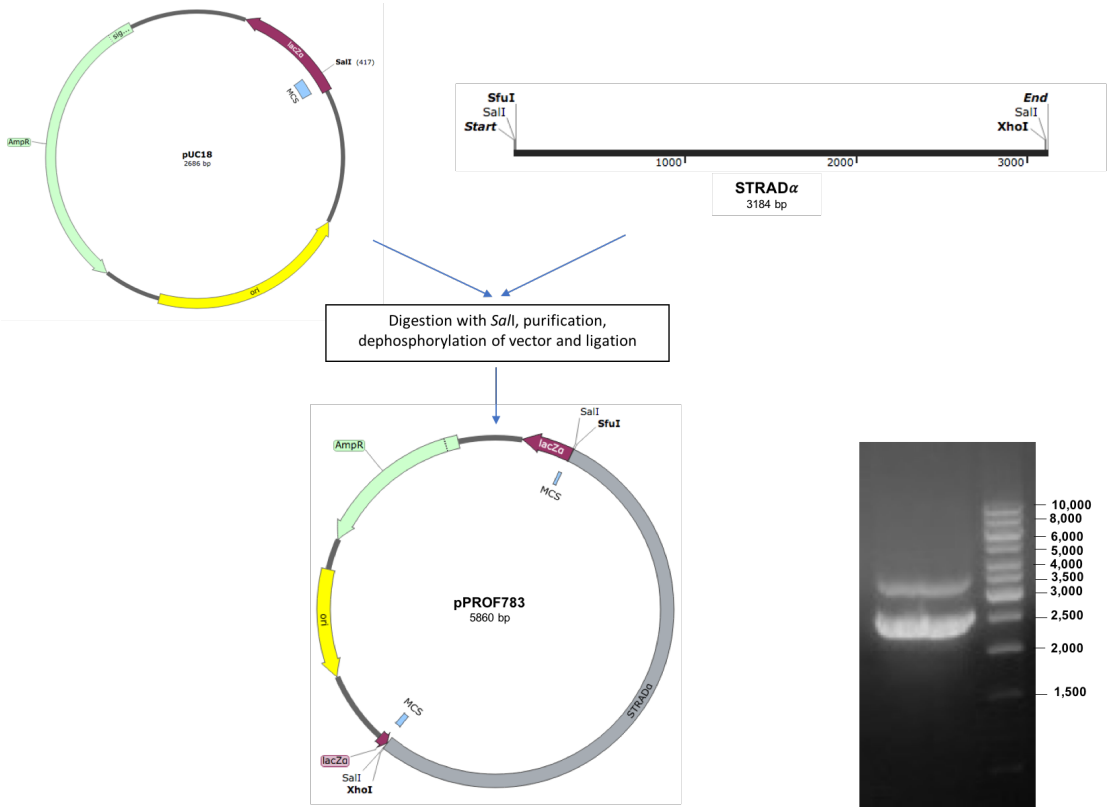

LANE	DNA	RESTRICTION ENZYME	FRAGMENT SIZE (bp)
1	1 Kb DNA ladder		
2	pPROF783	*Sal*1	2686 bp 3184 bp

Figure 3.23. Generation and restriction endonuclease digestion of pPROF783.
STRADα of length 3184bp, was amplified using primers STRADαF and StradαR, digested with *Sal*1 and cloned into pUC18 to produce the construct pPROF783. The constructs were verified by restriction enzyme analysis (the enzymes and fragment size are listed in the above table) and sequenced by AGRF.

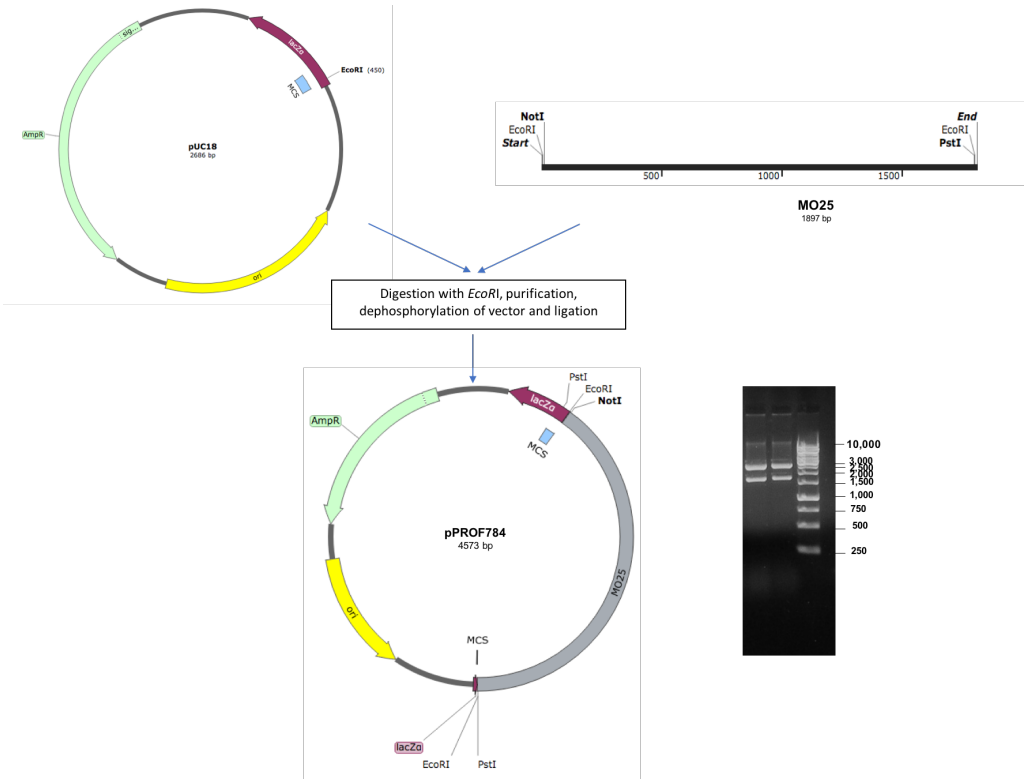

LANE	DNA	RESTRICTION ENZYME	FRAGMENT SIZE (bp)
1	1 Kb DNA ladder		
2	pPROF784	*Eco*RI	2686 bp, 1897 bp
3	pPROF784	*Eco*RI	2686 bp, 1897 bp

Figure 3.24. Generation and restriction endonuclease digestion of pPROF784.
The MO25 gene of length 1897bp, was amplified using primers MO25F and MO25R, digested with *Eco*RI and cloned into pUC18 to produce the construct pPROF784. The constructs were verified by restriction enzyme analysis (the enzymes and fragment size are listed in the above table) and sequenced by AGRF.

3.3.4. STRADα and MO25 gene sequencing

The cloned genes were sequenced by AGRF using the primers listed in Figure 2.5. The sequences were then aligned with the native gene sequence using the software Bioedit and were used for BLAST searches at the NCBI website to confirm that they represented the *D. discoideum* homologue of human LKB1. The results are shown in Appendix 8.

3.3.5. Creation of STRADα expression constructs in *D. discoideum* vectors

To create an overexpression construct, the full-length STRADα gene was excised from pPROF783 and subcloned into the *Not*1 and *Xho*1 sites of the *D. discoideum* expression vector pPROF267 removing the Tet cassette to form the pPROF267-STRADα construct named pPROF785 (Figure 3.25).

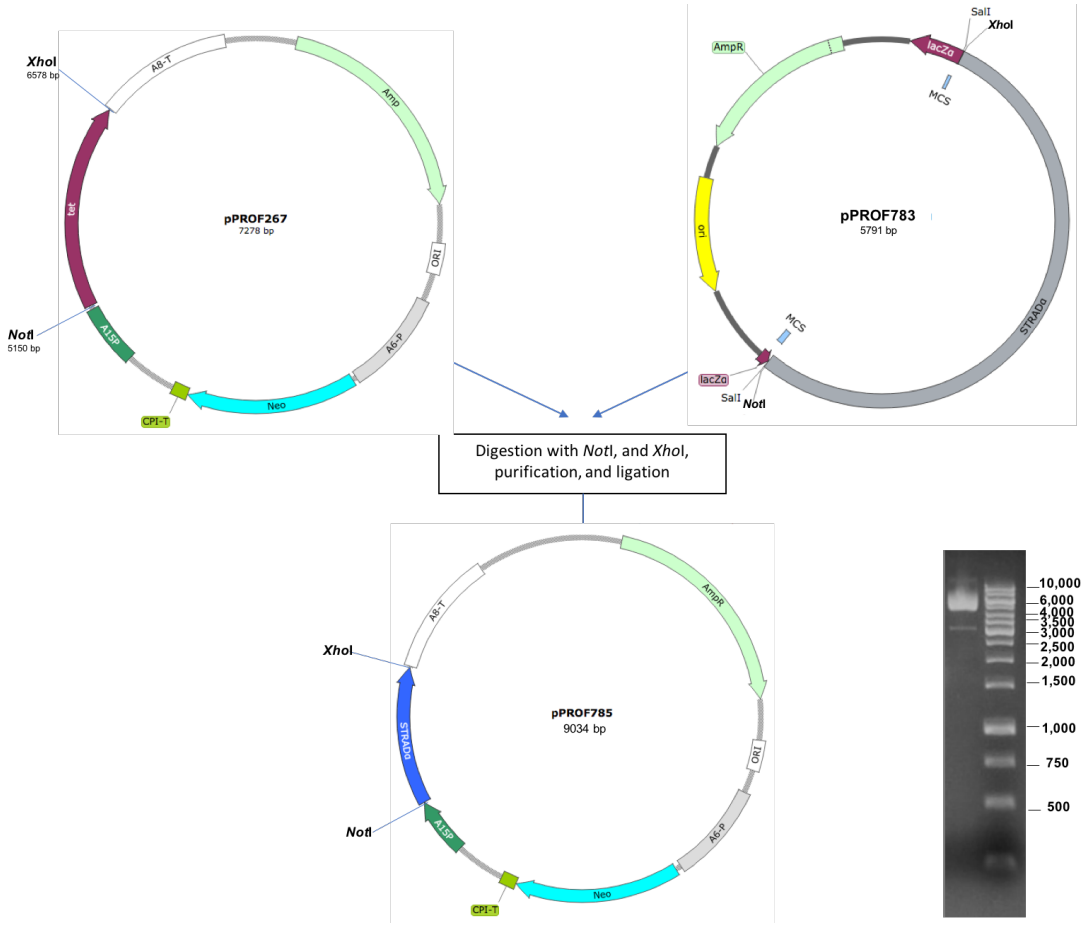

LANE	DNA	RESTRICTION ENZYME	FRAGMENT SIZE (bp)
1	1 kb DNA ladder		
2	pPROF785	*Not*1 and *Xho*1	5051 bp, 3184 bp

Figure 3.25. Generation and restriction endonuclease digestion of pPROF785.
STRADα was excised from pPROF783 and inserted into the *Not*I and *Xho*I sites of the *D. discoideum* expression vector pPROF267 to produce the construct pPROF785. The construct was verified by restriction enzyme analysis as listed in the table.

3.3.6. Creation of cotransformants with altered LKB1 and STRADα expression

To create cotransformants with altered levels of LKB1 and STRADα expression, the overexpression construct of LKB1 (pPROF781) and STRADα (pPROF785) were transformed concurrently into the parental *D. discoideum* strain AX2. In this process, multiple copies of the constructs are generated through rolling circle replication of the plasmid constructs in transformants, integrated at random sites in the *D. discoideum* genome via recombination (Barth *et al.,* 1998). The resultant transformants contain different numbers of copies of the construct and hence, express different levels of the gene. The number of copies of the implanted constructs were determined by qPCR (Section 2.3.4; Table 2.3) and relative expression levels in the cotransformants were verified by western blots using LKB1-antibodies (Figure 3.26). Antibodies against STRADα were not generated and obtaining antibodies in the future will further cement my findings. Accordingly in this thesis I follow the previously established convention of using construct copy numbers as an expression index (Bokko *et al*., 2007).

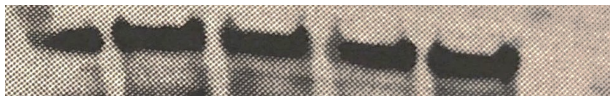

Figure 3.26. Western blot analysis of LKB1 in LKB1-STRADα cotransformants.
The western blot was performed on LKB1-STRADα cotransformants with various copy numbers of LKB1. Compared to the parental AX2 strain (rightmost lane), the figure shows elevated LKB1 protein expression in the cotransformants in the leftmost 5 lanes, presented in order of increasing LKB1 construct copy number. The copy numbers of the LKB1 and STRADα constructs in each transformant were respectively, from left to right, 32 and 66; 57 and 100; 59 and 113; 63 and 13; 89 and 22.

3.3.7. Phenotypic analysis of LKB1-STRADα co-transformants

To establish the effects of altering the levels of LKB1 and STRADα concurrently *in vivo* and the role of the STRADα in enhancing the activity of LKB1, the *D. discoideum* cotransformants overexpressing wild type LKB1 and STRADα were analysed phenotypically. In section 3.1.10.6 it was shown that overexpression of wild type LKB1 in *D. discoideum* results in aberrant phenotypes that depend on its kinase activity and resemble those caused by AMPK chronic activation and mitochondrial dysfunction (Annesley *et al.*, 2014). These biological activities of LKB1 are mediated by AMPK activity in most biological processes examined, the exceptions being nutrient uptake through pinocytosis and phagocytosis. The following experiments were carried out to determine whether the activity of LKB1 in LKB1-overexpressing *Dictyostelium* cells is amplified when the protein is coexpressed with STRADα.

3.3.7.1. Selection of LKB1-STRADα overexpression transformants

91 LKB1-STRADα overexpression cotransformants were obtained in the AX2 parental background with AX2 serving as the wild type parental control strain in these analyses. Each transformant had a different number of copies of the expression construct and initially 40 of these transformants were assessed on their ability to grow on bacterial lawns. Out of these 40 strains, 13 were chosen which displayed a range of growth rates, most likely due to them holding a range of diverse copy numbers. These selected cotransformants were then used for the ensuing phenotypic analysis.

3.3.7.2. LKB1-STRADα overexpression negatively affects plaque expansion in *D. discoideum*.

A phenotype which was identified in LKB1 overexpression and previously in AMPK overexpression and mitochondrially diseased strains was decreased growth on bacterial lawns (Bokko *et al.*, 2007). As shown in Section 3.1.10.2, LKB1 overexpression transformants showed slower plaque expansion rates in comparison to wild type AX2. To explore whether the activity of LKB1 in negatively affecting growth can be further

amplified in the presence of STRADα, the LKB1-STRADα overexpression cotransformants were observed for their ability to grow on normal agar plates covered with a lawn of *E. coli* B2. The rate of plaque expansion was calculated as described in Section 2.5.1. LKB1-STRADα overexpression cotransformants showed slower plaque expansion rates in comparison to wild type AX2 and this reduction was more pronounced than if LKB1 was overexpressed on its own. For example, in LKB1 overexpression cells, the plaque expansion rate was 0.205 mm/hr in a transformant with copy number 92, whereas in LKB1-STRADα overexpression cotransformants, the plaque expansion rate was 0.11 mm/hr in a transformant with 89 copies of the LKB1 construct. Accordingly, a given copy number of LKB1 in the LKB1-STRADα cotransformants can result in more dramatically aberrant phenotypes than a much higher copy number in transformants overexpressing only the LKB1 gene. In multiple regression analysis, the additional impairment of plaque expansion by coexpression of STRADαin cotransformants was entirely explained by the interaction between LKB1 and STRADα (Figure 3.27). I conclude that when LKB1 is coexpressed with STRADα, the LKB1 has a more potent effect on the growth of *Dictyostelium* cells than when only LKB1 is overexpressed. This is consistent with the kinase activity of LKB1 being enhanced by an interaction with STRADα as previously reported (Boudeau *et al.*, 2003a)

A.

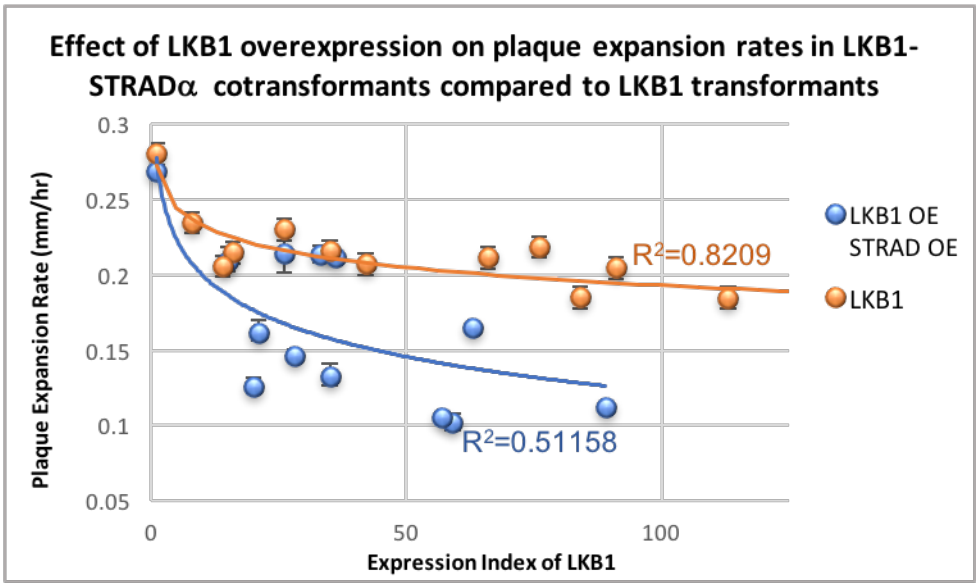

B.

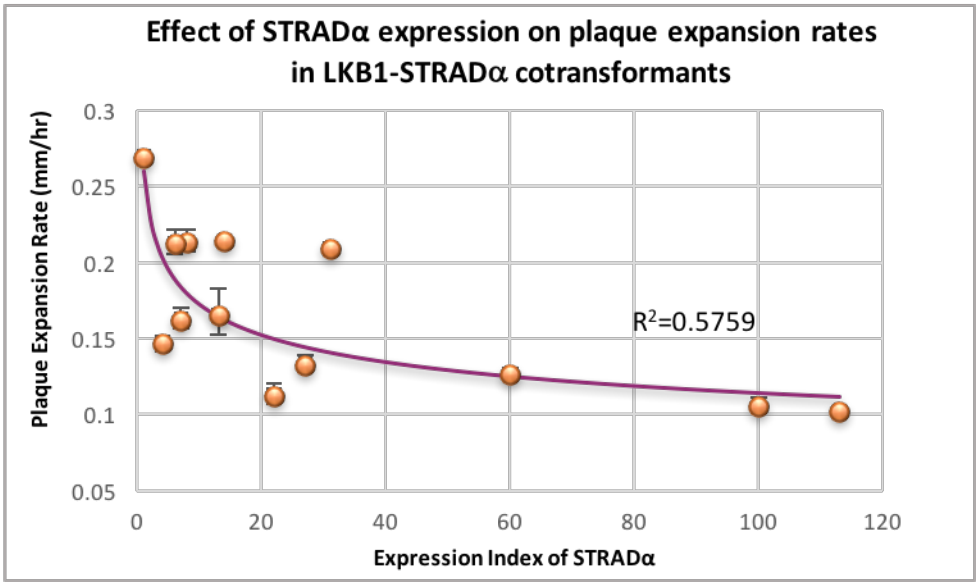

Figure 3.27. Plaque expansion rates of cotransformants with increased LKB1 and STRADα expression levels.

A. The effect of LKB1 overexpression in the LKB1-STRADα co-transformants was compared to its effect when it is solely overexpressed. A more dramatic decrease in plaque expansion rates occurred with low copy numbers of LKB1 when LKB1 is coexpressed with STRADα. **B**. The plaque expansion rates for the co-transformants were normalized against AX2 and plotted against their relative expression levels. An increase in the STRADα overexpression copy number also resulted in reduced plaque expansion rates. Multiple regression analysis of the plaque expansion rates against the logarithms of the copy numbers and an interaction term (product of the logarithms) showed that the effects of overexpression of LKB1 ($p=1.7x10^{-3}$, *t* test) and of the interaction with overexpressed STRADα ($p=1.4x10^{-6}$, *t* test) were highly significant. There was no additional, independent effect of STRADα ($p=0.76$, *t* test). Error bars are standard errors of the mean from 3 replicate measurements.

3.3.7.3. LKB1-STRADα overexpression negatively regulates phagocytosis in *D. discoideum*.

Plaque expansion rates of *D. discoideum* on bacterial lawns are determined by the phagocytosis rate, growth rate and motility of the amoebae. In earlier sections, it was shown that LKB1 overexpression inhibits both plaque expansion and phagocytosis, and that the interaction of coexpressed STRADα amplified the impairment of plaques expansion by LKB1. It was therefore important to establish whether STRADα interaction with LKB1 similarly enhanced the LKB1-mediated defect in phagocytosis.

The phagocytosis rates of AX2 and the LKB1-STRADα overexpression cotransformants were measured as described in Section 2.5.4. The results in Figure 3.28 show that overexpression of LKB1 in the presence of overexpressed STRADα exerted a more severe effect than overexpressing LKB1 alone. For example, in cells with 76 copies of the construct overexpressing LKB1 the phagocytosis rate was 64 % of the wild type, whereas in LKB1-STRADα overexpression cotransformants, 63 copies of the LKB1 construct produced an even lower phagocytosis rate at 50% of wild type. Accordingly, a given copy number of the LKB1 construct in the cotransformants can produce a similarly defective phenotype as a much higher copy number in transformants overexpressing only LKB1. In multiple regression analysis, the additional impairment of phagocytosis by coexpression of STRADα in cotransformants could be explained by the interaction between LKB1 and STRADα (Figure 3.28). Thus; LKB1 overexpression in conjunction with STRADα overexpression has a more potent effect on phagocytosis than when only LKB1 is overexpressed. As was the case for the impairment of growth on plates by LKB1, this is consistent with STRADα enhancing the kinase activity of LKB1 as previously reported (Boudeau *et al.,* 2003a).

A.

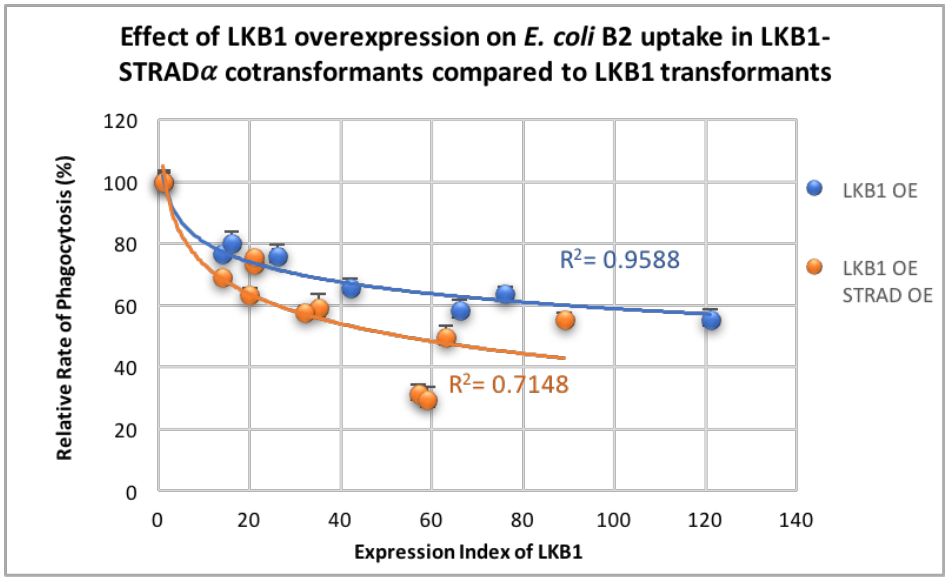

B.

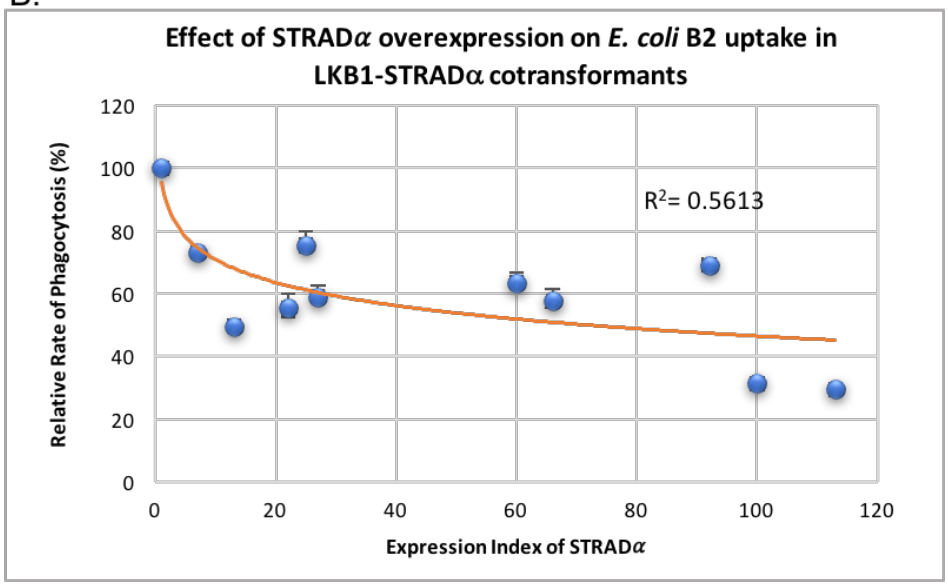

Figure 3.28. Phagocytosis rates of LKB1-STRADα overexpression cotransformants.
Bacterial uptake by LKB1 overexpression and STRADα overexpression cotransformants were determined using as prey an *E. coli* strain expressing DsRed. The hourly rate of consumption of bacteria by a single amoeba was calculated from the increase in fluorescence over 30 minutes, the fluorescence signal per million bacteria and the amoebal density. The phagocytosis rates were normalized against AX2 (100%) which served as an internal control within each experiment. **A.** The effect of LKB1 overexpression in the LKB1-STRADα cotransformants was compared to its effect when it is solely overexpressed. A low copy number of LKB1 in the LKB1-STRADα cotransformants is sufficient to cause a significant decrease in the phagocytosis rate. **B**. Overexpression of STRADα in the presence of overexpressed LKB1 leads to a decrease in phagocytosis. Multiple regression analysis of the phagocytosis rates against the logarithms of the copy numbers and an interaction term (product of the logarithms) showed that the effects of overexpression of LKB1 ($p=2.1x10^{-6}$, *t* test) and of the interaction with overexpressed STRADα ($p=1.1x10^{-4}$, *t* test) were highly significant. A separate effect of STRADα, independent of LKB1 expression, was not significant (p=0.06, *t* test). Error bars are standard errors of the mean from 3 independent experiments.

3.3.7.4. Increased LKB1 and STRADα expressions concurrently negatively regulates axenic growth in HL5 media

In section 3.1.10.4 increased expression of LKB1 in *D. discoideum* was shown to impair the axenic growth of transformants in HL-5 media. Since LKB1 had a more dramatic effect on growth on bacteria when hyperexpressed in combination with STRADα than when it was overexpressed alone, I examined whether the axenic growth of LKB1-STRADα cotransformants was more severely impaired than would be the case if only LKB1 were overexpressed. The generation times of wild type AX2 and LKB1-STRADα overexpression cotransformants were measured as described in Section 2.5.2. Figure 3.29 shows that the generation time significantly increases with increasing LKB1 and STRADα expression. Multiple regression analysis showed that the effect of STRADα is explained by a statistical interaction between STRADα and LKB1 overexpression, so that there was no separate, independent effect of STRADα. This is consistent with the effects of STRADα on plaque expansion rates and phagocytosis, as well as the reported enhancement of LKB1 kinase activity by STRADα (Boudeau *et al*., 2003a; Filippi *et al.,* 2011).

A.

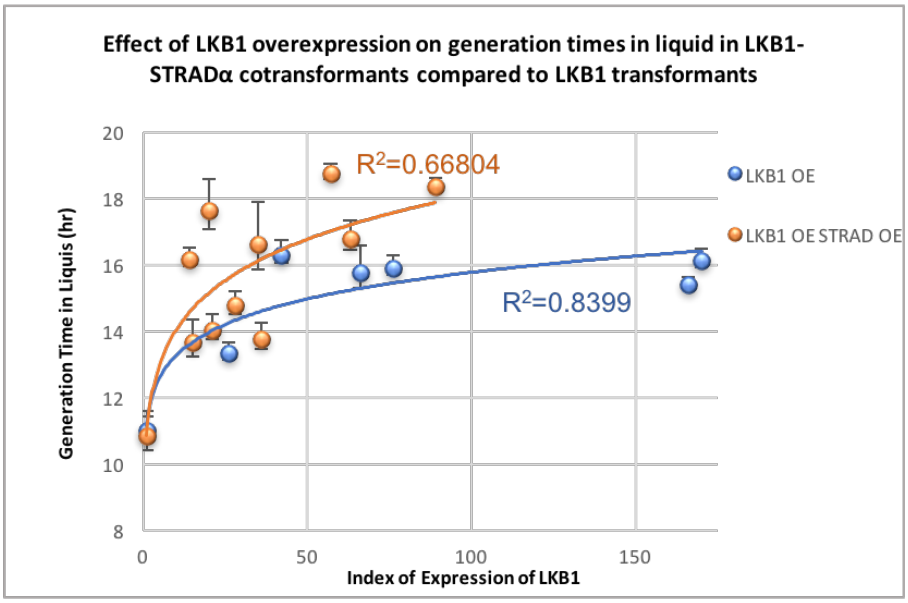

B.

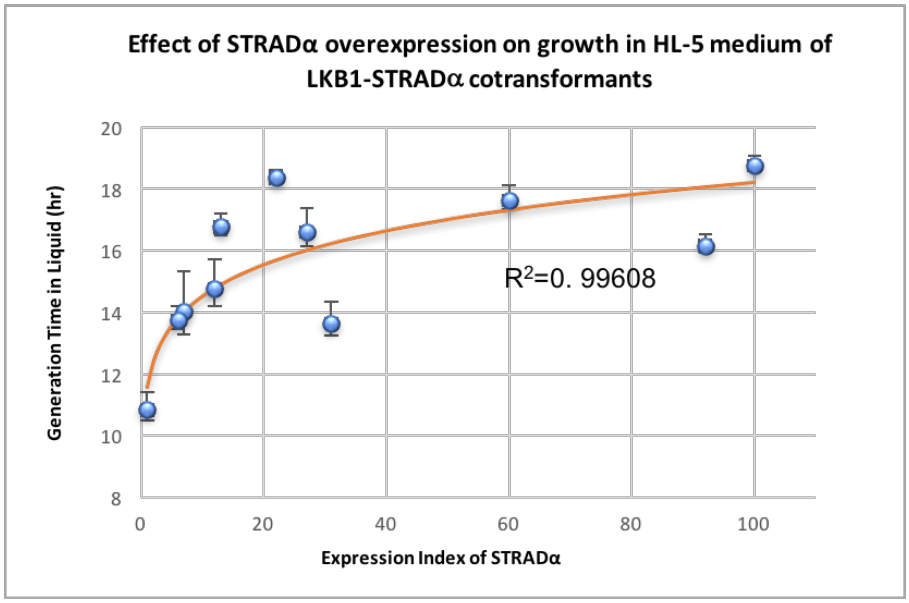

Figure 3.29. The effect of the overexpression of LKB1 and STRADα on the axenic growth of the transformants.

The generation time, which is the doubling time of strains during exponential phase, of LKB1-STRADα overexpression cotransformants was measured and compared with the parent strain, AX2. **A.** Increased expression of LKB1 in both the LKB1 overexpressing strains and in the LKB1-STRADα cotransformants resulted in an increase in the generation time. However, for a given copy number of the LKB1 expression construct the impairment of growth was more severe (generation time longer). **B.** Increased expression of STRADα in the cotransformants also caused slower growth. Multiple regression analysis of the logarithm of the generation times against the logarithms of the copy numbers and an interaction term (product of the copy number logarithms) showed that the effects of overexpression of LKB1 ($p=1.8\times10^{-8}$, *t* test) and of the interaction with overexpressed STRADα ($p=5.2\times10^{-5}$, *t* test) were highly significant. A separate effect of STRADα, statistically independent of LKB1 expression, was not significant (p=0.87, *t* test). Error bars are standard errors of the mean from 3 independent experiments.

3.3.7.5. LKB1-STRADα overexpression inhibits pinocytosis in D. discoideum.

As previously shown (section 3.1.10.5), LKB1 overexpression transformants exhibited a decrease in the rate of pinocytosis. As STRADα seemed to enhance other functions of LKB1 when coexpressed with it, I wanted to assess whether STRADα has the same effect in pinocytosis.

Compared to the effect of overexpressing LKB1 alone, Figure 3.30 shows that the copy number-dependent impairment of pinocytosis in cotransformants overexpressing LKB1 and STRADα is more severe. This suggests that as with the other phenotypes, STRADα overexpression enhanced the effect of the overexpressed LKB1. Thus a similar copy number of LKB1 in transformants coexpressing LKB1 and STRADα exerted the same effect as in transformants solely expressing LKB1. For example, the pinocytosis rate in LKB1 overexpression cells with 76 copies of the LKB1 construct was 68% of the wild type rate, whereas in LKB1-STRADα cotransformants with a lower LKB1 construct copy number of 63 the pinocytosis rate was 53% of wild type. Multiple regression analysis confirmed that, as with the other phenotypes, the effect of STRADα was explained entirely by its statistical interaction with LKB1. Hence, STRADα elevates the pinocytosis-inhibiting activity of LKB1 when the two proteins are overexpressed together.

A.

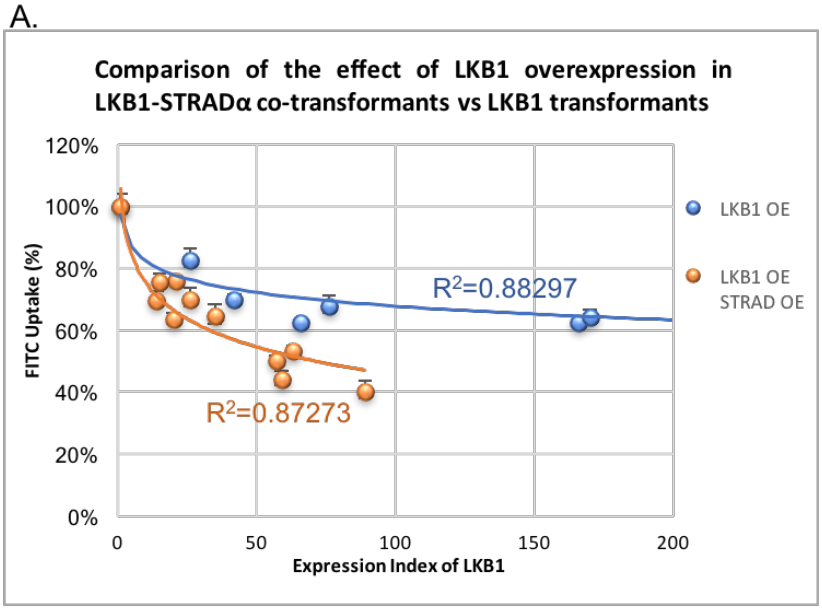

B.

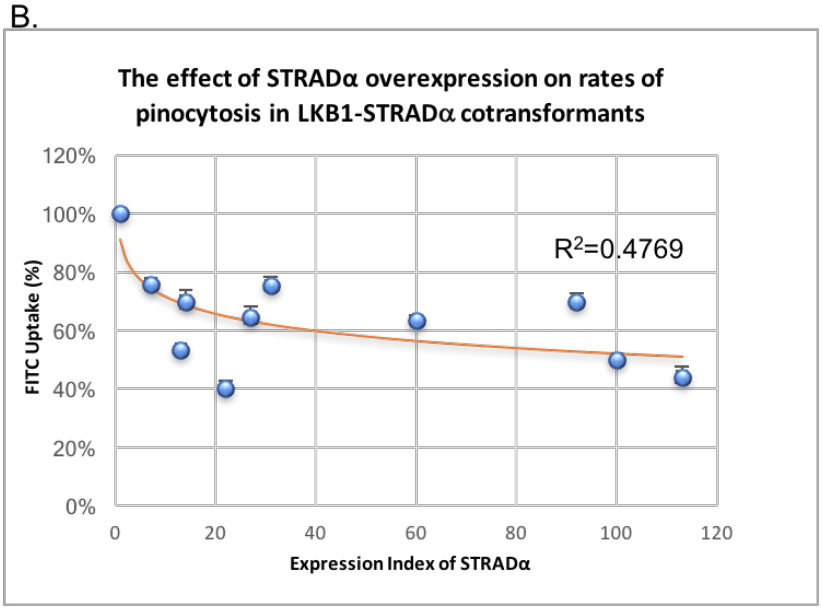

Figure 3.30. The pinocytosis rates of LKB1 and STRADα overexpression cotransformants.

AX2 and LKB1-STRADα overexpression co-transformants were grown in low fluorescence HL-5 medium containing FITC-dextran. **A.** The effect of LKB1 overexpression in the LKB1-STRADα cotransformants was compared to its effect when it alone is overexpressed. A low copy number of LKB1 in the LKB1-STRADα cotransformants is sufficient to cause a dramatic effect on the rate of pinocytosis. **B.** Increased expression of STRADα resulted in a decrease in the pinocytosis rates of the transformants. Multiple regression analysis was conducted using the logarithm of the generation times as the dependent variable (Y), the LKB1 construct copy number as the 1st independent variable (X_1), the logarithm of the STRADα construct copy number as the 2nd independent variable (X_2) and an interaction term ($X_3=X_1.X_2$). The results showed that the effects of overexpression of LKB1 ($p=1.8x10^{-8}$, *t* test) and of the interaction with overexpressed STRADα ($p=5.2x10^{-5}$, *t* test) were highly significant. A separate effect of STRADα, statistically independent of LKB1 expression, was not significant ($p=0.87$, *t* test). Error bars are standard errors of the mean from 3 independent experiments.

3.3.7.6. LKB1-STRADα overexpression impairs fruiting body morphology

Both mitochondrial disease in *Dictyostelium* and AMPK hyperactivity have been shown to result in impaired morphogenesis characterised with fewer fruiting bodies and short thick stalks (Kotsifas *et al*., 2002; Bokko *et al*., 2007). This is a result of misregulation in the stalk differentiation pathway (Chida *et al*., 2004). Increased LKB1 expression resulted in a similar phenotype - aberrant fruiting bodies with short thick stalks (Section 3.1.10.6). As the activity of LKB1 appears to be further enhanced when it is coexpressed with STRADα, the fruiting body morphogenesis of LKB1-STRADα co-transformants were assessed to determine the role of STRADα in affecting the severity of the morphological defects presented.

LKB1-STRADα cotransformants as well as the wild type AX2 were subcultured on plates containing a lawn of *K. aerogenes* and incubated at 21 ^{o}C for several days until fruiting bodies emerged. The fruiting bodies of the transformants were then inspected and compared to that of the wild type AX2 as described in Section 2.5.3. Increased LKB1-STRADα expression resulted in aberrant fruiting bodies with short thick stalks, a similar phenotype to that observed in cells with LKB1 overexpression (Figure 3.31). The morphological defect appeared to be more severe and to occur at a lower LKB1 copy number than in the transformants overexpressing only LKB1.

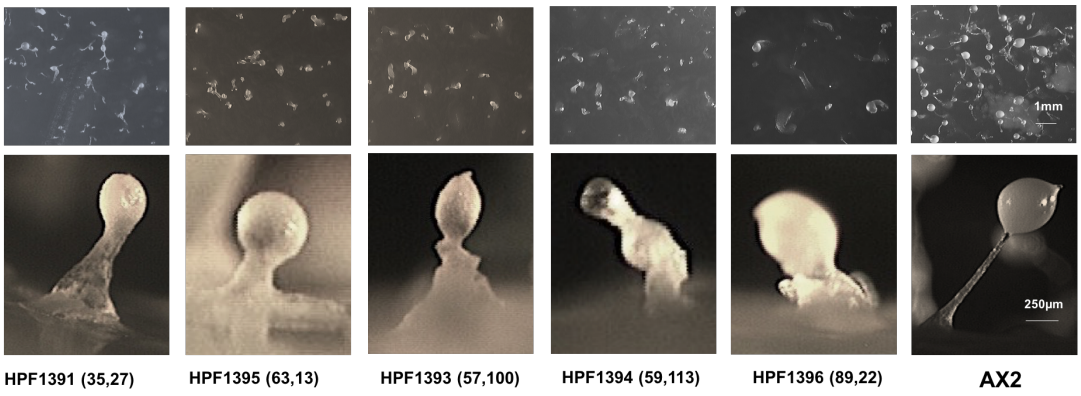

Figure 3.31. Fruiting body morphogenesis of transformants with increased LKB1 and STRADα expresssion.
Wild type AX2 fruiting bodies contain long slender stalks whereas transformants with increased expression of LKB1 and STRADα have short, aberrant and thicker stalks in comparison to wild type AX2. The severity of the defect correlates with the increase in LKB1 expression and is noticeable at a low copy number of LKB1. The bottom row shows the strain number of each transformant followed by a pair of copy numbers for each transformant, the 1st of each pair indicating the LKB1 construct and the 2nd indicating the STRADα construct.

3.3.8. The role of LKB1 activity in mitochondrial biogenesis when coexpressed with STRADα

3.3.8.1. LKB1 and STRADα concurrent overexpression has a more severe effect on mitochondrial mass and mitochondrial membrane potential than when only LKB1 is overexpressed

In mammalian cells, AMPK plays a crucial role in energy homeostasis of healthy cells. In muscle tissues particularly, the activity of AMPK results in mitochondrial proliferation as a response to strenuous physical training (Bergeron *et al.*, 2001; Zong *et al.*, 2002). Nevertheless, mitochondrial proliferation can also be a feature of mitochondrial diseases (Agostino *et al.*, 2003; Bokko *et al.,* 2007). In sections 3.1.11.1, I showed that overexpression of LKB1, an activating kinase of AMPK, causes an elevation of mitochondrial mass and a decrease in mitochondrial membrane potential and that this depends upon the protein's kinase activity. These results mirrored the effects of overexpression of the AMPKα catalytic domain reported previously by Bokko *et al.* (2007).

To determine whether the overexpression of STRADα concurrently with LKB1 would exacerbate this phenotype, the mitochondrial mass of the LKB1-STRADα overexpression

cotransformants was assessed for mitochondrial "mass" and membrane potential. Figure 3.32A,B shows that overexpression of LKB1 and STRADα resulted in an increase in mitochondrial mass, indicated by a stronger MitoTracker Green fluorescence signal per cell. Thus, similar effects were caused by overexpression of LKB1 in the cotransformants at a lower copy number of the LKB1 construct compared to transformants overexpressing LKB1 only. For example, in LKB1-STRADα cotransformants, an LKB1 copy number of only 35 resulted in a stronger Mitotracker Green signal (3.93 Rfu/10^6 cells) than LKB1 overexpression transformants with a copy number of 121 (2.85 Rfu/10^6 cells). Hence, STRADα significantly enhances the activity and function of LKB1 when overexpressed together with LKB1. Multiple regression analysis confirmed this and showed that, as with the other phenotypes, the effect of STRADα was explained entirely by its statistical interaction with LKB1. Therefore, STRADα elevates the activity of LKB1 in stimulating mitochondrial biogenesis when the two proteins are overexpressed together.

Whereas LKB1 and STRADα coexpression resulted in an increase in mitochondrial mass, it caused a decrease in mitochondrial membrane potential (Figure 3.32C,D). This effect was more severe than that caused by LKB1 overexpression alone and, as was the case with the other phenotypes tested, could be explained statistically by an interaction between LKB1 and STRADα with a separate, independent contribution from STRADα.

My results confirm that mitochondrial mass and membrane potential in *Dictyostelium* are regulated by LKB1 kinase activity and that this activity is enhanced by STRADα.

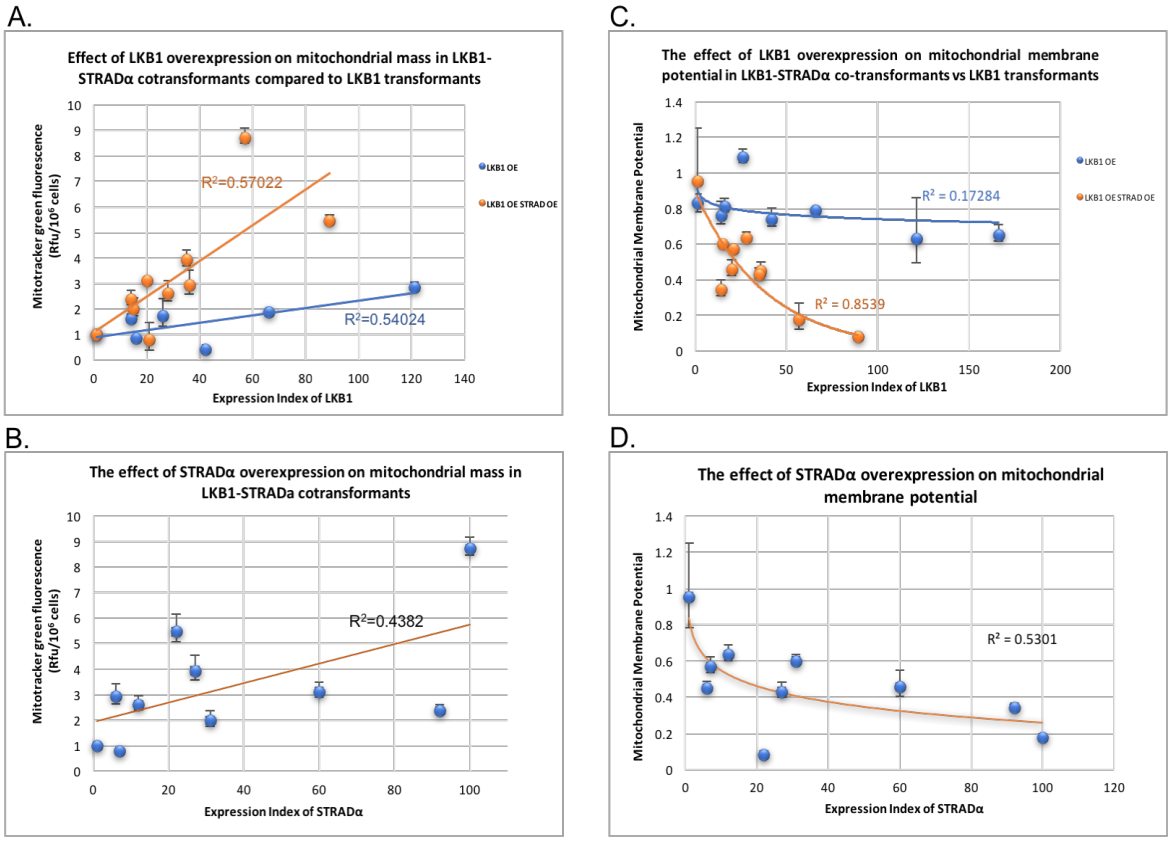

Figure 3.32. Effect of LKB1 and STRADα expression levels on mitochondrial mass and mitochondrial membrane potential in *Dictyostelium*.

The expression index indicates the copy numbers of the overexpression constructs of LKB1 and STRADα. Values for the wild-type parental strain AX2 are plotted at copy number 1, reflecting the single endogeneous copy of the wild type gene in each case. Mitochondrial mass is measured by fluorescence with the mitochondrion-specific dye MitoTracker Green after subtraction of autofluorescence from unstained cells from the same suspension. **A.** The effect of LKB1 overexpression in the LKB1-STRADα cotransformants was greater than its effect when it is solely overexpressed in LKB1 overexpressing strains. **B.** Increased expression of STRADα resulted in an increase in mitochondrial mass in the cotransformants.

Multiple regression of the mitochondrial mass against the copy numbers and an interaction term (product of the copy numbers of the two constructs) showed that the effects of overexpression of LKB1 ($p=0.013$, *t* test) and of the interaction with overexpressed STRADα ($p=1.9\times10^{-4}$, *t* test) were highly significant. There was no additional, independent effect of STRADα ($p=0.83$, *t* test). Error bars are standard errors of the mean from 3 replicate measurements.

C. The effect of LKB1 overexpression in the LKB1-STRADα cotransformants was greater than its effect when it is solely overexpressed in LKB1 overexpressing strains. **D.** Increased expression of STRADα resulted in a decrease in mitochondrial membrane potential of the cells.

Multiple regression analysis of the mitochondrial membrane potential against the logarithms of the copy numbers and an interaction term (product of the logarithms) showed that the effects of overexpression of LKB1 ($p=0.035$, *t* test) and of the interaction with overexpressed STRADα ($p=2.7\times10^{-6}$, *t* test) were highly significant. There was no additional, independent effect of STRADα ($p=0.46$, *t* test). Error bars are standard errors of the mean from 3 independent experiments.

4. Discussion

4.1. The role of LKB1 activity in *Dictyostelium discoideum*

In humans, LKB1, a serine/threonine tumour suppressor kinase, is comprised of 433 amino acids and has a conserved kinase catalytic domain located between the 49th and 309th amino acid. A BLAST search at dictyBase revealed a homologous protein of LKB1 in the *Dictyostelium* genome that has a 46 % identity and 63% similarity in the conserved 300 amino acid region homologous to the human LKB1. Most of this was the *Dictyostelium* LKB1 kinase domain (261 aa) which is 48 % identical and 66% similar to that of the human LKB1 (250 aa).

In mammalian cells, LKB1 is mainly localized in the nucleus due to the nuclear localization signal (NLS) found in its N-terminal noncatalytic region (residues 38-43) (Alessi *et al.,* 2006). Coexpression of LKB1 and STRADα targets the majority of LKB1 to the cytoplasm, although a significant amount remains nuclear. However, when LKB1 is expressed with STRADα and MO25, it becomes fully localised in the cytoplasm. Moreover, a mutation in the motif encompassing the nuclear localization signal (NLS) leads to the localization of LKB1 throughout the cell (Alessi *et al.,* 2006). These mutants still maintain the ability to inhibit cell growth like wild type LKB1, implying that the localization of LKB1 in the cytoplasm plays a crucial role in facilitating its tumour suppressor properties. Indeed, the importance of the cytoplasmic localization of LKB1 for its function is further demonstrated in PJS patients, in which mutant forms of LKB1, localized exclusively in the nucleus, are unable to suppress cell growth (Boudeau *et al.,* 2003). In *Dictyostelium,* the LKB1 protein lacks the nuclear targeting signal and hence, the subcellular localization of LKB1 in *D. discoideum* has been predicted to be cytoplasmic. Immunofluorescence analysis showed that LKB1 in *Dictyostelium discoideum* was indeed cytoplasmic (Figure 3.4). Presumably LKB1 in *Dictyostelium* is constitutively cytoplasmic and not subject to regulation by shuttling between the nucleus and cytoplasm like its human counterpart, which has been reported to exert its function only in the cytoplasm (Boudeau *et al.,* 2003).

To investigate the function of LKB1 in *D. discoideum*, a genetic approach was utilised to analyse the phenotypic effects of LKB1 activity. Transformants with an overexpression LKB1 construct were created to constitutively intensify the effects of LKB1 in

Dictyostelium and their resultant phenotypes were analysed. To confirm that the phenotypes examined in LKB1-overexpressing cells are due to its kinase activity, transformants that overexpress LKB1 Dead Kinase were also created. The LKB1 Dead Kinase construct was created using site directed mutagenesis by introducing two mutations into the LKB1 construct - K69M which disrupts the binding of ATP to LKB1 and abolishes the LKB1 kinase activity, and D186A in subdomain VII of the kinase domain which also renders LKB1 catalytically inactive. In mammalian cells, the equivalent LKB1 Dead Kinase is retained within the nucleus. However, since *Dictyostelium* LKB1 does not have a nuclear targeting signal, it is expected to be expressed and exert its phenotypic effects in the cytoplasm similar to wild type LKB1. Overexpression of LKB1 Dead Kinase construct was utilised in this study to competitively inhibit the function of LKB1 at different levels of severity in *Dictyostelium* cells. This is based on the fact that the point mutations introduced impair catalytic activity without impairing the protein's ability to bind to its substrates or its heterotrimeric partners, STRAD ✔ and MO25. The magnitude of the phenotypic effects observed in both LKB1 and LKB1 Dead Kinase transformants was highly correlated with the number of plasmid copies and expression levels.

In this work, I found that overexpression of wild type LKB1 dramatically impaired growth, both on a bacterial food source and in axenic medium in *Dictyostelium,* consistent with the growth-suppressing activity of its mammalian homologue in human cells (Inoki *et al*., 2003). Under metabolic stress, mammalian LKB1 phosphorylates and activates AMPK, which in turn inhibits protein synthesis and cell growth to conserve energy. LKB1 activation of AMPK inhibits cell growth through the direct phosphorylation of both TSC2 and raptor by AMPK and both of these lead to the inhibition of mTOR activity (Inoki *et al*., 2003; van Veelen *et al.,* 2011). mTOR is the active subunit of two patently distinctive protein complexes called mTORC1 and mTORC2 which play a significant role in initiating protein translation and cell growth and development (Zoncu *et al.,* 2011).

Overexpression of LKB1 is also implicated in supressing metastasis of cancer cells. In LKB1-deficient MDA–MB-435 breast cancer cells, overexpression of wild-type LKB1 can drastically impede the invasion and metastasis *in vitro* and *in vivo*. This effect accompanies the downregulation of matrix metalloproteinase 2 and 9 (MMP-2 and MMP-9) as well as vascular endothelial growth factor (VEGF) (Gan & Li, 2014). An equivalent inhibition of cell motility and ability to invade a bacterial lawn during growth on plates,

could contribute to the impaired plaque expansion I found to result from LKB1 overexpression. Conversely, the ability of LKB1 Dead Kinase to accelerate plaque expansion on bacterial lawns could be partly due to impairment of LKB1's role in cell motility. It would be valuable in future work to test directly the effect of LKB1 and LKB1 Dead Kinase on amoeboid motility in *Dictyostelium*.

The overexpression of LKB1 Dead Kinase in *Dictyostelium* resulted in accelerated growth rates not only on bacterial plates but also in axenic medium. The loss of LKB1 has similarly been shown to upregulate cell growth in mammalian cells. Dupuy *et al.* (2013) showed that the removal of LKB1 in ErbB2-mediated breast cancer resulted in tumour initiation and led to a characteristic change to aerobic glycolysis ('Warburg effect'). mTOR has been found to play a role in the metabolic reprogramming in these tumours, and the loss of LKB1 in these cells caused enhanced early tumour growth and improved migratory properties *in vitro*. Research conducted by Shen *et al.* (2002) in 116 cases of human breast cancer samples has correlated low LKB1 levels with higher histological grade of the tumour, larger tumour size and the presence of lymph node metastasis.

The results obtained in *Dictyostelium* in this thesis indicate that LKB1 regulates and restricts the rates of growth in healthy vegetative cells. The impairment of cell growth caused by overexpressing LKB1 is a *Dictyostelium* phenotypic equivalent of LKB1 tumour suppression activity and could be exploited for future studies of tumour progression in the *Dictyostelium discoideum* model. As tumorigenic transformation has been found to be associated with the aberrant activity of several well-defined pathways such as WNT/β-catenin (Zhan *et al.,* 2017), EGFR (Seshacharyulu *et al*., 2012) and NF-κB (Xia *et al.,*2014); potential studies can also be directed towards the functional analyses of these pathways in *Dictyostelium* upon LKB1 overexpression.

The rates of bacterial uptake in phagocytosis and of fluid uptake in pinocytosis were reduced in *Dictyostelium* by LKB1 overexpression and enhanced in strains expressing LKB1 Dead Kinase. These results show that the regulation of plaque expansion and axenic growth by LKB1 may also depend partly on the ability of the transformants to take up bacteria and fluid through phagocytosis and pinocytosis respectively.

Development in *Dictyostelium* is instigated by starvation-induced differentiation, in which the *D. discoideum* amoebae undergo chemotactic aggregation followed by multicellular differentiation resulting in the formation of a fruiting body - a sorus (spores) held by a

stalk and basal disk comprising of vacuolated cells (Strmecki *et al*., 2005; Willaims, 2006). The overexpression of LKB1 in an otherwise wild type *Dictyostelium* background caused impairment in the morphology of the fruiting bodies that worsened as the genetic defect became more severe. The aberrant fruiting bodies formed were stumpy with thick and short stalks, consistent with the developmental effects of AMPK overexpression and LKB1 knockdown previously reported (Bokko *et al*., 2007; Veeranki *et al.,* 2011).

The use of mitochondrial dyes (MitoTracker Green and Red) revealed that the overexpression of LKB1 in *Dictyostelium* cells resulted in increased mitochondrial mass indicative of mitochondrial proliferation, a feature of mitochondrial disease in humans (Rossignol *et al.,* 2003; McKenzie *et al.,* 2004), and in decreased mitochondrial membrane potential. Conversely in *Dictyostelium* cells overexpressing LKB1 Dead Kinase, the mitochondrial mass decreased and the mitochondrial membrane potential increased. These findings are consistent with observations in mammalian cells according to which mitochondrial biogenesis is enhanced in skeletal muscle in response to energy stress and nutrient deprivation (Zong *et al*., 2002). Furthermore, Bergeron *et al*., (2001) showed that LKB1 activation and chronic AMPK activation resulted in increased mitochondrial biogenesis. The role for LKB1 in maintaining mitochondrial biogenesis has also been demonstrated in loss-of-function experiments. Mice deficient in LKB1 (Tanner *et al*., 2013; Jeppesen *et al*., 2013) display reduced mitochondrial content in muscle, and mice with muscle-specific LKB1 knockout are incapable of enhancing mitochondrial biogenesis after exercise (Tanner *et al.*, 2013).

Hence, LKB1 not only regulates cell growth and development in *Dictyostelium* but also stimulates mitochondrial biogenesis as it does in mammalian cells. These functions of LKB1 are thus evolutionarily conserved from amoebae to humans.

4.2. AMPK mediates some but not all of LKB1's biological functions in *Dictyostelium discoideum*

Given the role of LKB1 as the main upstream kinase and activator of AMPK and as well as a key regulator in various cellular process mediated by AMPK activation, this thesis aimed to determine whether LKB1's biological functions in the *Dictyostelium* model are mediated by AMPK activation.

As the chronic activation of AMPK has been demonstrated to result from mitochondrial dysfunction in *Dictyostelium* and cause the phenotypic outcomes thereof (Bokko *et al.,* 2007), chronic hyperactivity of LKB1 was predicted to produce similar phenotypes. My observation that LKB1 overexpression impairs growth and morphogenesis, while the LKB1 Dead Kinase does the reverse is in keeping with this expectation. Furthermore, my results showed that the impaired growth and morphogenesis of *Dictyostelium* cells caused by LKB1 overexpression can be rescued by antisense-inhibiting AMPK, resulting in growth and fruiting body morphology similar to wild type AX2.

AMPK activation has also been shown to promote mitochondrial biogenesis. Zong *et al.*, (2002) showed that under energy stress, mice expressing a dominant-negative mutant of AMPK are unsuccessful in promoting mitochondrial biogenesis. O'Neill *et al;* (2001) also demonstrated reduced mitochondrial content in muscle in mice deficient in AMPK β1/β2 subunits. I showed here that antisense inhibition of AMPK activity counteracted the effects exerted by the overexpression of LKB1 resulting in mitochondrial mass and membrane potential similar to wild type AX2. I conclude that the high mitochondrial mass and decreased membrane potential caused by increased LKB1 expression are mediated by AMPK activation.

The rates of both phagocytosis and pinocytosis were previously reported to be unaffected either by catalytically active AMPK overexpression or by mitochondrial dysfunction (Bokko *et al.*, 2007). By contrast, I found that overexpression of LKB1 impaired both phagocytosis and pinocytosis, while LKB1 Dead Kinase overexpression did the reverse. This suggests that LKB1 may regulate these endocytic pathways by phosphorylating downstream target(s) other than AMPK. This was confirmed in this thesis by the phenotypes displayed by *Dictyostelium* cotransformants in which LKB1 was overexpressed and AMPK expression was antisense inhibited. AMPK knockdown failed to suppress the impairment of phagocytosis and pinocytosis caused by LKB1

overexpression. These findings imply that LKB1 may play a role in the regulation of nutritional stress responses through the activation of kinases other than AMPK. The rates of phagocytic and pinocytic ingestion depend upon signalling pathways coupled to the cell's nutritional status and contain both shared and distinct elements (Maniak, 2003) that could be downstream targets of LKB1. LKB1 is a ubiquitously expressed serine/threonine kinase known to phosphorylate 14 different protein kinases of the AMPK family (ARKs or AMPK Related Kinases). As homologues of most of these are encoded in the *Dictyostelium* genome, including MARK, BRSK and QIK (Goldberg *et al.,* 2006), it is probable that LKB1 phosphorylates and activates other ARKS as well as AMPK in *Dictyostelium*.

In conclusion, LKB1 appears to act as an upstream kinase of AMPK in the regulation of cell growth and development as well as mitochondrial biogenesis, but its regulation of phagocytosis and pinocytosis appear to occur independently of AMPK.

4.3. The function of LKB1 in *Dictyostelium discoideum* is enhanced when coexpressed with STRADα

LKB1 is normally found in its active form as a complex with two other subunits, STE20 related adapter (STRAD, a pseudokinase) and Mouse Protein 25 (MO25), in a 1:1:1 ratio to form the LKB1-STRAD-MO25 complex. The activity of LKB1 appears to be more enhanced when bound to STRADα and translocated to the cytoplasm (Baas *et al.,* 2003). The binding of the LKB1-STRAD complex to MO25 further enhances the stability and activity of LKB1 (Boudeau *et al*., 2003). MO25 alone has not been shown to have any effect on the localization of LKB1; however, but it cooperates with STRADα to facilitate cytosolic relocalization of LKB1 from the nucleus (Boudeau *et al*., 2003). In mammalian cells, STRADα and MO25α expressed on their own are localized throughout the cytoplasm and nucleus. However, when MO25α and STRADα are coexpressed, both proteins are relocalized to the cytoplasm and excluded from the nucleus (Boudeau *et al*., 2003). LKB1, when expressed with STRADα and MO25, becomes relocalised to the cytoplasm (Bass *et al*., 2003). A BLAST search at dictyBase showed the *Dictyostelium* genome to encode homologues of both STRADα and MO25, with the *Dictyostelium* gene

DDB0229911 sharing 34% identity with similar regions of STRADα, and the gene DDB0218587 sharing 55% identity with similar regions of MO25.

Like LKB1, the subcellular localization of STRADα and MO25 in *D. discoideum* is predicted to be cytoplasmic (Euk-mPLoc 2.0; Chou & Chen, 2010; Chou & Chen, 2008). As the activity of LKB1 when overexpressed appeared to regulate growth and morphogenesis of the *Dictyostelium* cells as well as their mitochondrial biogenesis, it was of interest to assess the severity of these phenotypes when overexpressing LKB1 alongside its binding partners STRADα and MO25.

To investigate the effect of STRADα and MO25 on the function of LKB1 in *D. discoideum*, I attempted to create transformants with concurrent overexpression of STRADα and MO25. However, I was unable to subclone the MO25 gene for expression in *Dictyostelium*, so I was only able to analyse the phenotypic outcomes resulting from coexpression of LKB1 and STRADα in *Dictyostelium* cells. The results revealed that when LKB1 is coexpressed with STRADα, the activity of LKB1 has a more potent effect on the phenotypes displayed by the *Dictyostelium* cells than when LKB1 is solely expressed. A lower copy number of LKB1 in the LKB1-STRADα cotransformants resulted in similar phenotypic outcomes as those resulting from overexpressing LKB1 alone at a much higher copy number. Multiple regression analysis confirmed that, for each of the phenotypes, the results were best explained statistically by LKB1 activity plus an interaction between LKB1 and STRADα with no separate, independent effect of STRADα.

These results confirm in *Dictyostelium* the role of STRADα in upregulating the activity of LKB1 as observed in mammalian cells. Thus, LKB1 can be constitutively active in *Dictyostelium*, presumably in the cytoplasm where its activity is not inhibited and this activity is amplified when bound to its partner STRADα. Presumably the LKB1-STRADα complex would have been even more potent if coexpressed with MO25.

4.4. Does LKB1 play a role in regulating mitochondrial dysfunction in *Dictyostelium discoideum*?

In humans, mitochondrial disease resulting from impaired mitochondrial oxidative

function give rise to an array of diverse disorders (Wallace, 1999; Rossignol *et al.,* 2003) such as cardiomyopathy, neuromuscular disorders and encephalomyopathies (Lehmann & Kelly, 2002; Schapira, 1999; Zeviani *et al.,* 1996; Kirvy *et al.*, 2004; Jain-Ghai *et al.*, 2013). Bokko *et al*. (2007) have previously shown that the cytopathological effects of mitochondrial dysfunction in *D. discoideum* are due to chronic activation of AMPK and can be suppressed by the antisense inhibition of AMPK activity. Mitochondrially diseased strains were created in *Dictyostelium* by antisense inhibiting the expression of chaperonin 60, an essential nuclear-encoded mitochondrial protein required for proper folding of mitochondrial proteins (Kotsifas *et al.,* 2002).

In this thesis, it was hypothesized that the overexpression of LKB1 would phenocopy the overexpression of constitutively active AMPK and mitochondrial dysfunction in *Dictyostelium.* Impaired growth and morphogenesis that were shown to be AMPK-dependent phenotypes in the *Dictyostelium* model, have also been shown to be typical of mitochondrial OXPHOS defects (Kotsifas *et al*., 2002; Bokko *et al*., 2007; Francione and Fisher, 2010). These defects were also caused by the overexpression of LKB1 in an AMPK-dependent manner as shown in this thesis. Both LKB1 (this thesis) and AMPK overexpression (Bokko *et al.*, 2007) cause an increase in mitochondrial mass, which can be a feature of mitochondrial disease in humans (Rossignal *et al.,* 2003; McKenzie *et al.,* 2004). However, this was not observed in mitochondrially compromised *Dictyostelium* cells by Bokko *et al*. (2007), who suggested that in the *Dictyostelium* model the effects on mitochondrial biogenesis of chaperonin 60 knockdown and of AMPK activation counterbalance one another. Alternatively, AMPK activation in these cells may not have reached a threshold required to cause mitochondrial proliferation, as this is a feature that arises only in severe mitochondrial disease at very late stages of progression.

My results suggest that the development of AMPK-dependent mitochondrial disease phenotypes is dependent on LKB1 activity, because LKB1 is the main upstream kinase of AMPK. To verify this directly, I conducted preliminary experiments with mitochondrially diseased *Dictyostelium* cells and showed that genetically inhibiting the kinase function of LKB1 led to the rescue of aberrant phenotypes caused by the antisense inhibition of chaperonin 60. Thus, mitochondrially compromised strains that would otherwise have exhibited severe growth defects on plates and in HL-5 liquid medium, were restored to wild type growth by overexpressing LKB1 Dead Kinase (Appendix 11). Furthermore, the overexpression of LKB1 Dead Kinase appears to have only a slight effect on

mitochondrial mass and membrane potential in the chaperonin 60 antisense-inhibited strains. This contrasts with the effects of LKB1 Dead Kinase expression in the wild type background which caused a clear reduction in mitochondrial mass. As was the case with antisense inhibition of AMPK expression (Bokko *et al*., 2007), this could indicate that the AMPK-mediated mitochondrial proliferation that should occur in mitochondrially compromised cells is counterbalanced by the inactivation of LKB1 and hence AMPK. Although, there is no direct interaction between these chaperonin 60 and LKB1, these preliminary results could provide an initial insight to the role of LKB1 in causing cytopathological changes that are associated with mitochondrial disorders.

4.5. Conclusion and future directions

In this thesis, the role of LKB1 has been investigated in the *Dictyostelium* model and shown to include the AMPK-dependent regulation of mitochondrial biogenesis, cell growth and morphogenesis as well as AMPK-independent regulation of endocytic nutrient uptake. These biological roles of LKB1 in the *Dictyostelium* model are consistent with its function in human cells including its activity as a tumour suppressor. The AMPK-dependent phenotypes associated with LKB1 hyperactivity are evident in mitochondrially diseased cells, because in those cells, AMPK is chronically activated by energy stress and this requires LKB1 as the upstream activating kinase.

However, as my results make clear, LKB1 also plays important roles in other AMPK-independent pathways in *Dictyostelium.* In particular, some downstream processes such as pinocytosis and phagocytosis are mediated by signalling pathways independent of AMPK. Since LKB1 is a main upstream activator of 14 AMPK-related kinases (ARKs), it is possible that LKB1 phosphorylates and activates other ARKS in conjunction with AMPK in the *Dictyostelium* transformants. The identification of the phenotypically relevant downstream kinases could be a subject for future work.

Although LKB1 normally occurs in a complex with two other subunits, it seems also to be constitutively active in *Dictyostelium* cells with sole overexpression of LKB1 appearing to be sufficient to exert phenotypic effects. This may be due to its lack of a nuclear localisation signal and hence its constitutive presence in the cytoplasm where its activity is not inhibited. However, as in mammalian cells, the overexpression of the

subunit STRADα enhanced the effects of overexpressing LKB1 in *Dictyostelium* cells. This indicates that when LKB1 binds to STRADα, its activity is further amplified. Unfortunately, I was unable to express the MO25 subunit in *Dictyostelium*, and hence it would be beneficial in future studies to further characterise *Dictyostelium* LKB1 as a part of a complex with both STRADα and MO25.

5. References

Adams, J., Chen Z. P., Van Denderen B. J., Morton, C. J., Parker, M. W., Witters, L. A., Stapleton, D., Kemp, B. E. (2004) Intrasteric control of AMPK via the gamma1 subunit AMP allosteric regulatory site. *Prot Sci* **13** (1), 155-165.

Agostino, A., Valletta, L., Chinnery, P. F., Ferrari, F., Taylor, R. W., Schaefer, A. M., Turnbull, D. M., Tiranti, V. & Zeviani, M. (2003) Mutations of *ANT1*, *Twinkle*, and *POLG1* in sporadic progressive external ophthalmoplegia (PEO). *Neurol* **60**, 1354–1356.

Agresti, C. A., Halkiadakis, P. N. & Tolias, P. (2018) MERRF and MELAS: current gene therapy trands and approaches. *J. Transl Gen Genom* **2**, 9.

Aitullina, A., Baumane, K., Zalite, S., Ranka, R., Zole, E., Pole, I., Sepetiene, S., Laganovska, G., Baumanis, V. & Pliss, L. (2013) Point mutations associated with Leber hereditary optic neuropathy in a Latvian population. *Mol Vision* **19**, 2343–2351.

Alers, S., Löffler, A. S., Wesselborg, S. & Stork, B. (2012) Role of AMPK-mTOR-Ulk1/2 in the Regulation of Autophagy: Cross Talk, Shortcuts, and Feedbacks. *Mol Cell Biol* **32**, 2-11.

Alessi, D. R., Sakamoto, K., Bayascas, J. R. (2006) LKB1-dependent signaling pathways. Annu Rev Biochem **75**, 137–163.

Alexander, A. & Walker, C. L. (2011) The role of LKB1 and AMPK in cellular responses to stress and damage. *FEBS Lett* **585**, 952 – 957.

Alexander, A., Cai, S. L., Kim, J., Nanez, A., Sahin, M., Maclean, K. H., Inoki, K., Guan, K. L., Shen, J., Person, M. D., Kusewitt, D., Mills, G. B., Kastan, M. B. & Walker, C. L. (2010a) ATM signals to TSC2 in the cytoplasm to regulate mTORC1 in response to ROS. *Proc Natl Acad Sci USA* **107**, 4153-4158.

Alexander, A., Kim, J. & Walker, C. L. (2010b) ATM engages the TSC2/mTORC1 signaling node to regulate autophagy. *Autophagy* **6**, 672 – 673.

Algire, C., Amrein, L., Bazile, M., David, S., Zakikhani, M. & Pollak, M. (2011) Diet and tumor LKB1 expression interact to determine sensitivity to anti-neoplastic effects of metformin in vivo. *Oncogene* **30**, 1174–1182.

Alhopuro, P., Phichith, D., Tuupanen, S., Sammalkorpi, H., Nybondas, M., Saharinen, J., Robinson, J. P., Yang, Z., Chen, L.-Q., Orntoft, T., Mecklin, J.-P., Jarvinen, H., Eng, C., Moeslein, G., Shibata, D., Houlston, R. S., Lucassen, A. & other authors (2008) Unregulated smooth-muscle myosin in human intestinal neoplasia. *Proc Nat Acad Sci* USA **105**, 5513-5518.

Alston, C. L., Lowe, J, Turnbull, D. M., Maddison, P. & Taylor, R. W. (2010) A novel mitochondrial tRNAGlu (MTTE) gene mutation causing chronic progressive external ophthalmoplegia at low levels of heteroplasmy in muscle. *J Neurol Sci* **298**, 140- 144.

Alston, C. L., Rocha, M. C., Lax, N. Z., Turnbull, D. M., & Taylor, R. W. (2017). The genetics and pathology of mitochondrial disease. *J Pathology* **241**, 236–250.

Amodeo, G. A., Rudolph, M. J. & Tong, L. (2007) Crystal structure of the heterotrimer core of Saccharomyces cerevisiae AMPK homologue SNF1. *Nat* **449**, 492–495.

Annesley, S. J., Chen, S., Francione, L. M., Sanislav, O., Chavan, A. J., Farah, C., De Piazza, S. W., Storey, C. L., Ilievska, J., Fernando, S. G., Smith, P. K., Lay, S. T. & Fisher, P. R. (2014) *Dictyostelium*, a microbial model for brain disease. *Biochim Biophys Acta (BBA) - General Subjects* **1840**, 1413-1432.

Annesley, S. J. & Fisher, P. R. (2009) *Dictyostelium discoideum*-a model for many reasons. *Mol Cell Biochem* **329**, 73-91.

Armata, H. L., Golebiowski, D., Jung, D. Y., Ko, H. J., Kim, J. K. & Sluss, H. K. (2010) Requirement of the ATM/p53 tumor suppressor pathway for glucose homeostasis. *Mol Cell Biol* **30**,5787 – 5794.

Asada, N. & Sanada, K. (2010) LKB1-Mediated Spatial Control of GSK3β and Adenomatous Polyposis Coli Contributes to Centrosomal Forward Movement and Neuronal Migration in the Developing Neocortex. *J Neuro* **30**, 8852-8865.

Asada, N., Sanada, K. & Fukada, Y. (2007) LKB1 regulates neuronal migration and neuronal differentiation in the developing neocortex through centrosomal positioning. *J Neurosci* **27**, 11769–11775.

Atkinson, D. E. & Walton, G. M. (1967) Adenosine triphosphate conservation in metabolic regulation. Rat liver citrate cleavage enzyme. *J Biol Chem* **242**, 3239-3241.

Attardi, G. (2002) Role of mitochondrial DNA in human aging. *Mitochondrion* **2**, 27–37.

Baas, A. F., Boudeau, J., Sapkota, G. P., Smit, L., Medema, R., Morrice, N. A., Alessi, D. R. & Clevers, H. C. (2003) Activation of the tumour suppressor kinase LKB1 by the STE20-like pseudokinase STRAD. *EMBO J* **22**, 3062–3072.

Baas, A. F., Kuipers, J., van der Wel, N. N., Batlle, E., Koerten, H. K., Peters, P. J. & Clevers, H. C. (2004) Complete polarization of single intestinal epithelial cells upon activation of LKB1 by STRAD. *Cell* **116**, 457–466.

Bai, B., Man, A. W. C., Yang, K., Guo, Y., Xu, C., Tse, H.-F., Han, W., Bloksgaard, M., De Mey, J. G. R., Vanhoutte, P. M., Xu, Aimin & Wang, Y. (2016) Endothelial SIRT1 prevents adverse arterial remodeling by facilitating HERC2-mediated degradation of acetylated LKB1. *Oncotarget* **7**, 39065-39081.

Bai, Y., Zhou, T., Fu, H., Sun, H. & Huang, B. (2012) 14-3-3 interacts with LKB1 via recognizing phosphorylated threonine 336 residue and suppresses LKB1 kinase function. *FEBS Lett* **586**, 1111-1119.

Banko MR, Allen JJ, Schaffer BE, et al. (2011) Chemical genetic screen for AMPKα2 substrates uncovers a network of proteins involved in mitosis. Mol Cell 44:878–92.

Banno, K., Kisu, I., Yanokura, M., Masuda, K., Ueki, A., Kobayashi, Y., Hirasawa, A. & Aoki, D. (2013) Hereditary gynecological tumors associated with Peutz-Jeghers syndrome. *Oncol Lett* **6**, 1184–1188.

Barnes, A. P., Lilley, B. N., Pan, Y. A., Plummer, L. J., Powell, A. W., Raines, A. N., Sanes, J. R. & Polleux, F. (2007) LKB1 and SAD kinases define a pathway required for the polarization of cortical neurons. *Cell* **129**, 549–563.

Barnes, K., Ingram, J. C., Porras, O. H., Barros, L. F., Hudson, E. R., Fryer, L. G. D., Foufelle, F., Carling, D., Hardie, D. G. & Baldwin, S. A. (2002) Activation of GLUT1 by metabolic and osmotic stress: potential involvement of AMP-activated protein kinase (AMPK). *J Cell Sci* **115**, 2433–2442.

Barth, C., Greferath, U., Kotsifas, M. & Fisher, P.R. (1999) Polycistronic transcription and editing of the mitochondrial small subunit (*SSU*) ribosomal RNA in *Dictyostelium discoideum. Curr Genet* **36**, 55-61.

Barth, C., Greferath, U., Kotsifas, M., Tanaka, Y., Alexander, S., Alexander, H. & Fisher, P.R. (2001) Transcript mapping and processing of mitochondrial RNA in *Dictyostelium discoideum*. *Curr Genet* **39**, 355-364.

Bateman, A. (1997) The structure of a domain common to archaebacteria and the homocystinuria disease protein. *Trends Biochem Sci* **22**, 12–13.

Baur, J. A., Pearson, K. J., Price, N. L., Jamieson, H. A., Lerin, C., Kalra, A., Prabhu, V. V., Allard, J. S., Lopez-Lluch, G., Lewis, K., Pistell, P. J., Poosala, S., Becker, K. G. & other authors (2006) Resveratrol improves health and survival of mice on a high-calorie diet. *Nat* **444**, 337–342.

Beg, Z. H., Allmann, D. W. & Gibson, D. M. (1973) Modulation of 3-hydroxy-3-methylglutaryl coenzyme A reductase activity with cAMP and wth protein fractions of rat liver cytosol. *Biochem Biophys Res Commun* **54**, 1362– 1369.

Bell, E. L., Emerling, B. M. & Chandel, N. S. (2005) Mitochondrial regulation of oxygen sensing. *Mitochondrion* **5**, 322-332.

Bender, A., Krishnan, K. J., Morris, C. M., Taylor, G. A., Reeve, A. K., Perry, R. H. & other authors (2006) High levels of mitochondrial DNA deletions in *substantia nigra* neurons in aging and Parkinson disease. *Nat Genet* **38**, 515-517.

Bensimon, A., Aebersold, R. & Shiloh, Y. (2011) Beyond ATM: the protein kinase landscape of the DNA damage response. *FEBS Lett* **585**, 1625 – 1639.

Bergeron, R., Ren, J. M., Cadman, K. S., Moore, I. K., Perret, P., Pypaert, M., Young, L. H., Semenkovich, C. F. & Shulman, G. I. (2001) Chronic activation of AMP kinase results in NRF-1 activation and mitochondrial biogenesis. *Am J Physiol Endocrinol Metab* **281**, E1340–E1346.

Betschinger, J. & Knoblich, J.A. (2004) Dare to be different: asymmetric cell division in Drosophila, C. elegans and vertebrates *Curr Biol* **14**, R674–R685.

Bettencourt-Dias, M., Giet, R., Sinka, R., Mazumdar, A., Lock, W. G., Blloux, F., Zafiropolous, P. J., Yamaguchi, S., Winter, S., Carthew, R. W., Cooper, M., Jones, D., Frenz, L. & Glover, D. M. (2004) Genome-wide survey of protein kinases required for cell cycle progression. *Nat* **432**, 980–987.

Bianchi K, Rimessi A, Prandini A, Szabadkai G, Rizzuto R. (2004) Calcium and mitochondria: mechanisms and functions of a troubled relationship. *Biochim Biophys Acta* **1742**, 119–131.

Boehlke, C., Kotsis, F., Patel, V., Braeg, S., Voelker, H., Bredt, S., Beyer, T., Janusch, H., Hamann, C., Godel, M., Muller, K., Herbst, M., Hornung, M., Doerken, M., Kottgen, M., Nitschke, R., Igarashi, P., Walz, G & Kuehn, E. W. (2010) Primary cilia regulate mTORC1 activ- ity and cell size through Lkb1. *Nat Cell Biol* **12**, 1115–1122.

Bokko, P. B., Francione, L., Bandala-Sanchez, E., Ahmed, A. U., Annesley, S. J., Huang, X., Khurana, T., Kimmel, A. R. & Fisher, P. R. (2007) Diverse cytopathologies in mitochondrial disease are caused by AMP-activated protein kinase Signalling. *Mol Biol Cell* **18**, 1874-1886.

Bonaccorsi, S., Mottier, V., Giansanti, M. G., Bolkan, B. J., Williams, B., Goldberg, M. L. & Gatti, M. (2007) The *Drosophila* Lkb1 kinase is required for spindle formation and asymmetric neuroblast division. *Develop* **134**, 2183–2193.

Bouchekioua-Bouzaghou, K., Poulard, C., Rambaud, J., Lavergne, E., Hussein, N., Billaud, M., Bachelot, T., Chabaud, S., Mader, S., Dayan, G., Treilleux, I., Corbo, L. & Le Romancer, M. (2014) LKB1 when associated with methylatedERα is a marker of bad prognosis in breast cancer. *Int J Cancer* **135**, 1307–1318.

Boudeau, J., Baas, A. F., Deak, M., Morrice, N. A., Kieloch, A., Schutkowski, M., Prescott, A. R., Clevers, H. C. & Alessi, D. R. (2003a) MO25alpha/beta interact with STRADalpha/beta enhancing their ability to bind, activate and localize LKB1 in the cytoplasm. *EMBO J* **22**, 5102– 5114.

Boudeau, J., Kieloch, A., Alessi, D. R., Stella, A., Guanti, G., & Resta, N. (2003b) Functional analysis of LKB1/STK11 mutants and two aberrant isoforms found in Peutz-Jeghers Syndrome patients. *Hum Mutat* **21**, 172.

Broustas, C. G. & Lieberman, H. B. (2014) DNA damage response genes and the development of cancer metastasis. *Radiation Res* **181**, 111-130.

Brown, G. C. & Borutaite, V. (2012) There is no evidence that mitochondria are the main source of reactive oxygen species in mammalian cells, *Mitochondrion* **12**, 1–4.

Bryan, H. K., Olayanju, A., Goldring, C. E. & Park, B. K. (2013) The Nrf2 cell

defence pathway: Keap1-dependent and -independent mechanisms of regulation. *Biochem Pharma* **85**, 705–717.

Buemi, M., Allegra, A., Rötig, A., Gubler, M. C., Aliosi, C., Corica, F., Pettinatto, G., Frisina, N, & Niaudet, P. (1997) Renal failure from mitochondrial cytopathies. *Nephron* **76**, 249-253.

Bultot, L., Horman, S., Neumann, D., Walsh, M. P., Hue, L. & Rider, M. H. (2009) Myosin light chains are not a physiological substrate of AMPK in the control of cell structure changes. *FEBS Lett* **583**, 25–28.

Bungard, D., Fuerth, B. J., Zeng, P. Y., Faubert, B., Maas, N. L., Viollet, B., Carling, D., Thompson, C. B., Jones, R. G., Berger, S. L. (2010) Signaling kinase AMPK activates stress-promoted transcription via histone H2B phosphorylation. *Sci* **329**, 1201 – 1205.

Burger, G., Gray, M. W., Forget, L. & Lang, B. F. (2013) Strikingly bacteria-like and gene-rich mitochondrial genomes throughout jakobid protists. *Genome Biol Evol* **5**, 418-438.

Burns, J. S. & Manda, G. (2017) Metabolic Pathways of the Warburg Effect in Health and Disease: Perspectives of Choice, Chain or Chance. *Int J Mol Sci* **18**, E2755.

Cai, W., Fu, Q., Zhou, X., Qu, J., Tong, Y. & Guan, M. X. (2008) Mitochondrial variants may influence the phenotypic manifestation of Leber's hereditary optic neuropathy-associated ND4 G11778A mutation. *J Genet. Genomics* **35,** 649-655.

Calabrese, M. F., Rajamohan, F., Harris, M. S., Caspers, N. L., Magyar, R., Withka, J. M., Wang, H., Borzilleri, K. A., Sahasrabudhe, P. V., Hoth, L. R., Geoghegan, K. F., Han, S., Brown, J., Subashi, T. A., Reyes, A. R. & other authors (2014) Structural basis for AMPK activation: natural and synthetic ligands regulate kinase activity from opposite poles by different molecular mechanisms. *Structure* **22**, 1161–1172.

Calabrese, V., Scapagnini, G., Giuffrida Stella, A. M., Bates, T. E., & Clark, J. B. (2001) Mitochondrial involvement in brain function and dysfunction: Relevance to aging, neurodegenerative disorders and longevity. *Neurochem Res* **26**, 739-764.

Calamaras, T. D., Lee, C., Lan, F., Ido, Y., Siwik, D. A., & Colucci, W. S. (2012) Post-translational modification of serine/threonine kinase LKB1 via Adduction of the

Reactive Lipid Species 4-Hydroxy-trans-2-nonenal (HNE) at lysine residue 97 directly inhibits kinase activity. *J Biol Chem* **287**, 42400–42406.

Calvo-Garrido, J., Carilla-Latorre, S., Kubohara, Y., Santos-Rodrigo, N., Mesquita, A., Soldati, T., Golstein, P. & Escalante, R. (2010) Autophagy in Dictyostelium: genes and pathways, cell death and infection. *Autophagy* **6**, 686-701.

Canto, C., Gerhart-Hines, Z., Feige, J. N., Lagouge, M., Noriega, L., Milne, J. C., Elliott, P. J., Puigserver, P. & Auwerx, J. (2009) AMPK regulates energy expenditure by modulating NAD+ metabolism and SIRT1 activity. *Nat* **458**, 1056-1060**.**

Carling D (2017) AMPK signalling in health and disease. *Curr Opin Cell Biol* **45**, 31–37.

Carling, D., Thornton, C., Woods, A. & Sanders, M. J. (2012) AMP-activated protein kinase: new regulation, new roles? *Biochem J* **445**, 11-27.

Carlson, C. A. & Kim, K. H. (1973) Regulation of hepatic acetyl coenzyme A carboxylase by phosphorylation and dephosphorylation. *J Biol Chem* **248**, 378–380.

Catarino, C. B., Ahting, U., Gusic, M., Iuso, A., Repp, B., Peters, K., Biskup, S., von Livonius, B., Prokish, H. & Klopstock, T. (2017) Characterization of a Leber's Hereditary Optic Neuropathy (LHON) Family Harboring Two Primary LHON Mutations m.11778G>A and m.14484T>C of the Mitochondrial DNA. *Mitochondrion* **36**, 15-20.

Cedikova, M., Kripnerova, M., Dvorakova, J., Pitule, P., Grundmanova, M., Babuska, V., Mullerova, D. & Kuncova, J. (2016) Mitochondria in white, brown, and beige adipocytes. *Stem Cells Int* **2016**, 1-11.

Chapman, A. G. & Atkinson, D. E. (1977) Adenine nucleotide concentrations and turnover rates. Their correlation with biological activity in bacteria and yeast. *Adv Microb Physiol* **15**, 253-306.

Chavez, J. A., Roach, W. G., Keller, S. R., Lane, W. S. & Lienhard, G. E. (2008) Inhibition of GLUT4 translocation by Tbc1d1, a Rab GTPase-activating protein abundant in skeletal muscle, is partially relieved by AMP-activated protein kinase activation. *J Biol Chem* **283**, 9187–9195.

Chen, J.-H., Zheng, J.-J., Guo, Q., Liu, C., Luo, B., Tang, S.-B., Cheng, J. D. & Huang, E.-W. (2017) A novel mutation in the *STK11* gene causes heritable Peutz-Jeghers syndrome - a case report. *BMC Med Genet* **18**, 19.

Chen, L., Jiao, Z. H., Zheng, L. S., Zhang, Y. Y., Xie, S. T., Wang, Z. X. & Wu, J. W. (2009) Structural insight into the autoinhibition mechanism of AMP-activated protein kinase. *Nat* **459**, 1146-1149.

Chen, L., Xin, F. J., Wang, J., Hu, J., Zhang, Y. Y., Wan, S., Cao, L. S., Lu, C., Li, P., Yan, S. F., Neumann, D., Schlattner, U., Xia, B., Wang, Z. X. & Wu, J. W. (2013) Conserved regulatory elements in AMPK. *Nat* **498**, E8–E10.

Chen, S. & Sang, N. (2016) Hypoxia-Inducible Factor-1: A Critical Player in the Survival Strategy of Stressed Cells. *J Cell Biochem* **117**, 267-278.

Chida, J., Yamaguchi, H., Amagai, A. & Maeda, Y. (2004) The necessity of mitochondrial genome DNA for normal development of *Dictyostelium* cells. *J Cell Sci* **117**,3141-3152.

Chinnery, P. F. & Hudson, G. (2013) Mitochondrial genetics. *Br Med Bull* **106**, 135-159.

Chinnery, P. F. & Turnbull, D. M. (2000) Mitochondrial DNA mutations in the pathogenesis of human disease. *Mol Med Today* **6**, 425-432.

Chisholm, R. L. & Firtel, R. A. (2004) Insights into morphogenesis from a simple developmental system. *Nat Rev Mol Cell Biol* **5**, 531-541.

Chou, K. C. & Shen, H. B. (2008) Cell-PLoc: A package of web-servers for predicting subcellular localization of proteins in various organisms. *Nat Prot* **3**, 153-162.

Chou, K. C & Shen, H. B. (2010) A New Method for Predicting the Subcellular Localization of Eukaryotic Proteins with Both Single and Multiple Sites: *Euk-mPLoc 2.0, PLoS ONE* **5**: e9931.

Chou, S. Z., Lee, Y. C., Chen, H. M., Chiang, M. C., Lai, H. L., Chang, H. H., Wu, Y. C., Sun, C. N., Chien, C. L., Lin, Y.S., Wang, S.C., Tung, Y. Y., Chang, C. & Chern, Y. (2005) CGS21680 attenuates symptoms of Huntington's disease in a transgenic mouse model**.** *J Neurochem* **93**, 310-320.

Chung, J., Kuo, C. J., Crabtree, G. R. & Blenis, J. (1992) Rapamycin-FKBP specifically blocks growth-dependent activation of and signaling by the 70 kd S6 protein kinases. *Cell* **69**, 1227–1236.

Ciafaloni, E., Ricci, E., Shanske, S., Moraes, C.T., Silvestri, G., Hirano, M., Simonetti, S., Angelini, C., Donati, M.A., Garcia, C., Martinuzzi, A., Mosewich, R., Servidei, S., Zammarchi, E., Bonilla, E., DeVivo, D.C., Rowland, L. P., Schon, E. A. & DiMauro, S. (1992) MELAS: Clinical Features, Biochemistry, and Molecular Genetics. *Ann Neurol* **31**, 391-398.

Collins, S. P., Reoma, J. L., Gamm, D. M. & Uhler, M. D. (2000) LKB1, a novel serine/threonine protein kinase and potential tumour suppressor, is phosphorylated by cAMP-dependent protein kinase (PKA) and prenylated in vivo. *Biochem J* **345**, 673–680.

Cooper, G. M. (2000) *The cell: A molecular approach, 2nd edition*. Sunderland (MA): Sinauer Associates.

Copeland, W. C. (2012) Defects in mitochondrial DNA replication and human disease. *Crit Rev Biochem Mol Biol* **47**, 64–74.

Corton, J. M., Gillespie, J. G. & Hardie, D. G. (1994) Role of the AMP-activated protein kinase in the cellular stress response. *Curr Biol* **4**, 315–324.

Corton, J. M., Gillespie, J. G., Hawley, S. A. & Hardie, D. G. (1995) 5-aminoimidazole-4- carboxamide ribonucleoside. A specific method for activating AMP-activated protein kinase in intact cells? *European J Biochem FEBS* **229**, 558–565.

Coskun, P. E., Beal, M. F. & Wallace, D. C. (2004) Alzheimer's brains harbor somatic mtDNA control-region mutations that suppress mitochondrial transcription and replication. *Proc Natl Acad Sci USA* **101**, 10726-10731.

Coughlan, K. A., Valentine, R. J., Ruderman, N. B. & Saha, A. K. (2014) AMPK activation: a therapeutic target for type 2 diabetes? *Diabetes Metab Syndr Obes* **7**, 241-253.

Cowan, C. R. & Hyman, A. A. (2007) Acto-myosin reorganization and PAR polarity in C. elegans. *Development* **134**, 1035–1043.

Creuzet, S. E., Martinez, S. & Le Douarin, N. M. (2006) The cephalic neural crest exerts a critical effect on forebrain and midbrain development. *Proc Natl Acad Sci USA* **103**, 14033–14038.

Crute, B. E., Seefeld, K., Gamble, J., Kemp, B. E. & Witters, L. A. (1998) Functional domains of the alpha-1 catalytic subunit of the AMP-activated protein

kinase. *J Biol Chem* **273**, 35347–35354.

Czubryt, M. P., McNally, J., Fishman, G. I. & Olson, E. N. (2003) Regulation of peroxisome proliferator-activated receptor gamma coactivator 1 alpha (PGC-1 alpha) and mitochondrial function by MEF2 and HDAC5. *Proc Natl Acad Sci USA* **100**, 1711-1716.

D'Aurelio, M., Vives-Bauza, C., Davidson, M. M., & Manfredi, G. (2010) Mitochondrial DNA background modifies the bioenergetics of NARP/MILS *ATP6*mutant cells. *Hum Mol Gen* **19**, 374–386.

Dahl, H. H & Thorburn, D. R. (2001) Mitochondrial diseases: beyond the magic circle. *Am J Med Genet* **106**, 1-3.

Dahmani, R., Just, P., Delay, a, Canal, F., Finzi, L., Prip-Buus, C., Lambert, M., Sujobert, P., Buchet-Poyau, K., Miller, E., Cavard, C., Marmier, S., Terris, B., Billaud, M. & Perret, C. (2014) A novel LKB1 isoform enhances AMPK metabolic activity and displays oncogenic properties. *Oncogene* **34**, 2337–2346.

Dai, D.-F., Rabinovitch, P. S. & Ungvari, Z. (2012) Mitochondria and Cardiovascular Aging. *Circulation Res* **110**, 10.

Dan, I., Watanabe, N. M. & Kusumi, A. (2001) The Ste20 group kinases as regulators of MAP kinase cascades. *Trends Cell Biol* **11**, 220–230.

Day, P., Shariff, A., Parra, L., Cleasby, A., Williams, M., Horer, S., Nar, H., Redemann, N, Tickle, I. & Yon, J. (2007) Structure of a CBS-domain pair from the regulatory gamma1 subunit of human AMPK in complex with AMP and ZMP. *Acta Crystallogr D Biol Crystallogr* **63**, 587-596.

De la Mata, M., Garrido-Maraver, J., Cotán, D., Cordero, M. D., Oropesa-Ávila, M., Izquierdo, L. G., De Miguel, M., Lorite, J. B., Infante, E. R., Ybot, P., Jackson, S. & Sánchez-Alcázar, J. A. (2012) Recovery of MERRF fibroblasts and cybrids pathophysiology by coenzyme Q10. *Neurotherap* **9**, 446-463.

Debray, F. G., Mitchell, G. A., Allard, P., Robinson, B. H., Hanley, J. A. & Lambert, M. (2007) Diagnostic accuracy of blood lactate- to-pyruvate molar ratio in the differential diagnosis of congenital lactic acidosis. *Clin Chem* **53**, 916-921.

Denison, F. C., Hiscock, N. J., Carling, D. & Woods, A. (2009) Characterization of an alternative splice variant of LKB1. *J Biol Chem* **284**, 67–76.

Denison, F. C., Smith, L. B., Muckett, P. J., O'Hara, L., Carling, D., & Woods, A. (2011) LKB1 is an essential regulator of spermatozoa release during spermiation in the mammalian testis. *PloS One* **6**, e28306.

DiMauro, S. (2004) Mitochondrial diseases. *Biochem Biophys Acta* **1658**, 80-88.

DiMauro, S. (2013) Mitochondrial encephalomyopathies--fifty years on: the Robert Wartenberg Lecture. *Neurol* **81**, 281-291.

DiMauro, S. & Davidzon, G. (2005) Mitochondrial DNA and disease. *Ann Med* **37**, 222-232.

DiMauro, S. & Schon, E. A. (2003) Mitochondrial respiratory-chain diseases. *N Engl J Med* **348**, 2656-2668.

DiMauro, S., Schon, E. A., Carelli, V., & Hirano, M. (2013) The clinical maze of mitochondrial neurology. *Nat Rev Neurol* **9**, 429-444.

Ditch, S. & Paull, T. T. (2012) The ATM protein kinase and cellular redox signaling: beyond the DNA damage response. *Trends Biochem Sci* **37**, 15 – 22.

Dorfman, J. & Macara, I. G. (2008) STRADalpha regulates LKB1 localization by blocking access to importin-alpha, and by association with Crm1 and exportin-7. *Mol Biol Cell* **19**, 1614–1626.

Drewes, G., Ebneth, A. & Mandelkow, E.M. (1998) MAPs, MARKs and microtubule dynamics. *Trends Biochem Sci* **23**, 307–311.

Dudley, P., Wood, C. K., Pratt, J. R. & Moore, A. L. (1997) Developmental regulation of the plant mitochondrial matrix located HSP70 chaperone and its role in protein import. *FEBS Lett* **417**, 321-324.

Dunlop, E. A. & Tee, A. R. (2014) mTOR and autophagy: A dynamic relationship governed by nutrients and energy. *Semin Cell Dev Biol* **36**, 121–129.

Dupuy, F., Griss, T., Blagih, J., Bridon, G., Avizonis, D., Ling, C., Dong, Z., Siwak, D. R., Annis, M. G., Mills, G. B., Muller, W. J., Siegel, P. M. & Jones, R. G. (2013) LKB1 is a central regulator of tumor initiation and pro-growth metabolism in ErbB2-mediated breast cancer. *Cancer & Metab* **1**, 18.

Elliott, H. R., Samuels, D. C., Eden, J. A., Relton, C. L. & Chinnery, P. F. (2008) Pathogenic mitochondrial DNA mutations are common in the general population. *Am J Hum Genet* **83**, 254–260.

Emile, S. H., El-Said, M. & Elfeki, H. (2018) Recurrent Intestinal Obstruction with Double-site Small Bowel Intussusception in Patient with Peutz-Jeghers Syndrome. *Int J Surg Proced* **1**, 105.

Eskelinen, E. & Saftig, P. (2009) Autophagy: A lysosomal degradation pathway with a central role in health and disease. *Biochem Biophys Acta (BBA) - Mol Cell Research*. **1793**, 664–673.

Estruch, F., Treitel, M. A., Yang, X. & Carlson, M. (1992) N-terminal mutations modulate yeast SNF1 protein kinase function. *Genet* **132**, 639-650.

Evans, J. M. M., Donnelly, L. A., Emslie-Smith, A. M., Alessi, D. R. & Morris, A. D. (2005) Metformin and reduced risk of cancer in diabetic patients. *BMJ Clinic Res* **330**, 1304–1305.

Falk, M. J. (2010) Neurodevelopmental Manifestations of Mitochondrial Disease. *J Dev Behav Pediatr* **31**, 610–621.

Faubert, B., Boily, G., Izreig, S., Griss, T., Samborska, B., Dong, Z., Dupuy, F., Chambers, C., Fuerth, B. J., Viollet, B., Mamer, O. A., Avizonis, D., DeBeradinis, R. J., Siegel, P. M. & Jones, R. G. (2013) AMPK is a negative regulator of the Warburg effect and suppresses tumor growth in vivo. *Cell Metab* **17**, 113–124.

Faubert, B., Vincent, E. E., Griss, T., Samborska, B., Izreig, S., Svensson, R. U., Mamer, O. A., Avizonis, D., Shackelford, D. B., Shae, R. J. & Jones, R. G. (2014) Loss of the tumor suppressor LKB1 promotes metabolic reprogramming of cancer cells via HIF-1α. *Proc Natl Acad Sci USA* **111**, 2554–2559.

Filippi, B. M., de los Heros, P., Mehellou, Y., Navratilova, I., Gourlay, R., Deak, M., Plater, L., Toth, R., Zeqiraj, E. & Alessi, D. R. (2011) MO25 is a master regulator of SPAK/OSR1 and MST3/MST4/YSK1 protein kinases. *EMBO J* **30**, 1730–1741.

Finsterer, J. (2001) Cerebrospinal-fluid lactate in adult mitochondriopathy with and without encephalopathy. *Acta Med Austriaca* **28**, 152-155.

Finsterer, J. (2008) Leigh and Leigh-like syndrome in children and adults. *Pediatr Neurol* **39**, 223–235.

Fisslthaler, B. & Fleming, I. (2009) Activation and signaling by the AMP-activated protein kinase in endothelial cells. *Circulation Res* **105**, 114–127.

Fogarty, S. & Hardie, D. G. (2010) Development of protein kinase activators: AMPK

as a target in metabolic disorders and cancer. *Biochem Biophys Acta* **1804**, 581– 591.

Fogarty, S., Hawley, S. A., Green, K. A., Saner, N., Mustard, K. J. & Hardie, D. G. (2010) Calmodulin-dependent protein kinase kinase-beta activates AMPK without forming a stable complex: synergistic effects of Ca2+ and AMP. *Biochem J* **426**, 109–118.

Forcet, C., Etienne-Manneville, S., Gaude, H., Founier, L., Debilly, S., Salmi, M., Baas, A., Olschwang, S., Clevers, H. & Billaud, M. (2005) Functional analysis of Peutz-Jeghers mutations reveals that the LKB1 C-terminal region exerts a crucial role in regulating both the AMPK pathway and the cell polarity. *Hum Mol Genet* **14**, 1283-1292.

Foretz, M., Hébrard, S., Leclerc, J., Zarrinpashneh, E., Soty, M., Mithieux, G., Sakamoto, K., Andreeli, F. & Viollet, B. (2010) Metformin inhibits hepatic gluconeogenesis in mice independently of the LKB1/AMPK pathway via a decrease in hepatic energy state. *J Clinic Investig* **120**, 2355–2369.

Francione, L. M., Annesley, S. J., Carilla-Latorre, S., Escalante, R. & Fisher, P. R. (2011) The *Dictyostelium* model for mitochondrial disease. *Semin Cell Dev Biol* **22**, 120-130.

Francione, L. M. & Fisher, P. R. (2010) Cytopathological mechanisms in mitochondrial disease**.** *Curr Chem Biol* **4**, 32-48.

Francione, L. M. & Fisher, P. R. (2011) Heteroplasmic mitochondrial disease in *Dictyostelium discoideum. Biochem Pharmacol* **82**, 1510-1520.

Francione, L. M., Smith, P. K., Accari, S. L., Taylor, P. E., Bokko, P. B., Bozzaro, S., Beech, P. L. & Fisher, P. R. (2009) *Legionella pneumophila* multiplication is enhanced by chronic AMPK signalling in mitochondrially diseased *Dictyostelium* cells. *Dis Model Mech* **2**, 479-489.

Frazier, A. E., Thorburn, D. R. & Compton, A. G. (2017) Mitochondrial energy generation disorders: genes, mechanisms and clues to pathology. *J Biol Chem* [Epub ahead of print]

Frey, T. G. & Mannella, C. A. (2000) The internal structure of mitochondria. *Trends Biochem Sci* **25**, 319–324.

Friedman, J. R. & Nunnari, J. (2014) Mitochondrial form and function. *Nat* **505**, 335-343.

Fryer, L. G., Parbu-Patel, A, & Carling, D. (2002) The Anti-diabetic drugs rosiglitazone and metformin stimulate AMP-activated protein kinase through distinct signaling pathways. *J Biol Chem* **277**, 25226–25232.

Fullerton, M. D., Galic, S., Marcinko, K., Sikkema, S., Pulinilkunnil, T., Chen, Z. P., O'Neill, H. M., Ford, R. J., Palanivel, R., O'Brien, M., Hardie, D. G., Macaulay, S. L., Schertzer, J. D., Dyck, J. R., van Denderen, B. J., Kemp, B. E & Steinberg, G. R. (2013) Single phosphorylation sites in Acc1 and Acc2 regulate lipid homeostasis and the insulin-sensitizing effects of metformin. *Nat med* **19,** 1649-1654.

Gadalla, A. E., Pearson, T., Currie, A. J., Dale, N., Hawley, S. A., Sheehan, M., Hirst, W., Michael, A. D., Randall, A., Hardie, D. G. & Frenguelli, B. G. (2004). AICA riboside both activates AMP-activated protein kinase and competes with adenosine for the nucleoside transporter in the CA1 region of the rat hippocampus. *J Neurochem* **88**, 1272–1282.

Galic, S., Fullerton, M. D., Schertzer, J. D., Sikkema, S., Marcinko, K., Walkley, C. R., Izon, D., Honeyman, J., Chen, Z., van Denderen, B. J., Kemp, B. E. & Steinberg, G. R. (2011) Hematopoietic AMPK β1 reduces mouse adipose tissue macrophage inflammation and insulin resistance in obesity. *J Clinic Invest* **121**, 4903–4915.

Gan, R. Y. & Li, H. B. (2014) Recent progress on liver kinase B1 (LKB1): expression, regulation, downstream signaling and cancer suppressive function. *Int J Mol Sci* **15**, 16698-16718.

Gao, J., Wang, L., Liu, J., Xie, F., Su, B. & Wang, X. (2017) Abnormalities of mitochondrial dynamics in neurodegenerative diseases. *Antioxidants* **6**, 25.

Garcia, D. & Shaw, R. J. (2017). AMPK: mechanisms of cellular energy sensing and restoration of metabolic balance. *Molecular Cell* **66**, 789–800.

García-Bermúdez, J. & Cuezva, J. M. (2016) The ATPase Inhibitory Factor 1 (IF1): A master regulator of energy metabolism and of cell survival. *Biochem Biophys Acta* **1857**, 1167-1182.

Garcia-Roves, P. M., Osler, M. E., Holmström, M. H. & Zierath, J. R. (2008) Gain-of-function R225Q mutation in AMP-activated protein kinase γ3 subunit increases mitochondrial biogenesis in glycolytic skeletal muscle. *J Biol Chem* **283**, 35724–35734.

Garrido, A., Brandt, M. & Djouder, N. (2016) Transport to Rhebpress activity. *Small GTPases* **7**, 12-15.

Gaude, H., Aznar, N., Delay, a, Bres, a, Buchet-Poyau, K., Caillat, C., Vigouroux, A., Rogon, C., Woods, A., Vanacker, J. M., Hohfeld, J., Perret, C., Meyer, P., Billaud, M. & Forcet, C. (2012) Molecular chaperone complexes with antagonizing activities regulate stability and activity of the tumor suppressor LKB1. *Oncogene* **31**, 1582–1591.

Giariello, F. M. & Trimbath, J. D. (2006) Peutz-Jeghers syndrome and management recommendations. *Clin Gastroeneter Hepatol* **4**, 408-415.

Giege, P., Sweetlove, L. J., Cognat, V. & Leaver, C. J. (2005) Coordination of nuclear and mitochondrial genome expression during mitochondrial biogenesis in *Arabidopsis*. *Plant Cell* **17,** 1497-1512.

Goldstein, B., & Macara, I. G. (2007) The PAR proteins: fundamental players in animal cell polarization. *Developmental Cell* **13**, 609–622.

Gloerich, M., ten Klooster, J.P., Vliem, M.J., Koorman, T., Zwartkruis, F.J., Clevers, H. & Bos, J.L. (2012) Rap2A links intestinal cell polarity to brush border formation. *Nat Cell Biol* **14**, 793–801.

Goldberg, J. M., Manning, G., Liu, A., Fey, P., Pilcher, K. E., Xu, Y., & Smith, J. L. (2006) The dictyostelium kinome--analysis of the protein kinases from a simple model organism. *PLoS Gen* **2**, e38.

Goto, Y., Nonaka, I. & Horai, S. (1990) A mutation in the tRNA(Leu)(UUR) gene associated with the MELAS subgroup of mitochondrial encephalomyopathies. *Nat* **348**, 651-653.

Goransson, O., McBride, A., Hawley, S. A., Ross, F. A., Shpiro, N., Foretz, M., Viollet, B., Hardie, D. G. & Sakamoto, K. (2007) Mechanism of action of A-769662, a valuable tool for activation of AMP-activated protein kinase. *J Biol Chem* **282**, 32549–32560.

Gowans, G. J., Hawley, S. A., Ross, F. A. & Hardie, D. G. (2013) AMP is a true physiological regulator of AMP-activated protein kinase, both by allosteric activation and by enhancing net phosphorylation. *Cell Metab* **18**, 556–566.

Grady, J. P., Campbell, G., Ratnaike, T., Blakely, E. L., Falkous, G., Nesbitt, V., Schaefer, A. M., McNally, R. J., Gorman, G. S., Taylor, R. W., Turnbull, D. M. &

McFarland, R. (2014) Disease progression in patients with single, large-scale mitochondrial DNA deletions. *Brain* **137**, 323–334.

Gray, M. W. (2012) Mitochondrial evolution. *Cold Spring Harbor Perspectives in Biology* **4**, a011403.

Greaves, L. C., Reeve, A. K., Taylor, R.W. & Turnbull, D. M. (2012) Mitochondrial DNA and disease. *J Pathol* **226**, 274–286.

Greaves, L. C., Yu-Wai-Man, P., Blakely, E. L., Krishnan, K. J., Beadle, N. E., Kerin, J., Barron, M. J., Griffiths, P. G., Dickinson, A. J., Turnbull, D. M. & Taylor, R. W. (2010) Mitochondrial DNA Defects and Selective Extraocular Muscle Involvement in CPEO. *Invest. Ophthalmol Vis Sci* **51**, 3340-3346.

Greer, E. L., Oskoui, P. R., Banko, M. R., Maniar, J. M., Gygi, M. P., Gygi, S. P. & Brunet, A. (2007) The energy sensor AMP-activated protein kinase directly regulates the mammalian FOXO3 transcription factor. *J Biol Chem* **282**, 30107–30119.

Gu, X., Yan, Y., Novick, S. J., Kovach, A., Goswami, D., Ke, J., Tan, M. H. E., Wang, L., Li, X., de Waart, P. W., Webb, M. R., Griffin, P. R., Xu, H. E. & Melcher, K. (2017) Deconvoluting AMP-activated protein kinase (AMPK) adenine nucleotide binding and sensing. *J Biol Chem* **292**, 12653-12666.

Guertin, D. A. & Sabatini, D. M. (2007) Defining the role of mTOR in cancer. *Cancer Cell* **12**, 9–22.

Guo, C., Sun, L., Chen, X. & Zhang, D. (2013) Oxidative stress, mitochondrial damage and neurodegenerative diseases. *Neural Regen Res* **8**, 2003-2014.

Gurgel-Giannetti, J., Oliveira, G., Filho, G. B., Martins, P., Vainzof, M., & Hirano, M. (2013) Mitochondrial Cardioencephalomyopathy Due to a Novel *SCO2*Mutation in a Brazilian Patient. *JAMA Neurol* **70**, 258–261.

Gwinn, D. M., Shackelford, D. B., Egan, D. F., Mihaylova, M. M., Mery, A., Vasquez, D. S., Turk, B. E. & Shaw, R. J. (2008) AMPK phosphorylation of raptor mediates a metabolic checkpoint. *Mol Cell* **30**, 214-226.

Haas, R. H., Parikh, S., Falk, M. J., Saneto, R. P., Wolf, N. I., Darin, N., Wong, L., Cohen, B. H. & Naviaux, R. K. (2008) The In-Depth Evaluation of Suspected Mitochondrial Disease: The Mitochondrial Medicine Society's Committee on Diagnosis. *Mol Genet and Metab* **94**, 16–37.

Haddock, B. A. & Hamilton, W. A. (1977) *Microbial Energetics 27th SYP,* Soc Gen Microbiol, Cambridge.

Haddock, B. A. & Jones, C. W. (1977) Bacterial respiration. *Bacteriol Rev* **41**, 47-99.

Hahn-Windgassen, A., Nogueira, V., Chen, C.-C., Skeen, J. E., Sonenberg, N. & Hay, N. (2005) Akt activates the mammalian target of rapamycin by regulating cellular ATP level and AMPK activity. *J Biol Chem* **280**, 32081–32089.

Han, D., Li, S.-J., Zhu, Y.-T., Liu, L. & Li, M.-X. (2013) LKB1/AMPK/mTOR signaling pathway in non-small-cell lung cancer. *Asian Pac J Cancer Prev* **14**, 4033–4039.

Handschin, C. & Spiegelman, B. M. (2011) PGC-1 coactivators and the regulation of skeletal muscle fiber-type determination. *Cell Metab* **13**, 351–352.

Hanks, S. K. & Hunter, T. (1995) Protein kinases 6. The eukaryotic protein kinase superfamily: kinase (catalytic) domain structure and classification. *FASEB J* **9**, 576-596.

Hardie, D. G. (2011) AMP-activated protein kinase: an energy sensor that regulates all aspects of cell function. *Genes Dev* **25**, 1895 – 1908.

Hardie, D. G. (2014) AMPK – sensing energy while talking to other signaling pathways. *Cell Metab* **20**, 939–952.

Hardie, D. G. & Alessi, D. R. (2013) LKB1 and AMPK and the cancer-metabolism link - ten years after. *BMC Biol* **11**, 36.

Hardie D. G. & Hawley S. A. (2001) AMP-activated protein kinase: the energy charge hypothesis revisited. *Bioessays* **23**, 1112–1119.

Hardie, D. G., Carling, D. & Gamblin, S. J. (2011) AMP-activated protein kinase: also regulated by ADP? *Trends Biochem Sci* **36**, 470–477.

Hardie, D. G., Ross, F. A. & Hawley, S. A. (2012) AMPK: a nutrient and energy sensor that maintains energy homeostasis. *Nat Rev Mol Cell Biol* **13**, 251-262.

Hasenour, C. M., Ridley, D. E., Hughey, C. C., James, F. D., Donahue, E. P., Shearer, J., Viollet, B., Foretz, M. & Wasserman, D. H. (2014) 5-Aminoimidazole-4-carboxamide-1-β-d-ribofuranoside (AICAR) Effect on Glucose Production, but Not Energy Metabolism, Is Independent of Hepatic AMPK *in Vivo*. *J Biol Chem* **289**, 5950–5959.

Hashimoto, T. & Shibasaki, F. (2015) Hypoxia-inducible factor as an angiogenic master switch. *Front Pediatr* **3**, 33.

Hawking, Z. L. (2016) Alzheimer's disease: the role of mitochondrial dysfunction and potential new therapies. *Biosci Horizons: Int J Student Res* **9**.

Hawley, S. A., Boudeau, J., Reid, J. L., Mustard, K. J., Udd, L., Mäkelä, T. P., Alessi, T. P. & Hardie, D. G. (2003) Complexes between the LKB1 tumor suppressor, STRAD alpha/beta and MO25 alpha/beta are upstream kinases in the AMP-activated protein kinase cascade. *J Biol* **2**, 28.

Hawley, S. A., Davison, M., Woods, A., Davies, S. P., Beri, R. K, Carling, D. & Hardie, D. G. (1996) Characterization of the AMP-activated protein kinase kinase from rat liver and identification of threonine 172 as the major site at which it phosphorylates AMP-activated protein kinase. *J Biol Chem* **271**, 27879–27887.

Hawley, S. A., Fullerton, M. D., Ross, F. A., Schertzer, J. D., Chevtzoff, C., Walker, K. J., Peggie, M. W., Zibrova, D., Green, K. A., Mustard, K. J., Kemp, B. E. and other authors (2012) The ancient drug salicylate directly activates AMP-activated protein kinase. *Sci* **336**, 918–922.

Hawley, S. A., Pan, D. A., Mustard, K. J., Ross, L., Bain, J., Edelman, A. M., Frenguelli, B. G. & Hardie, D. G. (2005) Calmodulin-dependent protein kinase kinase-beta is an alternative upstream kinase for AMP-activated protein kinase. *Cell Metab* **2**, 9–19.

Hawley, S. A., Ross, F. A., Chevtzoff, C., Green, K. A., Evans, A., Fogarty, S., Towler, M. C., Brown, L. J., Ogunbayo, O. A., Evans, A. M. & Hardie, D. G. (2010) Use of cells expressing gamma subunit variants to identify diverse mechanisms of AMPK activation. *Cell Metab* **11**, 554–565.

Haylett, W., Swart, C., vanderWesthuizen, F., vanDyk, H., vanderMerwe, L., vanderMerwe, C., Loos, B., Carr, J., Kinnear, C. & Bardien, S. (2016) Altered mitochondrial respiration and other features of mitochondrial function in Parkin-mutant fibroblasts from Parkinson's disease patients. *Parkinsons Dis* **2016**, 1819209.

Helm, M., Florentz, C., Chomyn, A. & Attardi, G. (1999) Search for differences in post-transcriptional modification patterns of mitochondrial DNA-encoded wild-type and mutant human tRNALys and tRNALeu(UUR). *Nucleic Acids Res* **27**, 756–763.

Hemminki, A., Markie, D., Tomlinson, I., Avizienyte, E., Roth, S., Loukola, A., Bignell, G., Warren, W., Aminoff, M., Hoglund, P., Jarvinen, H., Kristo, P., Pelin, K. and other authors (1998) A serine/threonine kinase gene defective in Peutz-Jeghers syndrome. *Nat* **391**, 184–187.

Hemminki, A. (1999) The molecular basis and clinical aspects of Peutz-Jeghers syndrome. *Cell Mol Life Sci* **55**, 735-750.

Herrmann, J. L., Byekova, Y., Elmets, C. A. & Athar, M. (2011) The Role of LKB1 in the Pathogenesis of Skin and Other Epithelial Cancers. *Cancer Lett* **306**, 1-9.

Herrero-Martín, G., Hoyer-Hansen, M., Garcia-Garcia, C., Fumarola, C., Farkas, T., Lopez-Rivas, A. & Jaattela, M. (2009) TAK1 activates AMPK-dependent cytoprotective autophagy in TRAIL-treated epithelial cells. *EMBO J* **28**, 677-685.

Herzig, S. & Shaw, R. J. (2018) AMPK: guardian of metabolism and mitochondrial homeostasis. *Nat rev. Mol Cell Bio* **19**, 121-135.

Hezel, A. F., Gurumurthy, S., Granot, Z., Swisa, A., Chu, G. C., Bailey, G., Dor, Y., Bardeesy, N. & Depinho, R. A. (2008) Pancreatic LKB1 deletion leads to acinar polarity defects and cystic neoplasms. *Mol Cell Biol* **28**, 2414–2425.

Hill, M. J., Suzuki, S., Segars, J. H. & Kino, T. (2015) CRTC2 Is a Coactivator of GR and Couples GR and CREB in the Regulation of Hepatic Gluconeogenesis. *Mol endocrin (Baltimore, Md.)* **30**, 104-117.

Hofhaus, G., Johns, D. R., Hurko, O., Attardi, G. & Chomyn, A. (1996) Respiration and Growth Defects in Transmitochondrial Cell Lines Carrying the 11778 Mutation Associated with Leber's Hereditary Optic Neuropathy. *J Bio Chem* **271**, 13155-13161

Hofmann, C., Shepelev, M. & Chernoff, J. (2004) The genetics of Pak. *J Cell Sci* **117**, 4343-4354.

Holt, I. J., Harding, A.E., Petty, R. K. H., Morgan-Hughes, J. A. (1990) A new mitochondrial disease associated with mitochondrial DNA heteroplasmy. *Am J Hum* Genet **46**, 428–433.

Holz, M. K., Ballif, B. A., Gygi, S. P. & Blenis, J. (2005) mTOR and S6K1 mediate assembly of the translation preinitiation complex through dynamic protein interchange and ordered phosphorylation events. *Cell* **123**, 569–580.

Hong, S. P., Leiper, F. C., Woods, A., Carling, D. & Carlson, M. (2003) Activation of yeast Snf1 and mammalian AMP-activated protein kinase by upstream kinases. *Proc Natl Acad Sci USA* **100**, 8839–8843.

Horike, N., Sakoda, H., Kushiyama, A., Ono, H., Fujishiro, M., Kamata, H., Nishiyama, K., Uchijima, Y., Kurihara, Y., Kurihara, H. & Asano, T. (2008) AMP-activated protein kinase activation increases phosphorylation of glycogen synthase kinase 3beta and thereby reduces cAMP-responsive element transcriptional activity and phosphoenolpyruvate carboxykinase C gene expression in the liver. *J Biol Chem* **283**, 33902–33910.

Hou, X., Xu, S., Maitland-Toolan, K. A., Sato, K., Jiang, B., Ido, Y., Lan, F., Walsh, K., Weirzbicki, M., Verbeuren, T. J., Cohen, R. A. & Zang, M. (2008). SIRT1 regulates hepatocyte lipid metabolism through activating AMP-activated protein kinase. *J Biol Chem* **283**, 20015–20026.

Houde, V. P., Ritorto, M. S., Gourlay, R., Varghese, J., Davies, P., Shpiro, N., Sakamoto, K. & Alessi, D. R. (2014) Investigation of LKB1 Ser431 phosphorylation and Cys433 farnesylation using mouse knockin analysis reveals an unexpected role of prenylation in regulating AMPK activity. *Biochem J* **458**, 41–56.

Huang, J. & Manning, B. D. (2008) The TSC1-TSC2 complex: a molecular switchboard controlling cell growth. *Biochem J* **412**, 179–190.

Huang, S. & Czech, M. P. (2007) The GLUT4 Clucose Transporter. *Cell Metab* **5**, 237-252.

Huang, X., Wullschleger, S., Shpiro, N., McGuire, V. A., Sakamoto, K., Woods, Y. L., McBurnie, W., Fleming, S. & Alessi, D. R. (2008). Important role of the LKB1-AMPK pathway in suppressing tumorigenesis in PTEN-deficient mice. *Biochem J* **412**, 211–221.

Hung, V., Zou, P., Rhee, H. W., Udeshi, N. D., Cracan, V., Svinkina, T., Carr, S. A., Mootha, V. K. & Ting, A. Y. (2014) Proteomic mapping of the human mitochondrial intermembrane space in live cells via ratiometric APEX tagging. *Mol Cell* **55**, 332-341.

Hurley, R. L., Anderson, K. A., Franzone, J. M., Kemp, B. E., Means, A. R., Witters, L. A. (2005) The Ca2+/calmoldulin-dependent protein kinase kinases are AMP-activated protein kinase kinases. *J Biol Chem* **280**, 29060–29066.

Hwang, J., Lee, H. W., Kim, S. J. & Chung., K. W. (2008) MELAS syndrome family harboring two mutations in mitochondrial genome. *Experimental & Molecular Medicine* **40**, 354-360.

Ienco, E. C., Orsucci, D., Montano, V., Ferrari, E., Petrozzi, L., Cheli, M., LoGerfo, A., Simoncini, C., Sicilano, G. & Mancuso, M. (2016) NEWS and VIEWS: mitochondrial encephalomyopathies. *Acta Myol* **35**, 135–140.

Ikenoue, T., Inoki, K., Yang, Q., Zhou, X. & Guan, K. L. (2008) Essential function of TORC2 in PKC and Akt turn motif phosphorylation, maturation and signalling. *EMBO J* **27**, 1919–1931.

Inazu, Y., Chae, S.C. & Maeda, Y. (1999) Transient expression of a mitochondrial gene cluster including rps4 is essential for the phase-shift of *Dictyostelium* cells from growth to differentiation. *Dev Genet* **25**, 339-352.

Inoki, K., Zhu, T. & Guan, K.-L. (2003) TSC2 mediates cellular energy response to control cell growth and survival. *Cell* **115**, 577–590.

Jain-Ghai, S., Cameron, J. M., Al Maawali, A., Blaser, S., MacKay, N., Robinson, B. & Raiman, J. (2013) Complex II deficiency—a case report and review of the literature. *Am J Med Genet A* **161A,** 285-294.

Jäger, S., Handschin, C., St.-Pierre, J. & Spiegelman, B. M. (2007) AMP-activated protein kinase (AMPK) action in skeletal muscle via direct phosphorylation of PGC-1α. *Proc Natl Acad Sci USA* **104**, 12017–12022.

Jansen, M., Ten Klooster, J. P., Offerhaus, G. J. & Clevers, H. (2009) LKB1 and AMPK family signaling: the intimate link between cell polarity and energy metabolism. *Physiolog Rev* **89**, 777–798.

Jeghers, H. (1944) Pigmentation of the skin. *N Engl J Med* **231**, 88-100.

Jenne, D. E., Reimann, H., Nezu, J., Friedel, W., Loff, S., Jeschke, R., Muller, O., Back, W. & Zimmer, M. (1998) Peutz-Jeghers syndrome is caused by mutations in a novel serine threonine kinase. *Nat Genet* **18**, 38-43.

Jensen, T. E., Rose, A. J., Jørgensen, S. B., Brandt, N., Schjerling, P., Wojtaszewski, J. F. P. & Richter, E. A. (2007) Possible CaMKK-dependent regulation of AMPK phosphorylation and glucose uptake at the onset of mild tetanic skeletal muscle contraction. *Am J Physiol Endocrinol Metab* **292**, E1308-E1317.

Jeon, S.-M., Chandel, N. S. & Hay, N. (2012) AMPK regulates NADPH homeostasis to promote tumour cell survival during energy stress. *Nat* **485**, 661–665.

Jeong, H., Huh, H. J., Youn, J., Kim, J. S., Cho, J. W. & Ki, C. S. (2014) Ataxia-telangiectasia with novel splicing mutations in the ATM gene. *Annals lab Med* **34**, 80-84.

Jeppesen, J., Maarbjerg, S. J., Jordy, A. B., Fritzen, A. M., Pehmøller, C., Sylow, L., Serup, A. K., Jessen, N., Thorsen, K., Prats, C., Kiens, B. & other authors (2013) LKB1 Regulates Lipid Oxidation During Exercise Independently of AMPK. *Diabetes* **62**, 1490–1499.

Ji, H., Ramsey, M. R., Hayes, D. N., Fan, C., McNamara, K., Kozlowski, P., Torrice, C., Wu, M. C., Shimamura, T., Perera, S. A., Liang, M. C., Cai, D., Naumov, G. N., Bao, L., Contreras, C. M., Li, D., Chen, L., Krishnamurthy, J., Koivunen, J., Chirieac, L. R., Padera, R. F., Bronson, R. T., Lindeman, N. I., Christiani, D. C., Lin, X., Shapiro, G. I., Janne, P. A., Johnson, B. E., Meyerson, M., Kwiatkowski, D. J., Castrillon, D. H., Bardeesy, N., Sharpless, N. E. & Wong, K. K. (2007) LKB1 modulates lung cancer differentiation and metastasis. *Nat* **448**, 807-810.

Jiang, S.-J., Dong, H., Li, J.-B., Xu, L.-J., Zou, X., Wang, K.-F., Lu, F.-E. & Yi, P. (2015) Berberine inhibits hepatic gluconeogenesis *via* the LKB1-AMPK-TORC2 signaling pathway in streptozotocin-induced diabetic rats. *World J Gastroenterology* **21**, 7777–7785.

Jonckheere, A.I., Smeitink, J.A. & Rodenburg, R.J. (2011) Mitochondrial ATP synthase: architecture, function and pathology. *J Inherit Metab Dis* **35**, 211-225.

Jørgensen, S. B., Wojtaszewski, J. F., Viollet, B., Andreelli, F., Birk, J. B., Hellsten, Y., Schjerling, P., Vaulont, S., Neufer, P. D., Richter, E. A. & Pilegaard, H. (2005) Effects of alpha-AMPK knockout on exercise-induced gene activation in mouse skeletal muscle. *FASEB J* **19**, 1146-1148.

Jornayvaz, F. R. & Shulman, G. I. (2010) Regulation of mitochondrial biogenesis. *Essays Biochem* **47**, 69–84.

Jung, C. H., Ro, S. H., Cao, J., Otto, N. M. & Kim, D. H. (2010) mTOR regulation of autophagy. *FEBS Lett* **584**, 1287–1295.

Kao, S., Chao, H. T. & Wei, Y. H. (1995) Mitochondrial deoxyribonucleic acid 4977-bp deletion is associated with diminished fertility and motility of human sperm. *Biol Reprod* **52**, 729-736.

Karos, M. & Fischer, R. (1999) Molecular characterization of HymA, an evolutionarily highly conserved and highly expressed protein of Aspergillus nidulans. *Mol Gen Genet* **260**, 510–521.

Karuman, P., Gozani, O., Odze, R. D., Zhou, X. C., Zhu, H., Shaw, R., Brien, T. P., Bozzuto, C. D., Ooi, D., Cantley, L. C. & Yuan, J. (2001) The Peutz-Jegher Gene Product LKB1 Is a Mediator of p53-Dependent Cell Death. *Mol Cell* **7**, 1307–1319.

Kazgan, N., Williams, T., Forsberg, L. J. & Brenman, J. E. (2010) Identification of a nuclear export signal in the catalytic subunit of AMP-activated protein kinase. *Mol Cell Biol* **21**, 3433-3442.

Kelly, D. P. & Strauss, A. W. (1994) Inherited cardiomyopathies. *N Engl J Med* **330**, 913-919.

Kemp, B. E., Oakhill, J. S. & Scott, J. W. (2007) AMPK structure and regulation from three angles. *Structure* **15**, 1161-1163.

Kemphues, K. J., Priess, J. R., Morton, D. G. & Cheng, N. S. (1988) Identification of genes required for cytoplasmic localization in early *C. elegans* embryos. *Cell* **52**, 311-320.

Kirby, D. M., Salemi, R., Sugiana, C., Ohtake, A., Parry, L., Bell, K. M., Kirk., E. P., Boneh, A., Taylor, R. W., Dahl, H. M., Ryan, M. T. & Thorburn, D. R. (2004) NDUFS6 mutations are a novel cause of lethal neonatal mitochondrial complex I deficiency. *J Clin Invest* **114**, 837-845.

Kirino, Y., Yasukawa, T., Ohta, S., Akira, S., Ishihara, K., Watanabe, K. & Suzuki, T. (2004) Codon-specific translational defect caused by a wobble modification deficiency in mutant tRNA from a human mitochondrial disease. *Proc Natl Acad Sci USA* **101**, 15070–15075.

Kishi, M., Pan, Y. A., Crump, J. G. & Sanes, J. R. (2005) Mammalian SAD kinases are required for neuronal polarization. *Sci* **307**, 929–932.

Kiyama, T., Chen, C. K., Wang, S. W., Pan, P., Ju, Z., Wang, J., Takada, S., Klein, W. H. & Mao, C. A. (2018) Essential roles of mitochondrial biogenesis regulator Nrf1 in retinal development and homeostasis. *Mol Neurodegen* **13**, 56.

Koay, A., Rimmer, K. A., Mertens, H. D., Gooley, P. R. & Stapleton, D. (2007) Oligosaccharide recognition and binding to the carbohydrate binding module of AMP-activated protein kinase. *FEBS Lett* **581**, 5055–5059.

Kojima, Y., Miyoshi, H., Clevers, H. C., Oshima, M., Aoki, M. & Taketo, M. M. (2007) Suppression of tubulin polymerization by the LKB1-microtubule-associated protein/microtubule affinity-regulating kinase signaling. *J Biol Chem* **282**, 23532–23540.

Korpelainen, H. (2004) The evolutionary processes of mitochondrial and chloroplast genomes differ from those of nuclear genomes. *Naturewissenschaften* **91**, 505-518.

Korsse, S.E., Peppelenbosch, M. P. & van Veelen, W. (2013) Targeting LKB1 signaling in cancer. *Biochem Biophysic Acta-Rev Cancer* **1835**, 194-210.

Korzeniewski, B. (2000) Regulation of ATP supply in mammalian skeletal muscle during resting state: intensive work transition. *Biophys Chem* **83**, 19–34.

Kotsifas, M., Barth, C., Lay, S. T., De Lozanne, A. & Fisher, P.R. (2002) Chaperonin 60 and mitochondrial disease in *Dictyostelium. J Mus Res Cell Motil* **23**, 839-852.

Kozlov, S. V., Waardenberg, A. J., Engholm-Keller, K., Arthur, J. W., Graham, M. E. & Lavin, M. (2016) Reactive Oxygen Species (ROS)-Activated ATM-Dependent Phosphorylation of Cytoplasmic Substrates Identified by Large-Scale Phosphoproteomics Screen. *Mol Cell Proteomics* **15**, 1032-1047.

Kraytsberg, Y., Kudryavtseva, E., McKee, A. C., Geula, C., Kowall, N. W. & Khrapko, K. (2006) Mitochondrial DNA deletions are abundant and cause functional impairment in aged human substantia nigra neurons. *Nat Genet* **38**, 518-520.

Kühlbrandt W. (2015) Structure and function of mitochondrial membrane protein complexes. *BMC Bio* 13, 89.

Kullmann, L. & Krahn, M. (2018) Controlling the master—upstream regulation of the tumor suppressor LKB1. *Oncogene* **37**, 3045-3057.

Kuo, I. Y. & Ehrlich, B. E. (2015) Signaling in muscle contraction. *Cold Spring Harb Perspect Biol* **7**, a006023.

Kurogouchi, F., Oguchi, T., Mawatari, E., Yamaura, S., Hora, K., Takei, M., Sekjima, Y., Ikeda, S. & Kiyosawa, K. (1998) A case of mitochondrial cytopathy with a typical point mutation MELAS, presenting with severe focal glomerulosclerosis as main clinical manifestations. *Am J Nephrol* **18**, 551-556.

Kurth-Kraczek, E. J., Hirshman, M. F., Goodyear, L. J. & Winder, W. W. (1999) 5' AMP- activated protein kinase activation causes GLUT4 translocation in skeletal muscle. *Diabetes* **48**, 1667–1671.

Laderoute, K. R., Amin, K., Calaoagan, J. M., Knapp, M., Le, T., Orduna, J., Foretz, M. & Viollet, B. (2006) 5'-AMP-activated protein kinase (AMPK) is induced by low-oxygen and glucose deprivation conditions found in solid-tumor microenvironments. *Mol Cell Biol* **26**, 5336–5347.

Lan, F., Cacicedo, J. M., Ruderman, N., & Ido, Y. (2008) SIRT1 modulation of the acetylation status, cytosolic localization, and activity of LKB1. Possible role in AMP-activated protein kinase activation. *J Biol Chem* **283**, 27628–27635.

Lang, B. F., Burger, G., O'Kelly, C. J., Cedergren, R., Golding, G. B., Lemieux, C., Sankoff, D., Turmel, M. & Gray, M. W. (1997) An ancestral mitochondrial DNA resembling a eubacterial genome in miniature. *Nat* **387**, 493–497.

Lantier, L., Fentz, J., Mounier, R., Leclerc, J., Treebak., J. T., Pehmøller, C., Sanz, N., Sakakibara, L., Saint-Armand, E., Viollet, B. & other authors (2014) AMPK controls exercise endurance, mitochondrial oxidative capacity, and skeletal muscle integrity. *FASEB J* **28**, 3211–3224.

Launonen, V. (2005) Mutations in the human LKB1/STK11 gene. *Hum Mutat* **26**, 291-297.

Le, P., Fisher, P. R., & Barth, C. (2009) Transcription of the *Dictyostelium discoideum* mitochondrial genome occurs from a single initiation site. *RNA* **15**, 2321-2330.

Leclerc, I. & Rutter, G. A. (2004) AMP-Activated Protein Kinase: A New Beta-Cell Glucose Sensor? Regulation by Amino Acids and Calcium Ions. *Diabetes* **53**, S67-S74.

Lee, I. C., El-Hattab, A. W., Wang, J., Li, F. Y., Weng, S.W. Craigen, W.J. & other authors (2012) SURF1-associated Leigh syndrome: a case series and novel mutations. *Hum Mutat* **33**, 1192-1200.

Lee, J. H., Koh, H., Kim, M., Kim, Y., Lee, S. Y., Karess, R. E., Lee, S. H., Shong, M., Kim, J. M., Kim, J. & Chung, J. (2007) Energy-dependent regulation of cell structure by AMP-activated protein kinase. *Nat* **447**, 1017–1020.

Lee, J. H., Giordano, S. & Zhang, J. (2012) Autophagy, mitochondria and oxidative stress: cross-talk and redox signaling. *Biochem* **441**, 523–540.

Lee, M.-J., Feliers, D., Sataranatarajan, K., Mariappan, M. M., Li, M., Barnes, J. L., Choudhury, C. G. & Kasinath, B. S. (2010) Resveratrol ameliorates high glucose-induced protein synthesis in glomerular epithelial cells. *Cell Signalling* **22**, 65–70.

Lee, Y. G., Lee, S. W., Sin, H. S., Kim, E. J. & Um, S. J. (2009) Kinase activity-independent suppression of p73alpha by AMP-activated kinase alpha (AMPKalpha). *Oncogene* **28**, 1040 – 1052.

Lehman, J. J., Barger, P. M., Kovacs, A., Saffitz, J. E., Medeiros, D. M. & Kelly, D. P. (2000) Peroxisome proliferator–activated receptor g coactivator-1 promotes cardiac mitochondrial biogenesis. *J Clin Investig* **106**, 847 – 856.

Lehman, J. J. & Kelly, D. P. (2002) Transcriptional activation of energy metabolic switches in the developing and hypertrophied heart. *Clin Exp Pharmacol Physiol* **29**, 339-345.

Leonard, J. V. & Schapira, A. H. (2000) Mitochondrial respiratory chain disorders I: mitochondrial DNA defects. *Lancet* **355**, 299-304.

Letellier, T., Malgat, M., and Mazat, J. P. (1993) Control of oxidative phosphorylation in rat muscle mitochondria: implications for mitochondrial myopathies. *Biochem Biophys Acta* **1141**, 58–64.

Li, X., Wang, L., Zhou, X. E., Ke, J., de Waal, P. W., Gu, X., Tan, M. H. E., Wang, D., Wu, D., Xu, H. E. & Melcher, K. (2015) Structural basis of AMPK regulation by adenine nucleotides and glycogen. *Cell Res* **25**, 50–66.

Li, Y., Xu, S., Mihaylova, M. M., Zheng, B., Hou, X., Jiang, B., Park, O., Luo, Z., Lefai, E., Shyy, J. Y. & other authors (2011) AMPK phosphorylates and inhibits SREBP activity to attenuate hepatic steatosis and atherosclerosis in diet-induced insulin-resistant mice. *Cell Metab* **13**, 376–388.

Liang, J., Shao, S. H., Xu, Z. X., Hennessy, B., Ding, Z., Larrea, M., Kondo, S., Dumont, D. J., Gutterman, J. U., Walker, C. L., Slingerland, J. M. & Mills, G. B. (2007) The energy sensing LKB1-AMPK pathway regulates p27(kip1) phosphorylation mediating the decision to enter autophagy or apoptosis. *Nat Cell Biol* **9**, 218–224.

Lim, H. W., Lim, H. Y. & Wong, K. P. (2009) Uncoupling of oxidative phosphorylation by curcumin: implication of its cellular mechanism of action. *Biochem Biophys Res Commun* **389**, 187-192.

Lim, M. A., Selak, M. A., Xiang, Z., Krainc, D., Neve, R. L., Kraemer, B. C.,

Watts, J. L. & Kalb, R. G. (2012) Reduced activity of AMP-activated protein kinase protects against genetic models of motor neuron disease**.** *Neurosci* **32**, 1123-1141.

Lin, J., Wu, H., Tarr, P. T., Zhang, C. Y., Wu, Z., Boss, O., Michael, L. F., Puigserver, P., Isotani, E., Olson, E.N., Lowell, B. B., Bassel-Duby, R. & Spiegelman, B. M. (2002) Transcriptional co-activator PGC-1α drives the formation of slow-twitch muscle fibres. *Nat* **418**, 797–801.

Linher-Melville, K., Zantinge, S., Sanli, T., Gerstein, H., Tsakiridis, T. & Singh, G. (2011) Establishing a relationship between prolactin and altered fatty acid β-oxidation via carnitine palmitoyl transferase 1 in breast cancer cells. *BMC Cancer* **11**, 56.

Lipmann, F. (1941) Metabolic generation and utilization of phosphate bond energy. *Adv Enzym Rel Areas Mol Bio* **1**, 99-162.

Lister, R., Hulett, J. M., Lithgow, T. & Whelan, J. (2005) Protein import into mitochondria: origins and functions today. *Mol Memb Biol* **22**, 87-100.

Liu, L., Siu, F.-M., Che, C.-M., Xu, A. & Wang, Y. (2012) Akt blocks the tumor suppressor activity of LKB1 by promoting phosphorylation-dependent nuclear retention through 14-3-3 proteins. *Am J Transl Res* **4**, 175-186.

Liu, Y., Lacal, J., Firtel, R. A. & Kortholt, A. (2016) Connecting G protein signaling to chemoattractant- mediated cell polarity and cytoskeletal reorganization. *Small GTPases* **85**, 1–5.

Lizcano, J. M., Göransson, O., Toth, R., Deak, M., Morrice, N. A., Boudeau, J., Hawley, S. A., Udd, L., Makela, T. P., Hardie, D. G. & Alessi, D. R. (2004) LKB1 is a master kinase that activates 13 kinases of the AMPK subfamily, including MARK/PAR-1. *EMBO J* **23**, 833–843.

Long, Y. C. & Zierath, J. R. (2006) AMP-activated protein kinase signaling in metabolic regulation. *J Clin Invest* **116**, 1776–1783.

Lopez-Lopez, C., Dietrich, M. O., Metzger, F., Loetscher, H., Torres-Aleman, I. (2007) Disturbed Cross Talk between Insulin-Like Growth Factor I and AMP-Activated Protein Kinase as a Possible Cause of Vascular Dysfunction in the Amyloid Precursor Protein/Presenilin 2 Mouse Model of Alzheimer's Disease**.** *J. Neurosci* **27**, 824-831.

Lott, M. T., Leipzig, J. N., Derbeneva, O., Xie, H. M., Chalkia, D., Sarmady, M., Procaccio, V. & Wallace, D. C. (2013) mtDNA variation and analysis using Mitomap

and Mitomaster. *Curr Protoc Bioinformatics* **44**: 1.23.21–1.23.26.

Luukko K., Ylikorkala A., Tiainen M. & Makela T.P. (1999) Expression of *LKB1* and *PTEN* tumor suppressor genes during mouse embryonic development. *Mech Dev* **83**, 187–190.

Ma, L., Niknejad, N., Gorn-Hondermann, I., Dayekh, K. & Dimitroulakos, J. (2012) Lovastatin Induces Multiple Stress Pathways Including LKB1/AMPK Activation That Regulate Its Cytotoxic Effects in Squamous Cell Carcinoma Cells. PLoS ONE 7(9): e46055.

Macara, I. G. (2004) Parsing the polarity code. *Mol Cell Biol* **5**, 220–231.

Maceluch, J. A. & Niedziela, M. (2006) The clinical diagnosis and molecular genetics of Kearns–Sayre syndrome: a complex mitochondrial encephalomyopathy. *Pediatr Endocrinol Rev* **4**, 117–137.

Machovic, M. & Janecek, S. (2006) Starch-binding domains in the post-genome era. *Cell Mol Life Sci* **63**, 2710-2724.

Man, P. Y., Turnbull, D. M. & Chinnery. P. F. (2002) Leber hereditary optic neuropathy. *J Med Genet* **39**, 162–169.

Mancuso, M., Orsucci, D., Angelini, C., Bertini, E., Carelli, V., Comi, G. P., Minetti, C, Moggio, M., Mongini, T., Servidei, S., Tonin, P., Toscano, A., Uziel, G. & other authors (2013) Phenotypic heterogeneity of the 8344A>G mtDNA "MERRF" mutation. *Neurol* **80**, 2049–2054.

Manfredi, G., Schon, E. A., Bonilla, E., Moraes, C. T., Shanske, S. & DiMauro, S. (1996) Identification of a mutation in the mitochondrial tRNA(Cys) gene associated with mitochondrial encephalopathy. *Hum Mutat* **7**, 158-163.

Manfredi, G., **Vu, T., Bonilla, E., Schon, E. A., DiMauro, S., Arnaudo, E., Zhang, L., Rowland, L. P. & Hirano, M. (1997)** Association of myopathy with large-scale mitochondrial DNA duplications and deletions: which is pathogenic? *Ann Neurol* **2**, 180–188.

Maniak M. (2003) Fusion and fission events in the endocytic pathway of *Dictyostelium*. *Traffic* **4**, 1-5.

Marignani, P. A., Kanai, F. & Carpenter, C. L. (2001) LKB1 associates with Brg1 and is necessary for Brg1-induced growth arrest. *J Biol Chem* **276**, 32415–32418.

Markham, A., Bains, R., Franklin, P. & Spedding, M. (2014) Changes in mitochondrial function are pivotal in neurodegenerative and psychiatric disorders: how important is BDNF? *Bri Jour Pharmacol* **171**, 2206-2229.

Martin, L. J. (2010) Mitochondrial and cell death mechanisms in neurodegenerative diseases. *Pharmaceut (Basel)* **3**, 839-915.

Martin, S. G. & St Johnston, D. (2003) A role for Drosophila LKB1 in anterior–posterior axis formation and epithelial polarity. *Nat* **421**, 379–384.

Martin-Belmonte, F. & Perez-Moreno, M. (2012) Epithelial cell polarity, stem cells and cancer. *Nat Rev Cancer* **12**, 23–38.

Martinez-Vicente, M. (2017) Neuronal mitophagy in neurodegenerative diseases. *Frontiers Mol Neurosci* **10**, 64.

Massa, V., Fernandez-Vizarra, E., Alshahwan, S., Bakhsh, E., Goffrini, P., Ferrero, I., Mereghetti, P., D'Adamo, P., Gasparini, P. & Zeviani, M. (2008) Severe infantile encephalomyopathy caused by a mutation in *COX6B1*, a nucleus-encoded subunit of cytochrome c oxidase. *Am J Hum Genet* **82**, 1281-1289.

Maselli, A., Laevsky, G. & Knecht, D.A. (2002) Kinetics of binding, uptake and degradation of live fluorescent (DsRed) bacteria by *Dictyostelium discoideum Microbiol* **148**, 413-420.

Matsuoka, S., Ballif, B. A., Smogorzewska, A., McDonald, E. R., Hurov, K. E., Luo, J., Bakalarski, C. E., Zhao, Z., Solimini, N., Lerentha, Y., Shiloh, Y., Gygi, S. P. & Elledge, S. J. (2007) ATM and ATR substrate analysis reveals extensive protein networks responsive to DNA damage. *Sci* **316**, 1160-1166.

McBride, A., Ghilagaber, S., Nikolaev, A. & Hardie, D. G. (2009) The glycogen-binding domain on the AMPK beta subunit allows the kinase to act as a glycogen sensor. *Cell Metab* **9**, 23–34.

McInnes, J. (2013) Mitochondrial-associated metabolic disorders: foundations, pathologies and recent progress. *Nutr Metab* **10**, 63.

McKenzie, M., Liolitsa, D. & Hanna, M. G. (2004) Mitochondrial disease: mutations and mechanisms. *Neurochem Res* **29**, 589-600.

Meena, N. P. & Kimmel, A. R. (2016) Biochemical responses to chemically distinct chemoattractants during the growth and development of dictyostelium. *Methods Mol Biol* **1407**, 141–151.

Mehenni, H., Gehrig, C., Nezu, J., Oku, A., Shimane, M., Rossier, C., Guex, N., Blouin, J. L., Scott, H. S. & Antonarakis, S. E. (1998) Loss of LKB1 kinase activity in Peutz–Jeghers syndrome, and evidence for allelic and locus heterogeneity. *Am J Hum Genet* **63**, 1641–1650.

Merrill, G. F., Kurth, E. J., Hardie, D. G., & Winder, W. W. (1997) AICA riboside increases AMP-activated protein kinase, fatty acid oxidation, and glucose uptake in rat muscle. *Am J Physio* **273**, E1107–1112.

Michiels, C., Minet, E., Mottet, D. & Raes, M. (2002) Regulation of gene expression by oxygen: NF-κB and HIF-1, two extremes. *Free Radic Biol Med* **33**, 1231-1242.

Mihaylova, M. M. & Shaw, R. J. (2011) The AMPK signalling pathway coordinates cell growth, autophagy and metabolism. *Nat Cell Biol* **13**, 1016–1023.

Milane, L., Trivedi, M., Singh, A., Talekar, M., & Amiji, M. (2015) Mitochondrial biology, targets, and drug delivery. *J Controlled Release* **207**, 40-58.

Milburn, C. C., Boudeau, J., Deak, M., Alessi, D. R. & van Aalten, D. M. (2004) Crystal structure of MO25 alpha in complex with the C terminus of the pseudo kinase STE20-related adaptor. *Nat Struct Mol Biol* **11**, 193–200.

Miranda, L., Carpentier, S., Platek, A., Hussain, N., Gueuning, M.-A., Vertommen, D., Ozkan, Y., Sid, B., Hue, L., Courtoy, P. J., Rider, M. H. & Horman, S. (2010) AMP-activated protein kinase induces actin cytoskeleton reorganization in epithelial cells. *Biochem Biophys Res Commun* **396**, 656–661.

Mirouse, V. & Billaud, M. (2011) The LKB1/AMPK polarity pathway. *FEBS Lett* **585**, 981–985.

Mishra, P. & Chan, D. C. (2014) Mitochondrial dynamics and inheritance during cell division, development and disease. *Nat Rev Mol Cell Biol* **15**, 634-646.

Miyaki, M., Iijima, T., Hosono, K., Ishii, R., Yasuno, M., Mori, T., Toi, M., Hishima, T., Shitara, N., Tamura, K., Utsunomiya, J., Kobayashi, N., Kuroki, T. & Iwama, T. (2000) Somatic mutations of LKB1 and beta-catenin genes in gastrointestinal polyps from patients with Peutz-Jeghers syndrome. *Cancer Res* **60**, 6311-6313.

Miyamoto, H., Matsushiro, A. & Nozaki, M. (1993) Molecular cloning of a novel mRNA sequence expressed in cleavage stage mouse embryos. *Mol Reprod Dev* **34**, 1–7.

Momcilovic, M., Hong, S. P. & Carlson, M. (2006) Mammalian TAK1 activates Snf1 protein kinase in yeast and phosphorylates AMP-activated protein kinase in vitro. *J Biol Chem* **281**, 25336-25343.

Monica, M. & Auerkari, E. I. (2018) Molecular genetics of Peutz-Jegher syndrome. *Adv Health Sci Res,* **4.**

Moraes, C. T., DiMauro, S., Zeviani, M., Lombes, A., Shanske, S., Miranda, A. F., Nakase, H., Bonilla, E., Werneck, L. C., Servidei, S., Nonaka, I., Koga, Y., Spiro, A. J. and other authors (1989) Mitochondrial DNA deletions in progressive external ophthalmoplegia and Kearns–Sayre syndrome. *New Engl J Med* **320**, 1293–1299.

Morén, A., Raja, E., Heldin, C.-H., & Moustakas, A. (2011) Negative regulation of TGFβ signaling by the kinase LKB1 and the scaffolding protein LIP1. *J Biol Chem* **286**, 341–353.

Morgan-Hughes, J. A., Sweeney, M. G., Cooper, J. M., Hammans, S. R., Brockington, M., Schapira, A. H., Harding, A. E. & Clark, J. B. (1995) Mitochondrial DNA (mtDNA) diseases: correlation of genotype to phenotype. *Biochem Biophys Acta* **1271**, 135-140.

Morgan-Smith, M., Wu, Y., Zhu, X., Pringle, J. & Snider, W. D. (2014) GSK-3 signaling in developing cortical neurons is essential for radial migration and dendritic orientation. *Elife* 1–24.

Mottillo, E. P., Desjardins, E. M., Crane, J. D., Smith, B. K., Green, A. E., Ducommun, S., Henriksen, T. I., Rebalka, I. A., Razi, A., Steinberg, G. R. & other authors (2016) Lack of Adipocyte AMPK Exacerbates Insulin Resistance and Hepatic Steatosis through Brown and Beige Adipose Tissue Function. *Cell Metab* **24**, 118–129.

Mounier, R., Théret, M., Lantier, L., Foretz, M. & Viollet, B. (2015) Expanding roles for AMPK in skeletal muscle plasticity. *Trends Endocrinol Metab* **26**, 275–286.

Nakano, A., & Takashima, S. (2012) LKB1 and AMP-activated protein kinase: regulators of cell polarity. *Genes to Cells*: *Mol Cell Mech* **17**, 737– 747.

Narkar, V. A., Downes, M., Yu, R. T., Embler, E., Wang, Y. X., Banayo, E., Mihaylova, M. M., Nelson, M. C., Zou, Y., Juguilon, H., Kang, H., Shaw, R. &

Evans, R. M. (2008) AMPK and PPARδ agonists are exercise mimetics. *Cell* **134**, 405–415.

Nesbitt, V., Pitceathly, R. D., Turnbull, D. M., Taylor, R. W., Sweeney, M. G., Mudanohwo, E. E., Rahman, S., Hanna, M. G. & McFarland, R. (2013) The UK MRC mitochondrial disease patient cohort study: clinical phenotypes associated with the m.3243A>G mutation--implications for diagnosis and management. *J Neurol Neurosurg Psychiatry* **84**, 936-938.

Nieminen, A. I., Eskelinen, V. M., Haikala, H. M., Tervonen, T. A., Yan, Y., Partanen, J. I. & Klefström, J. (2013) Myc-induced AMPK-phospho p53 pathway activates Bak to sensitize mitochondrial apoptosis. *Proc Natl Acad Sci USA* **110**, E1839 – E1848.

Niyazov, D. M., Kahler, S. G. & Frye, R. E. (2016) Primary Mitochondrial Disease and Secondary Mitochondrial Dysfunction: Importance of Distinction for Diagnosis and Treatment. *Mol Syndromol* **7**, 122-137.

Nony, P., Gaude, H., Rossel, M., Fournier, L., Rouault, J.-P., & Billaud, M. (2003) Stability of the Peutz-Jeghers syndrome kinase LKB1 requires its binding to the molecular chaperones Hsp90/Cdc37. *Oncogene* **22**, 9165–9175.

Nozaki, M., Onishi, Y., Togashi, S. & Miyamoto, H. (1996) Molecular characterization of the Drosophila Mo25 gene, which is conserved among Drosophila, mouse, and yeast. *DNA Cell Biol* **15**, 505–509.

O'Neill H. M., Maarbjerg, S. J., Crane, J.D., Jeppesen, J., Jørgensen, S. B., Schertzer, J. D., Shyroka, O., Kiens, B., van Denderen, B. J., Tarnopolsky. M. A., Kemp, B. E., Richter, E. A., Steinberg, G.R. (2011) AMP-activated protein kinase (AMPK) β1β2 muscle null mice reveal an essential role for AMPK in maintaining mitochondrial content and glucose uptake during exercise. *Proc Natl Acad Sci USA* **108**, 16092–16097.

Oakhill, J. S., Chen, Z. P., Scott, J. W., Steel, R., Castelli, L. A., Ling, N., Macaulay, S. L. & Kemp, B. E. (2010) beta-Subunit myristoylation is the gatekeeper for initiating metabolic stress sensing by AMP-activated protein kinase (AMPK). *Proc Natl Acad Sci USA* **107**, 19237–19241.

Ogawa, S., Yoshino, R., Angata, K., Iwamoto, M., Pi, M., Kuroe, K., Matsuo, K., Morio, T., Urushihara, H., Yanagisawa, K. & Tanaka, Y. (2000) The mitochondrial

DNA of *Dictyostelium discoideum*: complete sequence, gene content and genome organisation. *Mol Gen Genet* **263**, 514-519.

Oshima, T., Ueda, N., Ikeda, K., Abe, K. & Takasaka, T. (1996) Bilateral sensorineural hearing loss associated with the point mutation in mitochondrial genome. *Laryngoscope* **106**, 43-48.

Ossipova, O., Bardeesy, N., DePinho, R. A. & Green, J.B. (2003) LKB1 (XEEK1) regulates Wnt signalling in vertebrate development. *Nat Cell Biol* **5**, 889–894.

Owen, M. R., Doran, E. & Halestrap, A. P. (2000) Evidence that metformin exerts its anti-diabetic effects through inhibition of complex 1 of the mitochondrial respiratory chain. *Biochem J* **348**, 607–614.

Pan, D. (2010) The hippo signaling pathway in development and cancer. *Dev Cell* **19**, 491-505.

Pang, T., Xiong, B., Li, J. Y., Qiu, B. Y., Jin, G. Z., Shen, J. K. & Li, J. (2007) Conserved alpha-helix acts as autoinhibitory sequence in AMP-activated protein kinase alpha subunits. *J Biol Chem* **282**, 495-506.

Papadopoulou, L. C., Sue, C. M., Davidson, M. M., Tanji, K., Nishino, I., Sadlock, J. E., Krishna, S., Walker, W., Selby, J., Glerum, D. M. & other authors (1999) Fatal infantile cardioencephalomyopathy with COX deficiency and mutations in SCO2, a COX assembly gene. *Nat Genet* **23**, 333–337.

Parikh, S., Goldstein, A., Karaa, A., Koenig, M. K., Anselm, I. & Brunel-Guitton, C. (2017) Patient care standards for primary mitochondrial disease: a consensus statement from the Mitochondrial Medicine Society. *Genet Med* **19.**

Parker, S. J., Svensson, R. U., Divakaruni, A. S., Lefebvre, A. E., Murphy, A. N., Shaw, R. J. & Metallo, C. M. (2016) LKB1 promotes metabolic flexibility in response to energy stress. *Metabolic engineering* **43**, 208-217.

Partanen, J. I., Nieminen, A. I., Mäkelä, T. P. & Klefstrom, J. (2007) Suppression of oncogenic properties of c-Myc by LKB1-controlled epithelial organization. *Proc Natl Acad Sci USA* **104**, 14694–14699.

Paul, M. H. & Sperling, E. (1952) Cyclophorase system. XXIII. Correlation of cyclophorase activity and mitochondrial density in striated muscle. *Proc Soc Exp Biol Med* ***79,*** 352-354.

Paumard, P., Vaillier, J., Coulary, B., Schaeffer, J., Soubannier, V., Mueller, D. M., Brèthes, D., di Rago, J.-P. & Velours, J. **(2002)** The ATP synthase is involved in generating mitochondrial cristae morphology. *EMBO J* **21**, 221–230.

Payne, B. A. I., Wilson, I. J., Yu-Wai-Man, P., Coxhead, J., Deehan, D., Horvath, R., … Chinnery, P. F. (2013) Universal heteroplasmy of human mitochondrial DNA. *Human Mol Genet* **22**, 384–390.

Peutz J. L. A. (1921) Very remarkable case of familial polyposis of mucous membrane of intestinal tract and nasopharynx accompanied by peculiar pigmentation of skin and mucous membrane. *Ned Maandschr Verlosk Geneesk* **10**,134–146.

Pfeiffer, T., Schuster, S. & Bonhoeffer, S. (2001) Cooperation and competition in the evolution of ATP-producing pathways. *Sci* **292**, 504-507.

Pinton, P., Giorgi, C., Siviero, R., Zecchini, E. & Rizzuto, R. (2008) Calcium and apoptosis: ER-mitochondria Ca2+ transfer in the control of apoptosis. *Oncogene* **27**, 6407-6418.

Pitceathly, R. D. S. & McFarland, R. (2014) Mitochondrial myopathies in adults and children: Management and therapy development. *Curr Opin Neurol* **27**, 576–582.

Polekhina, G., Gupta, A., Michell, B. J., van Denderen, B., Murthy, S., Feil, S. C., Jennings, I. G., Campbell, D. J., Witters, L. A., Parker, M. W., Kemp, B. E. & Stapleton, D. (2003) AMPK beta subunit targets metabolic stress sensing to glycogen. *Curr Biol* **13**, 867–871.

Powis, G. & Kirkpatrick, L. (2004) Hypoxia inducible factor-1alpha as a cancer drug target. *Mol Cancer Therap* **3**, 647–654.

Preiss, T., Lowerson, S. A., Weber, K. & Lightowlers, R. N. (1995) Human mitochondria: distinct organelles or dynamic network? *Trends Genet* **11**, 211–212.

Puffenberger, E. G., Strauss, K. A., Ramsey, K. E., Craig, D. W., Stephan, D. A., Robinson, D. L., Hendrickson, C. L., Gottlieb, S., Ramsay, D. A., Siu, V. M., Heuer, G. G., Crino, P. B. & Morton, D. H. (2007) Polyhydramnios, megalencephaly and symptomatic epilepsy caused by a homozygous 7-kilobase deletion in LYK5. *Brain J Neurol* **130**, 1929–1941.

Quirós, P. M., Mottis, A. & Auwerx, J. (2016) Mitonuclear communication in homeostasis and stress. *Nat Rev Mol Cell Biol* **17**, 213-226.

Rahman, S. & Poulton, J. (2009) Diagnosis of mitochondrial DNA depletion syndromes. *Arch Dis Child* **94**, 3-5.

Rajakulendran, T., & Sicheri, F. (2010) Allosteric protein kinase regulation by pseudokinases: insights from STRAD. *Sci Signalling* **3**, pe8.

Ryan, M. T., & Hoogenraad, N. J. (2007) Mitochondrial-nuclear communications. *Annl Rev Biochem* **76**, 701-722.

Reeve, A. K., Krishnan, K. J., Turnbull, D. (2008) Mitochondrial DNA mutations in disease, aging, and neurodegeneration. *Ann NY Aca Sci* **1147**, 21–29.

Rena, G., Hardie, D. G., & Pearson, E. R. (2017) The mechanisms of action of metformin. *Diabetologia*, **60**, 1577–1585.

Rencurel, F., Stenhouse, A., Hawley, S. A., Friedberg, T., Hardie, D. G., Sutherland, C. & Wolf, C. R. (2005) AMP-activated protein kinase mediates phenobarbital induction of CYP2B gene expression in hepatocytes and a newly derived human hepatoma cell line. *J Biol Chem* **280:** 4367-4373.

Resta, N., Giorda, R., Bagnulo, R., Beri, S., Mina, E. D., Stella, A., Piglionica, M., Susca, F. C., Guanti, G., Zuffardi, O. & Ciccone, R. (2010) Breakpoint determination of 15 large deletions in Peutz-Jeghers subjects. *Hum Genet* **28**, 373-382.

Richter, C., Park, J. W., Ames, B. N. (1988) Normal oxidative damage to mitochondrial and nuclear DNA is extensive. *Proc Natl Acad Sci USA* **85**, 6465–6467.

Riek, U., Scholz, R., Konarev, P., Rufer, A., Suter, M., Nazabal, A., Ringler, P., Chami, M., Muller, S. A., Neumann, D., Forstner, M., Hennig, M., Zenobi, R., Engel, A., Svergun, D., Schlattner, U & Wallimann, T. (2008) Structural properties of AMP-activated protein kinase. Dimerization, molecular shape, and changes upon ligand binding. *J Biol Chem* **283**, 18331–18343.

Risinger, M. A. & Groden, J. (2004) Crosslinks and crosstalk: human cancer syndromes and DNA repair defects. *Cancer Cell* **6**, 539-545.

Rodriguez-Fraticelli, A. E., Auzan, M., Alonso, M.A., Bornens, M. & Martin-Belmonte, F. (2012) Cell confinement controls centrosome positioning and lumen initiation during epithelial morphogenesis, *J Cell Biol* **198**, 1011–1023.

Rosenthal, E. L., Kileny, P. R., Boerst, A. & Telian, S. A. (1999) Successful cochlear implantation in a patient with MELAS syndrome. *Am J Otology* **20**, 187-191.

Ross, F. A., Mackintosh, C. & Hardie, D. G. (2016) AMP-activated protein kinase: a cellular energy sensor that comes in 12 flavours. *FEBS J* **283**, 2987–3001.

Rossignol, R., Faustin, B., Rocher, C., Malgat, M., Mazat, J.-P., Letellier, T. (2003) Mitochondrial threshold effects. *Biochem J* **370**, 751-762.

Rossignol, R., Letellier, T., Malgat, M., Rocher, C. & Mazat, J. P. (2000) Tissue variation in the control of oxidative phosphorylation: implication for mitochondrial diseases. *Biochem J* **347**, 45-53.

Rowan, A., Churchman, M., Jefferey, R., Hanby, A., Poulsom, R. & Tomlinson, I. (2000) *In situ* analysis of *LKB1/STK11* mRNA expression in human normal tissues and tumours. J. Pathol. **192**, 203-206.

Ruhoy, I. S. & Saneto, R. P. (2014) The genetics of Leigh síndrome and its implications for clinical practice and risk management. *Appl clin Genet* **7**, 221-234.

Russell, R. R., Li, J., Coven, D. L., Pypaert, M., Zechner, C., Palmeri, M., Giordano, F. J., Mu, J., Birnbaum, M. J. & Young, L. H. (2004) AMP-activated protein kinase mediates ischemic glucose uptake and prevents postischemic cardiac dysfunction, apoptosis, and injury. *J Clinic Investig* **114**, 495–503.

Ryan, M. T., & Hoogenraad, N. J. (2007) Mitochondrial-nuclear communications. *Ann Rev Biochem* **76**, 701-722.

Sacconi, S., Salviati, L., Nishigaki, Y., Walker, W. F., Hernandez-Rosa, E., Trevisson, E., Severine, Delplace, Desnuelle, C. & other authors (2008) A functionally dominant mitochondrial DNA mutation. *Hum Mol Genet* **17**, 1814-1820.

Sahin, F., Maitra, A., Argani, P., Maehara, N., Montgomery, E., Goggins, M., Hruban, R. H. & Su, G. H. (2003) Loss of Stk11/Lkb1 expression in pancreatic and biliary neoplasms. *Mod Pathol* **16**, 686-691.

Sakamoto, K., McCarthy, A., Smith, D., Green, K. A., Hardie, G. D., Ashworth, A. & Alessi, D. R. (2005) Deficiency of LKB1 in skeletal muscle prevents AMPK activation and glucose uptake during contraction. *EMBO J* **24**, 1810–1820.

Sakamoto, K., Zarrinpashneh, E., Budas, G. R., Pouleur, A.-C., Dutta, A., Prescott, A. R., Vanoverschelde, J.-L., Ashworth, A., Jovanovic, A., Alessi, D. R. & Bertrand, L. (2006) Deficiency of LKB1 in heart prevents ischemia-mediated activation of AMPKα2 but not AMPKα1. *American Journal of Physiology. Endocrinology and Metabolism*, *290*(5), E780–E788.

Salt, I. P. & Hardie, G. D. (2017) AMP-Activated Protein Kinase. An Ubiquitous Signaling Pathway With Key Roles in the Cardiovascular System. *Circulation Res* **120**, 1825-1841.

Sanchez, A. M., Csibi, A., Raibon, A., Cornille, K., Gay, S., Bernardi, H. & Candau, R. (2012) AMPK promotes skeletal muscle autophagy through activation of forkhead FoxO3a and interaction with Ulk1. *J Cell Biochem* **113**, 695-710.

Sanchez-Cespedes, M. (2007) A role of LKB1 gene in human cancer beyond the Peutz-Jeghers syndrome. *Oncogene* **26**, 7825-7832

Sanders, M. J., Ali, Z. S., Hegarty, B. D., Heath, R., Snowden, M. A. & Carling, D. (2007) Defining the mechanism of activation of AMP-activated protein kinase by the small molecule A-769662, a member of the thienopyridone family. *J Biol Chem* **282**, 32539–32548.

Sanli, T., Steinberg, G. R., Singh, G. & Tsakiridis, T. (2014) AMP-activated protein kinase (AMPK) beyond metabolism. A novel genomic stress sensor participating in the DNA damage response pathway. *Cancer Biol Ther* **15**, 156-169

Sapkota, G. P., Boudeau, J., Deak, M., Kieloch, A., Morrice, N. & Alessi, D. R. (2002a) Identification and characterization of four novel phosphorylation sites (Ser31, Ser325, Thr336 and Thr366) on LKB1/STK11, the protein kinase mutated in Peutz–Jeghers cancer syndrome. *Biochem* **362**, 481–490.

Sapkota, G. P., Deak, M., Kieloch, A., Morrice, N., Goodarzi, A. A., Smythe, C., Shiloh, Y., Lees-Miller, S. P. & Alessi, D. R. (2002b) Ionizing radiation induces ataxia telangiectasia mutated kinase (ATM)-mediated phosphorylation of LKB1/STK11 at Thr-366. *Biochem J* **368**, 507- 516.

Sapkota, G. P., Kieloch, A., Lizcano, J. M., Lain, S., Arthur, J. S., Williams, M. R., Morrice, N., Deak, M. & Alessi, D. R. (2001). Phosphorylation of the protein kinase mutated in Peutz-Jeghers cancer syndrome, LKB1/STK11, at Ser431 by p90(RSK) and cAMP-dependent protein kinase, but not its farnesylation at Cys(433), is essential for LKB1 to suppress cell growth. *J Biol Chem* **276**, 19469–19482.

Saxton, R. A. & Sabatini, D. M. (2017) mTOR Signaling in Growth, Metabolism, and Disease. *Cell* **168**, 960-976.

Scarpelli, M., Zappini, F., Filosto, M., Russignan, A., Tonin, P. & Tomelleri, G. (2011) Mitochondrial Sensorineural Hearing Loss: A Retrospective Study and a

Description of Cochlear Implantation in a MELAS Patient. *Genet Res Int* **2012**, Article ID 287432, 5 pages.

Scarpulla R. C. (2011) Metabolic control of mitochondrial biogenesis through the PGC-1 family regulatory network. *Biochim Biophys Acta* **1813**, 1269-1278.

Schapira, A. H. (2006) Mitochondrial disease. *Lancet* **368,** 70-82.

Schapira, A. H. (1999) Mitochondrial involvement in Parkinson's disease, Huntington's disease, hereditary spastic paraplegia and Friedreich's ataxia. *Biochem Biophys Acta* **1410**, 159-170.

Scheffler, I. E. (2001) A century of mitochondrial research: achievements and perspectives. *Mitochondrion* **1**, 3-31**.**

Schmidt, O., Pfanner, N. & Meisinger, C. (2010) Mitochondrial protein import: From proteomics to functional mechanisms. *Nat Rev. Mol Cell Biol* **11**, 655- 667.

Schon, E. A. (2000) Mitochondrial genetics and disease. *Trends Biochem Sci* **25**, 555-560.

Schon, E. A., DiMauro, S. & Hirano, K. I. (2012) Human mitochondrial DNA: roles of inherited and somatic mutations. *Nat Rev Genet* **13**, 878–890

Schroder, R., Vielhaber, S., Wiedemann, F. R., Kornblum, C., Papassotiropoulos, A., Broich, P., Zierz, S., Elger, C. E. Reichmann, H. Seibel, P., Klockgether, T. & Kunz, W. S. (2000) New insights into the metabolic consequences of large- scale mtDNA deletions: a quantitative analysis of biochemical, morphological, and genetic findings in human skeletal muscle. J Neuropathol Exp Neurol **59**, 353-360.

Sciacco, M., Bonilla, E., Schon, E., DiMauro, S. and Moraes, C. (1994) Distribution of wild-type and common deletion forms of mtDNA in normal and respiration- deficient muscle fibers from patients with mitochondrial myopathy. *Hum Mol Genet* **3**, 13–19.

Scott, J. W., Ling, N., Issa, S. M., Dite, T. A., O'Brien, M. T., Chen, Z. P., Galic, S., Langendorf, C. G., Steinberg, G. R., Kemp, B. E. & Oakhill, J. S. (2014) Small molecule drug A-769662 and AMP synergistically activate naive AMPK independent of upstream kinase signaling. *Chem Biol* **21**, 619–627.

Scott, J. W., van Denderen, B. J., Jorgensen, S. B., Honeyman, J. E., Steinberg, G. R., Oakhill, J. S., Iseli, T. J., Koay, A., Gooley, P. R., Stapleton, D. & Kemp, B. E.

(2008) Thienopyridone drugs are selective activators of AMP-activated protein kinase beta1-containing complexes. *Chem Biol* **15**, 1220–1230.

Scott, K. D., Nath-Sain, S., Agnew, M. D. & Marignani, P. A. (2007) LKB1 catalytically deficient mutants enhance cyclin D1 expression. *Cancer Res* **67**, 5622–5627.

Scott, I. & Youle, R. J. (2010) Mitochondrial fission and fusion. *Essays biochem* **47**, 85-98.

Sebbagh, M., Olschwang, S., Santoni, M.-J., & Borg, J.-P. (2011) The LKB1 complex-AMPK pathway: the tree that hides the forest. *Familial Cancer* **10**, 415-424.

Seshacharyulu, P., Ponnusamy, M. P., Haridas, D., Jain, M. & Batra, S. K. (2012) Targeting the EGFR signalling pathway in cancer therapy. *Expert opin on therapeut targets* **16**, 15-31.

Senior, A. E., Nadanaciva, S. & Weber, J. (2002) The molecular mechanism of ATP synthesis by F_1F_0-ATP synthase. *Biochim Biophys Acta* **1553**, 188–211.

Sgarbi, G., Baracca, A., Lenaz, G., Valentino, L. M., Carelli, V. & Solaini, G. (2006) Inefficient coupling between proton transport and ATP synthesis may be the pathogenic mechanism for NARP and Leigh syndrome resulting from the T8993G mutation in mtDNA. *Biochem J* **395**,493–500.

Shackelford, D. B., Abt, E., Gerken, L., Vasquez, D. S., Seki, A., Leblanc, M., Wei, L., Fishbein, M. C., Czernin, J., Mischel, P. S. & Shaw, R. J. (2013) LKB1 inactivation dictates therapeutic response of non-small cell lung cancer to the metabolism drug phenformin. *Cancer Cell* **23**, 143–158.

Shackelford, D. B., Vasquez, D. S., Corbeil, J., Wu, S., Leblanc, M., Wu, C.-L., Vera, D. R. & Shaw, R. J. (2009) mTOR and HIF-1alpha-mediated tumor metabolism in an LKB1 mouse model of Peutz-Jeghers syndrome. *Proc Natl Acad Sci USA* **106**, 11137–11142.

Shang, L. & Wang, X. (2011) AMPK and mTOR coordinate the regulation of Ulk1 and mammalian autophagy initiation. *Autophagy* **7**, 924–926.

Shaw, R. J. (2008) LKB1: cancer, polarity, metabolism, and now fertility. *Biochem J* **416**, e1–3.

Shaw, R. J. (2009) LKB1 and AMP-activated protein kinase control of mTOR signalling and growth. *Acta physio (Oxford, England)* **196**, 65-80.

Shaw, R. J., Lamia, K. A., Vasquez, D., Koo, S. H., Bardeesy, N., Depinho, R. A., Montminy, M. & Cantley, L. C. (2005) The kinase LKB1 mediates glucose homeostasis in liver and therapeutic effects of metformin. *Sci* **310**, 1642–1646.

Shaw, R. J., Kosmatka, M., Bardeesy, N., Hurley, R. L., Witters, L.A., DePinho, R. A. & Cantley, L. C. (2004) The tumor suppressor LKB1 kinase directly activates AMP-activated kinase and regulates apoptosis in response to energy stress. *Proc Natl Acad Sci USA* **101***,* 3329–3335.

Shelly, M., Cancedda, L., Heilshorn, S., Sumbre, G. & Poo, M. M. (2007) LKB1/STRAD promotes axon initiation during neuronal polarization. *Cell* **129**, 565–577.

Shen, Y. A., Chen, Y., Dao, D. Q., Mayoral, S. R., Wu, L., Meijer, D., Ullian, E. M., Chan, J. R. & Lu, Q. R. (2014) Phosphorylation of LKB1/Par-4 establishes Schwann cell polarity to initiate and control myelin extent. *Nat Comm* **5**, Article 4991.

Shen, Z., Wen, X. F., Lan, F., Shen, Z. Z. & Shao, Z. M. (2002) The tumor suppressor gene LKB1 is associated with prognosis in human breast carcinoma. *Clin Cancer Res* **8**, 2085-2090.

Shoffner, J. M., Lott, M. T., Lezza, A. M., Seibel, P., Ballinger, S. W., and Wallace, D. C. (1990) Myoclonic epilepsy and ragged-red fiber disease (MERRF) is associated with a mitochondrial DNA tRNA(Lys) mutation. *Cell* **61**, 931-937.

Sinnett, S. E. & Brenman, J. E. (2016) The role of AMPK in Drosophila melanogaster. *Experientia supplementum (2012)* **107**, 389-401.

Skladal, D., Halliday, J. & Thorburn, D. R. (2003) Minimum birth prevalence of mitochondrial respiratory chain disorders in children. *Brain* **126**, 1905–1912.

Smith, D. P., Rayter, S. I., Niederlander, C., Spicer, J., Jones, C. M., & Ashworth, A. (2001) LIP1, a cytoplasmic protein functionally linked to the Peutz-Jeghers syndrome kinase LKB1. *Hum Mol Genet* **10**, 2869–2877.

Song, P., Xie, Z., Wu, Y., Xu, J., Dong, Y., & Zou, M.-H. (2008). Protein kinase Czeta-dependent LKB1 serine 428 phosphorylation increases LKB1 nucleus export and apoptosis in endothelial cells. *J Biol Chem* **283**, 12446–12455.

Spelbrink, J. N., Li, F. Y., Tiranti, V., Nikali, K., Yuan, Q.P., Tariq, M., Wanrooij, S., Garrido, N., Comi, G., Morandi, L., Santoro, L., Larsson, C. and more authors (2001) Human mitochondrial DNA deletions associated with mutations in the gene

encoding Twinkle, a phage T7 gene 4-like protein localized in mitochondria, *Nat Genet* **28**, 223–231.

Sriwijitkamol, A., Ivy, J. L., Christ-Roberts, C., DeFronzo, R. A., Mandarino, L. J. & Musi, N. (2006) LKB1-AMPK signaling in muscle from obese insulin-resistant Zucker rats and effects of training. *Am J Physio Endocrin Metab* **290**, E925–932.

Stahmann, N., Woods, A., Carling, D. & Heller, R. (2006) Thrombin activates AMP-activated protein kinase in endothelial cells via a pathway involving Ca^{2+}/calmodulin-dependent protein kinase kinase beta. *Mol Cell Biol* **26**, 5933–5945.

Steinberg, G. R., O'Neill, H. M., Dzamko, N. L., Galic, S., Naim, T., Koopman, R., Jørgensen, S. B., Honeyman, J., Hewitt, K., Chen, Z. P. & other authors (2010) Whole body deletion of AMP-activated protein kinase beta2 reduces muscle AMPK activity and exercise capacity. *J Biol Chem* **285**, 37198–37209.

Strange, K., Denton, J. & Nehrke, K. (2006) Ste20-Type Kinases: Evolutionarily Conserved Regulators of Ion Transport and Cell Volume. *Physio* **21**, 61-68.

Strmecki, L., Greene, D. M. & Pears, C. J. (2005) Developmental decisions in *Dictyostelium discoideum*. *Dev Biol* **284**, 25-36.

Suliman, B. & Piantadosi, C. A. (2016) Mitochondrial quality control as a therapeutic target. *Pharmacol Rev* **68,** 20-48.

Sullivan, J. E., Brocklehurst, K. J., Marley, A. E., Carey, F., Carling, D., & Beri, R. K. (1994) Inhibition of lipolysis and lipogenesis in isolated rat adipocytes with AICAR, a cell-permeable activator of AMP-activated protein kinase. *FEBS Lett* **353**, 33–36.

Sun, Y., Connors, K. E. & Yang, D. Q. (2007) AICAR induces phosphorylation of AMPK in an ATM-dependent, LKB1-independent manner. *Mol Cell Biochem* **306**, 239 – 245.

Suzuki, A., Okamoto, S., Lee, S., Saito, K., Shiuchi, T. & Minokoshi, Y. (2007) Leptin Stimulates Fatty Acid Oxidation and Peroxisome Proliferator-Activated Receptor {alpha} Gene Expression in Mouse C2C12 Myoblasts by Changing the Subcellular Localization of the {alpha}2 Form of AMP-Activated Protein Kinase. *Mol Cell Biol* **27**, 4317–4327.

Svensson, R. U., Parker, S. J., Eichner, L. J., Kolar, M. J., Wallace, M., Brun, S. N., Lombardo, P. S., Van Nostrand, J. L., Hutchins, A., Vera, L., Gerken, L., Greenwood, J., Bhat, S., Harriman, G., Westlin, W. F., Harwood, H. J., Saghatelian,

A., Kapeller, R., Metallo, C. M. & Shaw, R. J. (2016) Inhibition of acetyl-CoA carboxylase suppresses fatty acid synthesis and tumor growth of non-small-cell lung cancer in preclinical models. *Nat med* **22**, 1108-1119.

Swaney, K. F., Huang, C. H. & Devreotes, P. N. (2010) Eukaryotic chemotaxis: a network of signaling pathways controls motility, directional sensing, and polarity. *Ann Rev Biophys* **39**, 265-289.

Taanman, J. W. (1999) The mitochondrial genome: structure, transcription, translation and replication. *Biochim Biophys Acta Bioenerg* **1410,** 103-123.

Tamas, P., Hawley, S. A., Clarke, R. G., Mustard, K. J., Green, K., Hardie, D. G. & Cantrell, D. A. (2006) Regulation of the energy sensor AMP-activated protein kinase by antigen receptor and Ca2+ in T lymphocytes. *J Exp Med* **203**, 1665–1670.

Tanner C. B., Madsen, S. R., Hallowell, D. M., Goring, D. M. J., Moore, T. M., Hardman, S. E., Heninger, M. R., Atwood, D. R. & Thomson, D. M. (2013) Mitochondrial and performance adaptations to exercise training in mice lacking skeletal muscle LKB1. *Am J Physiol Endocrinol Metab* **305**, 1018–1029.

Taylor, R. W. & Turnbull, D. M. (2005) Mitochondrial DNA mutations in human disease. *Nat Rev Genet* **6**, 389-402.

Thorburn, D. R. (2004) Mitochondrial disorders: prevalence, myths and advances, *J Inherit Metab Dis* **27**, 349–362.

Tiainen, M., Vaahtomeri, K., Ylikorkala, A. & Makela, T. P. (2002) Growth arrest by the LKB1 tumor suppressor: induction of p21(WAF1/CIP1). *Hum Mol Genet* **11**, 1497–1504.

Tiainen, M., Ylikorkala, A. & Makela, T. P. (1999) Growth suppression by Lkb1 is mediated by a G1 cell cycle arrest. *Proc Natl Acad Sci USA* **96**, 9248-9251.

Tiranti, V., Hoertnagel, K., Carrozzo, R., Galimberti, C., Munaro, M., Granatiero, M, (1998) Mutations of SURF-1 in Leigh disease associated with cytochrome c oxidase deficiency. Am J Hum Genet. 63:1609–21.

Towler, M. C., Fogarty, S., Hawley, S. A., Pan, D. A., Martin, D. M., Morrice, N. A., McCarthy, A., Galardo, M. N., Meroni, S. B., Cigorraga, S. B., Ashworth, A., Sakamoto, K. & Hardie, D. G. (2008) A novel short splice variant of the tumour suppressor LKB1 is required for spermiogenesis. *Biochem J* **416**, 1-14.

Townley, R. & Shapiro, L. (2007) Crystal structures of the adenylate sensor from fission yeast AMP-activated protein kinase. *Sci* **315**, 1726–1729.

Trifunovic, A., Wredenberg, A., Falkenberg, M., Spelbrink, J. N., Rovio, A. T., Bruder, C. E., Bohlooly, -Y. M., Gidlöf, S., Oldfors, A., Wibom, R., Törnell, J., Jacobs, H. T., Larsson, N. G. (2004) Premature ageing in mice expressing defective mitochondrial DNA polymerase. *Nat* **429**, 417-423.

Tripathi, D. N., Chowdhury, R., Trudel, L. J., Tee, A. R., Slack, R. S., Walker, C. L., & Wogan, G. N. (2013) Reactive nitrogen species regulate autophagy through ATM-AMPK-TSC2-mediated suppression of mTORC1. *Proc Natl Acad Sci USA* **110**, E2950–2957.

Tsao, C. Y., Mendell, J. R. & Bartholomew, D. (2001) High mitochondrial DNA T8993G mutation (<90%) without typical features of Leigh's and NARP syndromes. *J Child Neurol* **16**, 533–535.

Tubbs, A. & Nussenzweig, A. (2017) Endogenous DNA damage as a source of genomic instability in cancer. *Cell* **168**, 644–656.

Tuppen, H. A. L., Blakely, E. M., Turnbull, D. M. & Taylor, R. W. (2010) Mitochondrial DNA mutations and human disease. *Biochim Biophys Acta (BBA) – Bioenerg* **1797**, 113–128.

Turner, N., Li, J. Y., Gosby, A., To, S. W., Cheng, Z., Miyoshi, H., Taketo, M. M., Cooney, G. J., Kraegen, E. W., James, D. E., Hu, L. H., Li, J. & Ye, J. M. (2008) Berberine and its more biologically available derivative, dihydroberberine, inhibit mitochondrial respiratory complex I: a mechanism for the action of berberine to activate AMP-activated protein kinase and improve insulin action. *Diabetes* **57**, 1414-1418.

Ui, A., Ogiwara, H., Nakajima, S., Kanno, S., Watanabe, R., Harata, M., Okayama, H., Harris, C. C., Yokota, J., Yasui, A. & Kohno, T. (2014) Possible involvement of LKB1-AMPK signaling in non-homologous end joining. *Oncogene* **33**, 1640-1648.

Uziel, G., Moroni, I., Lamantea, E., Fratta, G. M., Ciceri, E., Carrara, F. & Zeviani, M. (1997) Mitochondrial disease associated with the T8993G mutation of the mitochondrial ATPase 6 gene: a clinical, biochemical, and molecular study in six families. *J Neurol Neurosurg Psychiatry* **63**, 16–22.

Varelas, X. (2014) The Hippo pathway effectors TAZ and YAP in development, homeostasis and disease. *Develop* **141**, 1614-1626.

van Veelen, W., Korsse, S. E., van de Laar, L. & Peppelenbosch, M. P. (2011) The long and winding road to rational treatment of cancer associated with LKB1/AMPK/TSC/mTORC1 signaling. *Oncogene* **30**, 2289-2303.

Vander Heiden, M. G., Cantley, L. C., & Thompson, C. B. (2009) Understanding the Warburg effect: the metabolic requirements of cell proliferation. *Sci NY* **324**, 1029–1033.

Vaseva, A. V., Marchenko, N. D., Ji, K., Tsirka, S. E., Holzmann, S. & Moll, U. M. (2012) p53 opens the mitochondrial permeability transition pore to trigger necrosis. *Cell* **149**, 1538-1548.

Vazquez-Martin, A., López-Bonet, E., Oliveras-Ferraros, C., Pérez-Martínez, M. C., Bernadó, L. & Menendez, J. A. (2009) Mitotic kinase dynamics of the active form of AMPK (phospho-AMPKalphaThr172) in human cancer cells. *Cell Cycle* **8**, 788–791.

Veeranki, S., Hwang, S.-H., Sun, T., Kim, B., & Kim, L. (2011) LKB1 regulates development and the stress response in *Dictyostelium*. *Developl Biol* **360**, 351–357.

Veleva-Rotse, B. O., Smart, J. L., Baas, A. F., Edmonds, B., Zhao, Z. M., Brown, A., Klug, L. R., Hansen, K., Reilly, G., Gardner, A. P., Subbiah, K. and other authors (2014) STRAD pseudokinases regulate axogenesis and LKB1 stability. *Neural Dev* **9**, 5.

Viollet, B., Guigas, B., Leclerc, J., Hébrard, S., Lantier, L., Mounier, R., ... Foretz, M. (2009) AMP-activated protein kinase in the regulation of hepatic energy metabolism : from physiology to therapeutic perspectives. *Acta Physiologica* **196**, 81–98.

Vital, A & Vital, C. (2012) Mityochondria and peripheral Neuropathies. *J Neuropathol Exp Neurol* **71**, 1036-1046.

Wakerhage, H. & Woods, N. M. (2002) Exercise-induced signal transduction and gene regulation in skeletal muscle. *J Sports Sci Med* **1**, 103– 114.

Wallace, D.C. (1999) Mitochondrial diseases in man and mouse. *Sci* **283**, 1482-1488.

Wallace, D.C. (2010) Mitochondrial DNA mutations in disease and aging**.** *Environ Mol Mutagen* **51**, 440-450.

Wallace, D. C. & Fan, W. (2010) Energetics, epigenetics, mitochondrial genetics. *Mitochondrion* **10**, 12–31.

Wang, Q., Liang, B., Shirwany, N. A. & Zou, M. H. (2011) 2-Deoxy-D-glucose treatment of endothelial cells induces autophagy by reactive oxygen species-mediated activation of the AMP-activated protein kinase. *PLoS One* **6**, e17234.

Wang, R., Qi, X., Liu, X. & Guo, X. (2016) Peutz-Jeghers syndrome: Four cases in one family. *Intractable & Rare Diseases Res* **5**, 42-43.

Wani, W., Boyer-Guittaut, M., Dodson, M., Chatham, J., Darley-Usmar, V. & Zhang, J. (2015). Regulation of autophagy by protein post-translational modification. *Lab Invest* **95**, 14–25.

Watanabe, T., Hosoya, H. & Yonemura, S. (2007) Regulation of myosin II dynamics by phosphorylation and dephosphorylation of its light chain in epithelial cells. *Molecular biology of the cell* **18**, 605-616.

Watts, J. L., Morton, D. G., Bestman, J. & Kemphues, K. J. (2000) The *C. elegans* par-4 gene encodes a putative serine-threonine kinase required for establishing embryonic asymmetry. *Development* **127**, 1467–1475.

Wei, C., Bhattaram, V. K., Igwe, J. C., Fleming, E. & Tirnauer, J. S. (2012) The LKB1 tumor suppressor controls spindle orientation and localization of activated AMPK in mitotic epithelial cells. *PLoS One* **7**, e41118.

Westerman, A. M., Entius, M. M., de Baar, E., Boor, P. P. C., Koole, R., van Velthuysen, M. L. F., Offerhaus, G. J. A., Lindhout, D., de Rooij, F. W. M. & Wilson, J. H. P. (1999) Peutz-Jeghers syndrome: 78-year follow-up of the original family. *Lancet* **353**, 1211-1215.

Whittaker, R. G., Devine, H. E., Gorman, G. S., Schaefer, A. M., Horvath, R., Ng, Y., Nesbitt, V., Lax, N. Z., McFarland, R., Cunningham, M. O., Taylor, R. W. & Turnbull, D. M. (2015) Epilepsy in adults with mitochondrial disease: A cohort study. *Ann Neurol* **78**, 949-957.

Wilczynska, Z., Barth, C. & Fisher, P. R. (1997) Mitochondrial mutations impair signal transduction in *Dictyostelium discoideum* slugs. *Biochem Biophys Res Commun* **234**, 39-43.

Williams, J. G. (2006) Transcriptional regulation of *Dictyostelium* pattern formation. *EMBO Reports* **7**, 694–698.

Wittenhagen, L.M. & Kelley, S.O. (2002) Dimerization of a pathogenic human mitochondrial tRNA. *Nat Struct Biol* **9,** 586–590.

Woods, A., Azzout-Marniche, D., Foretz, M., Stein, S. C., Lemarchand, P., Ferré, P., Foufelle, F. & Carling, D. (2000) Characterization of the role of AMP-activated

protein kinase in the regulation of glucose-activated gene expression using constitutively active and dominant negative forms of the kinase. *Mol Cell Biol* **20**, 6704–6711.

Woods, A., Dickerson, K., Heath, R., Hong, S. P., Momcilovic, M., Johnstone, S. R., Carlson, M. & Carling, D. (2005) Ca2+/calmodulin-dependent protein kinase kinase-beta acts upstream of AMP-activated protein kinase in mammalian cells. *Cell Metab* **2**, 21–33.

Woods, A., Johnstone, S. R., Dickerson, K., Leiper, F. C., Fryer, L. G. D., Neumann, D., Schlattner, U., Wallimann, T., Carlson, M. & Carling, D. (2003) LKB1 is the upstream kinase in the AMP-activated protein kinase cascade. *Curr Biol* **13***,* 2004-2008.

Wu, L., Valkema, R., Van Haastert, P. J. & Devreotes, P. N. (1995) The G protein beta subunit is essential for multiple responses to chemoattractants in Dictyostelium. *J Cell Biol* **129**, 1667–1675.

Wu, Z., Puigserver, P., Andersson, U., Zhang, C., Adelmant, G., Mootha, V., Troy, A., Cinti, S., Lowell, B., Scarpulla, R. C. & Spiegelman, B. M. (1999) Mechanisms controlling mitochondrial biogenesis and respiration through the thermogenic coactivator PGC-1. *Cell* **98**, 115-124.

Xia, Y., Shen, S. & Verma, I. M. (2014) NF-κB, an active player in human cancers. *Cancer Immunol Res* **2**, 823-830.

Xiao B, Heath R, Saiu P., Leiper, F. C., Leone, P., Jing, C., Walker, P. A, Haire, L., Eccleston, J. F., Davis, C. T., Martin, S. R., Carling, D. & Gamblin, S. J. (2007) Structural basis for AMP binding to mammalian AMP-activated protein kinase. *Nat* **449**, 496–500.

Xiao, B., Sanders, M. J., Underwood, E., Heath, R., Mayer, F. V., Carmena, D., Jing, C., Walker, P. A., Eccleston, J. F., Haire, L. F., Saiu, P., Howell, S. A., Aasland, R., Martin, S. R., Carling, D. & Gamblin, S. J. (2011) Structure of mammalian AMPK and its regulation by ADP. *Nat* **472**, 230-233.

Xie, Z., Dong, Y., Scholz, R., Neumann, D., & Zou, M.-H. (2008) Phosphorylation of LKB1 at serine 428 by protein kinase C-zeta is required for metformin-enhanced activation of the AMP-activated protein kinase in endothelial cells. *Circulation* **117**, 952–962.

Xie, Z., Dong, Y., Zhang, J., Scholz, R., Neumann, D., & Zou, M.-H. (2009) Identification of the serine 307 of LKB1 as a novel phosphorylation site essential for its

nucleocytoplasmic transport and endothelial cell angiogenesis. *Mol Cell Biol* **29**, 3582–3596.

Xie, M., Zhang, D., Dyck, J. R., Li, Y., Zhang, H., Morishima, M., Mann, D. L., Taffet, G. E., Baldini, A., Khoury, D. S. & Schneider, M. D. (2006) A pivotal role for endogenous TGF-beta-activated kinase-1 in the LKB1/AMP-activated protein kinase energy-sensor pathway. *Proc Natl Acad Sci USA* **103**, 17378–17383.

Yajima, H., Isomoto, H., Nishioka, H., Yamaguchi, N., Ohnita, K., Ichikawa, T., Takeshima, F., Shikuwa, S., Ito, M., Nakao, K., Tsukamoto, K. & Kohno, S. (2013) Novel serine/threonine kinase 11 gene mutations in Peutz-Jeghers syndrome patients and endoscopic management. *World J Gastrointest Endoscopy* **5**, 102-110.

Yamamoto, M., Clemens, P. R. & Engel, A. G. (1991) Mitochondrial DNA deletions in mitochondrial myopathies: observations in 19 patients**.** *Neurol* 41, 1822-1828.

Yang, Y., Li, W., Liu, Y., Sun, Y., Li, Y., Yao, Q., Li, J., Zhang, Q., Gao, Y., Gao, L., & Zhao, J. (2014) Alpha-lipoic acid improves high-fat diet-induced hepatic steatosis by modulating the transcription factors SREBP-1, FoxO1 and Nrf2 via the SIRT1/LKB1/AMPK pathway. *J Nutr Biochem* **25**, 1207–1217.

Yang, Y., Atasoy, D., Su, H. H. & Sternson, S. M. (2011) Hunger states switch a flipflop memory circuit via a synaptic AMPK-dependent positive feedback loop. *Cell* **146**, 992–1003.

Yasukawa, T., Suzuki, T., Ishii, N., Ueda, T., Ohta, S. & Watanabe, K. (2000) Defect in modification at the anticodon wobble nucleotide of mitochondrial tRNA(Lys) with the MERRF encephalomyopathy pathogenic mutation. *FEBS Lett* **467**, 175-178.

Yasukawa, T., Suzuki, T., Ueda, T., Ohta, S. & Watanabe, K. (2000) Modification defect at anticodon wobble nucleotide of mitochondrial $tRNAs^{Leu(UUR)}$ with pathogenic mutations of mitochondrial myopathy, encephalopathy, lactic acidosis, and stroke-like episodes. *J Biol Chem* **275,** 4251–4257.

Yoneda, M., Tanno, Y., Horai, S., Ozawa, T., Miyatake, T. & Tsuji, S. (1990) A common mitochondrial DNA mutation in the t-RNA(Lys) of patients with myoclonus epilepsy associated with ragged-red fibers. *Int J Biochem* **21**, 789–796.

Yu, F. X., Zhao, B. & Guan, K. L. (2015) Hippo Pathway in Organ Size Control, Tissue Homeostasis, and Cancer. *Cell* **163**, 811-828.

Yu, N., Zhang, Y., Zhang, K., Xie, Y., Lin, X. & Di, Q. (2016) MELAS and Kearns–Sayre overlap syndrome due to the mtDNA m. A3243G mutation and large-scale mtDNA deletions. *eNeurologicalSci* **4**, 15–18.

Zagórska, A., Deak, M., Campbell, D. G., Banerjee, S., Hirano, M., Aizawa, S., Prescott, A. R. & Alessi, D. R. (2010) New roles for the LKB1-NUAK pathway in controlling myosin phosphatase complexes and cell adhesion. *Sci Signaling* **3**, ra25.

D. Zala, U. Schlattner, T. Desvignes, J. Bobe, A. Roux, P. Chavrier, M. Boissan (2017) The advantage of channelling nucleotides for very processive functions. *F1000 Res* **6,** p. e674.

Zeqiraj, E., Filippi, B. M., Deak, M., Alessi, D. R., & van Aalten, D. M. F. (2009) Structure of the LKB1-STRAD-MO25 complex reveals an allosteric mechanism of kinase activation. *Sci* NY **326**, 1707–1711.

Zeviani, M., Bertagnolio, B. & Uziel, G. (1996) Neurological presentations of mitochondrial diseases. *J Inherit Metab Dis* **19**, 504-520.

Zeviani, M. & Carelli, V. (2007) Mitochondrial disorders. *Curr Opin Neurol* **20**, 564-571.

Zeviani, M., Moraes, C. T., DiMauro, S., Nakase, H., Bonilla, E., Schon, E. A. & Rowland, L. P. (1988) Deletions of mitochondrial DNA in Kearns-Sayre syndrome. *Neur* **38**, 1339-1346.

Zeviani, M., Servidei, S., Gellera, C., Bertini, E., DiMauro, S. & DiDonato, S. (1989) An autosomal dominant disorder with multiple deletions of mitochondrial DNA starting at the D-loop region. *Nat* **339**, 309–311.

Zhan, Y., Chen, Y., Zhang, Q., Zhuang, J., Tian, M., Chen, H. Z., Zhang, L. R., Zhang, H. K., He, J. P., Wang, W. J., Wu, R., Wang, Y., Shi, C., Yang, K., Wu, Q. & other authors (2012) The orphan nuclear receptor Nur77 regulates LKB1 localization and activates AMPK. *Nat Cheml Biol* **8**, 897–904.

Zhan, T., Rindtroff, N. & Boutros, M. (2017) Wnt signaling in cancer. *Oncog* **36**, 1461-1473.

Zhang, F. & Broughton, R. E. (2013) Mitochondrial–Nuclear Interactions: Compensatory Evolution or Variable Functional Constraint among Vertebrate Oxidative Phosphorylation Genes? *Genome Biol Evol* **5**, 1781–1791.

Zhang, L., Li, J., Young, L. H. & Caplan, M. J. (2006) AMP-activated protein kinase regulates the assembly of epithelial tight junctions. *Proc Natl Acad Sci USA* **103**, 17272–17277.

Zhang, Z. J., Zheng, Z. J., Shi, R., Su, Q., Jiang, Q. & Kip, K. E. (2012) Metformin for liver cancer prevention in patients with type 2 diabetes: a systematic review and meta-analysis. *J Clin Endocrinol Metab* **97**, 2347-2353.

Zhao, R.-X. & Xu, Z.-X. (2014) Targeting the LKB1 Tumor Suppressor. *Curr Drug Targets* **15**, 32-52.

Zheng, B. & Cantley, L. C. (2007) Regulation of epithelial tight junction assembly and disassembly by AMP-activated protein kinase. *Proc Natl Acad Sci U S A* **104**, 819–822.

Zheng, D., MacLean, P. S., Pohnert, S. C., Knight, J. B., Olson, A. L., Winder, W. W., & Dohm, G. L. (2001) Regulation of muscle GLUT-4 transcription by AMP-activated protein kinase. *J Appl Physio* **91**, 1073–1083.

Zheng, Z., Chen, H., Li, J., Li, T., Zheng, B., Zheng, Y., Jin, H., He, Y., Gu, Q. & Xu, X. (2012) Sirtuin 1-mediated cellular metabolic memory of high glucose via the LKB1/AMPK/ROS pathway and therapeutic effects of metformin. *Diabetes* **61**, 217–228.

Zheng, X., Boyer, L., Jin, M., Mertens, J., Kim, Y., Ma, L., Hamm, M., Gage, F. H. & Hunter, T. (2016) Metabolic reprogramming during neuronal differentiation from aerobic glycolysis to neuronal oxidative phosphorylation eLife**, 5,** p. e13374.

Zhu, H., Moriasi, C. M., Zhang, M., Zhao, Y. & Zou, M.-H. (2013) Phosphorylation of Serine 399 in LKB1 Protein Short Form by Protein Kinase Cζ Is Required for Its Nucleocytoplasmic Transport and Consequent AMP-activated Protein Kinase (AMPK) Activation. *J Bio Chem* **288**, 16495-16505.

Zippel, N., Malik, R. A., Fromel, T., Popp R., Bess, E., Strilic, B., Wettschureck, N., Fleming, I. & Fisslthaler, B. (2013) Transforming Growth Factor-β–Activated Kinase 1 Regulates Angiogenesis via AMP-Activated Protein Kinase-α1 and Redox Balance in Endothelial Cells. Arterioscler. *Thromb Vasc Biol* **33**, 2792–2799.

Zoncu, R., Efeyan, A. & Sabatini, D. M. (2011) mTOR: from growth signal integration to cancer, diabetes and ageing. *Nat Rev Mol Cell Biol* **12**, 21–35.

Zong, H., Ren, J. M., Young, L. H., Pypaert, M., Mu, J., Birnbaum, M. J., & Shulman, G. I. (2002) AMP kinase is required for mitochondrial biogenesis in skeletal

muscle in response to chronic energy deprivation. *Proc Natl Acad Sci USA* **99**, 15983–15987.

Zu, Y., Liu, L., Lee, M. Y. K., Xu, C., Liang, Y., Man, R. Y., Vanhoutte, P. M. & Wang, Y. (2010) SIRT1 promotes proliferation and prevents senescence through targeting LKB1 in primary porcine aortic endothelial cells. *Circulation Res* **106**, 1384–1393.

6. Appendix

6.1. Appendix 1 Main chemicals, reagents and suppliers

Chemical	**Supplier**
Acetic acid (glacial)	Ajax
Acrylamide mix	Bio-Rad
Adenosine triphosphate (ATP)	Roche
Agar (Technical no.3)	Oxoid
Agarose (Mol. Biol. Grade)	Promega
Ammonium acetate	APS
Ammonium persulfate (APS)	Sigma
Ampicillin	Roche
Bacteriological peptone	Oxoid
Bacto® Proteose peptone	Difco
Bacto® Tryptone	Difco
Bacto® Yeast extract	Difco

Bis/Acrylamide Mix	Bio-Rad
Blocking Reagent	Qiagen
Boric acid	Sigma
Bovine serum albumin	Sigma
Bromophenol blue	Sigma
Butanol (sec)	Sigma
Calcium acetate	Sigma
Cesium chloride	Roche
Chloroamphenicol	Sigma
Chloroform	Ajax
Coomassie brilliant blue	Sigma
Cyclic AMP	Roche
D-glucose	BDH
Diethyl pyrocarbonate (DEPC)	Sigma
Dimethyl sulphoxide (DMSO)	Ajax

Dipotassium hydrogen orthophospate	Ajax
DNAzol	Molecular Research Center
ECF	Amersham
EDTA (Ethylenediamine-tetracetic acid)	Sigma
Ethanol (absolute)	May & Baker
Ethidium Bromide	Sigma
Fluorescein isothiocyanate (FITC)-dextran	Sigma
Formamide	Ajax
Formaldehyde	Ajax
Gene Ruler^{TM} 1kb DNA ladder	Thermo Fisher Scientific
Geneticin (G418)	Promega
Glycerol	Ajax
Glycine	APS
HEPES (N-Hydroxyethylpiperazine-N)	Sigma
HL-5 medium without glucose	Formedium

Horse Blood Serum	Sigma-Aldrich
Hydrochloric acid	Ajax
Imidazole	Sigma
Iso-amul alcohol	Ajax
Isopropanol	Ajax
Isopropyl-1-thio-β-D-galactoside (IPTG)	Roche
N-Lauroyl Sarcosine	Sigma
L-cysteine	Sigma
Magnesium acetate	Ajax
Magnesium chloride	Ajax
Magnesium sulphate	APS
2-mercaptoethanol	Sigma
MES (2-(N-Morpholino) ethane-sulphonic acid)	Sigma
Methanol	Ajax
Mineral oil	Promega

Mitotracker red CMX-Ros	Invitrogen
Nonidet P40 substitute (NP40)	Sigma
Nu-PAGE running buffer (20X)	Invitrogen
Nu-PAGE transfer buffer (20X)	Invitrogen
Phenol	Sigma
Ponceau S	Sigma
Potassium acetate	Ajax
Potassium Chloride	Ajax
Potassium dihydrogen orthophosphate	Ajax
Potassium hydroxide	APS
Potassium phosphate	Ajax
Resin	Clontech
Skim milk powder	New Zealand Dairy
SM agar	Formedium
Sodium acetate	Ajax

Sodium azide	Sigma
Sodium chloride	Ajax
Tri-sodium citrate	Ajax
Sodium dihydrogen orthophosphate	Ajax
Sodium dodecyl sulphate (SDS)	Ajax
Di-sodium hydrogen orthophosphate	Ajax
Sodium hydroxide	Univar
Sodium phosphate	APS
Streptomycin	Boehringer Mannheim
Sucrose	Ajax
T4 ligase buffer (10X)	Promega
TE Buffer	Invitrogen
TEMED	Sigma
Tetracycline (hydrochloride)	Sigma
Tris	Bio-Rad

Triton® X-100	Sigma
TRIzol®	Invitrogen
Tryptone	Difco
Tween®20 (polyoxyethylene-sorbitan monolaurata)	Sigma-aldrich
Ultramount	Thermo fisher scientific
Yeast Extract	Oxoid

Full names of suppliers

Airpure Australia, Pty. Ltd., St Marys, NSW, AUS
Ajax Chemicals Pty. Ltd., Auburn, NSW, AUS
Alpha Innotech Corporation, San Leandro, CA, USA
Amersham Biosciences Ltd., Buckinghamshire, UK
APS Pty. Ltd., Seven Hills, NSW, AUS
Artisan technology group, Illinois, USA
Astral Scientific, Gymea, NSW, AUS Atherton Pty. Ltd., Queensland, AUS
Australian Scientific Instruments Pty. Ltd., Fishwick, ACT, AUS
BeliMed Inc., Edisonstrasse 7a, 84453 Mühldorf am Inn, DE
BD Biosciences, San Jose, California, USA
BDH, Laboratory Suppliers Pty. Ltd., Poole, England, UK
Bibby Scientific Ltd., Staffordshire, OSA, UK
Bio-Rad Australia Pty. Ltd., Reagent Park, NSW, AUS
Boehringer-Mannheim Australia Pty. Ltd., Castle Hill, NSW, AUS
Bollé Australia Pty. Ltd., Heatherton, VIC, AUS
Capitol Scientific Inc., Austin, Texas, USA
Clontech Laboratories, Inc., Mountain View, CA.
Coldtech Pty. Ltd., South Windsor, NSW, AUS
Contherm Scientific Ltd., Petone, Wellington, NZ
CSL Ltd., Parkville, VIC, AUS
Difco Laboratories Pty. Ltd., Detroit, MI, USA
Data Weighing Systems, Inc., Illinois, USA
Electrolux Kelvinator, AUS
Eppendorf South Pacific Pty. Ltd., North Ryde, NSW, AUS
Fisher & Paykel, Cleveland, QLD, AUS
Flow Laboratories Inc., McLean, Virginia, USA
Food service direct Inc., Hampton, Virginia, USA

Forma Scientific, Florida, USA
ICN Biochemical Australasia, Seven Hills, NSW, AUS
Invitrogen Australia Pty. Ltd., Mount Waverley, VIC, AUS Jencons Australia, Noble Park, VIC, AUS
Kimberly-Clark Corporation, Albury, NSW, AUS
Laboratory Systems Group Pty. Ltd., Kilsyth, VIC, AUS
LG Corporation, Seoul, Korea
Life Technologies Ltd., (GIBCO BRL), Gaithersburg, MD, USA
Living Stone Industries, Inc., Greeneville, Tennessee, USA
May & Baker Nigeria PLC., Ikeja, Lagos, Nigeria
Menzel Vision & Robotics Pvt Ltd., Chembur, Mumbai, India
Merck Pty. Ltd., Kilsyth, VIC, AUS
Millipore Australia Pty. Ltd., North Ryde, NSW, AUS
Molecular Dynamics Inc., Sunnyvale, CA, USA
MP Biomedicals Australasia Pty. Ltd., Seven Hills, NSW, AUS
Nalge Nunc International Corporation, Rochester, New York, USA
NEC Australia, Mulgrave, VIC, AUS
New Zealand Dairy Products Bangladesh Ltd., Dhaka, Bangladesh.
Nikon Australia Pty. Ltd., Lidcombe, NSW, AUS
NuAire Corporation, Plymouth, Minnesota, USA
NuncTM. Part of Thermo Fisher Scientific, Rochester, NY, USA
Olympus Pty. Ltd., North Ryde, NSW, AUS
Origene Technologies, Inc., Rockville, MD
Oxoid Australia Pty. Ltd., Adelaide, South Australia, AUS
Pharmacia Biotech Pty. Ltd., Westerville, OH, USA
Polaroid Australiasia, Scoresby, VIC, AUS
Promega Corporation, Annandale, NSW, AUS
Pro-Tek Australia, Campbellfield, VIC, AUS
Oiagen Pty. Ltd., Chadstone Center, VIC, AUS
Quality Scientific Plastics, Inc., Holm Road, Petaluna, CA, USA
Qualitex Solidstat, VIC, AUS
Ratek Instruments Pty. Ltd., Boronia, VIC, AUS
Roche Diagnostics Australia Pty. Ltd., Castle Hill, NSW, AUS
Sarstedt Australia Pty. Ltd., South Australia, AUS
Sartorious Australia Pty. Ltd., Oakleigh, VIC, AUS
Savant Instruments Inc., Minnesota, USA
Scotsman Ice Systems, Vernon Hills, Illinois, USA
Sigma-Aldrich Pty. Ltd., Castle Hill, NSW, AUS
Starna Pty. Ltd., Thornleigh, NSW, AUS
Terumo Corporation, North Ryde, NSW, AUS
Thermo Fisher Scientific, Scoresby, VIC, AUS TPS Pty. Ltd., Springwood, QLD, AUS
Turner Biosystems, Sunnyvale, CA, USA
UVP Bio-strategy Distribution Pty. Ltd., Hawthorn East, VIC, AUS
Veeder-Root company, Simsbury, Connecticut, USA

6.2. Appendix 2 Composition of media

Medium	**Concentration**	**Component**
D. discoideum storage medium	45 % (v/v)	Horse blood serum
	45 % (v/v)	Saline Solution
	10 % (v/v)	Dimethyl sulfoxide
HL-5 (Ph 6.4-6.6 with glacial acetic)	1.0 % (w/v)	Difco Proteose Peptone
	1.0 % (w/v)	Glucose
	0.5 % (w/v)	Difco Yeast Extract
	2.4 mM	$Na_2HPO_4.2H_2O$
	2.6 mM	KH_2PO_4
HL-5 (pH 6.4-6.6 with glacial acetic)	1.0 % (w/v)	Glucose
	2.2 % (w/v)	HL-5 without Glucose
LoFlo HL-5 medium (Filter sterilize)	0.385 % (w/v)	D-Glucose
	0.18 % (w/v)	Proteose peptone
	0.385 % (w/v)	Yeast extract

	0.385 % (w/v)	KH_2PO_4
	0.385 % (w/v)	Na_2HPO_4
Luria Bertani (LB) Broth	1.0 % (w/v)	Difco bacto tryptone
	1.0 % (w/v)	Difco bacto yeast extract
	1.0 % (w/v)	NaCl
	1 mM	NaOH
Luria Agar	Luria Broth	
	1.0 % (w/v)	Oxoid agar
MES-HL-5 (Ph 7.2-7.3 with 2M NaOH)	0.13 % (w/v)	MES
	1.0 % (w/v)	Glucose
	1.0 % (w/v)	Oxoid bacteriological
	0.6 % (w/v)	Oxoid yeast extract
Normal Agar	2.0 % (w/v)	Difco bacto agar
	0.1 % (w/v)	Difco bacto peptone
	0.11 % (w/v)	Glucose

	0.2 % (w/v)	KH_2PO_4
	2.5 mM	Na_2HPO_4
Nutrient Broth	2.5 % (w/v)	$NB^{\#2}$
	0.5 % (w/v)	Oxoid yeast extract
Standard Medium (SM) Agar	1.0 % (w/v)	Oxoid bacteriological
	1.0 % (w/v)	Oxoid agar
	1.0 % (w/v)	Glucose
	0.1 % (w/v)	Oxoid yeast extract
	0.22 % (w/v)	KH_2PO_4
	0.1 % (w/v)	K_2HPO_4
	0.1 % (w/v)	$MgSO_4.7H_2O$
SM Agar	4.17 % (w/v)	Formedium SM agar
Water Agar	1.0 % (w/v)	Oxoid agar
Super Optimal Culture medium	2.0 % (w/v)	Difco bacto tryptone
	0.25 % (w/v)	Difco bacto yeast extract

(S.O.C.)	20 mM	Glucose
	10 mM	NaCl
	10 mM	$MgCl_2$
	10 mM	$MgSO_4$
	2.5 mM	KCL

6.3. Appendix 3 Composition of buffers

Buffer	**Concentration**	**Component**
General buffers		
EDTA (pH8.0)	0.5 M	Ethylenediaminetetraacetic acid
Ethidium bromide stock	1 mg ml^{-1}	Ethidium bromide
Saline solution	8.6 mM	NaCl
	10 mM	KCl
	2.7 mM	$CaCl.2H_20$
Sodium Acetate (pH 5.2)	3 M	Sodium acetate
TE (pH 8.0)	10 mM	Tris-HCl
	1 mM	EDTA
X-gal	2 % (w/v)	X-gal in DMSO
Isolation of genomic DNA (Cesium Chloride)		
EDTA/Sarkosyl Buffer (pH 8.4)	0.2 M	EDTA
	2 % (w/v)	N-Lauroyl sarcosine sodium

Nuclear lysis buffer (pH 7.5)	10 mM	Mg acetate
	10 mM	NaCl
	30 mM	Hepes
	10 % (w/v)	Sucrose
	2 % (v/v)	NP-40
Polymerase Chain Reacyion (PCR)		
PCR buffer (10 X)	500 mM	Potassium chloride
	200 mM	Tris-HCl (pH 8.8)
Taq polymerase	5 U ml^{-1}	
PCR Nucleotide Mix	20 mM	dNTPs
Magnesium Chloride	50 mM	$MgCl_2$
Alkaline lysis minipreps		
Resuspension Buffer	50 mM	Tris-HCl, pH 8.0
	10 mM	EDTA
	100 g ml^{-1}	RNAse A

Lysis Solution (NaOH/SDS)	0.2 M	NaOH
	10 % (v/v)	SDS
Neutralisation (pH 4.8 with KOH)	5 M	Potassium acetate
Restriction digestion		
One-Phor-All buffer (10X)	0.1 M	Tris-acetate (pH 7.5)
	0.1 M	Magnesium acetate
	0.5 M	Potassium acetate
Gel Electrophoresis		
Agarose Gel	1.0 (w/v)	Agarose
	0.5 μg ml^{-1}	Ethidium Bromide
	10 % (v/v)	TBE (10X)
	90 % (v/v)	dH_2O
DNA ladder (working)	16.7 % (v/v)	1 kb Gene Ruler DNA ladder
	16.7 % (v/v)	6 x loading dye solution

	67.6 % (v/v)	dH_2O
SBE (3X)	50 % (v/v)	Sucrose
	2.2 mM	Bromophenol blue
	4 % (v/v)	0.5 M EDTA (pH 8.0)
TBE stock (10X)	0.89 M	Tris
	0.89 M	Boric acid
	20 mM	EDTA
Transformation of *D. discoideum*		
Calcium Chloride solution	2 M	$CaCl_2$
Glycerol solution (60%)	60 % (v/v)	Glycerol
HBS (2X, pH 7.05)	0.27 M	NaCl
	9.66 mM	KCl
	1.40 mM	Na_2HPO_4
Pinocytosis		
FITC-dextran	20 mg ml^{-1}	FITC-dextran in HL-5

Sodium Phosphate-Triton-X100	0.25 % (v/v)	Triton-X100
	100 mM	Na_2HPO_4
Sorensen's buffer (pH 6.0)	2 mM	Na_2HPO_4
	14.67 mM	KH_2PO_4
Phagocytosis		
Phosphate buffer 20mM	2.35 mM	Na_2HPO_4
	17.21 mM	KH_2PO_4
Sodium Azide stock	400 mM	Sodium Azide in phosphate
Mitochondrial Mass and Mitochondrial Membrane Potential		
MitoTracker Red stock in DMSO	200 μM	MitoTracker Red (CMXROS)
MitoTracker Green stock in DMSO	400 μM	MitoTracker Green (CMXROS)
Immunofluorescence		
Blocking buffer in PBS (pH 6.5)	0.05 % (v/v)	Tween 20
	1 % (v/v)	Bovine Serum Albumin

	1 % (v/v)	Cold water fish skin gelatin
DAPI stock	1 mg ml^{-1}	DAPI
MitoTracker Red stock in DMSO	1 mM	MitoTracker Red (CMXROS)
PBS (pH 6.5)	12 mM	Na_2HPO_4
	12 mM	NaH_2PO_4
SDS-PAGE analysis		
SDS-PAGE sample buffer (5X)	15 % (v/v)	Mercaptoethanol
	15 % (v/v)	SDS
	15 % (v/v)	Bromophenol blue
	50 % (v/v)	Glycerol
Coomassie Blue	50 % (v/v)	Methanol
	10 % (v/v)	Acetic acid
	40 % (v/v)	dH_2O
	0.05 % (w/v)	Coomassie brilliant blue G
Coomassie Blue	5 % (v/v)	Methanol

Destaining	7 % (v/v)	Acetic acid
	88 % (v/v)	dH_2O
Electrophoresis running buffer (5X)	0.5 M	Tris base
	1.92 M	Glycine
	0.5 % (w/v)	SDS
Western blotting and protein detection		
Laemmli buffer	62.5 mM	Tris-Cl (pH 6.8)
	10 % (v/v)	Glycerol
	2 % (v/v)	SDS
	5 % (v/v)	2-mercaptoethanol
	0.05 % (w/v)	Bromophenol blue
Transfer buffer	150 mM	Glycine
	25 mM	Trisbase
	20 % (v/v)	Methanol
Blocking buffer	10 % (w/v)	Skim milk powder in TBS

TBS (pH 7.5)	10 mM	Trisbase
	150 mM	NaCl
TBS-Tween (TBST, pH 7.5)	20 mM	Trisbase
	0.5 M	NaCl
	0.05 % (v/v)	Tween 20
TBS Tween-Triton	99.8 % (v/v)	TBST (pH 7.5)
	0.2 % (v/v)	Triton X-100
AEC chromogen substrate	37.5 mM	Acetate buffer (pH 7.5)
	0.75 % (v/v)	AEC chromogen
	0.75 % (v/v)	H_2O_2 (3%)
Blocking reagent solution	0.5 % (w/v)	Blocking reagent
	10 % (v/v)	Blocking reagent buffer
	0.1 % (v/v)	Tween 20
	89.4 % (v/v)	dH_2O

6.4. Appendix 4 Enzymes

Enzyme	**Supplier**
DNase I	Roche
Restriction endonucleases	Promega
RNase A	Invitrogen
Taq polymerase recombinant	Invitrogen
T4 DNA ligase	Promega
Thermosensitive Alkaline Phosphatase (TSAP)	Promega

6.5. Appendix 5 Kits

Kit	**Supplier**
AEC chromogen kit	Sigma
ECF western blotting kit	Amersham
Gene Images ECF detection kit	Amersham
PureLink™ HiPure Plasmid Filter Purification Kit	Invitrogen
PureLink™ HiPure Plasmid Filter Maxiprep Kit	Invitrogen
PureLink™ Quick Gel Extraction Kit	Invitrogen
PureLink™ HiPure precipitator module	Invitrogen
Wizard SV gel & PCR clean-up system	Promega

6.6. Appendix 6 Gene sequences

1. LKB1 genomic sequence from *D. discoideum*

DDB0229349|DDB_G0279629 |Genomic DNA|gene: lkb1 on chromosome: 3 position 2335074 to 2337125

5′ATGGAAGTTGAACAACAACCATCATATACATCGAATTTTATAATTCATTTAAATGAA
AATGAAGATAATGGCATTTCATATAGATCAAGAAAATCTACACCAAAATTAGTTAAACA
TTATATATTAGGTGAAGTTTTAGGTGAAGGTATTTTTCAATCGATTATATATATATATA
TATATATATATATATCATTATATATATAGTATGAAATATATTAATTTATTATTTATTAA
TTATTTTTAGGTGCTTATGGTAAAGTTAAAGATGGCATGGATTCATTTACACAAAAAAG
AGTAGCAGTTAAAATATTAAAAAGAGCAAGATTAAAAAAAGATTCCTGGCGGGGAAGCAT
CAGTTTTAAAAGAGATTAATATTACAAAAAAGTTACACAATAAACATATAATCAAATTA
ATTGATCATTTCATTATAGAGGAAAAAGGTAAACTGTACATTGTCTATGAATATGTTGG
TGGTGGAACTTCACAAAATATTTTAGAAAATGCACCAAATGGTAGATTACCACCACACC
AATCACAATTGTATGTATTATTTATTTTTTAAAATTTTTATATTTTATTTTTATTATTA
AATAAAATATTTTATTAATAATAATAATAATTACAGTATATTTAGACAATTAATTGAAG
CATGTGAATATATTCATTCACAAAAGATATTACATCGTGATATTAAACCTGATAATATA
CTATTTACACATGCAAATGTATTGAAATTGAGTGATTTTGGAGTTGCAGAGGATAGTAG
CCAATTGGAAGATTTTGAATGTTTATCAAGAAGTTATGGTTCACCAGCATTTCAACCAC
CAGAGTTAACACAATTTCAAACTACATTTTCACCATTTAAAATCGATATTTGGGCAATG
GGTGTAACATTATACCTTATGACCATTGGTAAATTCCCTTTTTCCGGTGCAAATATGTT
TGTACTTTTTGAAAATATCTCTAAATGTAAAATAGAATTTCCAAATGATCTCGATAAAG
ATTTGGTTAATTTAATTAAAGGTATTTTACAAGTTGATCATATTCAAAGATTTTCATTA
GGTCAAATTAAAAATCATCCGTAAAGTATTAAATAAATAAATAATAATAATAATAATAA
TAAAACTATTTAAATAGATAAGAGAGAGATAAATATTAATACCTTTTTTTTTATTTTCA
TAAATTTAGGTGGTGTATTAAATATATACCAGAGGTAGAACCATTTGTGCCATTATTAG
AAGAAAGTAAATTTTTACCATTAGAGATGGCATATGGTGATGATGAAGGTGATGATGGT
GGAGGTGGTAGAGGAGGAGGAGGAGATGATGAACTTATTTTTGGTTATGAAAATGATGG
AAATACAATAGATTTACAAGATCCAGAATATATACCCTCTATATCAGTGGGTGATCAAC
CACCATCAACTCCAATATTACATAGTAGTGATCATCATCATCATCATCATCATAATAAC
CAACATCAACATCAACAACAACAACAGCAACTACAACAATCACAACAATTTCATGGTAA
TGGAGATAATAATTTATTATTTGATTCAAATAATAATTTAATATTTGATTCAAATAATA
ATTTATTATTTAATACAAATAATAATGAACATTTAATTAATGGTTTACCAGTGCACCCA
ATTGAACTCGACCCTGTAAATATTAAAAAGAGTTCAATTGGTACAAATATTTCTGATGT
GGCTTTAATTCGTGAGAATTATATATGCTCTGATAATGATGCTAGTAGTGGTCAAGATG
ATGAAGACTATTCAGATGATAATGAAATTAGTGGTGAAGATTTAAATCCAACAAATCAC
CACCACCACCGTGCTGATAGAGTTGGCTCACGTGATAAGAGTTCAAGATCAAGTAAAAG
AAAGAATAGTAGTAGTAATAATAATAATAATTCCACTTCTCCAAAAGTTGAATTTA
ATCCAAACCGTTCTTCACCTCAACCACCTTTAAGAAATTCAAGTAATAGAAGGCCAAAA
ATTACTTTTGAATCTCCACATAATAAGTCAAAATGTATCATTAATTAA **3′**

2. STRADα genomic sequence from *D. discoideum*

DDB0229911|DDB_G0276577 |Genomic DNA|gene: fray2 on chromosome: 2 position 6994954 to 6998137

5′ATGTCCGATGATAAATATCATCATGATAAACATCATGATAAGCATCATATAGATTCA
AAGCAAAGTACAGCAGCAGCATTATCATCATCATCGACATTAGCTTCATCCTCCTCCAT
GACAACAACAACAACAACAACGTCAACAACAACAACGGCAGCATCTCCAATAACACCAA
AACCAAGAAAAAATTACCCAAATTCAGCAGATCAATATGAACTTAAGGAAACCATTGGT
AAAGGTGGAAGCGGATTAGTACAACGTGCAATATGTTTACCATTTCAAGAGAATGTAGC
TATAAAGATTATAGATTTAGAGCATTGTAAAAACGTATCATTAGAAGAGATTAGAAAGG
AAATACAGGCAATGAGTCTTTGTCATCATCCAAATGTAGTTGCATACCACACAAGTTTT
GTATATAACGAGTCACTATGGGTAATTATGGATTTTT*TATCAGCTGGCTCATGCTCTG
ATATCATGAGATTTTCATTCCCTCAAGGTTTTGAAGAACATGTTATCGCCACTATCCTC
AAAGAAGCTTTGAAAGCAATTTGCTATTTTCATAAAACTGGCAGAATTCATAGAGATAT
TAAATCTGGTAATATTTTAATCGATTCAAATGGTAACATTCAATTAAGTGATTTTGGTG
TTAGTGCAACATTAATTGATACTGGTGAAACAAGTAGAAATACTTTTGTTGGTACACCT
TGTTGGATGGCACCTGTAAGTTTAAATTTTAAATTTTTTTTAAAAAAAAAAAAAAAAAA
AAAAAAAAAATATAATATTAATTATTTTATTTTATTTTTTTTAAAAAATTTAGGAAATT
ATGGAACAAGTTAATTATGATTATGCAGTTGATATTTGGTCATTTGGTATTACAGCATT
AGAACTTGCAAGAGGTAAGGCACCTTTTGCAGAATATCCACCAATGAAAGTTTTATTAT
TGACACTTCAAAACCCACCACCATCATTGGAGGGGGATGGCGAAAGTAAATGGTCTCAT
AGTTTTAAAGATTTAGTTGAAAAATGTCTTCAAAAGGATCCATCTAAAAGACCATTACC
TTCAAAACTTTTAGAACATAGATTCTTTAAGCAAGCAAAGAAACCAGATTATTTAGTTC
AACATATTTTGGCAAAATTACCACCATTAGGTCAAAGATATCAAATGTTATCCGAAGAT
TCATTTGCTATGCTTAGAAATACTTCTTCACCACAATTTGATACTGGTCATAGTAATTC
AGCTGATGAATGGATATTTCCAAATGAAAATAATGATAATAATAATTCATCAACTACAA
CTACAACAACTACAACTACAACTACAAATCCATCAAATAATAATAATAATAATAATAAT
AAAACTAAAGAAAATTTAACTCAATCACCATTTGAAACGCCATCACACACACCATCAAC
ATCACCAGGTTCAACACCAAGTCATAGTAGAACATCTACACCAACAAGTAATCATACAG
CACTTGGATCATCATCGACTGTCGTTCCTCCACCAGTTGTACCATTAACCTTACCAACA
GCTATTCCAGTTACTGCAGCTGCTTATCACCAACAACAACAACATCATCATTTATCCCA
TTCATCTGGAAGTATACCGAACCATAACGCCAGTAGTAATTTGGGTGCAAGCGCACATA
GTAATGTTCATGGTTTAGCACATAGTTCAATTCACCCAACATCTTCAGCAGCATCAACA
ACTGTTGTAAATAACACTCAACAACCTCAAACCTTACAACCACCACAACAACAACATCA
ACTACAACAACCAATTAAAACTCCAAGTCCGATCAACGCTATAAATATTGTTAAATTAA
ATCAATCTGATTTAATAACTCCACCAAAAACCTCACCAAAGAAAGAAGGTAGTATACCA
TCCTCTTCATCTCATGGTAATATTCCATCATTGGTTACAACCTCACCAAAATCACCATT
ACAACATCAACAACAAATACCACAACAACAACAAGATCCAGCTATGATAAATAGTAATA
ATAGTAGTATTAGTAGTAATGGCGCATACAATAGAGAATTAATATCTGCATCGGGTAGT
GCTCTATCAAAACCCCCATCTCCATCTTCCGATAAAGAAAATAACTCTACCAGTAAATC
AAATAAATCAAAATCTAGACAATCATCAAGAGCCTCCTCTTTATCAGAGAGTTCAGATT
CAACCTCTCATACTTCGAGCTCTGATGAACACTCTAGTAGATATGAAAGTGATAGAAAA
TCTTATAAAAAGAAAAAGAGCAGTAGCAGTAGTAGCAATAGTAAAAGAGATCGTGAACG
TGAACGTGACCGTGATCGTTCTAATAAAACCTATAAAAACTCTAGAAGTAGAAATGTTA
GTAGAGACAGAGAAAGAGAAAGAGATAGACATAATCGTTCAAGAGACAGAGATAGAGAA
AGAGAAAGGGAAAGAGATAGAGACAGAGAAAGAGATAGAGACAGAAGTAGAGATCGTTC
AAGAGATAGAAGTAGAGATAGAGAAAGAGATAGAAGTAGAGATCGTTCAAGAGATAGAG
ATAGAAGTAGAGATCGTTCAAGAGATAGAAGTAGAGAAAGGGATAGAGATAGAAGTAGA
GATAGAAGCAGAGATCGTTCAAGAAGTAGAGATTCTGATAGTAGGGATAGAAGTAGAGA
TCGTTCAAGAAGTCATTCCAACAGAAGAAGAAGTAGAAGTCGTGATAGTAGAAATAAAT
CCAGAGATAGATCATCTGATTCTGATAGAAGTAGAGACAGAAGTAGAGATAGAGATTAT
AAATCTTCAAAATATAAAAAGAGTAGTAGAGGTACCAGTGGTAGAAAGAATAATAAAAT
TCAATCAAAACTCGACTCCCAAGCAACTCATATTTCCTATCTTGAAGATAAGATATCCA

CACTCACCAATTGGCTTCAACAACAAAACCTTCTCAATACTAGTAATGGTCAAGTTTTA
TCTCCAACCGATCCAAATTTGGTTTCTAAACTTCAAACTCAATTGGATGTTCTTCAATC
AGAAAATTCTTATCTAAGAAATGAAAATATTAACTTGAAAACAATTGTAAATGGTTCAA
ATTCAACAAATAATTCATTAAATCAAAGTTCTGGTATGGCTTTTAGAAATAGCGTTTCT
TCTTTACATCAATTAAATATGAGTAATAGTAGTAATAATAGTAGACCACAAACTCAATA
A **3′**

*The nucleotides highlighted in green correspond to the WIF sequence motif, which is involved in aiding the binding of the pseudokinase STRAD to MO25 (Section 3.3.1).

3. MO25 genomic sequence from *D. discoideum*

DDB0304446|DDB_G0284307 |Genomic DNA|gene: DDB_G0284307 on chromosome: position 1707062 to 1708958

5′ATGAAATTAGAGAAAGGGATTTTCATGAAGATGAAGCTGAAGAAGATTGTCCAACAA
GTTGTTCAAGTGATGACCATGATGACACTTAAAAAGACAATAGAACAGGTCCAAATGAT
GTAAAATCCTTTATTCAAGTTAAAAAAAGCTTCAAATAATTTCAAAAAAACAAATAAAA
AAAAAAAAAAAGAACTCTTTAAAAACAAGAAATATTTTTATTTTATTTTTTTTTATTTT
ATTTTCTCTTTTTTTTATTACTATTACTATTTGTTTTTTTTTGGTTTTCTTTTTTTTTT
TTTTTTTTTTTTTTTTTTTTTTAAAATATGAGTTGATTTTAAAAAAAAAATAAAAAAAT
AAAAAAAAAAATTAATTTTTTTAAAAATTTTTTTTTTTTTAAAAAATTTTTTTTTTTTT
TTTTTTTTTTTTTCTCAATAATAACTAAAAATAATACGCCACAAAGTCAAAAGAGTATT
GTTTTTGCTATATCATATAGTATATAGATAATCGTTAAAATTATATATTTAATATATTT
TATAAAAAATTAAAGTAAAAAATAATAATAATAATAAAGAAATTTAATATATAAAC
AAAAAAAAAGAGACAAAGAGAGAGAAAATAAAATGAATATCTTTTTTAATAAAAAACAA
AAGACCCCATCAGAATTGGTTAAATCCATTAAAGAAAGCCTTGCTTCAATGGATAAAAG
TGGTCCAAACTCTAAATCAACCGAAAAGGTAAGCTATTTTTAATCATTGGAATCATTTT
CTATTTATATCTTATTTTTAAAAATAAAATAAAATAAAATAAAATAAAATAAAATAAAA
TAAAAAAAAAAAAAAAGATCATACCACAGTGACTATCAATTTTTTTTTTCTTTTACTCTT
TCTTTCCTTCTTTCTTCCTTAATAAATATTAACATTATCACACCCTCCTTCAATTTAAT
CAAAAAAATTTTTAAAAAAAAAAAAAAAAAAAAAAAAAAATAAAAGGCATCAGAAGAAAT
TTCAAAATGTTTACAAGAGATTAAAAAGATATTACATGGTGATTCAGAGCATGAACCAA
ATCAAGAGGTTGTTGCTGTATTATCAAATGAAATATGTACCAGTGATTTGGTACAAATC
CTTATTAAAGATTTAAACAAACTCGAGTTTGAAGCTAAAAAAGATGTAGCTCAAATTTT
CAATATTTTATTAAGACATAAAAATGGTGCTCGTTCACCAATTGTAGAATATATCGCTA
AAAATCCAGAAATTTTAGATTCATTAGTTAAAGGGTAATTAGTACTTAAATATAGTATA
ATAGACAGATAAAATATACATACCTACAGGAGTGATCGATCGATAGATAGGTAGATAGA
TATATAGATAAATAAATAATTATAGGAAGATAGTGATAGTTTAGTAATAATAGAAAATA
TCATTCCTCCCTCCCTCCAATTAATATCAAATACTGACATAAAATACCTAAATAAACAC
ATACATACATACATACATAAATAATCATTTATTTTAAATTATTAGTTACGAACAACAGG
ATATTGCATTAAATTGTGGTACAATGCTTAGGGAATGTATCAAGCATGAATCATTGGCT
AAAATTTTAATATATTCACCAAACTTTTGGGAGTTCTTTGAATTTGTTGAAGTTTCAAA
TTTTGATGTTGCTTCTGATACATTTGCCACCTTTAAAGAGATTTTAACAAAACATAAAA
CACTTAGCGCTGAATTTTTAGAAAAGAATTACGATCAGGTATATTTCATATATATATTT
ATTTATTTTTAG **3′**

6.7. Appendix 7 Primers and their features

Name	Sequence (5'-3')	TM (^{0}C)	Direction
Primers designed for PCR or Sequencing			
LKB1F	GC**GAATTCGCGGCCGC**ATGGAAGTTGAACAACA ACCATCATATACATCG	71	Forward
LKB1R	GC**GAATTCCTCGAG**TTAATTAATGATACATTTT GACTTATTATGTGGAG	65	Reverse
STRADF	GC**GTCGACGCGGCCGC**ATGTCCGATGATAAATATCATCATGATAAACATC	71	Forward
STRADR	GC**GTCGACCTCGAG**TTATTGAGTTTGTGGTCTACTATTATTACTACTATTACTC	68.5	Reverse
MO25F	GC**GAATTCGCGGCCGC** ATGAAATTAGAGAAAGGGATTTTC	67	Forward
MO25R	GC**GAATTCCTGCAG**CTAAAAATAAATAAATATATATATGAAATATACCTGATCG	64	Reverse
Primers designed for Sequencing			
LKB1F (Start site: 342)	CGGGGAAGCATCAGTTTTAAAAG	58.5	Forward
LKB1F (Start site: 810)	CAGCATTTCAACCACCAGAGTTA	59	Forward
LKB1R (Start site: 1241)	TTCTTCTAATAATGGCACAAATGG	59.5	Reverse
STRADF (Start site: 387)	TGTAGTTGCATACCACACAAGTT	58.5	Forward
STRADF (Start site: 903)	CACCTTTTGCAGAATATCCACCA	59	Forward
STRADF (Start site: 1393)	GCCATCACACACACCATCAA	59	Forward
STRADF (Start site:	TGGCTTCAACAACAAAACCTTC	58	Forward

2900)			
STRADR (Start site: 276)	TGGTAAACATATTGCACGTTGTAC	58	Reverse
STRADR (Start site: 1799)	TCGGACTTGGAGTTTTAATTGGT	58	Reverse
STRADR (Start site: 2811)	CCACTGGTACCTCTACTACTCTTTT	59	Reverse
MO25F (Start site: 707)	TGGTCCAAACTCTAAATCAACCG	59	Forward
MO25F (Start site: 1205)	GTGCTCGTTCACCAATTGTAGA	59	Forward
MO25R (Start site: 1078)	CAGCAACAACCTCTTGATTTGG	58	Reverse
MO25R (Start site: 1569)	CATTCCCTAAGCATTGTACCACA	59	Reverse
Primers designed for QPCR			
Fil1588F	CCCTCAATGATGAAGCC	47	
Fil1688R	CCATCTAAACCTGGACC	47	
LKB1QF	GCGCACCGTGCTGATAGAGTTGGCTCA	64	
LKB1QR	GCGCAAGGTGGTTGAGGTGAAGAACGGT	64	
STRADQF	GCGCACATAGTAATGTTCATGG	53	
STRADQR	GGTTTGAGGTTGTTGAGTGTTATT	52	
AMPKASQF	CAAGTTGTGGTTCACCCAATTAC	54	

AMPKASQR	CACCACAAGACCAAACATCAAC	53	

6.7. Appendix 8 Sequencing alignments

pPROF780 (pUC18-LKB1)

Length = 2052
Score = 10260
Identity = 2052 /2052 (100 %)
Similarity: 2052 /2052 (100 %)

```
1     ATGGAAGTTGAACAACAACCATCATATACATCGAATTTTATAATTCATTT     50
      |||||||||||||||||||||||||||||||||||||||||||||||||||
1     ATGGAAGTTGAACAACAACCATCATATACATCGAATTTTATAATTCATTT     50

51    AAATGAAAATGAAGATAATGGCATTTCATATAGATCAAGAAAATCTACAC    100
      |||||||||||||||||||||||||||||||||||||||||||||||||||
51    AAATGAAAATGAAGATAATGGCATTTCATATAGATCAAGAAAATCTACAC    100

101   CAAAATTAGTTAAACATTATATATTAGGTGAAGTTTTAGGTGAAGGTATT    150
      |||||||||||||||||||||||||||||||||||||||||||||||||||
101   CAAAATTAGTTAAACATTATATATTAGGTGAAGTTTTAGGTGAAGGTATT    150

151   TTTCAATCGATTATATATATATATATATATATATATATATCATTATATAT    200
      |||||||||||||||||||||||||||||||||||||||||||||||||||
151   TTTCAATCGATTATATATATATATATATATATATATATCATTATATAT    200

201   ATAGTATGAAATATATTAATTTATTATTTATTAATTATTTTTAGGTGCTT    250
      |||||||||||||||||||||||||||||||||||||||||||||||||||
201   ATAGTATGAAATATATTAATTTATTATTTATTAATTATTTTTAGGTGCTT    250

251   ATGGTAAAGTTAAAGATGGCATGGATTCATTTACACAAAAAAGAGTAGCA    300
      |||||||||||||||||||||||||||||||||||||||||||||||||||
251   ATGGTAAAGTTAAAGATGGCATGGATTCATTTACACAAAAAAGAGTAGCA    300

301   GTTAAAATATTAAAAAGAGCAAGATTAAAAAAGATTCCTGGCGGGGAAGC    350
      |||||||||||||||||||||||||||||||||||||||||||||||||||
301   GTTAAAATATTAAAAAGAGCAAGATTAAAAAAGATTCCTGGCGGGGAAGC    350

351   ATCAGTTTTAAAAGAGATTAATATTACAAAAAAGTTACACAATAAACATA    400
      |||||||||||||||||||||||||||||||||||||||||||||||||||
351   ATCAGTTTTAAAAGAGATTAATATTACAAAAAAGTTACACAATAAACATA    400

401   TAATCAAATTAATTGATCATTTCATTATAGAGGAAAAAGGTAAACTGTAC    450
      |||||||||||||||||||||||||||||||||||||||||||||||||||
401   TAATCAAATTAATTGATCATTTCATTATAGAGGAAAAAGGTAAACTGTAC    450

451   ATTGTCTATGAATATGTTGGTGGTGGAACTTCACAAAATATTTTAGAAAA    500
      |||||||||||||||||||||||||||||||||||||||||||||||||||
451   ATTGTCTATGAATATGTTGGTGGTGGAACTTCACAAAATATTTTAGAAAA    500

501   TGCACCAAATGGTAGATTACCACCACACCAATCACAATTGTATGTATTAT    550
      |||||||||||||||||||||||||||||||||||||||||||||||||||
501   TGCACCAAATGGTAGATTACCACCACACCAATCACAATTGTATGTATTAT    550

551   TTATTTTTTAAAATTTTTATATTTTATTTTTATTATTAAATAAAATATTT    600
      |||||||||||||||||||||||||||||||||||||||||||||||||||
551   TTATTTTTTAAAATTTTTATATTTTATTTTTATTATTAAATAAAATATTT    600

601   TATTAATAATAATAATAATTACAGTATATTTAGACAATTAATTGAAGCAT    650
```

```
     ||||||||||||||||||||||||||||||||||||||||||||||||||||||||
601  TATTAATAATAATAATAATTACAGTATATTTAGACAATTAATTGAAGCAT    650

651  GTGAATATATTCATTCACAAAAGATATTACATCGTGATATTAAACCTGAT    700
     ||||||||||||||||||||||||||||||||||||||||||||||||||||||||
651  GTGAATATATTCATTCACAAAAGATATTACATCGTGATATTAAACCTGAT    700

701  AATATACTATTTACACATGCAAATGTATTGAAATTGAGTGATTTTGGAGT    750
     ||||||||||||||||||||||||||||||||||||||||||||||||||||||||
701  AATATACTATTTACACATGCAAATGTATTGAAATTGAGTGATTTTGGAGT    750

751  TGCAGAGGATAGTAGCCAATTGGAAGATTTTGAATGTTTATCAAGAAGTT    800
     ||||||||||||||||||||||||||||||||||||||||||||||||||||||||
751  TGCAGAGGATAGTAGCCAATTGGAAGATTTTGAATGTTTATCAAGAAGTT    800

801  ATGGTTCACCAGCATTTCAACCACCAGAGTTAACACAATTTCAAACTACA    850
     ||||||||||||||||||||||||||||||||||||||||||||||||||||||||
801  ATGGTTCACCAGCATTTCAACCACCAGAGTTAACACAATTTCAAACTACA    850

851  TTTTCACCATTTAAAATCGATATTTGGGCAATGGGTGTAACATTATACCT    900
     ||||||||||||||||||||||||||||||||||||||||||||||||||||||||
851  TTTTCACCATTTAAAATCGATATTTGGGCAATGGGTGTAACATTATACCT    900

901  TATGACCATTGGTAAATTCCCTTTTTCCGGTGCAAATATGTTTGTACTTT    950
     ||||||||||||||||||||||||||||||||||||||||||||||||||||||||
901  TATGACCATTGGTAAATTCCCTTTTTCCGGTGCAAATATGTTTGTACTTT    950

951  TTGAAAATATCTCTAAATGTAAAATAGAATTTCCAAATGATCTCGATAAA   1000
     ||||||||||||||||||||||||||||||||||||||||||||||||||||||||
951  TTGAAAATATCTCTAAATGTAAAATAGAATTTCCAAATGATCTCGATAAA   1000

1001 GATTTGGTTAATTTAATTAAAGGTATTTTACAAGTTGATCATATTCAAAG   1050
     ||||||||||||||||||||||||||||||||||||||||||||||||||||||||
1001 GATTTGGTTAATTTAATTAAAGGTATTTTACAAGTTGATCATATTCAAAG   1050

1051 ATTTTCATTAGGTCAAATTAAAAATCATCCGTAAAGTATTAAATAAATAA   1100
     ||||||||||||||||||||||||||||||||||||||||||||||||||||||||
1051 ATTTTCATTAGGTCAAATTAAAAATCATCCGTAAAGTATTAAATAAATAA   1100

1101 ATAATAATAATAATAATAATAAAACTATTTAAATAGATAAGAGAGAGATA   1150
     ||||||||||||||||||||||||||||||||||||||||||||||||||||||||
1101 ATAATAATAATAATAATAATAAAACTATTTAAATAGATAAGAGAGAGATA   1150

1151 AATATTAATACCTTTTTTTTTATTTTCATAAATTTAGGTGGTGTATTAAA   1200
     ||||||||||||||||||||||||||||||||||||||||||||||||||||||||
1151 AATATTAATACCTTTTTTTTTATTTTCATAAATTTAGGTGGTGTATTAAA   1200


1201 TATATACCAGAGGTAGAACCATTTGTGCCATTATTAGAAGAAAGTAAATT   1250
     ||||||||||||||||||||||||||||||||||||||||||||||||||||||||
1201 TATATACCAGAGGTAGAACCATTTGTGCCATTATTAGAAGAAAGTAAATT   1250

1251 TTTACCATTAGAGATGGCATATGGTGATGATGAAGGTGATGATGGTGGAG   1300
     ||||||||||||||||||||||||||||||||||||||||||||||||||||||||
1251 TTTACCATTAGAGATGGCATATGGTGATGATGAAGGTGATGATGGTGGAG   1300

1301 GTGGTAGAGGAGGAGGAGGAGATGATGAACTTATTTTTGGTTATGAAAAT   1350
     ||||||||||||||||||||||||||||||||||||||||||||||||||||||||
1301 GTGGTAGAGGAGGAGGAGGAGATGATGAACTTATTTTTGGTTATGAAAAT   1350

1351 GATGGAAATACAATAGATTTACAAGATCCAGAATATATACCCTCTATATC   1400
     ||||||||||||||||||||||||||||||||||||||||||||||||||||||||
1351 GATGGAAATACAATAGATTTACAAGATCCAGAATATATACCCTCTATATC   1400
```

```
1401 AGTGGGTGATCAACCACCATCAACTCCAATATTACATAGTAGTGATCATC   1450
     ||||||||||||||||||||||||||||||||||||||||||||||||||
1401 AGTGGGTGATCAACCACCATCAACTCCAATATTACATAGTAGTGATCATC   1450

1451 ATCATCATCATCATCATAATAACCAACATCAACATCAACAACAACAACAG   1500
     ||||||||||||||||||||||||||||||||||||||||||||||||||
1451 ATCATCATCATCATCATAATAACCAACATCAACATCAACAACAACAACAG   1500

1501 CAACTACAACAATCACAACAATTTCATGGTAATGGAGATAATAATTTATT   1550
     ||||||||||||||||||||||||||||||||||||||||||||||||||
1501 CAACTACAACAATCACAACAATTTCATGGTAATGGAGATAATAATTTATT   1550

1551 ATTTGATTCAAATAATAATTTAATATTTGATTCAAATAATAATTTATTAT   1600
     ||||||||||||||||||||||||||||||||||||||||||||||||||
1551 ATTTGATTCAAATAATAATTTAATATTTGATTCAAATAATAATTTATTAT   1600

1601 TTAATACAAATAATAATGAACATTTAATTAATGGTTTACCAGTGCACCCA   1650
     ||||||||||||||||||||||||||||||||||||||||||||||||||
1601 TTAATACAAATAATAATGAACATTTAATTAATGGTTTACCAGTGCACCCA   1650

1651 ATTGAACTCGACCCTGTAAATATTAAAAAGAGTTCAATTGGTACAAATAT   1700
     ||||||||||||||||||||||||||||||||||||||||||||||||||
1651 ATTGAACTCGACCCTGTAAATATTAAAAAGAGTTCAATTGGTACAAATAT   1700

1701 TTCTGATGTGGCTTTAATTCGTGAGAATTATATATGCTCTGATAATGATG   1750
     ||||||||||||||||||||||||||||||||||||||||||||||||||
1701 TTCTGATGTGGCTTTAATTCGTGAGAATTATATATGCTCTGATAATGATG   1750

1751 CTAGTAGTGGTCAAGATGATGAAGACTATTCAGATGATAATGAAATTAGT   1800
     ||||||||||||||||||||||||||||||||||||||||||||||||||
1751 CTAGTAGTGGTCAAGATGATGAAGACTATTCAGATGATAATGAAATTAGT   1800

1801 GGTGAAGATTTAAATCCAACAAATCACCACCACCACCGTGCTGATAGAGT   1850
     ||||||||||||||||||||||||||||||||||||||||||||||||||
1801 GGTGAAGATTTAAATCCAACAAATCACCACCACCACCGTGCTGATAGAGT   1850

1851 TGGCTCACGTGATAAGAGTTCAAGATCAAGTAAAAGAAAGAATAGTAGTA   1900
     ||||||||||||||||||||||||||||||||||||||||||||||||||
1851 TGGCTCACGTGATAAGAGTTCAAGATCAAGTAAAAGAAAGAATAGTAGTA   1900


1901 GTAATAATAATAATAATAATTCCACTTCTCCAAAAGTTGAATTTAATCCA   1950
     ||||||||||||||||||||||||||||||||||||||||||||||||||
1901 GTAATAATAATAATAATAATTCCACTTCTCCAAAAGTTGAATTTAATCCA   1950

1951 AACCGTTCTTCACCTCAACCACCTTTAAGAAATTCAAGTAATAGAAGGCC   2000
     ||||||||||||||||||||||||||||||||||||||||||||||||||
1951 AACCGTTCTTCACCTCAACCACCTTTAAGAAATTCAAGTAATAGAAGGCC   2000

2001 AAAAATTACTTTTGAATCTCCACATAATAAGTCAAAATGTATCATTAATT   2050
     ||||||||||||||||||||||||||||||||||||||||||||||||||
2001 AAAAATTACTTTTGAATCTCCACATAATAAGTCAAAATGTATCATTAATT   2050

2051 AA   2052
     ||
2051 AA   2052
```

Note: The query sequence is from the construct sequenced by AGRF and the subject sequence is from the native gene sequence acquired from dictyBase.

pPROF782 (pPROF267-LKB1 DEAD KINASE)

Length = 2052
Score = 10233
Identity = 2049 /2052 (99.9 %)
Similarity: 2049 /2052 (99.9 %)

```
1     ATGGAAGTTGAACAACAACCATCATATACATCGAATTTTATAATTCATTT     50
      ||||||||||||||||||||||||||||||||||||||||||||||||||
1     ATGGAAGTTGAACAACAACCATCATATACATCGAATTTTATAATTCATTT     50

51    AAATGAAAATGAAGATAATGGCATTTCATATAGATCAAGAAAATCTACAC    100
      ||||||||||||||||||||||||||||||||||||||||||||||||||
51    AAATGAAAATGAAGATAATGGCATTTCATATAGATCAAGAAAATCTACAC    100

101   CAAAATTAGTTAAACATTATATATTAGGTGAAGTTTTAGGTGAAGGTATT    150
      ||||||||||||||||||||||||||||||||||||||||||||||||||
101   CAAAATTAGTTAAACATTATATATTAGGTGAAGTTTTAGGTGAAGGTATT    150

151   TTTCAATCGATTATATATATATATATATATATATATATATCATTATATAT    200
      ||||||||||||||||||||||||||||||||||||||||||||||||||
151   TTTCAATCGATTATATATATATATATATATATATATATCATTATATAT    200

201   ATAGTATGAAATATATTAATTTATTATTTATTAATTATTTTTAGGTGCTT    250
      ||||||||||||||||||||||||||||||||||||||||||||||||||
201   ATAGTATGAAATATATTAATTTATTATTTATTAATTATTTTTAGGTGCTT    250

251   ATGGTAAAGTTAAAGATGGCATGGATTCATTTACACAAAAAAGAGTAGCA    300
      ||||||||||||||||||||||||||||||||||||||||||||||||||
251   ATGGTAAAGTTAAAGATGGCATGGATTCATTTACACAAAAAAGAGTAGCA    300

301   GTTAAAATATTAAAAAAGAGCAAGATTAAAAAAGATTCCTGGCGGGGAAGC    350
      |||||  ||||||||||||||||||||||||||||||||||||||||||
301   GTTAATGTATTAAAAAAGAGCAAGATTAAAAAAGATTCCTGGCGGGGAAGC    350

351   ATCAGTTTTAAAAGAGATTAATATTACAAAAAAGTTACACAATAAACATA    400
      ||||||||||||||||||||||||||||||||||||||||||||||||||
351   ATCAGTTTTAAAAGAGATTAATATTACAAAAAAGTTACACAATAAACATA    400

401   TAATCAAATTAATTGATCATTTCATTATAGAGGAAAAAGGTAAACTGTAC    450
      ||||||||||||||||||||||||||||||||||||||||||||||||||
401   TAATCAAATTAATTGATCATTTCATTATAGAGGAAAAAGGTAAACTGTAC    450

451   ATTGTCTATGAATATGTTGGTGGTGGAACTTCACAAAATATTTTAGAAAA    500
      ||||||||||||||||||||||||||||||||||||||||||||||||||
451   ATTGTCTATGAATATGTTGGTGGTGGAACTTCACAAAATATTTTAGAAAA    500

501   TGCACCAAATGGTAGATTACCACCACACCAATCACAATTGTATGTATTAT    550
      ||||||||||||||||||||||||||||||||||||||||||||||||||
501   TGCACCAAATGGTAGATTACCACCACACCAATCACAATTGTATGTATTAT    550

551   TTATTTTTTAAAATTTTTATATTTTATTTTTATTATTAAATAAAATATTT    600
      ||||||||||||||||||||||||||||||||||||||||||||||||||
551   TTATTTTTTAAAATTTTTATATTTTATTTTTATTATTAAATAAAATATTT    600

601   TATTAATAATAATAATAATTACAGTATATTTAGACAATTAATTGAAGCAT    650
      ||||||||||||||||||||||||||||||||||||||||||||||||||
601   TATTAATAATAATAATAATTACAGTATATTTAGACAATTAATTGAAGCAT    650
```

```
651  GTGAATATATTCATTCACAAAAGATATTACATCGTGATATTAAACCTGAT    700
     ||||||||||||||||||||||||||||||||||||||||||||||||||
651  GTGAATATATTCATTCACAAAAGATATTACATCGTGATATTAAACCTGAT    700

701  AATATACTATTTACACATGCAAATGTATTGAAATTGAGTGATTTTGGAGT    750
     |||||||||||||||||||||||||||||||||||||| |||||||||
701  AATATACTATTTACACATGCAAATGTATTGAAATTGAGTGCTTTTGGAGT    750

751  TGCAGAGGATAGTAGCCAATTGGAAGATTTTGAATGTTTATCAAGAAGTT    800
     ||||||||||||||||||||||||||||||||||||||||||||||||||
751  TGCAGAGGATAGTAGCCAATTGGAAGATTTTGAATGTTTATCAAGAAGTT    800

801  ATGGTTCACCAGCATTTCAACCACCAGAGTTAACACAATTTCAAACTACA    850
     ||||||||||||||||||||||||||||||||||||||||||||||||||
801  ATGGTTCACCAGCATTTCAACCACCAGAGTTAACACAATTTCAAACTACA    850

851  TTTTCACCATTTAAAATCGATATTTGGGCAATGGGTGTAACATTATACCT    900
     ||||||||||||||||||||||||||||||||||||||||||||||||||
851  TTTTCACCATTTAAAATCGATATTTGGGCAATGGGTGTAACATTATACCT    900

901  TATGACCATTGGTAAATTCCCTTTTTCCGGTGCAAATATGTTTGTACTTT    950
     ||||||||||||||||||||||||||||||||||||||||||||||||||
901  TATGACCATTGGTAAATTCCCTTTTTCCGGTGCAAATATGTTTGTACTTT    950

951  TTGAAAATATCTCTAAATGTAAAATAGAATTTCCAAATGATCTCGATAAA   1000
     ||||||||||||||||||||||||||||||||||||||||||||||||||
951  TTGAAAATATCTCTAAATGTAAAATAGAATTTCCAAATGATCTCGATAAA   1000

1001 GATTTGGTTAATTTAATTAAAGGTATTTTACAAGTTGATCATATTCAAAG   1050
     ||||||||||||||||||||||||||||||||||||||||||||||||||
1001 GATTTGGTTAATTTAATTAAAGGTATTTTACAAGTTGATCATATTCAAAG   1050

1051 ATTTTCATTAGGTCAAATTAAAAATCATCCGTAAAGTATTAAATAAATAA   1100
     ||||||||||||||||||||||||||||||||||||||||||||||||||
1051 ATTTTCATTAGGTCAAATTAAAAATCATCCGTAAAGTATTAAATAAATAA   1100

1101 ATAATAATAATAATAATAATAAAACTATTTAAATAGATAAGAGAGAGATA   1150
     ||||||||||||||||||||||||||||||||||||||||||||||||||
1101 ATAATAATAATAATAATAATAAAACTATTTAAATAGATAAGAGAGAGATA   1150

1151 AATATTAATACCTTTTTTTTTATTTTCATAAATTTAGGTGGTGTATTAAA   1200
     ||||||||||||||||||||||||||||||||||||||||||||||||||
1151 AATATTAATACCTTTTTTTTTATTTTCATAAATTTAGGTGGTGTATTAAA   1200

1201 TATATACCAGAGGTAGAACCATTTGTGCCATTATTAGAAGAAAGTAAATT   1250
     ||||||||||||||||||||||||||||||||||||||||||||||||||
1201 TATATACCAGAGGTAGAACCATTTGTGCCATTATTAGAAGAAAGTAAATT   1250

1251 TTTACCATTAGAGATGGCATATGGTGATGATGAAGGTGATGATGGTGGAG   1300
     ||||||||||||||||||||||||||||||||||||||||||||||||||
1251 TTTACCATTAGAGATGGCATATGGTGATGATGAAGGTGATGATGGTGGAG   1300

1301 GTGGTAGAGGAGGAGGAGGAGATGATGAACTTATTTTTGGTTATGAAAAT   1350
     ||||||||||||||||||||||||||||||||||||||||||||||||||
1301 GTGGTAGAGGAGGAGGAGGAGATGATGAACTTATTTTTGGTTATGAAAAT   1350

1351 GATGGAAATACAATAGATTTACAAGATCCAGAATATATACCCTCTATATC   1400
     ||||||||||||||||||||||||||||||||||||||||||||||||||
1351 GATGGAAATACAATAGATTTACAAGATCCAGAATATATACCCTCTATATC   1400

1401 AGTGGGTGATCAACCACCATCAACTCCAATATTACATAGTAGTGATCATC   1450
     ||||||||||||||||||||||||||||||||||||||||||||||||||
1401 AGTGGGTGATCAACCACCATCAACTCCAATATTACATAGTAGTGATCATC   1450
```

```
1451 ATCATCATCATCATCATAATAACCAACATCAACATCAACAACAACAACAG   1500
     ||||||||||||||||||||||||||||||||||||||||||||||||||
1451 ATCATCATCATCATCATAATAACCAACATCAACATCAACAACAACAACAG   1500

1501 CAACTACAACAATCACAACAATTTCATGGTAATGGAGATAATAATTTATT   1550
     ||||||||||||||||||||||||||||||||||||||||||||||||||
1501 CAACTACAACAATCACAACAATTTCATGGTAATGGAGATAATAATTTATT   1550

1551 ATTTGATTCAAATAATAATTTAATATTTGATTCAAATAATAATTTATTAT   1600
     ||||||||||||||||||||||||||||||||||||||||||||||||||
1551 ATTTGATTCAAATAATAATTTAATATTTGATTCAAATAATAATTTATTAT   1600

1601 TTAATACAAATAATAATGAACATTTAATTAATGGTTTACCAGTGCACCCA   1650
     ||||||||||||||||||||||||||||||||||||||||||||||||||
1601 TTAATACAAATAATAATGAACATTTAATTAATGGTTTACCAGTGCACCCA   1650


1651 ATTGAACTCGACCCTGTAAATATTAAAAAGAGTTCAATTGGTACAAATAT   1700
     ||||||||||||||||||||||||||||||||||||||||||||||||||
1651 ATTGAACTCGACCCTGTAAATATTAAAAAGAGTTCAATTGGTACAAATAT   1700

1701 TTCTGATGTGGCTTTAATTCGTGAGAATTATATATGCTCTGATAATGATG   1750
     ||||||||||||||||||||||||||||||||||||||||||||||||||
1701 TTCTGATGTGGCTTTAATTCGTGAGAATTATATATGCTCTGATAATGATG   1750

1751 CTAGTAGTGGTCAAGATGATGAAGACTATTCAGATGATAATGAAATTAGT   1800
     ||||||||||||||||||||||||||||||||||||||||||||||||||
1751 CTAGTAGTGGTCAAGATGATGAAGACTATTCAGATGATAATGAAATTAGT   1800

1801 GGTGAAGATTTAAATCCAACAAATCACCACCACCACCGTGCTGATAGAGT   1850
     ||||||||||||||||||||||||||||||||||||||||||||||||||
1801 GGTGAAGATTTAAATCCAACAAATCACCACCACCACCGTGCTGATAGAGT   1850

1851 TGGCTCACGTGATAAGAGTTCAAGATCAAGTAAAAGAAAGAATAGTAGTA   1900
     ||||||||||||||||||||||||||||||||||||||||||||||||||
1851 TGGCTCACGTGATAAGAGTTCAAGATCAAGTAAAAGAAAGAATAGTAGTA   1900


1901 GTAATAATAATAATAATAATTCCACTTCTCCAAAAGTTGAATTTAATCCA   1950
     ||||||||||||||||||||||||||||||||||||||||||||||||||
1901 GTAATAATAATAATAATAATTCCACTTCTCCAAAAGTTGAATTTAATCCA   1950

1951 AACCGTTCTTCACCTCAACCACCTTTAAGAAATTCAAGTAATAGAAGGCC   2000
     ||||||||||||||||||||||||||||||||||||||||||||||||||
1951 AACCGTTCTTCACCTCAACCACCTTTAAGAAATTCAAGTAATAGAAGGCC   2000

2001 AAAAATTACTTTTGAATCTCCACATAATAAGTCAAAATGTATCATTAATT   2050
     ||||||||||||||||||||||||||||||||||||||||||||||||||
2001 AAAAATTACTTTTGAATCTCCACATAATAAGTCAAAATGTATCATTAATT   2050

2051 AA   2052
     ||
2051 AA   2052
```

Note: The query sequence is from the construct sequenced by AGRF and the subject sequence is from the native gene sequence acquired from dictyBase. The nucleotides highlighted in yellow are mutated via site directed mutagenesis (Section 2.3.3).

pPROF783 (pUC18-STRAD)

Length: 3184
Score: 15920.0
Identity: 3184/3184 (100.0%)
Similarity: 3184/3184 (100.0%

```
1     ATGTCCGATGATAAATATCATCATGATAAACATCATGATAAGCATCATAT     50
      ||||||||||||||||||||||||||||||||||||||||||||||||||
1     ATGTCCGATGATAAATATCATCATGATAAACATCATGATAAGCATCATAT     50

51    AGATTCAAAGCAAAGTACAGCAGCAGCATTATCATCATCATCGACATTAG    100
      ||||||||||||||||||||||||||||||||||||||||||||||||||
51    AGATTCAAAGCAAAGTACAGCAGCAGCATTATCATCATCATCGACATTAG    100

101   CTTCATCCTCCTCCATGACAACAACAACAACAACAACGTCAACAACAACA    150
      ||||||||||||||||||||||||||||||||||||||||||||||||||
101   CTTCATCCTCCTCCATGACAACAACAACAACAACAACGTCAACAACAACA    150

151   ACGGCAGCATCTCCAATAACACCAAAACCAAGAAAAAATTACCCAAATTC    200
      ||||||||||||||||||||||||||||||||||||||||||||||||||
151   ACGGCAGCATCTCCAATAACACCAAAACCAAGAAAAAATTACCCAAATTC    200

201   AGCAGATCAATATGAACTTAAGGAAACCATTGGTAAAGGTGGAAGCGGAT    250
      ||||||||||||||||||||||||||||||||||||||||||||||||||
201   AGCAGATCAATATGAACTTAAGGAAACCATTGGTAAAGGTGGAAGCGGAT    250

251   TAGTACAACGTGCAATATGTTTACCATTTCAAGAGAATGTAGCTATAAAG    300
      ||||||||||||||||||||||||||||||||||||||||||||||||||
251   TAGTACAACGTGCAATATGTTTACCATTTCAAGAGAATGTAGCTATAAAG    300

301   ATTATAGATTTAGAGCATTGTAAAAACGTATCATTAGAAGAGATTAGAAA    350
      ||||||||||||||||||||||||||||||||||||||||||||||||||
301   ATTATAGATTTAGAGCATTGTAAAAACGTATCATTAGAAGAGATTAGAAA    350

351   GGAAATACAGGCAATGAGTCTTTGTCATCATCCAAATGTAGTTGCATACC    400
      ||||||||||||||||||||||||||||||||||||||||||||||||||
351   GGAAATACAGGCAATGAGTCTTTGTCATCATCCAAATGTAGTTGCATACC    400

401   ACACAAGTTTTGTATATAACGAGTCACTATGGGTAATTATGGATTTTTTA    450
      ||||||||||||||||||||||||||||||||||||||||||||||||||
401   ACACAAGTTTTGTATATAACGAGTCACTATGGGTAATTATGGATTTTTTA    450

451   TCAGCTGGCTCATGCTCTGATATCATGAGATTTTCATTCCCTCAAGGTTT    500
      ||||||||||||||||||||||||||||||||||||||||||||||||||
451   TCAGCTGGCTCATGCTCTGATATCATGAGATTTTCATTCCCTCAAGGTTT    500

501   TGAAGAACATGTTATCGCCACTATCCTCAAAGAAGCTTTGAAAGCAATTT    550
      ||||||||||||||||||||||||||||||||||||||||||||||||||
501   TGAAGAACATGTTATCGCCACTATCCTCAAAGAAGCTTTGAAAGCAATTT    550

551   GCTATTTTCATAAAACTGGCAGAATTCATAGAGATATTAAATCTGGTAAT    600
      ||||||||||||||||||||||||||||||||||||||||||||||||||
551   GCTATTTTCATAAAACTGGCAGAATTCATAGAGATATTAAATCTGGTAAT    600

601   ATTTTAATCGATTCAAATGGTAACATTCAATTAAGTGATTTTGGTGTTAG    650
      ||||||||||||||||||||||||||||||||||||||||||||||||||
601   ATTTTAATCGATTCAAATGGTAACATTCAATTAAGTGATTTTGGTGTTAG    650

651   TGCAACATTAATTGATACTGGTGAAACAAGTAGAAATACTTTTGTTGGTA    700
```

```
     ||||||||||||||||||||||||||||||||||||||||||||||||||||||
651  TGCAACATTAATTGATACTGGTGAAACAAGTAGAAATACTTTTGTTGGTA    700

701  CACCTTGTTGGATGGCACCTGTAAGTTTAAATTTTAAATTTTTTTTAAAA    750
     ||||||||||||||||||||||||||||||||||||||||||||||||||||||
701  CACCTTGTTGGATGGCACCTGTAAGTTTAAATTTTAAATTTTTTTTAAAA    750

751  AAAAAAAAAAAAAAAAAAAAAAAATATAATATTAATTATTTTATTTTATT    800
     ||||||||||||||||||||||||||||||||||||||||||||||||||||||
751  AAAAAAAAAAAAAAAAAAAAAAAATATAATATTAATTATTTTATTTTATT    800

801  TTTTTTAAAAAATTTAGGAAATTATGGAACAAGTTAATTATGATTATGCA    850
     ||||||||||||||||||||||||||||||||||||||||||||||||||||||
801  TTTTTTAAAAAATTTAGGAAATTATGGAACAAGTTAATTATGATTATGCA    850

851 GTTGATATTTGGTCATTTGGTATTACAGCATTAGAACTTGCAAGAGGTAA    900
    ||||||||||||||||||||||||||||||||||||||||||||||||||||||
851 GTTGATATTTGGTCATTTGGTATTACAGCATTAGAACTTGCAAGAGGTAA    900

901 GGCACCTTTTGCAGAATATCCACCAATGAAAGTTTTATTATTGACACTTC    950
    ||||||||||||||||||||||||||||||||||||||||||||||||||||||
901 GGCACCTTTTGCAGAATATCCACCAATGAAAGTTTTATTATTGACACTTC    950

951 AAAACCCACCACCATCATTGGAGGGGGATGGCGAAAGTAAATGGTCTCAT   1000
    ||||||||||||||||||||||||||||||||||||||||||||||||||||||
951 AAAACCCACCACCATCATTGGAGGGGGATGGCGAAAGTAAATGGTCTCAT   1000

1001 AGTTTTAAAGATTTAGTTGAAAAATGTCTTCAAAAGGATCCATCTAAAAG   1050
     ||||||||||||||||||||||||||||||||||||||||||||||||||||||
1001 AGTTTTAAAGATTTAGTTGAAAAATGTCTTCAAAAGGATCCATCTAAAAG   1050

1051 ACCATTACCTTCAAAACTTTTAGAACATAGATTCTTTAAGCAAGCAAAGA   1100
     ||||||||||||||||||||||||||||||||||||||||||||||||||||||
1051 ACCATTACCTTCAAAACTTTTAGAACATAGATTCTTTAAGCAAGCAAAGA   1100

1101 AACCAGATTATTTAGTTCAACATATTTTGGCAAAATTACCACCATTAGGT   1150
     ||||||||||||||||||||||||||||||||||||||||||||||||||||||
1101 AACCAGATTATTTAGTTCAACATATTTTGGCAAAATTACCACCATTAGGT   1150

1151 CAAAGATATCAAATGTTATCCGAAGATTCATTTGCTATGCTTAGAAATAC   1200
     ||||||||||||||||||||||||||||||||||||||||||||||||||||||
1151 CAAAGATATCAAATGTTATCCGAAGATTCATTTGCTATGCTTAGAAATAC   1200

1201 TTCTTCACCACAATTTGATACTGGTCATAGTAATTCAGCTGATGAATGGA   1250
     ||||||||||||||||||||||||||||||||||||||||||||||||||||||
1201 TTCTTCACCACAATTTGATACTGGTCATAGTAATTCAGCTGATGAATGGA   1250


1251 TATTTCCAAATGAAAATAATGATAATAATAATTCATCAACTACAACTACA   1300
     ||||||||||||||||||||||||||||||||||||||||||||||||||||||
1251 TATTTCCAAATGAAAATAATGATAATAATAATTCATCAACTACAACTACA   1300

1301 ACAACTACAACTACAACTACAAATCCATCAAATAATAATAATAATAATAA   1350
     ||||||||||||||||||||||||||||||||||||||||||||||||||||||
1301 ACAACTACAACTACAACTACAAATCCATCAAATAATAATAATAATAATAA   1350

1351 TAATAAAACTAAAGAAAATTTAACTCAATCACCATTTGAAACGCCATCAC   1400
     ||||||||||||||||||||||||||||||||||||||||||||||||||||||
1351 TAATAAAACTAAAGAAAATTTAACTCAATCACCATTTGAAACGCCATCAC   1400

1401 ACACACCATCAACATCACCAGGTTCAACACCAAGTCATAGTAGAACATCT   1450
     ||||||||||||||||||||||||||||||||||||||||||||||||||||||
1401 ACACACCATCAACATCACCAGGTTCAACACCAAGTCATAGTAGAACATCT   1450
```

```
1451 ACACCAACAAGTAATCATACAGCACTTGGATCATCATCGACTGTCGTTCC   1500
     ||||||||||||||||||||||||||||||||||||||||||||||||||
1451 ACACCAACAAGTAATCATACAGCACTTGGATCATCATCGACTGTCGTTCC   1500

1501 TCCACCAGTTGTACCATTAACCTTACCAACAGCTATTCCAGTTACTGCAG   1550
     ||||||||||||||||||||||||||||||||||||||||||||||||||
1501 TCCACCAGTTGTACCATTAACCTTACCAACAGCTATTCCAGTTACTGCAG   1550

1551 CTGCTTATCACCAACAACAACAACATCATCATTTATCCCATTCATCTGGA   1600
     ||||||||||||||||||||||||||||||||||||||||||||||||||
1551 CTGCTTATCACCAACAACAACAACATCATCATTTATCCCATTCATCTGGA   1600

1601 AGTATACCGAACCATAACGCCAGTAGTAATTTGGGTGCAAGCGCACATAG   1650
     ||||||||||||||||||||||||||||||||||||||||||||||||||
1601 AGTATACCGAACCATAACGCCAGTAGTAATTTGGGTGCAAGCGCACATAG   1650

1651 TAATGTTCATGGTTTAGCACATAGTTCAATTCACCCAACATCTTCAGCAG   1700
     ||||||||||||||||||||||||||||||||||||||||||||||||||
1651 TAATGTTCATGGTTTAGCACATAGTTCAATTCACCCAACATCTTCAGCAG   1700

1701 CATCAACAACTGTTGTAAATAACACTCAACAACCTCAAACCTTACAACCA   1750
     ||||||||||||||||||||||||||||||||||||||||||||||||||
1701 CATCAACAACTGTTGTAAATAACACTCAACAACCTCAAACCTTACAACCA   1750

1751 CCACAACAACAACATCAACTACAACAACCAATTAAAACTCCAAGTCCGAT   1800
     ||||||||||||||||||||||||||||||||||||||||||||||||||
1751 CCACAACAACAACATCAACTACAACAACCAATTAAAACTCCAAGTCCGAT   1800

1801 CAACGCTATAAATATTGTTAAATTAAATCAATCTGATTTAATAACTCCAC   1850
     ||||||||||||||||||||||||||||||||||||||||||||||||||
1801 CAACGCTATAAATATTGTTAAATTAAATCAATCTGATTTAATAACTCCAC   1850

1851 CAAAAACCTCACCAAAGAAAGAAGGTAGTATACCATCCTCTTCATCTCAT   1900
     ||||||||||||||||||||||||||||||||||||||||||||||||||
1851 CAAAAACCTCACCAAAGAAAGAAGGTAGTATACCATCCTCTTCATCTCAT   1900

1901 GGTAATATTCCATCATTGGTTACAACCTCACCAAAATCACCATTACAACA   1950
     ||||||||||||||||||||||||||||||||||||||||||||||||||
1901 GGTAATATTCCATCATTGGTTACAACCTCACCAAAATCACCATTACAACA   1950


1951 TCAACAACAAATACCACAACAACAACAAGATCCAGCTATGATAAATAGTA   2000
     ||||||||||||||||||||||||||||||||||||||||||||||||||
1951 TCAACAACAAATACCACAACAACAACAAGATCCAGCTATGATAAATAGTA   2000

2001 ATAATAGTAGTATTAGTAGTAATGGCGCATACAATAGAGAATTAATATCT   2050
     ||||||||||||||||||||||||||||||||||||||||||||||||||
2001 ATAATAGTAGTATTAGTAGTAATGGCGCATACAATAGAGAATTAATATCT   2050

2051 GCATCGGGTAGTGCTCTATCAAAACCCCCATCTCCATCTTCCGATAAAGA   2100
     ||||||||||||||||||||||||||||||||||||||||||||||||||
2051 GCATCGGGTAGTGCTCTATCAAAACCCCCATCTCCATCTTCCGATAAAGA   2100

2101 AAATAACTCTACCAGTAAATCAAATAAATCAAAATCTAGACAATCATCAA   2150
     ||||||||||||||||||||||||||||||||||||||||||||||||||
2101 AAATAACTCTACCAGTAAATCAAATAAATCAAAATCTAGACAATCATCAA   2150

2151 GAGCCTCCTCTTTATCAGAGAGTTCAGATTCAACCTCTCATACTTCGAGC   2200
     ||||||||||||||||||||||||||||||||||||||||||||||||||
2151 GAGCCTCCTCTTTATCAGAGAGTTCAGATTCAACCTCTCATACTTCGAGC   2200

2201 TCTGATGAACACTCTAGTAGATATGAAAGTGATAGAAAATCTTATAAAAA   2250
```

```
     ||||||||||||||||||||||||||||||||||||||||||||||||||
2201 TCTGATGAACACTCTAGTAGATATGAAAGTGATAGAAAATCTTATAAAAA   2250


2251 GAAAAAGAGCAGTAGCAGTAGTAGCAATAGTAAAAGAGATCGTGAACGTG   2300
     ||||||||||||||||||||||||||||||||||||||||||||||||||
2251 GAAAAAGAGCAGTAGCAGTAGTAGCAATAGTAAAAGAGATCGTGAACGTG   2300

2301 AACGTGACCGTGATCGTTCTAATAAAACCTATAAAAACTCTAGAAGTAGA   2350
     ||||||||||||||||||||||||||||||||||||||||||||||||||
2301 AACGTGACCGTGATCGTTCTAATAAAACCTATAAAAACTCTAGAAGTAGA   2350

2351 AATGTTAGTAGAGACAGAGAAAGAGAAAGAGATAGACATAATCGTTCAAG   2400
     ||||||||||||||||||||||||||||||||||||||||||||||||||
2351 AATGTTAGTAGAGACAGAGAAAGAGAAAGAGATAGACATAATCGTTCAAG   2400

2401 AGACAGAGATAGAGAAAGAGAAAGGGAAAGAGATAGAGACAGAGAAAGAG   2450
     ||||||||||||||||||||||||||||||||||||||||||||||||||
2401 AGACAGAGATAGAGAAAGAGAAAGGGAAAGAGATAGAGACAGAGAAAGAG   2450

2451 ATAGAGACAGAAGTAGAGATCGTTCAAGAGATAGAAGTAGAGATAGAGAA   2500
     ||||||||||||||||||||||||||||||||||||||||||||||||||
2451 ATAGAGACAGAAGTAGAGATCGTTCAAGAGATAGAAGTAGAGATAGAGAA   2500

2501 AGAGATAGAAGTAGAGATCGTTCAAGAGATAGAGATAGAAGTAGAGATCG   2550
     ||||||||||||||||||||||||||||||||||||||||||||||||||
2501 AGAGATAGAAGTAGAGATCGTTCAAGAGATAGAGATAGAAGTAGAGATCG   2550

2551 TTCAAGAGATAGAAGTAGAGAAAGGGATAGAGATAGAAGTAGAGATAGAA   2600
     ||||||||||||||||||||||||||||||||||||||||||||||||||
2551 TTCAAGAGATAGAAGTAGAGAAAGGGATAGAGATAGAAGTAGAGATAGAA   2600

2601 GCAGAGATCGTTCAAGAAGTAGAGATTCTGATAGTAGGGATAGAAGTAGA   2650
     ||||||||||||||||||||||||||||||||||||||||||||||||||
2601 GCAGAGATCGTTCAAGAAGTAGAGATTCTGATAGTAGGGATAGAAGTAGA   2650

2651 GATCGTTCAAGAAGTCATTCCAACAGAAGAAGAAGTAGAAGTCGTGATAG   2700
     ||||||||||||||||||||||||||||||||||||||||||||||||||
2651 GATCGTTCAAGAAGTCATTCCAACAGAAGAAGAAGTAGAAGTCGTGATAG   2700

2701 TAGAAATAAATCCAGAGATAGATCATCTGATTCTGATAGAAGTAGAGACA   2750
     ||||||||||||||||||||||||||||||||||||||||||||||||||
2701 TAGAAATAAATCCAGAGATAGATCATCTGATTCTGATAGAAGTAGAGACA   2750

2751 GAAGTAGAGATAGAGATTATAAATCTTCAAAATATAAAAAGAGTAGTAGA   2800
     ||||||||||||||||||||||||||||||||||||||||||||||||||
2751 GAAGTAGAGATAGAGATTATAAATCTTCAAAATATAAAAAGAGTAGTAGA   2800

2801 GGTACCAGTGGTAGAAAGAATAATAAAATTCAATCAAAACTCGACTCCCA   2850
     ||||||||||||||||||||||||||||||||||||||||||||||||||
2801 GGTACCAGTGGTAGAAAGAATAATAAAATTCAATCAAAACTCGACTCCCA   2850

2851 AGCAACTCATATTTCCTATCTTGAAGATAAGATATCCACACTCACCAATT   2900
     ||||||||||||||||||||||||||||||||||||||||||||||||||
2851 AGCAACTCATATTTCCTATCTTGAAGATAAGATATCCACACTCACCAATT   2900

2901 GGCTTCAACAACAAAACCTTCTCAATACTAGTAATGGTCAAGTTTTATCT   2950
     ||||||||||||||||||||||||||||||||||||||||||||||||||
2901 GGCTTCAACAACAAAACCTTCTCAATACTAGTAATGGTCAAGTTTTATCT   2950

2951 CCAACCGATCCAAATTTGGTTTCTAAACTTCAAACTCAATTGGATGTTCT   3000
     ||||||||||||||||||||||||||||||||||||||||||||||||||
2951 CCAACCGATCCAAATTTGGTTTCTAAACTTCAAACTCAATTGGATGTTCT   3000
```

```
3001 TCAATCAGAAAATTCTTATCTAAGAAATGAAAATATTAACTTGAAAACAA   3050
     ||||||||||||||||||||||||||||||||||||||||||||||||||
3001 TCAATCAGAAAATTCTTATCTAAGAAATGAAAATATTAACTTGAAAACAA   3050

3051 TTGTAAATGGTTCAAATTCAACAAATAATTCATTAAATCAAAGTTCTGGT   3100
     ||||||||||||||||||||||||||||||||||||||||||||||||||
3051 TTGTAAATGGTTCAAATTCAACAAATAATTCATTAAATCAAAGTTCTGGT   3100

3101 ATGGCTTTTAGAAATAGCGTTTCTTCTTTACATCAATTAAATATGAGTAA   3150
     ||||||||||||||||||||||||||||||||||||||||||||||||||
3101 ATGGCTTTTAGAAATAGCGTTTCTTCTTTACATCAATTAAATATGAGTAA   3150

3151 TAGTAGTAATAATAGTAGACCACAAACTCAATAA   3184
     ||||||||||||||||||||||||||||||||||
3151 TAGTAGTAATAATAGTAGACCACAAACTCAATAA   3184
```

Note: The query sequence is from the construct sequenced by AGRF and the subject sequence is from the native gene sequence acquired from dictyBase. The nucleotides highlighted in green correspond to the WIF sequence motif, which is involved in aiding the binding of the pseudokinase STRAD to MO25 (Section 3.3.1).

pPROF784 (pUC18-MO25)

Length: 1780
Score: 8900.0
Identity: 1780/1780 (100.0%)
Similarity: 1780/1780 (100.0%)

```
1    ATGAAATTAGAGAAAGGGATTTTCATGAAGATGAAGCTGAAGAAGATTGT     50
     ||||||||||||||||||||||||||||||||||||||||||||||||||
1    ATGAAATTAGAGAAAGGGATTTTCATGAAGATGAAGCTGAAGAAGATTGT     50

51   CCAACAAGTTGTTCAAGTGATGACCATGATGACACTTAAAAAGACAATAG    100
     ||||||||||||||||||||||||||||||||||||||||||||||||||
51   CCAACAAGTTGTTCAAGTGATGACCATGATGACACTTAAAAAGACAATAG    100

101  AACAGGTCCAAATGATGTAAAATCCTTTATTCAAGTTAAAAAAAGCTTCA    150
     ||||||||||||||||||||||||||||||||||||||||||||||||||
101  AACAGGTCCAAATGATGTAAAATCCTTTATTCAAGTTAAAAAAAGCTTCA    150

151  AATAATTTCAAAAAAACAAATAAAAAAAAAAAAAAAAGAACTCTTTAAAAA    200
     ||||||||||||||||||||||||||||||||||||||||||||||||||
151  AATAATTTCAAAAAAACAAATAAAAAAAAAAAAAAAAGAACTCTTTAAAAA    200

201  CAAGAAATATTTTTATTTTATTTTTTTTTATTTTATTTTCTCTTTTTTTT    250
     ||||||||||||||||||||||||||||||||||||||||||||||||||
201  CAAGAAATATTTTTATTTTATTTTTTTTTATTTTATTTTCTCTTTTTTTT    250

251  ATTACTATTACTATTTGTTTTTTTTTGGTTTTCTTTTTTTTTTTTTTTTT    300
     ||||||||||||||||||||||||||||||||||||||||||||||||||
251  ATTACTATTACTATTTGTTTTTTTTTGGTTTTCTTTTTTTTTTTTTTTTT    300
```

```
301  TTTTTTTTTTTTTTTAAAATATGAGTTGATTTTAAAAAAAAAATAAAAAA   350
     ||||||||||||||||||||||||||||||||||||||||||||||||||
301  TTTTTTTTTTTTTTTAAAATATGAGTTGATTTTAAAAAAAAAATAAAAAA   350

351  ATAAAAAAAAAAATTAATTTTTTTAAAAATTTTTTTTTTTTTTAAAAAATT   400
     ||||||||||||||||||||||||||||||||||||||||||||||||||
351  ATAAAAAAAAAAATTAATTTTTTTAAAAATTTTTTTTTTTTTTAAAAAATT   400

401  TTTTTTTTTTTTTTTTTTTTTTTTCTCAATAATAACTAAAAATAATACGC   450
     ||||||||||||||||||||||||||||||||||||||||||||||||||
401  TTTTTTTTTTTTTTTTTTTTTTTTCTCAATAATAACTAAAAATAATACGC   450

451  CACAAAGTCAAAAGAGTATTGTTTTTGCTATATCATATAGTATATAGATA   500
     ||||||||||||||||||||||||||||||||||||||||||||||||||
451  CACAAAGTCAAAAGAGTATTGTTTTTGCTATATCATATAGTATATAGATA   500

501  ATCGTTAAAATTATATATTTAATATATTTTATAAAAAATTAAAGTAAAAA   550
     ||||||||||||||||||||||||||||||||||||||||||||||||||
501  ATCGTTAAAATTATATATTTAATATATTTTATAAAAAATTAAAGTAAAAA   550

551  ATAATAATAATAATAATAAAGAAATTTAATATATAAACAAAAAAAAAGAG   600
     ||||||||||||||||||||||||||||||||||||||||||||||||||
551  ATAATAATAATAATAATAAAGAAATTTAATATATAAACAAAAAAAAAGAG   600

601  ACAAAGAGAGAGAAAATAAAATGAATATCTTTTTTAATAAAAAACAAAAG   650
     ||||||||||||||||||||||||||||||||||||||||||||||||||
601  ACAAAGAGAGAGAAAATAAAATGAATATCTTTTTTAATAAAAAACAAAAG   650

651  ACCCCATCAGAATTGGTTAAATCCATTAAAGAAAGCCTTGCTTCAATGGA   700
     ||||||||||||||||||||||||||||||||||||||||||||||||||
651  ACCCCATCAGAATTGGTTAAATCCATTAAAGAAAGCCTTGCTTCAATGGA   700

701  TAAAAGTGGTCCAAACTCTAAATCAACCGAAAAGGTAAGCTATTTTTAAT   750
     ||||||||||||||||||||||||||||||||||||||||||||||||||
701  TAAAAGTGGTCCAAACTCTAAATCAACCGAAAAGGTAAGCTATTTTTAAT   750

751  CATTGGAATCATTTTCTATTTATATCTTATTTTTAAAAATAAAATAAAAT   800
     ||||||||||||||||||||||||||||||||||||||||||||||||||
751  CATTGGAATCATTTTCTATTTATATCTTATTTTTAAAAATAAAATAAAAT   800

801  AAAATAAAATAAAATAAAATAAAATAAAAAAAAAAAAAAAGATCATACCAC   850
     ||||||||||||||||||||||||||||||||||||||||||||||||||
801  AAAATAAAATAAAATAAAATAAAATAAAAAAAAAAAAAAAGATCATACCAC   850

851  AGTGACTATCAATTTTTTTTTTCTTTTACTCTTTCTTTCCTTCTTTCTTC   900
     ||||||||||||||||||||||||||||||||||||||||||||||||||
851  AGTGACTATCAATTTTTTTTTTCTTTTACTCTTTCTTTCCTTCTTTCTTC   900

901  CTTAATAAATATTAACATTATCACACCCTCCTTCAATTTAATCAAAAAAA   950
     ||||||||||||||||||||||||||||||||||||||||||||||||||
901  CTTAATAAATATTAACATTATCACACCCTCCTTCAATTTAATCAAAAAAA   950

951  TTTTTAAAAAAAAAAAAAAAAAAAAAAAAAAATAAAAGGCATCAGAAGAAA  1000
     ||||||||||||||||||||||||||||||||||||||||||||||||||
951  TTTTTAAAAAAAAAAAAAAAAAAAAAAAAAAATAAAAGGCATCAGAAGAAA  1000

1001 TTTCAAAATGTTTACAAGAGATTAAAAAGATATTACATGGTGATTCAGAG  1050
     ||||||||||||||||||||||||||||||||||||||||||||||||||
1001 TTTCAAAATGTTTACAAGAGATTAAAAAGATATTACATGGTGATTCAGAG  1050

1051 CATGAACCAAATCAAGAGGTTGTTGCTGTATTATCAAATGAAATATGTAC  1100
     ||||||||||||||||||||||||||||||||||||||||||||||||||
```

```
1051 CATGAACCAAATCAAGAGGTTGTTGCTGTATTATCAAATGAAATATGTAC   1100

1101 CAGTGATTTGGTACAAATCCTTATTAAAGATTTAAACAAACTCGAGTTTG   1150
     ||||||||||||||||||||||||||||||||||||||||||||||||||
1101 CAGTGATTTGGTACAAATCCTTATTAAAGATTTAAACAAACTCGAGTTTG   1150

1151 AAGCTAAAAAAGATGTAGCTCAAATTTTCAATATTTTATTAAGACATAAA   1200
     ||||||||||||||||||||||||||||||||||||||||||||||||||
1151 AAGCTAAAAAAGATGTAGCTCAAATTTTCAATATTTTATTAAGACATAAA   1200


1201 AATGGTGCTCGTTCACCAATTGTAGAATATATCGCTAAAAATCCAGAAAT   1250
     ||||||||||||||||||||||||||||||||||||||||||||||||||
1201 AATGGTGCTCGTTCACCAATTGTAGAATATATCGCTAAAAATCCAGAAAT   1250

1251 TTTAGATTCATTAGTTAAAGGGTAATTAGTACTTAAATATAGTATAATAG   1300
     ||||||||||||||||||||||||||||||||||||||||||||||||||
1251 TTTAGATTCATTAGTTAAAGGGTAATTAGTACTTAAATATAGTATAATAG   1300

1301 ACAGATAAAATATACATACCTACAGGAGTGATCGATCGATAGATAGGTAG   1350
     ||||||||||||||||||||||||||||||||||||||||||||||||||
1301 ACAGATAAAATATACATACCTACAGGAGTGATCGATCGATAGATAGGTAG   1350

1351 ATAGATATATAGATAAATAAATAATTATAGGAAGATAGTGATAGTTTAGT   1400
     ||||||||||||||||||||||||||||||||||||||||||||||||||
1351 ATAGATATATAGATAAATAAATAATTATAGGAAGATAGTGATAGTTTAGT   1400

1401 AATAATAGAAAATATCATTCCTCCCTCCCTCCAATTAATATCAAATACTG   1450
     ||||||||||||||||||||||||||||||||||||||||||||||||||
1401 AATAATAGAAAATATCATTCCTCCCTCCCTCCAATTAATATCAAATACTG   1450

1451 ACATAAAATACCTAAATAAACACATACATACATACATACATAAATAATCA   1500
     ||||||||||||||||||||||||||||||||||||||||||||||||||
1451 ACATAAAATACCTAAATAAACACATACATACATACATACATAAATAATCA   1500

1501 TTTATTTTAAATTATTAGTTACGAACAACAGGATATTGCATTAAATTGTG   1550
     ||||||||||||||||||||||||||||||||||||||||||||||||||
1501 TTTATTTTAAATTATTAGTTACGAACAACAGGATATTGCATTAAATTGTG   1550

1551 GTACAATGCTTAGGGAATGTATCAAGCATGAATCATTGGCTAAAATTTTA   1600
     ||||||||||||||||||||||||||||||||||||||||||||||||||
1551 GTACAATGCTTAGGGAATGTATCAAGCATGAATCATTGGCTAAAATTTTA   1600

1601 ATATATTCACCAAACTTTTGGGAGTTCTTTGAATTTGTTGAAGTTTCAAA   1650
     ||||||||||||||||||||||||||||||||||||||||||||||||||
1601 ATATATTCACCAAACTTTTGGGAGTTCTTTGAATTTGTTGAAGTTTCAAA   1650

1651 TTTTGATGTTGCTTCTGATACATTTGCCACCTTTAAAGAGATTTTAACAA   1700
     ||||||||||||||||||||||||||||||||||||||||||||||||||
1651 TTTTGATGTTGCTTCTGATACATTTGCCACCTTTAAAGAGATTTTAACAA   1700

1701 AACATAAAACACTTAGCGCTGAATTTTTAGAAAAGAATTACGATCAGGTA   1750
     ||||||||||||||||||||||||||||||||||||||||||||||||||
1701 AACATAAAACACTTAGCGCTGAATTTTTAGAAAAGAATTACGATCAGGTA   1750

1751 TATTTCATATATATATTTATTTATTTTTAG   1780
     ||||||||||||||||||||||||||||||
1751 TATTTCATATATATATTTATTTATTTTTAG   1780
```

Note: The query sequence is from the construct sequenced by AGRF and the subject sequence is from the native gene sequence acquired from dictyBase.

6.8. Appendix 9 Mutagenesis of LKB1

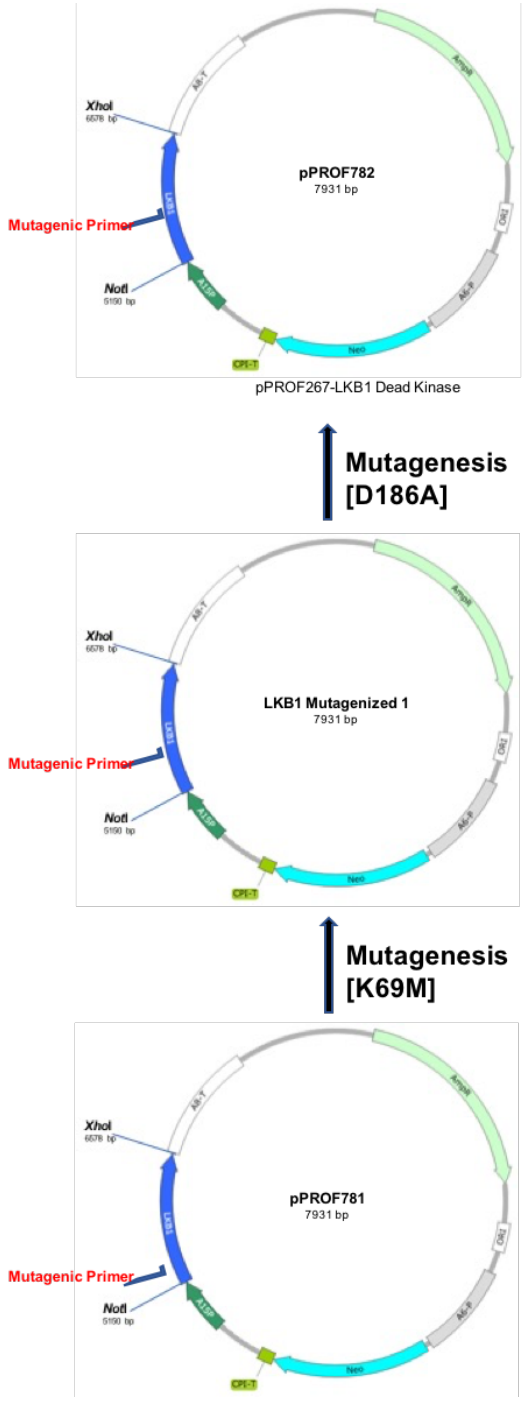

Figure A.9 Site directed mutagenesis of LKB1 to create LKB1 Dead Kinase.
Two mutations were introduced into the LKB1 construct subcloned in the *Dictyostelium* plasmid (pPROF781): K69M which disrupts the binding of ATP to LKB1 and abolishes the LKB1 kinase activity; and D186A in subdomain VII of the kinase domain rendering LKB1 catalytically inactive.

6.9. Appendix 10 Laboratory materials, instruments and equipment

Material	
Item	**Supplier**
Aluminium foil	Food service direct
Cell counter	Veeder-Root
Cell culture flasks (50 ml)	BD Biosciences
Cell culture flasks (160 ml)	Nunc
Cell culture flasks (200 ml & 500 ml)	Sigma-Aldrich
Centrifuge tubes (10 ml & 50 ml)	Sarstedt
Cling wrap	Food service direct
Cover slips	Menzel
Delicate task wipers	Kimberly-Clark
Driplock wash bottle	Bibby sterilin
Electroporation Cuvette	Bio-Rad

Ethanol bottle	Nalgene
Filter paper (0.025 μm)	Millipore
Hemacytometer	Scientific instruments
Hemacytometer cover glass	Thermo Fisher
Amersham Hybond^{TM}- P+ nylon membrane	GE Healthcare
Latex(nitrile) examination gloves	Pro-tek Australia
Microcentrifuge tubes 1.5 ml	Sarstedt
Micropipette (0.5-10 μl, 10-100 μl, 100-1000 μl)	Eppendorf
Micropipette tips (10 μl ,100 μl, 1000 μl)	Sarstedt
Microseal “B” seal	Bio-Rad
Microscope slides	Thermo Fisher
Microtitration 96-well plate with cover (0.35 ml)	Flow Laboratories
Multiwell (24 well) plate with cover	Nunc
Needles (sterile)	Terumo
Nitrocellulose membrane	Amersham

Parafilm	Thermo Fisher
PCR tubes	Sarstedt
Petridishes	Sarstedt
Pippet aids (easypet)	Eppendorf
Protect glasses	Bollé
PVDF membrane	Amersham
qPCR plate (96 wells)	Bio-Rad
Quartz cuvette	Starna
Surgical blade	Living stone
Surgical mask	Kimberly-clark
Syringes (1 cc ml^{-1}, 2 cc ml^{-1}, 5 cc ml^{-1}, 10 cc ml^{-1}, 20 cc ml^{-1})	Terumo
Syringe filter (0.2 µm)	Sartorious
UV blocking faceshield (uvc-803)	Capital Scientific
Instruments and equipments	

Item	Model	Supplier
AlphaDigiDoc RT		Alpha Innotech
Autoclave	LST-V	BeliMed
Balance DeltaRange	Mettler Toledo XS204	Thermo Fisher
Camera	C5060	Olympus
Centrifuge	5424	Eppendorf
Centrifuge	5702	Eppendorf
Centrifuge	Beckman Coulter L870	Thermo Fisher
Centrifuge	Minispin	Eppendorf
Centrifuge	Sorvall RC 5C	Thermo Fisher
Centrifuge	Sorvall RT6000B	Thermo Fisher
Fridgerator	Cyclic defrost 380	Kelvinator
DNA speedvac	110	Savant
Dry block heater		Ratek

Electroporation system	Gene-pulser	Bio-Rad
Electrophoresis cell	Sub-Cell® GT Cell	Bio-Rad
Fluorometer	Turner Biosystems Modulus	Promega
Freezer (-80 ^{o}C)	Glacier NU-9668	NuAire
Freezer (-80 ^{o}C)	Forma Scientific Bio-Freezer 8538	Thermo Fisher
Fume hood		labsystems
Ice flaker	Scotsman MF26	Scotsman Ice systems
Freezer (-20 ^{o}C)	Fisher & Paykel N388	Fisher& Paykel
Imager	Gel Doc EZ	Bio-Rad
Incubator	catalogue	Contherm
Incubator	Gallenkamp Cooled incubator	Artisan technology
Laminar flow	Gelman Science CF435	Airpure Australia
Microscope	IMT2 (Inverted)	Olympus
Microscope	FX-35 (Binocular)	Nikon

Microscope	S261(Dissecting)	Olympus
Microscope	CH2 (Binocular)	Olympus
Microscope	BX61 (Motorized fluorescence)	Olympus
Microwave oven	MS3848XRSK	LG
Orbital Benchtop		Ratek
Orbital mixer	EOM5	Ratek
pH meter	Orion Star A211	Thermo Fisher
phosphorimager	Storm 860	Amersham
Pipetting Aid	Easypet	Eppendorf
Platform shaker		Ratek
Power Pack	^{TM} HC	Bio-Rad
Real-time PCR	Icycler IQ multicolour	Bio-Rad
Scale	Sartorius BP 1200	Data Weighing
Shaking water bath	SWB20D	Ratek

Sonifier	Branson 250	Thermo Fisher
Spectrophotometer	Ultrospec 1000 UV/Visible	Amersham
Thermal Cycler	PTC-150 minicycler	Bio-Rad
Transfer System	Trans-Blot® Turbo™	Bio-Rad
UV transilluminator	TM-36	UVP
Vortex mixer		Ratek
Waterbath		Ratek
Water purification system		Millipore

6.10. Appendix 11

A.11. Over-expression of LKB1 Dead Kinase and Chaperonin 60 Antisense- inhibition co-transformants in mitochondrially diseased cells.

A.11.1. Overexpression of LKB1 Dead Kinase rescues impaired growth caused by the antisense inhibition of Chaperonin 60 in D. discoideum.

A phenotype which was identified previously in mitochondrially diseased strains, created by the antisense inhibition of Chaperonin 60, was decreased growth on bacterial lawns (Bokko *et al.,* 2007). This phenotype was also exhibited in strains overexpressing LKB1; and conversely rescued in *Dictyostelium* strains expressing LKB1 Dead Kinase. To explore whether the slow growth rate of mitochondrially diseased transformants can be rescued by inhibiting the expression of LKB1, transformants co-expressing LKB1 Dead Kinase and Chaperone 60 antisense-inhibited constructed were created and then observed for their ability to grow on normal agar plates covered with a lawn of *E. coli* B2. The rate of plaque expansion was calculated as depicted in Section 2.5.1. The co-transformants showed relatively similar plaque expansion rate in comparison to wild type AX2 indicating a rescue in the phenotypes depicted previously by mitochondrially diseased strains (Bokko *et al.,* 2007). This result shows that the plaque expansion in mitochondrially diseased cells can be regulated by the activity of LKB1.

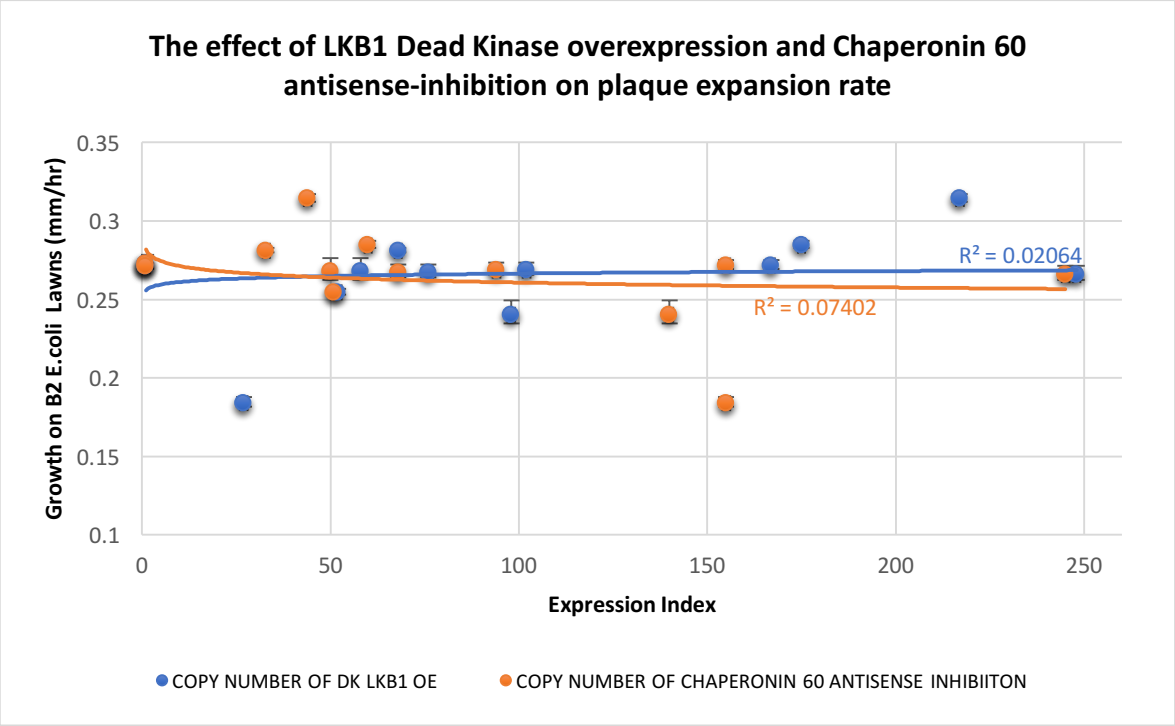

Figure A.11.1 Plaque expansion rates of co-transformants with LKB1 Dead Kinase overexpression and Chaperonin 60 antisense inhibition constructs.

The plaque expansion rates for the transformants were normalized against AX2 and plotted against their relative expression levels. An increase in the LKB1 Dead Kinase overexpression construct copy number and hence in the levels of expression, resulted in mostly similar plaque expansion rates to AX2. This result is mirrored with the increase in the Chapronin 60 antisense inhibition construct copy number and hence in the levels of expression. Hence, the co-transformation of both constructs shows to grow in a similar fashion to wild type AX2. The figures show the coefficient of variation, R^2, representing the fraction of the variance in plaque expansion rates that was attributable to the regression relationship. Error bars are standard errors of the mean from 3 replicate measurements.

A.11.2. LKB1 Dead Kinase overexpression- Chaperonin 60 antisense-inhibition co-transformants positively regulate growth in HL5 liquid.

LKB1 Dead Kinase overexpression showed to rescue the slow growth of transformants with antisense inhibition of Chaperonin 60 (depicted previously by Bokko *et al.,* 2007) on bacterial lawns to resemble the normal growth of wild type AX2. These co-transformants were also subcultured in HL-5 media to determine whether they had similar effects on axenic growth; that is if LKB1 Dead Kinase overexpression can reverse the effects caused by Chaperonin 60 antisense-inhibited levels.

The generation times of wild type AX2 and the co-transformants were measured as described in Section 2.5.2. Figure A.11.2 shows that the generation time is relatively similar in comparison to wild type AX2 indicating a rescue in the phenotypes depicted previously by Chaperonin 60 antisense-inhibition. This result shows that the axenic growth in mitochondrially diseased *Dictyostelium* cells can be regulated by the activity of LKB1.

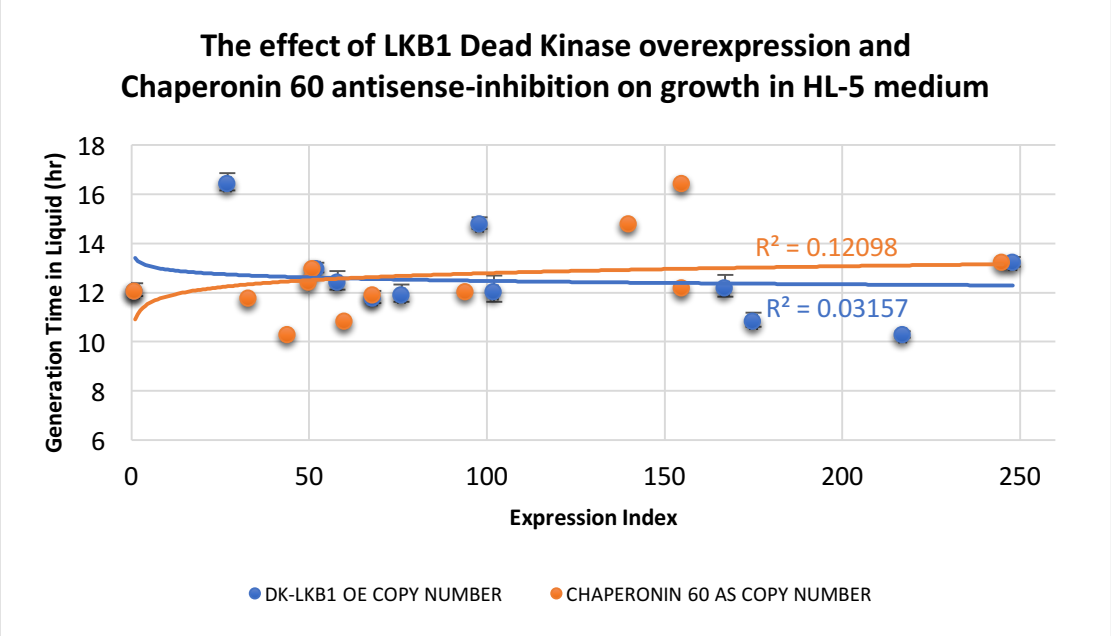

Figure A.11.2 The effect of LKB1 Dead Kinase overexpression in mitochondrial diseased *Dictyostelium* cells on the axenic growth of the co-transformants.
The generation times, which is the doubling time of strains during exponential phase, of the co-transformants were measured and compared with the parent strain, AX2. Antisense-inhibited Chaperonin 60 was shown by Bokko *et al.,* (2007) to result in an increase in the generation time; however, increased LKB1 Dead Kinase expression levels rescued this phenotype depicted as shown by a normal generation time of the strains in comparison to AX2. The figure shows the coefficient of variation, R^2, representing the fraction of the variance in generation time that was attributable to the regression relationship. Error bars are standard errors of the mean from 3 independent experiments.

A.11.3. The role of LKB1 Kinase activity in regulating mitochondrial biogenesis in mitochondrially diseased Dictyostelium cells.

Mitochondrial proliferation was shown to be a feature of mitochondrial diseases (Campos *et al.*, 1997; Agostino *et al.*, 2003). Bokko *et al.* (2007) showed that the mitochondrial mass and biogenesis remained unaltered in the mitochondrially diseased cells of *Dictyostelium.*

Bokko *et al*. (2007) also evaluated the role of AMPK activation in mitochondrial biogenesis in *Dictyostelium* revealing that increased AMPK expression resulted in elevated mitochondrial mass whereas a decrease in AMPK attenuated expression resulted in decreased mitochondrial mass. An elevation in mitochondrial mass was indicative of increased mitochondrial proliferation. An increase or decrease in LKB1 expression appeared to phenocopy the regulation of mitochondrial mass and biogenesis as presented by altered AMPK expression respectively.

We therefore examined whether the inactivation of LKB1, an upstream kinase of AMPK, might affect the phenotype exhibited in mitochondrially diseased *Dictyostelium* cells.

The overexpression of LKB1 Dead Kinase appears to only have a slight effect on the mitochondrial mass and membrane potential in the chaperonin 60 antisense inhibited strains, which could possibly indicate that mitochondrial proliferation that should occur in mitochondrially compromised cells is counterbalanced by the inactivation of LKB1 and hence AMPK; resulting in amending the delirious effects caused by mitochondrial dysfunction.

A.

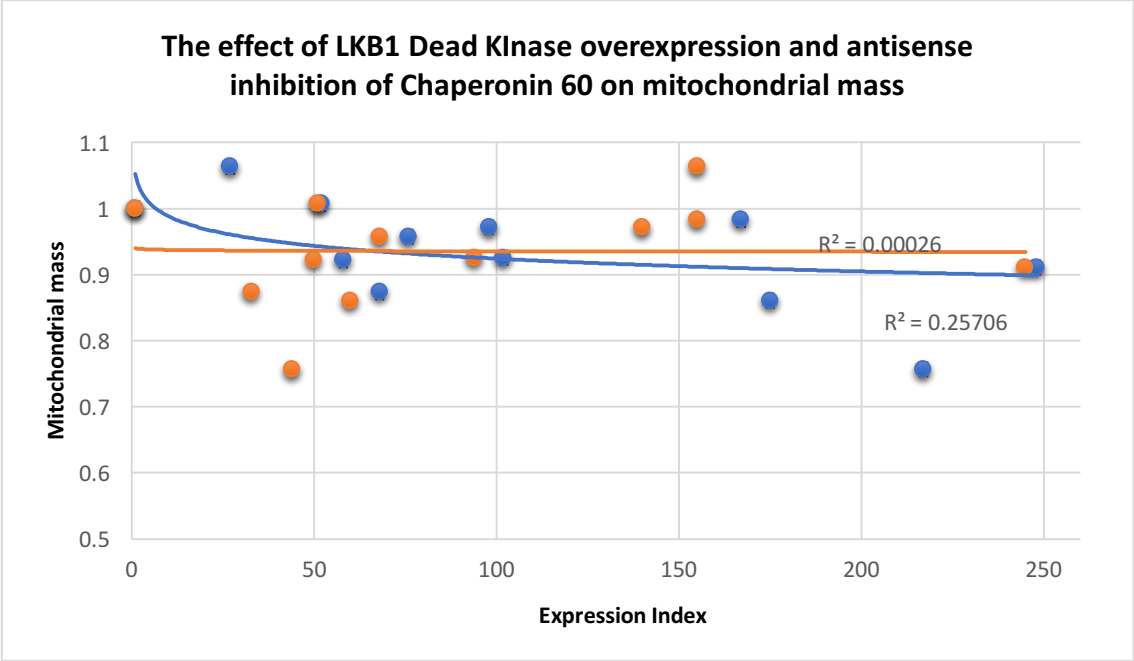

B.

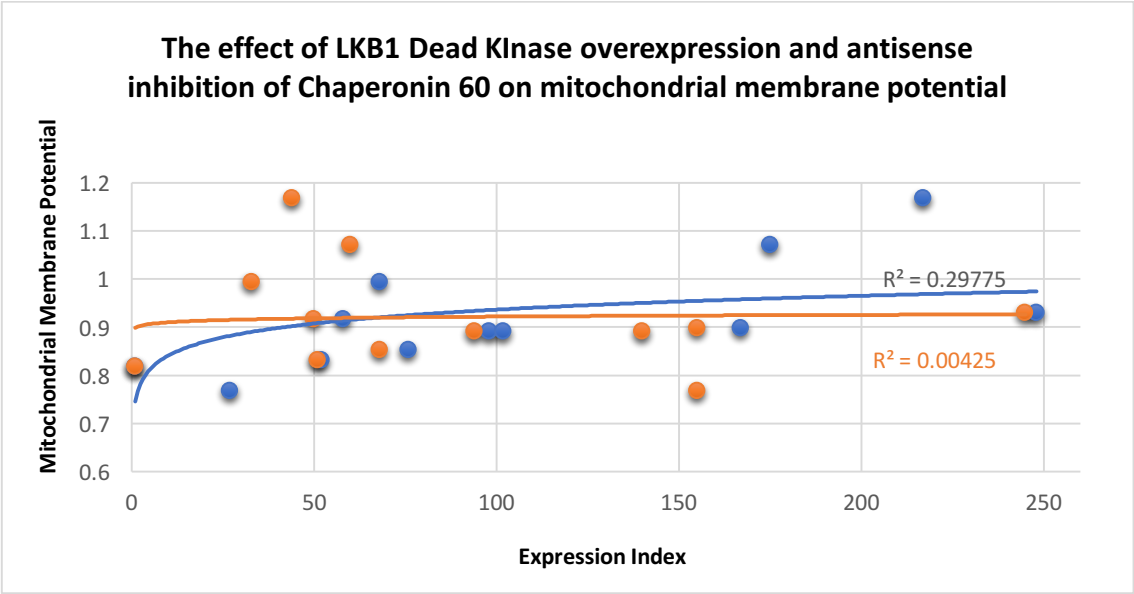

Figure A.11.3 Effect of LKB1 Dead Kinase and Chaperonin 60 antisense-inhibited expression levels on mitochondrial mass and mitochondrial membrane potential in *Dictyostelium*.

The expression index indicates the copy numbers of the overexpression constructs of LKB1 Dead Kinase (Blue) and antisense-inhibited construct of Chaperonin 60 (Orange). Copy numbers of zero refer to the wild-type parental strain AX2. **A.** Mitochondrial mass is measured by fluorescence with the mitochondrion-specific dye MitoTracker Green after subtraction of autofluorescence from unstained cells from the same suspension. LKB1 Dead Kinase overexpression-Chaperonin 60 antisense-inhibited transformants appear to have a range of mitochondrial masses similar to wild type AX2. **B.** The mitochondrial membrane potential of the co-transformants is not altered and resembles that of wild type AX2. The figures show the coefficient of variation, R^2, representing the fraction of the variance in mitochondrial mass and mitochondrial membrane potential rates that were attributable to the regression relationship.